NON-INVASIVE MONITORING OF GLUCOSE AND LACTATE IN HUMANS BY REVERSE IONTOPHORESIS

CONGO T.S. CHING

NON-INVASIVE MONITORING OF GLUCOSE AND LACTATE IN HUMANS BY REVERSE IONTOPHORESIS

Thesis presented for the degree of

Doctor of Philosophy

by

Congo T.S. Ching, M.Phil.

Bioengineering Unit

University of Strathclyde

Glasgow

May 2005

Abstract

Blood glucose and lactate monitoring are beneficial to many patients, e.g. diabetes mellitus patients, critical care patients, etc. However, there are very few non-invasive or continuous monitoring systems for these parameters and significant clinical benefit could be achieved if such systems were readily available. Therefore, this study focused on the development of a prototype monitoring system for non-invasive monitoring of blood glucose and lactate in human subjects.

The current study consisted of three parts. In the first part of the study, *in vitro* experiments were performed using a model system for the optimisation of glucose and lactate extraction by reverse iontophoresis. In the second part of the study, a portable and programmable constant current device for iontophoresis was designed, developed and evaluated. This newly-developed device was then used in the final part of the study.

In the third part of the study, screen-printed silver-silver chloride electrodes were fabricated and studied. Finally, the newly-developed device and electrodes were then used on healthy volunteers to study long duration bipolar direct current iontophoresis effects on transdermal glucose and lactate extraction and on the electrical properties of human skin.

Importantly, the results show that reverse iontophoresis extraction of glucose and lactate needs careful optimisation of extraction times and current waveforms. In addition, significant temporary changes in skin impedance occurred as a result of reverse iontophoresis. These impedance changes show promise for their use in the calibration of iontophoresis devices for human use.

Acknowledgements

I acknowledge with gratitude to my chief supervisor Prof. P Connolly (Department of Bioengineering, University of Strathclyde, Glasgow, UK) for her constructive advice, useful discussion and encouragement throughout this work.

I will always be grateful to the late Mr. IG Camilleri (Canniesburn Plastic Surgery Unit, Glasgow Royal Infirmary, UK) for his encouragement, valuable medical knowledge, and comments on my work during the earlier stages of this research. The loss of such an eminent colleague and collaborator during the project was keenly felt by myself and the Bioengineering Unit.

I am indebted to John Swire & Sons Ltd. (HK) for the award of the James Henry Scott Scholarship which allowed me to pursue the first two years of my PhD study in Glasgow, and for sponsoring my conference travel in the later years. I am also indebted to University of Strathclyde for the award of the University Postgraduate Studentship which allowed me to pursue the third year of my PhD study in Glasgow.

I would like to express my gratitude to all the staff in the Department of Bioengineering, in particular Ms. R Kirk, Mr. B Cartlidge, Mr. J Maclean and Mr. I Tullis, who have helped me with this research work.

I also would like to thank all my colleagues in the Department of Bioengineering, in particular Mr. D McColl, Ms. F Angeli and Mr. A Smith are praised for giving me moral support throughout this project.

Last but not least, I extend my special and sincere thanks to my parents and family members for their loving support and patience during my study.

Congo Ching

Table of Contents

List of Abbreviations

Ag/AgCl	Silver-Silver Chloride
ANOVA	Analysis of Variance
CCU	Critical Care Unit
DC	Direct Current
DPDT	Double Pole Double Throw
FDA	Food and Drug Administration
GOD	Glucose Oxidase
HPLC	High Performance Liquid Chromatography
IC	Integrated Circuit
LOD	Lactate Oxidase
LSD	Least Significant Difference
MC	Methylcellulose
MIR	Mid Infrared Radiation
MWCO	Molecular Weight Cut-Off
NIR	Near Infrared
PBS	Phosphate Buffer Solution
POD	Peroxidase
SPE	Screen-Printed Electrode
SPST	Single Pole Single Throw
TRAM	Transverse Rectus Abdominis Myocutaneous

■ *Chapter 1*

Introduction

Chapter 1 Introduction

Homeostatic disturbances, such as the interruption of energy supply to organs, can develop rapidly into life threatening situations. Therefore, fine adjustment of the uptake and release of metabolites in different organs and regulation of the circulation is essential to prevent the build up of concentration differences beyond the limits acceptable for life (i.e. homeostasis). Nowadays, physicians make an attempt at anticipating sudden pathological events by frequently monitoring a patient's metabolites. In the clinical setting, body fluids of critical care patients are often monitored continuously for energy metabolism substrates and products such as oxygen, carbon dioxide and hydrogen ions (pO_2, pCO_2 and pH).

This thesis focuses on development of a monitoring system for non-invasive monitoring of the metabolites glucose and lactate. These metabolites are of major importance for large patient groups such as diabetes mellitus patients and critical care patients. To date it has not been possible in any clinical setting to monitor both of these parameters in a continuous non-invasively manner.

Diabetes is a global health problem that presents one of the 21st century's biggest medical challenges. Globally there are already over 171 million people with diabetes (Wild *et al.* 2004). Around 1.8 million people in the UK today have diagnosed diabetes (Diabetes UK 2004, Boyle *et al.* 1998). At least a million more are thought to have diabetes but do not know it yet (Diabetes UK 2004, Simmons *et al.* 1991, Harris *et al.* 1987, Forrest *et al.* 1986). Diabetes increases the risk of ill health and shortens life (Panzram 1987). Complications include blindness (Evans 1995), and amputation (Davis *et al.* 2004, Bild *et al.* 1989). Diabetes can cause death from heart disease (Laing *et al.* 1999a and 1999b, Stephenson *et al.* 1995, Rosengren *et al.* 1989), stroke

(Stephenson *et al.* 1995, Bell 1994) and kidney failure (Brancati *et al.* 1997, Wang *et al.* 1996, Stephenson *et al.* 1995, Cameron and Challah 1986). The number of people with diabetes is rising in UK due to lifestyle changes and obesity (Gatling *et al.* 1998, Amos *et al.* 1997, Neil *et al.* 1987, Gatling *et al.* 1985). Although there is no definitive source, a considerable increase in the number of people worldwide developing Type 2 diabetes is forecast (Amos *et al.* 1997, King *et al.* 1993).

Diabetes generates a substantial economic burden. It accounts for some nine per cent of the annual NHS budget (Currie *et al.* 1997). This represents a total of approximately £5.2 billion a year. Clearly, with the continuing increase in the economic burden, strategies have to be implemented to monitor and control blood glucose levels. Evidence showed that tight monitoring and control of blood glucose levels can reduce the prevalence of complications in both type 1 and type 2 diabetes (The UK Prospective Diabetes Study Group 1998a, 1998b, 1998c and 1998d, The Diabetes Control and Complication Trial Research Group 1993).

Type 1 diabetes, often called insulin-dependent diabetes mellitus, develops if the body is unable to produce any insulin. This type of diabetes usually appears before the age of 40. It is treated by insulin injections and diet and regular exercise is recommended. Type 2 diabetes, also known as non insulin dependent diabetes mellitus, develops when the body can still make some insulin, but not enough, or when the insulin that is produced does not work properly. This type of diabetes usually appears in people over the age of 40. It is treated by diet and exercise alone or by diet, exercise and tablets or by diet, exercise and insulin injections.

In fact, monitoring of metabolites is of major importance for many patient groups. Glucose monitoring is beneficial to the diabetes mellitus patient while both glucose and lactate monitoring is beneficial to the critical care patient. In critical care units, high lactate levels in the blood have a strong prognostic value (Vincent 1996), with lactate levels over 5 mM (normally 0.6 – 2.4 mM) associated with a poor outcome (Bakker *et al.* 1991). It is possible to predict organ failure from serial lactate

measurements (Gersh, and Anderson 1993). Lactate monitoring has been suggested to be valuable for many patients in emergency medicine: for trauma patients, for patients with head injury or cerebral ischemia (Menzel *et al.* 1999, Zauner *et al.* 1998, Mendelowitsch *et al.* 1998, Artru *et al.* 1998, Valadka *et al.* 1998), acute intestinal ischemia (Murray *et al.* 1994), transplanted organ surveillance e.g. myocutaneous flaps (Rojdmark *et al.* 1998), and patients with septic shock (Levraut *et al.* 1998, de Boer *et al.* 1994, Bakker *et al.* 1991). In summary, large patient groups may benefit from glucose and lactate monitoring devices.

In recent years, several promising techniques have been evolved for invasive and non-invasive monitoring. Subcutaneous implantable biosensors has been employed for glucose monitoring (Wilson *et al.* 1992) while a combination of biosensors with microdialysis sampling has been employed for lactate monitoring (Volpe *et al.* 1995). Non-invasive monitoring of glucose, using near infrared (NIR) spectroscopy has been proposed (Fischbacher *et al.* 1997, Müller *et al.* 1997, Marbach *et al.* 1993, Haaland *et al.* 1992). Reverse iontophoresis, the use of low levels of DC current through skin, has also been shown to be capable of monitoring glucose non-invasively (Potts *et al.* 2002, Tierney *et al.* 2000, Rao *et al.* 1993). Non-invasive monitoring is preferred for patients who need to monitor their metabolites frequently as invasive monitoring still has the chance of inducing infection at the insertion site. Moreover, surgical intervention is required for the invasive monitoring techniques mentioned above.

NIR spectroscopy is an indirect approach to monitoring metabolites while reverse iontophoresis directly and non-invasively extracts metabolites out of the human body through the intact skin. The extracted metabolites can be quantified by either biosensor or spectroscopic approaches. More importantly, NIR spectroscopy is not particularly accurate even in the normal physiological range (Van Heuvelen 1987) and it has been reported that NIR spectroscopy has a subject-dependent concentration bias (Ward *et al.* 1992). Although there are some problems for the reverse iontophoresis

technique, e.g. lag time of at least 20 minutes from the beginning of an extraction cycle until a blood glucose level can be reported (Potts *et al.* 2002), this technique is accurate and allows multiple measurements over a 24-hour period (Tierney *et al.* 2000).

In the present study, the reverse iontophoresis technique was selected for the development of a prototype monitoring system for non-invasive monitoring of glucose and lactate. The principal objectives of this study are:

(1) to investigate the optimum current waveforms for reverse iontophoresis for glucose and lactate extraction;

(2) to design, develop and evaluate a low-cost, low-power, miniature, programmable constant current device used for reverse iontophoresis;

(3) to design, develop and evaluate low-cost and reliable screen-printed electrodes for reverse iontophoresis;

(4) to investigate the effect of long duration bipolar direct current on human transdermal extraction of glucose and lactate;

(5) to investigate the effect of long duration bipolar direct current on the electrical properties of human skin.

■ *Chapter 2*

Literature Review

Chapter 2 Literature Review

Diabetes results in long-term health disorders and a heavy burden is imposed on the patient and on health care resources. Most of these disorders are due to the devastating influences of diabetes on both the small and the large blood vessels. The influence of diabetes on the small blood vessels can cause eye, kidney and nerve damage, whereas the influence on the large blood vessels can cause accelerated atherosclerosis, with increased rates of coronary heart disease, peripheral vascular disease and stroke.

Theoretically, returning blood glucose levels to normal by replacement insulin injections, dietary control and other treatments in diabetes should prevent complications. However, near-normal blood glucose concentrations are very difficult to achieve and maintain in many patients, particularly those with type 1 diabetes. In these patients, blood glucose levels can swing between high (hyperglycaemia) and low (hypoglycaemia) in an unpredictable manner. Because intermittent blood glucose monitoring may miss episodes of hyperglycaemia and hypoglycaemia, it is necessary to continuously detect blood glucose levels and to adjust therapy accordingly so as to maintain normal glucose levels. To date, most type 1 and type 2 diabetic patients measure their own blood glucose several times a day by obtaining finger-prick capillary samples and applying the blood to a reagent strip for analysis in a portable meter (Pickup 2003). However, this method is painful, cumbersome, aesthetically unpleasant and inconvenient. More importantly, this method is not a continuous monitoring method and therefore blood glucose monitoring cannot be performed during sleeping and whilst the subject is occupied, such as during driving a motor vehicle. This provides considerable impetus for the development of non-invasive methods for continuous blood glucose monitoring.

2.1 EPIDEMIOLOGICAL STUDIES OF DIABETES

Epidemiological studies have shown that the prevalence of diabetes is steadily increasing and is a widespread problem in modern society (Wild *et al.* 2004, Amos *et al.* 1997, King *et al.* 1993). The number of cases of diabetes worldwide in 2000 among adults ≥ 20 years of age was estimated to be 171 million (Wild *et al.* 2004) and in 2003 this was estimated to be 194 million (International Diabetes Federation 2003). By 2025, the number of people with diabetes is expected to exceed 333 million (International Diabetes Federation 2003). In the United Kingdom, approximately 1.8 million people today have been diagnosed as diabetics (Diabetes UK 2004, Boyle *et al.* 1998) and at least a million more are thought to have diabetes but do not know it yet (Diabetes UK 2004, Simmons *et al.* 1991, Harris *et al.* 1987). Apart from the United Kingdom, reports from other countries also reveal a high incidence of diabetes, such as India (35.5 million), China (23.8 million), the United States (16 million), Russia (9.7 million), Japan (6.7 million) and so on (International Diabetes Federation 2003). The reasons for the increased prevalence are not known, however it is suspected that lack of regular exercise is considered to be a major risk factor for the development of diabetes in all people, especially when linked with obesity. Changes in eating style (more and more people taking fast food) are also suspected to increase the prevalence.

Diabetes increases the risk of ill health and shortens life. It is the leading cause of blindness and visual impairment (International Diabetes Federation 2003, Evans 1995) as well as of amputation which is not the result of an accident (Davis *et al.* 2004, International Diabetes Federation 2003, Bild *et al.* 1989). People with diabetes are two to four times more likely to develop cardiovascular disease and about three times more likely to die through cardiovascular disease than people without diabetes (International Diabetes Federation 2003, Laing *et al.* 1999a and 1999b, Stephenson *et al.* 1995, Rosengren *et al.* 1989). People with diabetes are also significantly more likely to have a stroke (International Diabetes Federation 2003, Stephenson *et al.* 1995, Bell 1994)

and kidney failure (International Diabetes Federation 2003, Brancati *et al.* 1997, Wang *et al.* 1996, Stephenson *et al.* 1995, Cameron and Challah 1986).

The devastating complications of diabetes impose a huge and substantial economic burden not just on healthcare services but also on industry and commerce. It is estimated that diabetes accounts for between 5% and 10% of a nation's health budget (International Diabetes Federation 2003). In the United Kingdom, diabetes accounts for some 9% of the annual NHS budget (Currie *et al.* 1997) and this represents a total of approximately £5.2 billion a year. The economic impact of diabetes was also demonstrated in other countries. In the United States, diabetes cost an estimated £73.9 billion in 2002, an amount made up of medical expenditures (£51.4 billion) and lost productivity (£22.5 billion) (American Diabetes Association 2003), up from £54.9 billion in 1997 (American Diabetes Association 1998). It is estimated that the annual cost for diabetes could rise to an estimated £87.4 billion by 2010 and to £107.5 billion by 2020 (American Diabetes Association 2003).

Clearly, with the continuing increase in the economic burden, strategies have to be implemented to monitor and control blood glucose levels in diabetics. Evidence showed that tight monitoring and control of blood glucose levels can reduce the prevalence of complications in both type 1 and type 2 diabetes (The UK Prospective Diabetes Study 1998a, 1998b, 1998c and 1998d, The Diabetes Control and Complication Trial Research Group 1993). Given the scale of the problem, it is important to find ways to monitor blood glucose levels in order to reduce the prevalence of complications for diabetic patients.

2.2 CRITICAL CARE PATIENTS IN THE CRITICAL CARE UNIT

Critical care patients in the critical care unit (CCU) require complex care across a broad range of acute illnesses. CCUs consist about 10% of acute care hospital beds

(Groeger *et al.* 1993). The number of CCU admissions in Scotland (cohort of some 20 CCUs) is estimated to be about 6500 patients in 2001, up from about 5600 patients in 1995 (Scottish Intensive Care Society Audit Group 2003). On the other hand, the number of annual CCU admissions is estimated to be 4.4 million patients in the United State (Young and Birkmeyer 2000). On account of an ageing population and the growing acuity of illness of hospitalized patients, both the total number of CCU patients and their proportional share of hospital admissions are expected to grow (Angus *et al.* 2000).

CCU patients usually have mortality rates between 12% and 17% (Al-Asadi *et al.* 1996). It is believed that this mortality could be reduced by intensive monitoring of metabolites of the patient. Indeed, monitoring of lactate is beneficial to the critical care patient as the trend in lactate levels is known to be a superior indicator of patient viability (Abramson *et al.* 1993). Blood lactate levels have been used for prognosis of critical illness and assessing effects of therapeutic manoeuvres (Moomey *et al.* 1998, Vincent 1998, Cairns *et al.* 1997, Marecaux *et al.* 1996, Abramson *et al.* 1993), because blood lactate is an extremely fast indicator of oxygen deprivation at the cellular level, increasing within seconds of a life threat and decreasing within seconds of appropriate therapy (Bakker *et al.* 1991). Blood lactate has been reported to be superior to other variables (e.g. oxygen-derived variables) as a predictor of outcome (Moomey *et al.* 1998). In CCUs, high lactate levels in the general circulation have a strong prognostic value (Vincent 1996), with lactate levels over 5 mM (normally 0.6 – 2.4 mM) are associated with a poor outcome (Bakker *et al.* 1991). Therefore, it is possible to predict organ failure from serial lactate measurements (Gersh and Anderson 1993).

Lactate monitoring has been suggested to be valuable for many patients in emergency medicine, such as trauma patients (Slomovitz *et al.* 1998, Manikis *et al.* 1995). Inadequate oxygen delivery to tissues causes a shift to anaerobic metabolism and increased production of lactate. A metabolic acidosis secondary to accumulation of

lactate suggests inadequate tissue oxygen delivery. Manikis *et al.* (1995) investigated the correlation between blood lactate, mortality, and organ failure in 129 trauma patients, including 100 intensive care unit survivors and 29 intensive care unit fatalities. They found that initial lactate and highest lactate levels were significantly higher in patients with organ failure than without organ failure. They also found that not only the initial or the highest lactate value but also the duration of hyperlactatemia can be correlated with the development of organ failure. Their observations stress the importance of the initial resuscitation in the prevention of organ failure. Therefore, they suggested that serial blood lactate measurements are reliable indicators of morbidity and mortality after trauma.

Lactate monitoring has also been employed on patients with head injury or cerebral ischemia (Goodman *et al.* 1999, Menzel *et al.* 1999, Zauner *et al.* 1998, Mendelowitsch *et al.* 1998, Artru *et al.* 1998, Valadka *et al.* 1998). Lactate is produced in the brain from glucose by anaerobic metabolism when oxygen is not available. Usually, the increase of the brain lactate concentration is associated with more serious brain injury (Mendelowitsch *et al.* 1998). Goodman *et al.* (1999) studied cerebral glucose and lactate metabolism in 126 head-injured patients using microdialysis. They found that elevated extracellular lactate, reduced glucose, and an elevated lactate/glucose ratio were observed with cerebral hypoxia and ischemia. More importantly, they found that elevated lactate and an increased lactate/glucose ratio strongly correlated with death.

Moreover, lactate monitoring has been used on patients with acute intestinal ischemia (Murray *et al.* 1994). For example, Murray *et al.* (1994) conducted a prospective study to evaluate preoperative D(-)-lactate levels in 31 patients undergoing laparotomy for acute abdominal emergencies, including suspected acute mesenteric ischemia. They reported that peripheral D(-)-lactate levels are elevated only at two hours after onset of experimental intestinal ischemia and demonstrated the clinical usefulness in diagnosing acute ischemia, such as acute mesenteric ischemia.

Besides, lactate monitoring has been suggested to be valuable for patients with transplanted organ surveillance, such as myocutaneous flaps (Udesen *et al.* 2000, Rojdmark *et al.* 1998). Udesen *et al.* (2000), using microdialysis, postoperatively measured glucose, glycerol and lactate concentrations for continuous period of 72 hours in the flaps of 14 women, who underwent reconstruction with a free transverse rectus abdominis myocutaneous (TRAM) flap. The measured metabolites were compared with those in a reference catheter that was placed subcutaneously in the femur. They found that, during flap ischemia, the concentration of glucose was reduced, while the lactate and glycerol levels increased. However, after reperfusion of the flaps, the concentrations of glucose, lactate, and glycerol approached normal. They therefore concluded that monitoring of glucose, glycerol and lactate concentrations with microdialysis can detect ischemia in free flaps at an early stage, making early surgical intervention possible.

Last but not least, lactate monitoring has also been employed on patients with septic shock (Levraut *et al.* 1998, de Boer *et al.* 1994, Bakker *et al.* 1991). For instance, Bakker *et al.* (1991) examined measurements of cardiac output, oxygen-derived variables, and blood lactate levels in 48 patients with documented septic shock. In their investigation, twenty-seven patients survived but twenty-one patients died from the shock episode. They found that survivors had significantly lower blood lactate levels both initially and in the final phase of septic shock, and only the survivors had a significant decrease in blood lactate levels during the course of septic shock. Because blood lactate levels are closely related to ultimate survival from septic shock and decreases in blood lactate levels during the course of septic shock could indicate a favorable outcome, they therefore concluded that blood lactate levels can serve as a reliable clinical guide to therapy.

Because a large number of patient groups may benefit from lactate monitoring, there is a drive to find ways to monitor blood lactate levels in the CCU.

2.2.1 Monitoring of Free Flaps (Skin Grafts)

One drive for the current project was to develop a method of monitoring free flaps (skin grafts) following plastic surgery. Flaps have become an increasingly popular and useful method of tissue reconstruction nowadays in plastic surgery. It is important that the flap is successful i.e. that the skin graft stays in place, is vascularised and healthy. In the past twenty years, flap success rate has steadily improved (Khouri 1992) with overall flap success rates greater than 95% (Hidalgo *et al.* 1998, Kind *et al.* 1998, Kroll *et al.* 1996, Schusterman *et al.* 1994). Although the accrued technical expertise of the surgeon is usually the most important factor, close postoperative monitoring and subsequent early detection of a problem can successfully resolve vascular compromise resulting in salvage rates of 70% to 100% by surgical reintervention (Lineaweaver and Buncke 1986, Lidman and Daniel 1981). The most critical period is usually the first 24 to 48 hours following surgery when venous or arterial obstruction can cause rapid changes.

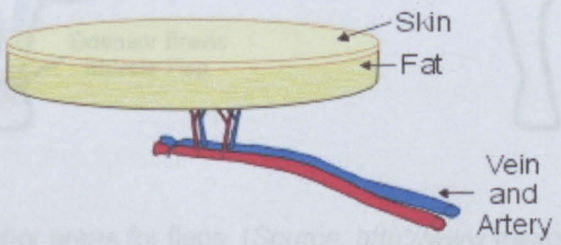

Figure 2.1 – The anatomy of a flap. (*Source: http://www.microsurgeon.org*)

A flap is a unit of tissue, moved from one part of the body (donor site) to another (recipient site), which carries its own nutrition through a pedicle or base by which it remains attached at all stages of transfer (see Figure 2.1). This makes it independent of the vascularity of the defect on which it is placed. In the human body, more than thirty-three donor areas can be chosen as flaps (see Figure 2.2). For

example, fibula bone flap is most commonly used for mandibular reconstruction (Lutz *et al.* 2004) while transverse rectus abdominus myocutaneous flap is the most common flap used for microvascular breast reconstruction (Behnam *et al.* 2003).

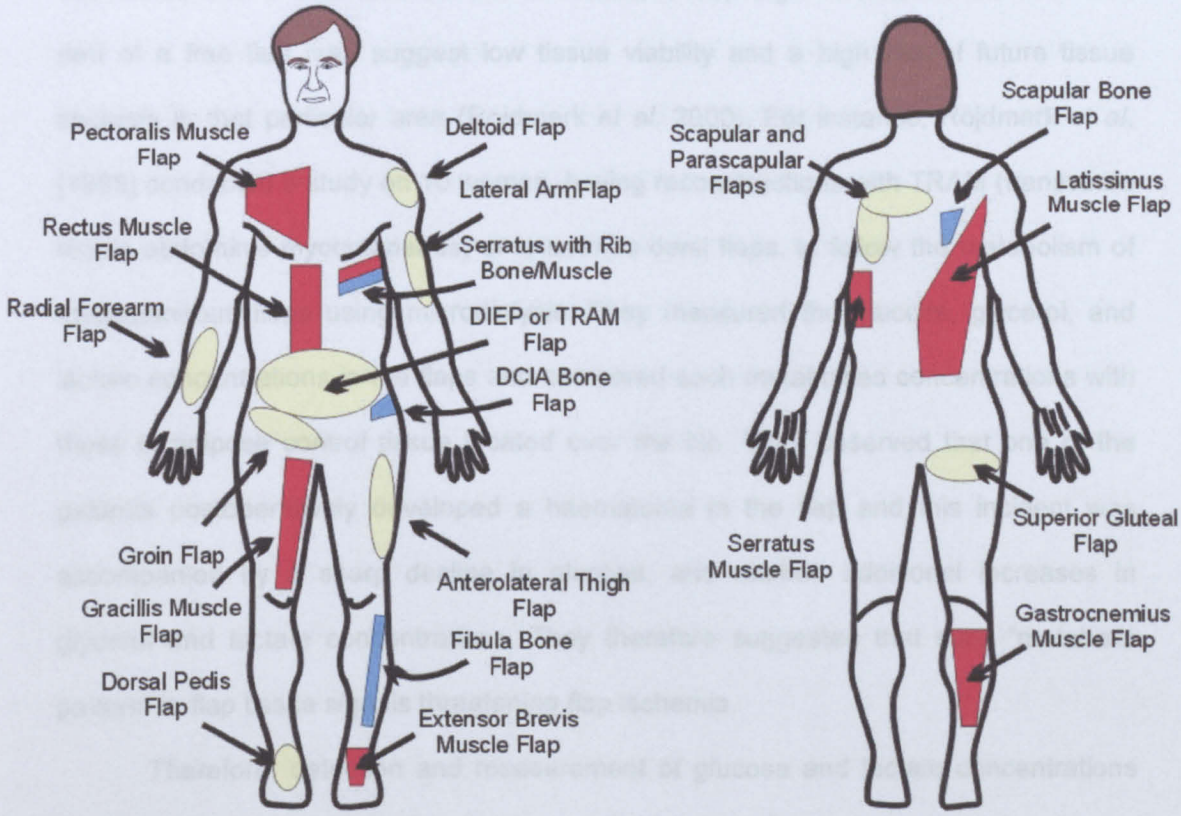

Figure 2.2 – Donor areas for flaps. (*Source: http://www.microsurgeon.org*)

There are many metabolites in a free flap and the monitoring of glucose, lactate, urea and others is of special medical interest as a guide to the metabolic state. However, the most important and valuable metabolites for flap monitoring are glucose and lactate (Edsander-Nord *et al.* 2002, Rojdmark *et al.* 2000, Rojdmark *et al.* 1998). This is because that glucose is a substance of high metabolic importance, the main energy carrier for tissue, and its concentration level can reflect the nutritional supply

condition of a free flap while lactate is produced from glucose by anaerobic metabolism when oxygen is not available and therefore its concentration level can be used to indicate the oxygen supply of a free flap. Decreasing glucose concentration in combination with increasing lactate level, a metabolic pattern which may be typical of complete flap ischemia (Edsander-Nord *et al.* 2002, Rojdmark *et al.* 1998), is associated with arterial and venous occlusions. Also, "high" lactate level in a certain part of a free flap may suggest low tissue viability and a high risk of future tissue necrosis in that particular area (Rojdmark *et al.* 2000). For instance, Rojdmark *et al.* (1998) conducted a study on 10 women, having reconstructions with TRAM (transverse rectus abdominis myocutaneous) or latissimus dorsi flaps, to follow the metabolism of myocutaneous flaps using microdialysis. They measured the glucose, glycerol, and lactate concentrations in the flaps and compared such metabolites concentrations with those in adipose control tissue located over the hip. They observed that one of the patients postoperatively developed a haematoma in the flap and this incident was accompanied by a sharp decline in glucose, and marked additional increases in glycerol and lactate concentrations. They therefore suggested that such "metabolic pattern" in flap tissue signals threatening flap ischemia.

Therefore, detection and measurement of glucose and lactate concentrations will be the starting point of this project.

2.3 TECHNIQUES FOR METABOLITE MONITORING

In recent years, several promising techniques have been evolved for invasive and non-invasive monitoring of glucose or lactate. Invasive techniques include: subcutaneous implantable biosensors (Wilson *et al.* 1992) or a combination of biosensors with microdialysis sampling (Volpe *et al.* 1995). For example, Volpe *et al.* (1995) coupled a microdialysis technique and a flow-through cell assembled with a

lactate amperometric sensor for continuous monitoring of lactate in human subcutaneous tissue and they found a lactate increase during physical exercise with the results correlating well with a reference spectrophotometric procedure. These invasive monitoring techniques require implantation which is associated with biocompatibility problems if the implantation is prolonged. Also, invasive monitoring techniques mentioned above still have a chance of inducing infection at the insertion site and surgical intervention is required. Therefore, non-invasive monitoring is preferred for patients who need to monitor their blood glucose or lactate frequently.

Techniques used for non-invasive monitoring involve either radiation or fluid extraction. With radiation techniques, an energy beam is applied to the body, which is then modified in proportion to the concentration of glucose or lactate in the blood. The blood glucose or lactate concentration is then calculated. The most promising radiation techniques used for non-invasive monitoring include: near infrared (NIR) spectroscopy (Fischbacher *et al.* 1997, Müller *et al.* 1997, Marbach *et al.* 1993, Haaland *et al.* 1992), mid infrared radiation spectroscopy (Malchoff *et al.* 2002), radio wave impedance (Pfutzner *et al.* 2004, Caduff *et al.* 2003) and optical rotation of polarized light (Cameron *et al.* 1999, Cote *et al.* 1992).

With fluid extraction techniques, a body fluid is extracted and measured. The blood glucose or lactate concentration is then calculated. There are two ways for the fluid extraction: Fluid extraction from skin and interstitial fluid harvesting. Usually, interstitial fluid harvesting is classified as "nearly non-invasive" as it can still cause very minimal micro trauma. The most promising techniques for fluid extraction from skin is reverse iontophoresis (Potts *et al.* 2002, Tierney *et al.* 2000, Rao *et al.* 1993).

2.3.1 Near Infrared Spectroscopy

Near infrared (NIR) spectroscopy uses an external light source in the near infrared spectrum, wavelengths from 780 to 2500 nm, to penetrate various types of

tissue. The light passes through or is reflected by a part of the body, and glucose and other parts of the blood and tissue absorb a small amount of the light at each wavelength. The reflected light is analyzed by spectroscopy and is compared to a detection beam (Kajiwara *et al.* 1993, Robinson *et al.* 1992) this can be calibrated against a blood glucose value (Hall and Pollard 1992).

NIR measurements are usually performed at places on the body that are relatively well perfused with blood. For example, the tips of fingers, earlobes, inner lip or oral mucosa. A number of commercial devices (Dream-beam®, Diasensor® and Glucocontrol®) have been introduced based on this principle, however, no or limited scientific *in vivo* studies have been reported. This may be due to variations in sweat, changes in the local blood circulation and/or interference from other body compounds (Guilbault 1988). Therefore, the accuracy of these techniques has found to be only good within a set of well prepared ensemble of patients.

NIR spectroscopy was the first non-invasive glucose monitoring technology reviewed by the Food and Drug Administration (FDA) panel in 1996 (Diabetes test nixed 1996). Although it provides a fast, convenient and easy-to-use blood glucose measurement for patients (Kaiser 1979), it suffers from low sensitivity, limited resolution and insufficient precision (Koschinsky and Heinemann 2001, Klonoff 1997). More importantly, it is not particularly accurate in the physiologic glucose range (Robinson *et al.* 1992, Van Heuvelen 1987). Moreover, it suffers from poor selectivity because NIR can be absorbed by other body substances (Chung *et al.* 1996, Guilbault 1988). Furthermore, measurements may be affected by variables at the measurement site (Wilkins *et al.* 1996), such as skin location, skin and tissue structure, and skin contamination by foreign substances. All these problems create the necessity for frequent recalibration of the NIR spectroscopy for blood glucose monitoring and this resulted in FDA's denial of market approval (Klonoff 1997).

2.3.2 Mid Infrared Radiation Spectroscopy

Mid infrared radiation (MIR) spectroscopy measures natural thermal emissions or body heat, wavelengths from 5000 to 12000 nm. The human body emits thermal radiation or body heat with wavelengths in the MIR spectrum. When the radiation passes out of the body, part of it is absorbed by glucose. The absorption in the "glucose band", around 9400 nm (Back *et al.* 1984), is related to its concentration. The amount of radiation absorbed can be spectroscopically determined by comparing measured and predicted amounts of thermal energy at the skin surface and the difference can be converted into a measure of the blood glucose concentration (Goldstein and Chiang 1985). The problem with using MIR spectroscopy for blood glucose monitoring is the small signal size of human thermal emissions, the limited resolution and insufficient precision (Koschinsky and Heinemann 2001, Klonoff 1997).

2.3.3 Radio Wave Impedance

The radio wave impedance spectrum of glucose can be examined when an alternating current at high frequency (1 – 200 MHz) passes through the blood (Caduff *et al.* 2003). In blood, glucose is the substance present at the highest sugar concentration compared to other solutes. The glucose interacts with the radio wave to attenuate the amplitude and shift its phase. The alternating current is applied to a body part like a finger and the exiting current is compared to the reference current and the difference represents the impedance caused by glucose and other substances. This impedance is proportionate to the glucose concentration and it can be expressed as such. The main difficulty with this technique is that factors other than glucose, such as concentration of electrolytes in the blood, finger width, body temperature and etc, can also affect the impedance. This must be accounted for, to choose the correct

frequency, to determine the relationship between impedance and blood glucose concentration (Caduff *et al.* 2003).

2.3.4 Optical Rotation of Polarized Light

A beam of infrared polarized light can be passed through a body component, such as the ocular aqueous humor being the transparent liquid present between the cornea and the iris which has glucose present in a concentration proportional to that of blood (March *et al.* 1982), and the beam is shifted by an angle proportional to the concentration of glucose (Cote *et al.* 1992). This angle can then be converted to a glucose value. The problem with this technique for blood glucose monitoring is the small signal size (i.e. angle of rotation) due to the small concentration of glucose in the ocular aqueous humor. Therefore, it is necessary to use sensitive detection and software to convert this angle into an actual blood glucose equivalent. Moreover, other optically active substances contribute to the signals, increasing or decreasing the polarization angle, thus compromising the specificity of the technique. Also, there is a delay between blood glucose changes and aqueous humor glucose. Other problems include corneal rotation and eye motion artifact.

2.3.5 Reverse Iontophoresis

The details of reverse iontophoresis technique are described in section 2.6. Reverse iontophoresis involves the application of a micro-current to the skin with the current pulling sodium ions and other ions and charged molecules through the intact skin. Electroosmosis ensures that water and uncharged molecules such as glucose also some through. The glucose concentration in this fluid is proportional to the concentration in blood (Rao *et al.* 1993, Glikfeld *et al.* 1988). This technique is very

promising because of the range of molecules and ions which might be examined if successfully extracted. There are some problems with this technique: (1) a lag time before a blood glucose value can be reported (Potts *et al.* 2002), (2) a low concentration of glucose in the fluid, and (3) skin could be adversely affected by prolonged reverse iontophoresis (Tierney *et al.* 2001, Tierney *et al.* 2000a).

The GlucoWatch® (see Figure 2.3), made by Cygnus Inc. of Redwood City, CA is FDA approved device which can read glucose levels up to three times an hour and can sound an alarm if glucose levels fall too low or rise too high. The manufacturer states that the device has been tested clinically and is as accurate as current glucose monitors (Tierney *et al.* 2001, Tierney *et al.* 2000a, Tierney *et al.* 2000b).

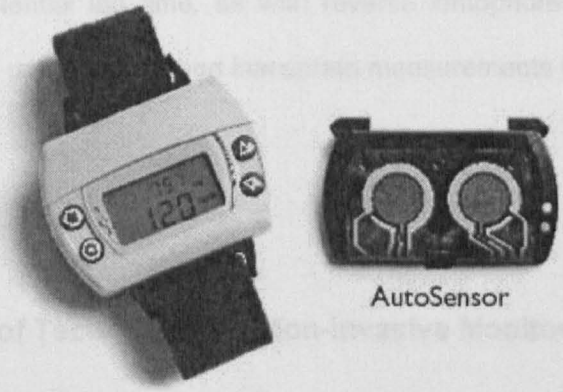

Figure 2.3 – The GlucoWatch® biographer for non-invasive glucose monitoring via reverse iontophoresis. (*Source: http://www.mendosa.com/glucowatch.htm*)

2.3.6 Interstitial Fluid Harvesting

Transcutaneous harvesting of interstitial fluid can be accomplished with nearly no skin trauma and minimal sensation. Therefore, this technology is normally classified not as "non-invasive" but rather as "nearly non-invasive".

A number of recent studies have shown that interstitial fluid can serve as a reliable surrogate for blood in the measurement of physiological glucose (Smith *et al.* 1999, Bantle and Thomas 1997, Klonoff 1997). Interstitial fluid harvesting involves penetration into the superficial layers of the skin (causing very minimal micro trauma) where are almost free of blood capillaries and nerve endings, followed by the extraction of fluid from the superficial layers of the skin, and finally by the measurement of the fluid metabolites concentration. For example, in one hand-held device (LifeGuide, Integ Inc., Minnesota), the skin is penetrated by a hollow needle and a small volume of interstitial fluid is harvested and measured for glucose using far infrared radiation spectroscopy technology. Usually, interstitial fluid harvesting technique uses many microneedles rather than just a single microneedle.

There is a problem with interstitial fluid technology for blood glucose monitoring. Because of the potential lag time, as with reverse iontophoresis technology, some treatment decisions may be based on inaccurate measurements if blood glucose levels are shifting rapidly.

2.3.7 Summary of Techniques for Non-invasive Monitoring of Blood Parameters

Except for the reverse iontophoresis technique and interstitial fluid harvesting technique, all of the non-invasive techniques mentioned above are indirect approaches to monitoring metabolites. Both the reverse iontophoresis technique and interstitial fluid harvesting technique can directly extract metabolites out of the human body through the intact skin and the extracted metabolites can be quantified by various means such as a biosensor.

It has been reported that NIR spectroscopy is not particularly accurate even in the normal physiological range (Robinson *et al.* 1992, Van Heuvelen 1987) and has a

subject-dependent concentration bias (Ward *et al.* 1992). In general, both NIR and MIR spectroscopy techniques have low sensitivity, limited resolution and insufficient precision (Koschinsky and Heinemann 2001, Klonoff 1997). Therefore, they are not suitable for metabolite monitoring. In addition, radio wave impedance techniques can also be affected by many other factors and similarly the optical rotation of polarized light can be influenced by corneal rotation and eye motion.

For the interstitial fluid harvesting technique, it involves penetration into the superficial layers of the skin by microneedles. Although the diameter and height of a single microneedle is respectively small (30 μm – 200 μm) and short (1 mm – 7 mm) (Talbot and Pisano 1998, Lin and Pisano 1999), it still causes a micro trauma on the skin. Normally, interstitial fluid harvesting technique uses many microneedles, rather than only one single microneedle, to extract substance out of body. Therefore, the area for microneedles to penetrate the skin is large and this leads to a large area of micro trauma. For example, 100 microneedles, with each single microneedle with a diameter of 30 μm and height of 1 mm, penetrated into the superficial layers of the skin can result in an area of micro trauma of at least 0.07 mm^2 and a volume of micro trauma of at least 0.07 mm^3. The more the number of microneedles used, the greater is the area and volume of a micro trauma. Therefore, this technique is only nearly non-invasive because it causes micro trauma even though the micro trauma is at the superficial layers of the skin.

Compared with interstitial fluid harvesting, reverse iontophoresis is a truly non-invasive technique as it does not cause micro trauma on the skin. Even though there are some problems for reverse iontophoresis, e.g. lag time of at least 20 minutes from the beginning of a fluid extraction cycle until a blood glucose level can be reported (Potts *et al.* 2002), this technique is accurate and produces multiple measurements over a 24-hour period (Tierney *et al.* 2000). Therefore, reverse iontophoresis was chosen for this study as the preferred non-invasive method for the development of a prototype monitoring system for non-invasive monitoring of glucose and lactate.

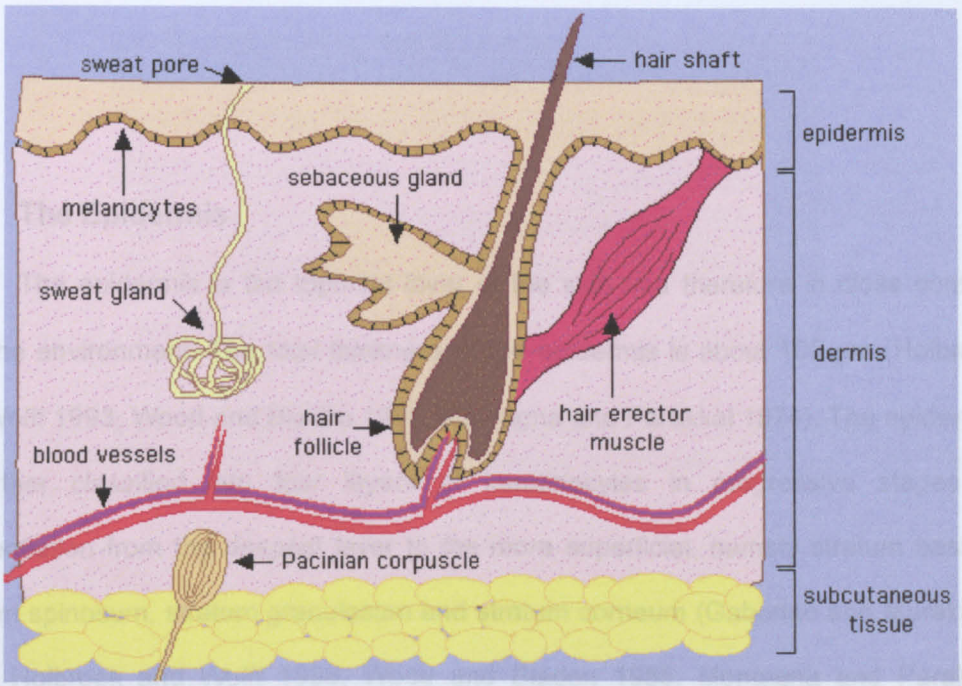

Figure 2.4 – The structure of the skin. (*Source: http:// www.enchantedlearning.com*)

2.4 THE STRUCTURE OF THE SKIN

Because the reverse iontophoresis technique is employed on the skin, basic knowledge on the structure of the skin can help in understanding the pathways of substances extracted through the skin during reverse iontophoresis.

Skin is an important organ system necessary for all mammalian life, forming the boundary between the body and the external world. It is a permselective membrane that, at physiological pH, supports a net negative charge (Burnette and Ongpipattanakul 1987). It serves as a protective barrier against physical and chemical assault. Because of the barrier function of the skin, transdermal extraction or delivery of substances is very difficult. Skin also helps to provide sensory perception, thermoregulation, immunologic surveillance, and control of insensible fluid loss.

Histologically, the skin is a complex three-layered organ (Gaboriau and Murakami 2001, Holbrook and Wolff 1993) with a total thickness of about 4 mm (Wood

and Bladon 1985). The three layers are epidermis, dermis and subcutis (see Figure 2.4).

2.4.1 The Epidermis

The epidermis is the topmost layer of the skin and therefore in close contact with the environment. The total thickness of the epidermis is about 100 μm (Holbrook and Wolff 1993, Wood and Bladon 1985, Montagna and Parakkal 1974). The epidermis is further classified into four layers of keratinocytes in progressive stages of differentiation from the deepest layer to the more superficial, namely stratum basale, stratum spinosum, stratum granulosum and stratum corneum (Gaboriau and Murakami 2001, Holbrook and Wolff 1993, Wood and Bladon 1985, Montagna and Parakkal 1974).

The stratum corneum, a primary protective barrier from the external environment, consists of as many as 25 or more layers of horny skin cells (corneocytes) which are connected via desmosomes (protein-rich appendages of the cell membrane) (Holbrook and Wolff 1993, Montagna and Parakkal 1974). The corneocytes are embedded in a lipid matrix. The stratum corneum lipid content is critical to its retention of water in the skin. It also affects its electronic properties. The structure of the stratum corneum can be roughly described by a "brick and mortar" model (Elias 1983). The corneocytes of hydrated keratin comprise the bricks and the epidermal lipids fill the space between the dead cells like mortar (see Figure 2.5). The stratum granulosum contains 2 to 5 layers of flattened, diamond-shaped cells while the stratum spinosum is made up of 8 to 10 layers of many-sided cells. The stratum basale is composed of a single layer of columnar cells with the basement membrane of the epidermis attached to the dermis.

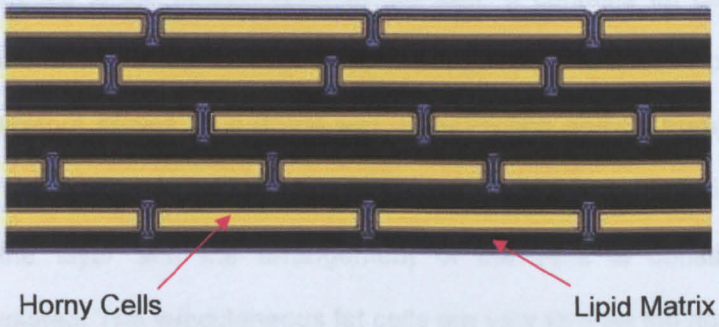

Figure 2.5 – Schematic structure of the stratum corneum according to the brick and mortar model. The horny cells are embedded in a lamellar structured lipid matrix. (*Source: http://www.scf-online.com/*)

2.4.2 The Dermis

The dermis is the middle layer of the skin located between the epidermis and subcutaneous tissue. It is the thickest layer of the skin (about 4 mm) and mainly consists of collagens, elastic fibres and ground substances with blood vessels, lymph nodes, nerves and cells dispersed throughout it (Wood and Bladon 1985).

Collagens are responsible for the structural support of the skin (Wood and Bladon 1985). Elastic fibres are responsible for resisting deformational forces and returning the skin to its resting shape (Wood and Bladon 1985). Ground substances, e.g. hyaluronic acid, chondroitin sulfates and etc, play an important role in skin hydration and help to preserve the tensile elasticity of the skin (Wood and Bladon 1985). Fibroblasts produce and secrete collagen, elastin and other structural molecules necessary for maintaining the overall skin health.

The dermis also contains blood-vessels, sweat glands, sebaceous glands, hair follicles and erector pili muscle.

2.4.3 The Subcutis

The subcutis is the bottom layer of the skin. It contains fat cells as well as nutrients, blood-vessels, sebaceous glands, sweat glands and erector pili muscles for the hairs. It therefore serves as a depot and as protection against bumps (Wood and Bladon 1985). Normally the fat cells are the main component. Their volume, the thickness of the layer and the arrangement of the cells is constitutionally and hormonally regulated. The subcutaneous fat cells are very rare on the nose, the eyelids and the outer ear.

2.5 PATHWAYS OF METABOLITE TRANSPORT THROUGH THE SKIN DURING REVERSE IONTOPHORESIS

In general, a molecule under the influence of electric current through skin can take either an appendageal pathway (i.e. through hair follicles, sweat ducts, and secretary glands) or non-appendageal pathway (i.e. across the stratum corneum: intracellularly and intercellularly) (Riviere and Heit 1997, Singh and Bhatia 1996, Cullander 1992, Schnetz and Fartasch 1991) (see Figure 2.6 & 2.7). Both pathways are in parallel, but the former normally predominates in accordance with the established fact that ions tend to take the path of least resistance (Del Terzo *et al.* 1989, Burnette and Ongipipattanakul 1988, Burnette and Marrero 1986). This has been recently proved by laser scanning confocal microscopy and vibrating probe electrode techniques (Guy 1998).

Non-follicular transport however has been recently identified in playing a significant role in the overall transport of ionic molecules. This route has been identified as the intercellular pathway, which consists of polar regions in the lipid lamella (Jadoul *et al.* 1999). These aqueous pathways are primarily due to the voltage-dependent pore

formation in the stratum corneum and are attributed to the flip-flop movements of polypeptide helices in the stratum corneum.

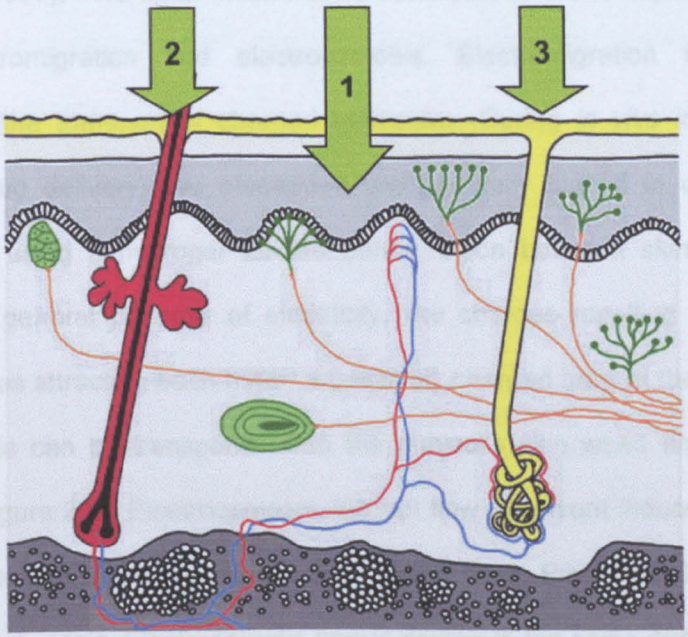

Figure 2.6 – Possible pathways for a penetrant to cross the skin barrier. (1) across the intact horny layer, (2) through the hair follicles with the associated sebaceaous glands, or (3) via the sweat glands. (*Source: http://www.scf-online.com/*)

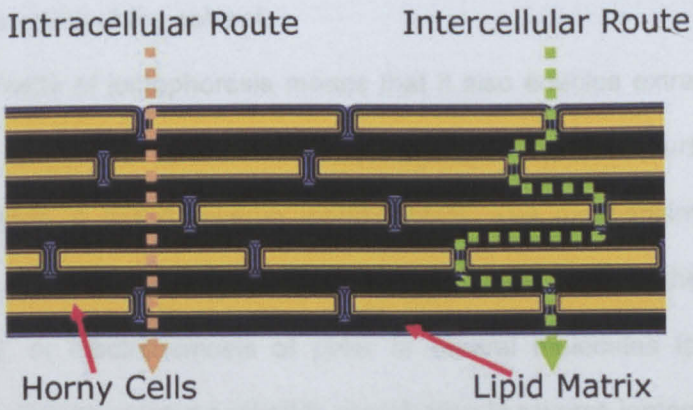

Figure 2.7 – Schematic diagram of the two microroutes of penetration. (*Source: http://www.scf-online.com/*)

2.6 REVERSE IONTOPHORESIS TECHNIQUE

Iontophoresis refers to the passage of a low level of current through a synthetic or biological membrane to promote the transport of both charged and neutral molecules (Merino *et al.* 1997). Two main mechanisms contribute to the iontophoresis, and they are the electromigration and electroosmosis. Electromigration is the primary mechanism in the transport of charged molecules. During *in vivo* iontophoresis for transdermal drug delivery, two electrodes are generally placed in contact with the subject's skin, using a hydrogel for the buffer region between skin and electrode. Based on the general principle of electricity, like charges repelling each other and opposite charges attracting each other, a positively charged drug at the hydrogel of the anode electrode can be transported into the subject's skin when an electric field is applied (see Figure 2.8). Electroosmosis, the net flow of solvent induced by the flow of ions across the skin under an electric field (Pikal 1990; Pikal and Shah 1990), also enhances iontophoresis. Electroosmotic flow is always in the same direction as the flow of counter ions. Since human skin is negatively charged under physiological conditions (Burnette and Ongpipattanakul 1987), the counter ions are cations and the electroosmotic flow is thus from anode to cathode (Pikal 2001, Guy *et al.* 2000) (see Figure 2.8). Thus, the transport of both charged and uncharged molecules is enhanced by the convective action of the solvent.

The symmetry of iontophoresis means that it also enables extraction of solute molecules from within the subdermal compartment to the skin surface, and this extraction technique is called reverse iontophoresis. The mechanism of extraction mainly involves either electromigration of charged molecules to the electrode of opposite polarity, or electroosmosis of polar or neutral molecules to the cathode. Passive diffusion also provides a negligible contribution to reverse iontophoresis.

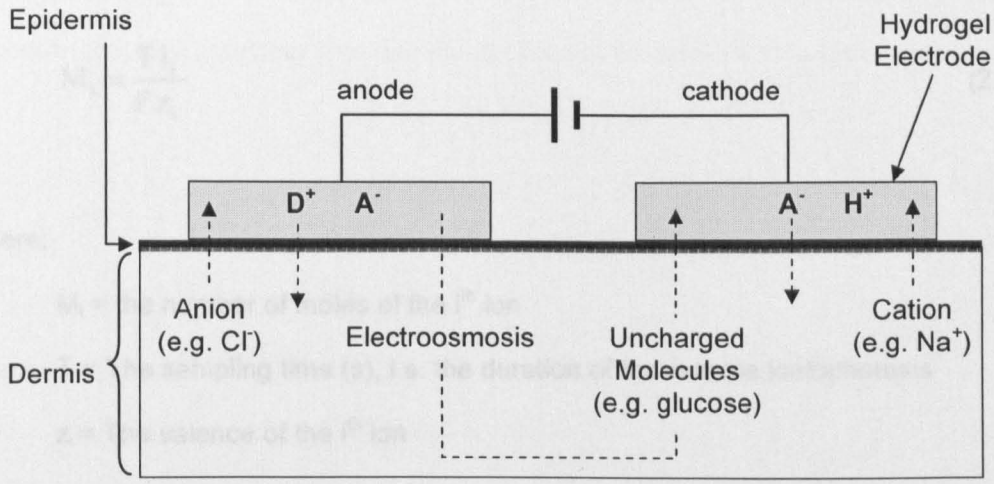

Figure 2.8 – Schematic illustration of the drug molecule delivery using iontophoresis. D^+ is a positively charged drug. A^- in the anode electrode is the counterion of the positively charged drug. Both H^+ and A^- in the cathode electrode are buffer ions. Both Cl^- and Na^+ are primary anion and cation components of the extracellular fluid of the skin, respectively. Electroosmosis enhances uncharged molecules moving to cathode.

2.6.1 Mechanisms of Transport during Reverse Iontophoresis

The total flux of a solute during reverse iontophoresis is the sum of electromigration, electroosmosis, and passive diffusion. However, the contribution of passive diffusion on the total flux is extremely small compared to either electromigration or electroosmosis, and therefore the passive flux contribution can normally be neglected.

Electromigration: Electromigration is the movement of small ions across the skin under the direct influence of the electric field. Electron fluxes are transformed into ionic fluxes via the electrode reactions; and ionic transport proceeds through the skin to maintain electroneutrality (Phipps and Gyory 1992, Sage and Riviere 1992, Burnette 1989). Faraday's law applies to steady-state transport and relates the number of ions crossing the membrane to the electric current, the time of current passage and the charge per ion (Sage and Riviere 1992, Burnette 1989):

$$M_i = \frac{T i_i}{F z_i} \qquad (2.1)$$

where:

M_i = the number of moles of the i^{th} ion

T = The sampling time (s), i.e. the duration of the reverse iontophoresis

z_i = The valence of the i^{th} ion

F = Faraday's constant

i_i = The current (A) carried by the i^{th} species

Current passage sets in motion a number of ions across the skin, and all of them compete to carry a fraction of the current. The contribution of each ion to charge transport is called its transport number:

$$t_i = \frac{i_i}{I} \qquad (2.2)$$

where:

t_i = The transport number of the i^{th} ion

I = The total current passage (A)

Substituting Equation 2.2 into Equation 2.1 gives:

$$M_i = \frac{t_i I T}{F z_i} \qquad (2.3)$$

The extraction flux of each ion is defined by the ratio of the number of moles transported to the sampling time (i.e. the duration of the reverse iontophoresis):

$$J_{EM} = \frac{M_i}{T} = \frac{t_i}{Fz_i} I \qquad (2.4)$$

where:

J_{EM} = The extraction flux of each ion (mol s^{-1})

As reported by Phipps and Gyory (1992), the transport number of the ion of interest (the i^{th} ion) may also be expressed as follows:

$$t_i = \frac{c_i z_i u_i}{\sum_{j=1}^{n} (c_j z_j u_j)} \qquad (2.5)$$

where:

c_i = The concentration (mol cm^{-3}) of the i^{th} ion

z_i = The valence of the i^{th} ion

u_i = The mobility (cm^2 s^{-1} V^{-1}) of the i^{th} ion

c_j = The concentration (mol cm^{-3}) of each of the "n" ions in the system

z_j = The valence of each of the "n" ions in the system

u_j = The mobility (cm^2 s^{-1} V^{-1}) of each of the "n" ions in the system

Given that sodium ion (Na^+) and chloride ion (Cl^-) are the principal extracellular electrolytes present in the body at high concentrations, they will invariably carry a major part of the current during reverse iontophoresis *in vivo*.

As shown in Equation 2.3, iontophoretic extraction is determined by the total current passage for the reverse iontophoresis, the duration of the reverse iontophoresis, the charge and the transport number of the ion of interest. The total current passage is directly and easily controlled by the power supply but is limited, for safety reasons and practical purposes *in vivo*, to not more than 0.5 mA/cm^2 (Brand and Iversen 1996, Ledger 1992). The duration of each extraction must be sufficiently long to ensure that sufficient analyte is available for detection but not so long that clinically significant changes in the systemic concentration may have occurred.

Electroosmosis: Electroosmosis is the principal transport mechanism of uncharged molecules (Pikal 1992). The skin is negatively charged at physiological pH (Burnette and Ongpipattanakul 1987), and acts therefore as a permselective membrane to cations. This preferential passage of counterions induces an electroosmotic solvent flow that carries neutral molecules in the anode-to-cathode direction.

There are two important characteristics of this mechanism of electrotransport. They are that the solvent volume flow (i.e. volume × time^{-1} × area^{-1}) is proportional to the potential gradient across the skin (Pikal 1992 & 1990, Burnette and Ongpipattanakul 1987) and that the electroosmotic flux of solute is independent of molecular size (Pikal 1992 & 1990). As reported by Pikal and Shah (1990), the electroosmotic flux contribution to the transport of a solute "s" present in the anodal compartment at a molar concentration is:

$$J_{EO} = J_{vs}\, c_s \qquad (2.6)$$

where:

J_{EO} = The electroosmotic flux of the solute "s"

J_{vs} = The solvent volume flow ($\mu l\ h^{-1}\ mA^{-1}$)

c_s = The molar concentration of the solute "s"

As well as the current density, the pH and the ionic strength are electrode formulation parameters that may modulate electroosmosis (Santi and Guy 1996). Altering the pH on either side of the skin can change the skin's permselectivity and hence may change the direction of the electroosmotic flow (Santi and Guy 1996). Practically speaking, only the surface pH (i.e. the pH of the electrode formulation) can be altered *in vivo*, of course.

By lowering the ionic strength of the electrode formulation, electroosmotic flow can be increased for cathodal extraction (Santi and Guy 1996, Merino *et al.* 1999). For anodal extraction, this phenomenon is less obvious (Santi and Guy 1996). However, it is important that a finite level of electrolyte must be present in the electrode chambers, particularly at the anode, to support the Ag/AgCl electrochemistry.

Passive diffusion: The principle of diffusion is the flux of a chemical species from an area of high concentration to an area of low concentration. According to Fick's first laws of diffusion, the net flux of solute "j" across a permeable surface in a given time is proportional to the difference in the concentrations between the species (Eddowes 1990):

$$J_P = D_j \frac{\delta c_j}{\delta h} \qquad (2.7)$$

where:

J_P = The passive diffusion flux of the solute "j"

D_j = The aqueous diffusivity of the solute "j"

$\frac{\delta c_j}{\delta h}$ = The concentration gradient of the solute "j" across the skin

As shown in Equation 2.7, the rate of diffusion is dependent on the difference in concentration between the 2 regions, the greater the difference in concentration, the faster the rate of diffusion.

The dominant mechanism (electromigration or electroosmosis):

Electromigration is clearly the principal mechanism for small mobile ions, whereas for neutral, polar substances, electroosmosis dominates as there is no electromigration possible from the electrode. Both electromigration and electroosmosis depend upon the applied current (Padmanabhan *et al.* 1990, Phipps *et al.* 1989), with the effect being less marked for electroosmosis (Delgado-Charro and Guy 1994, Burnette and Ongpipattanakul 1987). As the size of an ion increases, the mobility of the ion is therefore reduced and this results in electromigration being compromised. Therefore, for cations, the dominant mechanism switches from electromigration to electroosmosis with increasing the size of ions (Guy *et al.* 2001).

2.6.2 Applications of Reverse Iontophoresis in Human Medicine

Although used since the latter half of the 19th Century, iontophoresis is only now being studied systematically for its application in human medicine to the fields of drug delivery, non-invasive diagnosis and patient monitoring. Iontophoresis provides a means of local, non-invasive, painless drug administration when compared with the traditional administration of a drug by needle insertion. Importantly, iontophoresis can be used to deliver peptides and protein drugs not suitable for oral administration (Green *et al.* 1992). Schmidt *et al.* (1995) treated 18 women, who had acne scars, with estriol iontophoresis and 28 subjects (9 men and 19 women), who had atrophic acne

scars, with tretinoin iontophoresis twice weekly for a period of 3 months. They found that both iontophoresis treatments were clinically effective in decreasing acne scars.

Merino *et al.* (1999) have recently demonstrated the possibility of measuring systemic phenylalanine levels, using reverse iontophoresis, which is useful for diagnosing phenylketonuria, a potentially fatal metabolic disease in infants of missing an enzyme to biotransform phenylalanine. Reverse iontophoresis also offers some promise for developing a skin sensitivity testing system that measures prostaglandin E2 (PGE2) levels through the skin (Mize *et al.* 1997). Mize *et al.* (1997) monitored PGE2 in response to the transdermal delivery of irritant drugs (chlorpromazine, chloroquine, promazine, tetracaine and metoclopramide), and they reported that a significant increases in PGE2 (monitored non-invasively by reverse iontophoresis), which is generated in response to transdermally applied drug irritants, were observed that correlated well with more classic determinations of irritation (e.g., the Draize test, lesion score). Very recently, the extraction of urea by reverse iontophoresis has been performed in 17 patients (21–35 years) with impaired kidney function (Degim *et al.* 2003). Urea was extracted by electroosmosis to the cathode by current application for 5 minutes at the current density of 0.1 mA cm^{-2}. The extracted amounts correlated well with urea levels in the blood (r^2 = 0.88). This gives some promise for developing a system to determine when dialysis should be performed in pediatric patients with kidney disease.

Topically, the most successful iontophoresis application for patient monitoring has been non-invasive blood glucose detection (Potts *et al.* 2002, Tierney *et al.* 2001, Rao *et al.* 1995). Rigorous control of blood glucose levels through a combination of frequent glucose measurements and insulin injections can reduce the occurrence of long term complications in type I diabetes. However, the current monitoring methods, mainly finger-stick sampling, for repetitive blood glucose measurement are painful, aesthetically unpleasant and inconvenient. This provides considerable impetus for the development of non-invasive methods for monitoring blood glucose. Following initial

feasibility studies (Rao *et al.* 1995, 1993), it has now been shown in diabetics that reverse iontophoresis can non-invasively monitor blood glucose levels as efficiently as the currently-used finger-stick sampling (Tamada *et al.* 1995).

2.6.3 Factors Affecting Reverse Iontophoresis

Because of the perfect barrier properties of the epidermis, not all metabolites can be transdermally extracted out of the human skin. There are size limitations of ions and molecules in transdermal reverse iontophoresis and this is governed by the pore size of the human skin. The skin pores sizes are estimated to be in the region of 10 – 25Å. For metabolites with molecular size smaller than the pore size of the human skin, it was found that the permeability coefficients of a series of positively charged, negatively charged and uncharged solutes across excised human skin are a function of molecular size (Yoshida and Roberts 1993). When the molecular size increases, the permeability coefficient decreases (Yoshida and Roberts 1993).

Recently, work has been carried out to optimise the efficiency of reverse iontophoresis on the transport of molecules. Optimisation of reverse iontophoresis across skin has focussed on several parameters in the system which can be adjusted such as the pH (Santi and Guy 1996) of the external skin buffer, current strength (Santi and Guy 1996) and variation of the waveform of the applied current (Tomohira *et al.* 1997, Santi and Guy 1996, Hirvonen *et al.* 1995).

pH: The pH is of importance for the reverse iontophoresis. Hydrogen and hydroxyl ions are the two ionic species inherently present in the external skin buffer and the skin. The effect of pH of the external skin buffer on reverse iontophoresis has been investigated by Santi and Guy (1996). They used a vertical diffusion cell, in which both electrode chambers are located on the epidermal side of the hairless mouse skin as shown in Figure 2.9, to study the effect of the pH of the electrode chamber buffer on

electroosmotic flow during reverse iontophoresis. They found that cathodal extraction was enhanced by increasing the pH of the electrode chamber buffer while lowering the pH could facilitate the anodal extraction (see Figure 2.10). Under physiological conditions, with the external skin buffer set at 7.4 approximately, the membrane has a net negative charge and electroosmotic flow is from anode to cathode (Pikal 1990, Pikal and shah 1990, Burnette and Ongpipattanakul 1987). Because the isoelectric point of the skin is about 4, at higher pH, the negative charge density of the skin increases and this further enchances the electroosmotic flow from anode to cathode. However, at lower pH, the negative charge density of the skin decreases and this reduces the electroosmotic flow from anode to cathode. That is the reason why Santi and Guy (1996) found a higher cathodal extraction at higher pH and higher anodal extraction at lower pH.

However, the practical application of this strategy, that is to employ electrode solution of specific pH, is limited. This is because that the skin will not tolerate extremes of pH for anything but the shortest period before showing signs of inflammation. However, at least, there is the potential to use different pH solutions in the anode and cathode to maximize electroosmotic flow into each.

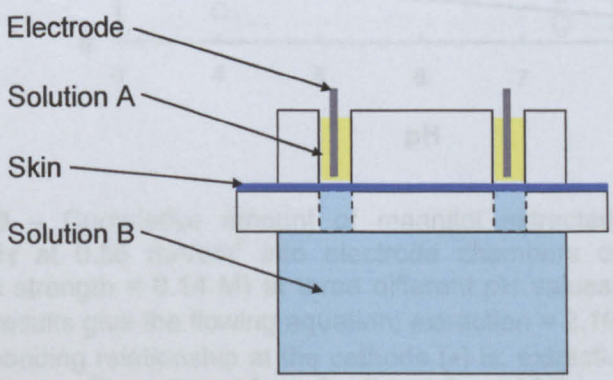

Figure 2.9 – Schematic diagram of a vertical diffusion cell.

In the clinical situation, the external skin buffer is normally set to pH 7.4 (physiological pH), because pH of the external skin buffer set too high or too low can cause skin irritation. In this study, glucose is extracted out of the human skin for monitoring. Because glucose is an uncharged molecule, it is extracted mainly by electroosmosis. Therefore, glucose is extracted to the cathode if the external skin buffer is set to a value equal to or higher than the physiological pH. According to the finding reported by Santi and Guy (1996), higher cathodal extraction can be achieved by setting the external skin buffer at higher pH. Therefore, in order to get a higher glucose extraction at the cathode without causing skin irritation, the external skin buffer is set to pH 7.4 in this study.

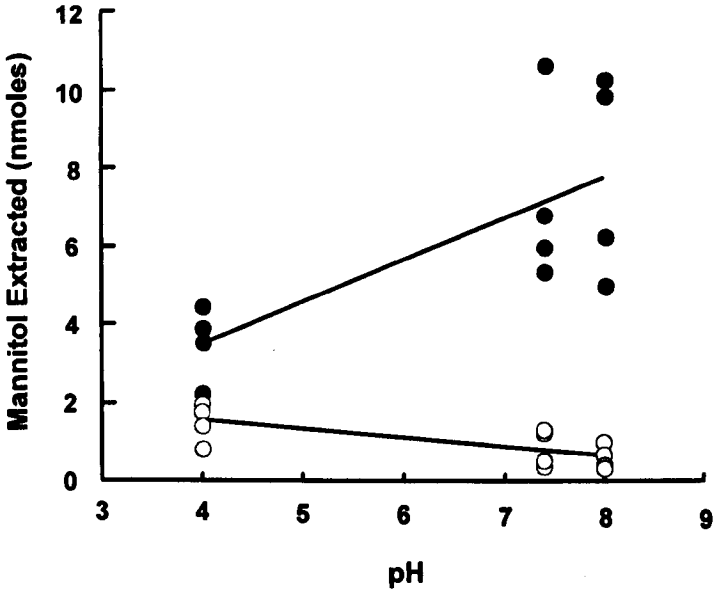

Figure 2.10 – Cumulative amount of mannitol extracted during 2 h of reverse iontophoresis at 0.56 mA/cm^2 into electrode chambers containing Hepes-buffered saline (ionic strength = 0.14 M) at three different pH values. Linear regression of the anodal (O) results give the flowing equation: extraction = 2.19 – 0.17·pH, with r^2 = 0.61. The corresponding relationship at the cathode (•) is: extraction = -0.98 + 1.13·pH, with r^2 = 0.73. (*Source: Reproduced from Santi and Guy 1996*)

Current strength: Based on Equation 2.4, there is a linear relationship between the observed flux of a number of compounds and the applied current. The higher the applied current, the higher is the observed flux.

However, the maximum strength of the current that can be used is limited by human safety consideration, and the upper limiting value of current has been suggested to be 0.5 mA/cm^2 (Brand and Iversen 1996, Ledger 1992). Delgado-Charro and Guy (1994) reported that the efficiency of electroosmotic flow is only weakly dependent upon current density in the range of 0.14 – 0.55 mA/cm^2. Santi and Guy (1996) reported that amount extracted by 0.3 mA/cm^2 has no significant different with the amount extracted by 0.5 mA/cm^2 although amount extracted by 0.5 mA/cm^2 is a little bit more than that by 0.3 mA/cm^2. Therefore, based on the information mentioned above, current density of 0.3 mA/cm^2 is used in this study so that it is adequate enough to extract glucose out of the human skin without causing skin irritation and it is safe to the human.

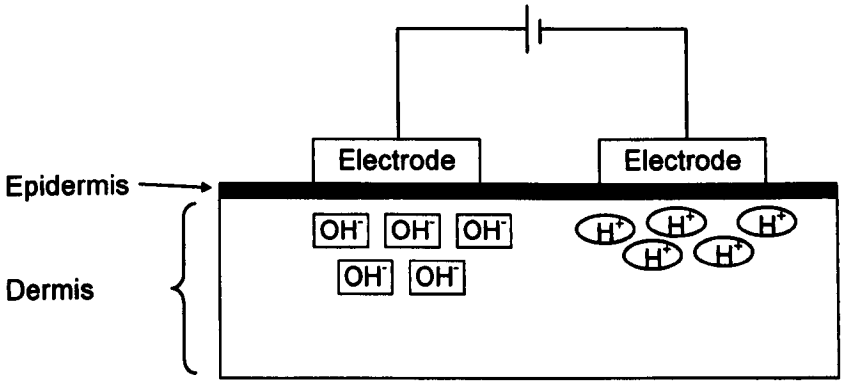

Figure 2.11 – Schematic illustration of the polarization of skin during constant direct current iontophoresis. OH^- is the hydroxyl ion and H^+ is the hydrogen ion.

Current waveforms: Hydrogen and hydroxyl ions are the two ionic species inherently present in the skin. Use of constant direct current (DC) may localise hydrogen ion at the cathodal skin region and hydroxyl ion at the anodal skin region (see Figure 2.11) and this can cause a polarization of the skin which leads to stinging and erythrema (Howard *et al.* 1995). Such skin polarization can be overcome by using pulsed DC (Chien *et al.* 1990, Chien *et al.* 1987), which is a constant DC delivered periodically. During the "off time"", the skin naturally gets depolarized by itself and returned to its near initial electric condition. Skin polarization can also be overcome by using bipolar current (Tomohira *et al.* 1997, Howard *et al.* 1995), which is a constant DC changed its current flow direction periodically. For example, when constant DC flows from electrode A (anode) to electrode B (cathode), hydroxyl ion is localised at skin with electrode A and hydrogen ion is localised at skin with electrode B. Once the direction of current flow is reversed, that is current flowing from electrode B (anode) to electrode A (cathode), hydrogen ion is localised at skin with electrode A and hydroxyl ion is localised at skin with electrode B. This process therefore helps to depolarise the skin.

Tomohira *et al.* (1997) used an *in vivo* rat abdominal skin model to study the effect of electrode polarity switching (i.e. bipolar DC current profile) in iontophoresis of insulin and calcitonin. They found that bipolar DC current profile could enhance the absorption of the insulin and calcitonin.

Hirvonen *et al.* (1995) used a vertical diffusion cell (see Figure 2.9) with mouse skin to study the impact of different applied current profiles in regulating the permeation of two charged amino acids, lysine and glutamic acid. They found that bipolar current profiles and constant DC current profile resulted in comparable transport rates which are higher than that of pulsed DC current profile. Therefore, in order to achieve a high transport rate, it is better to use bipolar current profile or constant DC current profile rather than pulsed DC current profile. However, constant DC is thought to cause a polarization of the skin which leads to stinging and erythrema (Howard *et al.* 1995).

Therefore, bipolar current profile is used in this study as it can provide a high transport rate and reduce skin irritation.

At present, little has been reported about the effect of bipolar current profiles on iontophoresis (Tomohira *et al.* 1997, Hirvonen *et al.* 1995). In order to get a better understanding of the effect of a bipolar current profile on iontophoresis, the present study has focused long duration bipolar DC (i.e. passage of constant current with the polarity of electrodes reversing at different time intervals in the range of several minutes). Three different time interval conditions were tested using a pre-clinical, model iontophoresis system to select the optimum conditions for extraction of glucose and lactate. The results were used to design an iontophoresis device which was tested in healthy volunteers for the transdermal extraction of glucose and lactate.

2.7 DEVICES FOR REVERSE IONTOPHORESIS

Nowadays, many iontophoresis devices are commercially available in the market. Major companies that are involved in the development of iontophoresis devices include IOMED Inc. (Salt Lake City, Utah), Empi Inc. (St Paul, Minnesota), Life-Tech Inc. (Houston, Texas), Cygnus Inc. (Redwood City, California) and etc. (see Table 2.1).

Hypothetically, an iontophoresis device can be utilised in the field of reverse iontophoresis for transdermal extraction of substances as both iontophoresis and reverse iontophoresis techniques require the application of a low level constant current to transdermally deliver drugs or extract metabolites. An Iontophoresis device is generally used with a battery as the power supply and this reduces the chances of electric shocks, thus increasing patient compliance and acceptability.

Table 2.1 – Iontophoresis products listed by manufacturer.

Manufacturer	Commercial Name / System	Production Status	Disease / treatment	Power supply	Current mode	Reference
Cygnus Inc.	GlucoWatch®	On the market	Glucose monitoring system based on reverse iontophoresis	Battery		- Panchagula *et al.* 2000 - Website 1
EMPI Inc.	Dupel® Iontophoresis system	On the market		Battery	Two channel DC	- Website 2
General Medical Co.	Drionic® Device	On the market	Hyperhidrosis treatment	Battery		- Website 3
Hidrex GmbH	1. Hidrex GS 2. Hidrex PS	On the market	Hyperhidrosis treatment	Battery or mains	1. DC 2. Pulsed DC	- Website 4
IOMED Inc.	Phoresor® Dose Controller (PM 850 & 900)	On the market		Battery	DC	- Website 5
Life-Tech Inc.	- Microphor® Model 6121 - Iontophor® Model 6111PM/DX	On the market		Battery	Two channel DC	- Website 6
Optis	Eyegate II, Ocular applicator and device	C.E. marked and about to be commercialised		Battery		- Halhal *et al.* 2004 - Website 7
R.A. Fischer Co.	MD-1a Galvanic Unit	On the market	Hyperhidrosis	Mains	DC	- Website 8
Vyteris Inc.	Pre-filled lidocaine patch and preprogrammed microcomputer	On the market	Dermal anesthesia	Battery		- Kalia *et al.* 2004 - Website 9
Wescor	Macroduct® Sweat collection system Model 3700	On the market	Diagnosis of cystic fibrosis	Battery		- Website 10

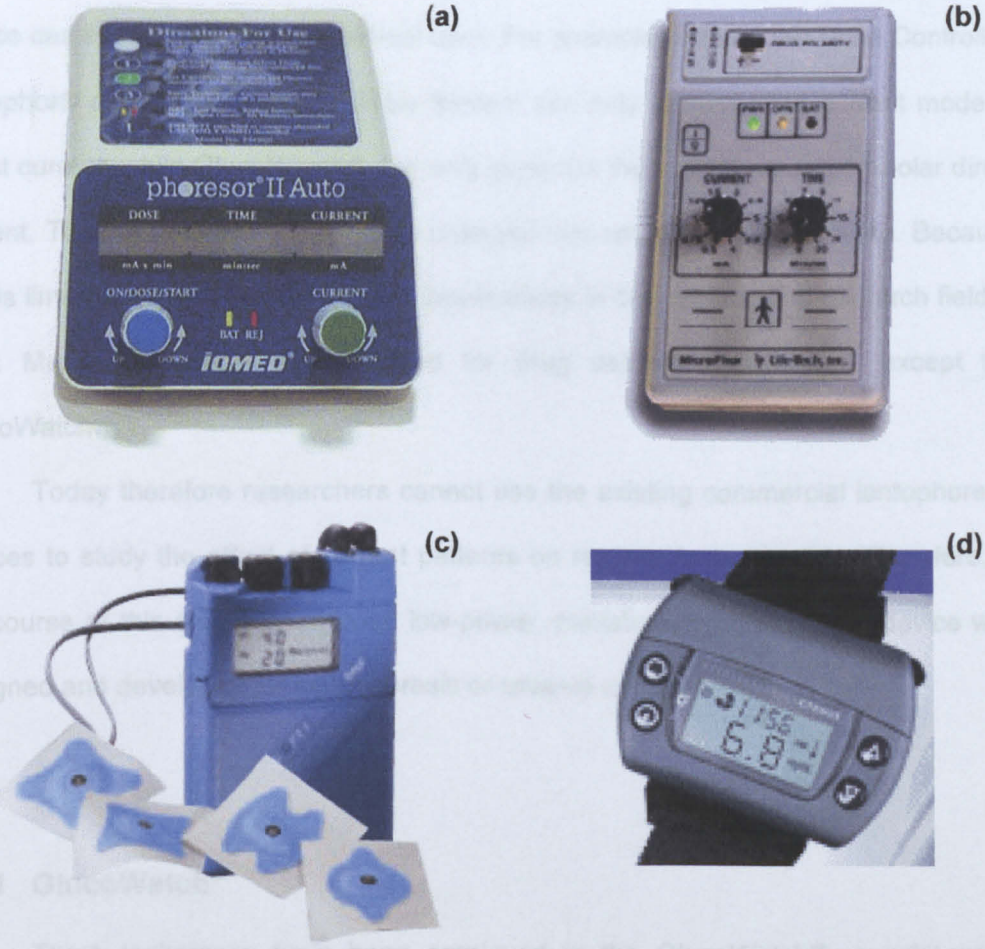

Figure 2.12 – Iontophoresis devices available in the commercial market. (a) Phoresor® Dose Controller (PM850, IOMED, Inc., UT) (*Source: http://imwellness.com/electrotherapy.htm*). (b) Microphor® (model 6121, Life-Tech, Inc., TX) (*Source: http://www.life-tech.com/pns/fr_index.html?/pns/ab1.html*). (c) Dupel® Iontophoresis System (EMPI CANADA, CN) (*Source: http://www.empi.com/products/ionto/DupelDoc.pdf*). (d) GlucoWatch® (Cygnus Inc, California) (*Source: http://www.glucowatch.com/uk/professional/index.html*).

Although there are many iontophoresis devices available in the commercial market (see Figure 2.12), such as Phoresor® Dose Controller (PM850, IOMED, Inc., UT), Microphor® (model 6121, Life-Tech, Inc., TX), Dupel® Iontophoresis System (EMPI CANADA, CN) and GlucoWatch® (Cygnus Inc, California), the only device to have been utilised for reverse iontophoresis is the GlucoWatch® (see section 2.7.1 for a full explanation of the mode of action of this device). More importantly, many of them

are non-programmable (i.e. preset programs, particularly the current mode, of the device can not be amended for clinical use). For example, Phoresor® Dose Controller, Iontophor® and Dupel® Iontophoresis System can only generate the current mode of direct current, while GlucoWatch® can only generate the current mode of bipolar direct current. Their current mode cannot be changed into any other current mode. Because of this limitation, they have had limited applications in the medical and research field to date. Mostly they have been utilised for drug delivery applications, except the GlucoWatch®.

Today therefore researchers cannot use the existing commercial iontophoresis devices to study the effect of current patterns on reverse iontophoresis. Therefore, in the course of this study, a low-cost, low-power, miniature, programmable device was designed and developed for iontophoresis or reverse iontophoresis.

2.7.1 GlucoWatch®

Three techniques have been employed in the GlucoWatch®, a wrist-watch device, and they are the reverse iontophoresis for glucose sample extraction, biosensing techniques for glucose sample measurement, and data verification and conversion leading to a display of the glucose reading.

A hydrogel pad is used as the conducting contact between the GlucoWatch® and the skin, and also to collect the extracted fluid. The Hydrogel pad used in the GlucoWatch® is composed of an aqueous salt solution in a cross-linked polymer which contains glucose oxidase to break down glucose in creating hydrogen peroxide (Kurnik *et al.* 1998).

A diagram of the electrode configuration of the GlucoWatch® is shown in Figure 2.13a. There are 2 separate pairs of circular array electrodes on the base of the GlucoWatch® and each electrode contains a ring shaped reverse iontophoresis electrode and a disc shaped sensing electrode as shown in Figure 2.13b. The sensing

electrode is made from platinum and is activated by the application of a potential of 0.3 – 0.8 V related to a silver-silver chloride reference electrode (Kurnik *et al.* 1998).

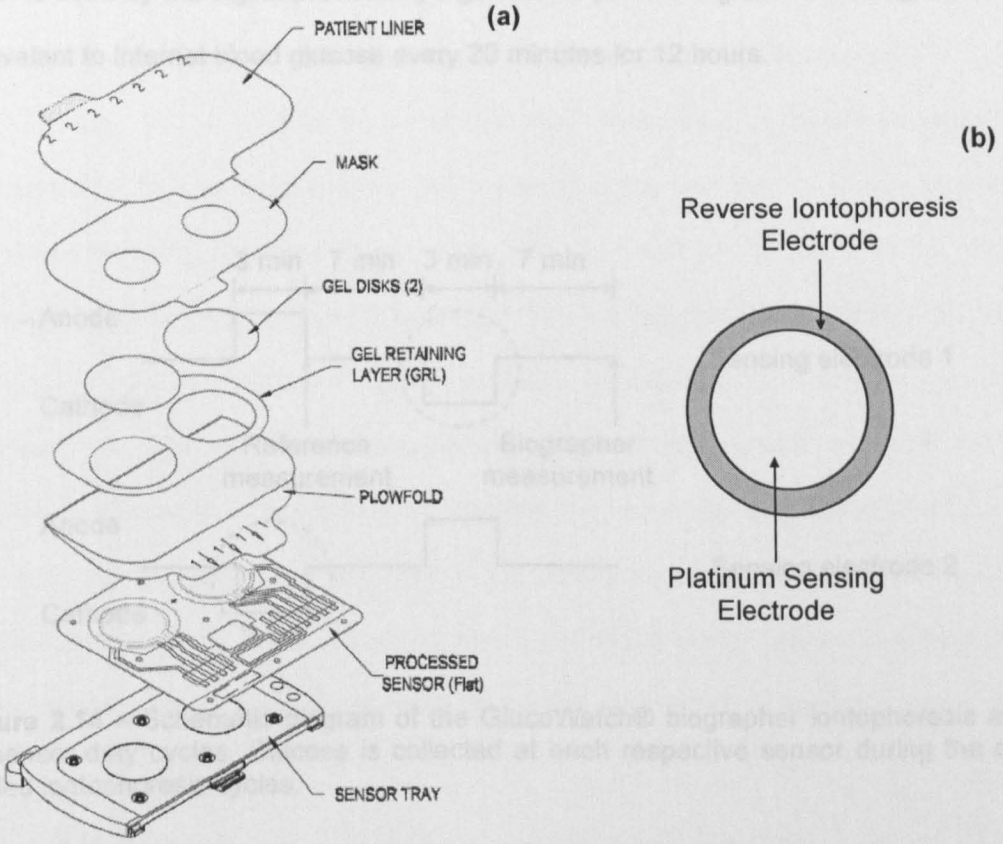

Figure 2.13 – (a) Electrode configuration illustrating how disposable part of the GlucoWatch® Biographer is composed using iontophoresis electrodes, sensing electrode, hydrogel pads and glucose mask (*Source: Tierney et al. 2001*). (b) Electrode array on the base of the GlucoWatch® Biographer. The outer ring is used to extract fluid from the body and the inner electrode is used to detect hydroxide peroxide.

The working principle of the GlucoWatch® is summarised in Figure 2.14. Reverse iontophoresis (iontophoresis current = 0.3 mA) is applied for 3 minutes to collect glucose (about 50 – 500 picomol of glucose will be extracted) then reverse iontophoresis is subsequently stopped and the sensing electrode is activated for 7 minutes to convert the hydrogen peroxide. The polarity of the iontophoresis current is

then reversed and the process is repeated. The integrated currents of the two sensing electrodes are summed and input to a signal processing algorithm (Kurnik *et al.* 1999). A single finger-stick blood glucose measurement is performed after 3 hours of wearing the device to provide a one-point calibration of the system. After that, the calibration factor is used by the signal processing algorithm to provide a glucose reading which is equivalent to internal blood glucose every 20 minutes for 12 hours.

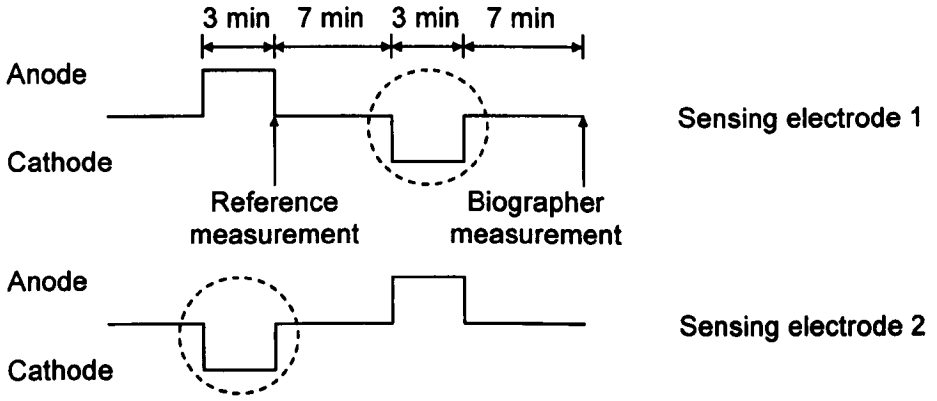

Figure 2.14 – Schematic diagram of the GlucoWatch® biographer iontophoresis and biosensor duty cycles. Glucose is collected at each respective sensor during the dot circled iontophoresis cycles.

2.8 ELECTRODES FOR REVERSE IONTOPHORESIS

Electrodes are very important for reverse iontophoresis and they can be classified as polarizable or non-polarizable electrodes. For an ideally polarizable electrode, it behaves like a capacitor and there is no actual charge transfer across the electrode-electrolyte interface when current is applied. That is, the potential of the electrode will change significantly from its equilibrium potential with the application of even a small current density. The reason for this behaviour is that the electrode reaction is inherently slow (has a small exchange current density). An example of a material that approximates a polarizable electrode is platinum.

For an ideally non-polarizable electrode, it is not easily polarizable and current passes freely across the electrode-electrolyte interface. That is, the potential of the electrode will not change significantly from its equilibrium potential with the application of even a large current density. The reason for this behaviour is that the electrode reaction is inherently fast (has a large exchange current density). An example of a material that approximates a non-polarizable electrode is silver-silver chloride.

Phipps *et al.* (1989) demonstrated the importance of electrode material selection in optimizing drug delivery by investigating the transport of lithium across a polyvinyl alcohol hydrogel membrane. They used platinum as the anode in the donor compartment and this caused a pH decrease from 5.9 to 2.6 after 6 hours at 1 mA. The decrease in pH was attributed to the oxidation of water to form oxygen gas and hydrogen ion. The increased presence of hydrogen ions coupled with their faster mobility as compared to the lithium ion resulted in a lithium delivery efficiency of about only 20% of total lithium. It is well known that polarizable electrodes cause electrolysis of water leading to pH shifts caused by hydrogen ions at the anode and hydroxyl ions at the cathode, whereas non-polarizable electrodes overcome this problem:

At anode: $2\ H_2O\ (l) \longrightarrow O_2\ (g) + 4\ H^+\ (aq) + 4\ e^-$ $E° = -1.23V$

At cathode: $2\ H_2O\ (l) + 2\ e^- \longrightarrow H_2\ (g) + 2\ OH^-$ $E° = -0.83V$

Overall reaction: $2\ H_2O\ (l) \longrightarrow 2\ H_2\ (g) + O_2\ (g)$ $E° = -2.06V$

Since the process of reverse iontophoresis is pH sensitive (Santi and Guy 1996) and it desirable to maintain near neutral pH for substances in contact with skin, non-polarizable electrodes are recommended to be used on the field of reverse iontophoresis. In this study, silver-silver chloride electrodes were used because they

are capable of delivering significant current without inducing changes in the pH of the bathing solutions (Jahn 1900). This is because that the redox potential for this system is lower than for water enabling electroneutrality to be maintained at anode and cathode. During reverse iontophoresis, silver at the anode oxidizes under the applied potential and reacts with chloride ion to form insoluble silver chloride. On the other hand, at the cathode, the reduction of the silver chloride to silver metal liberates chloride ion. Therefore, electrochemical reactions do not involve electrolysis of water and pH changes are eliminated.

At anode: $Ag\ (s) + Cl^-\ (aq) \longrightarrow AgCl\ (s) + e^-$ $E° = -0.22V$

At cathode: $AgCl\ (s) + e^- \longrightarrow Ag\ (s) + Cl^-\ (aq)$ $E° = 0.22V$

The detail of the preparation of the silver-silver chloride electrodes is described in section 3.1.1.

2.9 CONDUCTING MEDIUM BETWEEN ELECTRODES AND SKIN DURING REVERSE IONTOPHORESIS

During *in vivo* reverse iontophoresis for transdermal metabolite extraction, a conducting medium is placed in the region between skin and electrode to allow current transmission from the electrode to the skin. The medium normally can be a gel or an aqueous solution. Most of the studies in the literature have been carried out with aqueous solutions. However, to hold promise for further clinical application, gels would be the most suitable formulation. This is because gels have several advantages over liquids, like ease of fabrication for a device, suitability of use with various electrode designs, deformability into skin contours, better occlusion, and better stability.

Moreover, there is always a great volume of water employed in gel formulation and this can in turn provide an advantageous electro-conductive base for clinical use (Zhang *et al.* 1996). Therefore, iontophoretic devices often utilize gels as a contact interface between the skin and the electrodes (Phipps *et al.* 1989, Alvarez-Figueroa and Blanco-Mendez 2001, Banga and Chien 1993).

In this study, methylcellulose (MC) was used to prepare a gel. MC is a non-toxic polymer used as a food additive and in tablet formulation for medicines. The viscosity of the aqueous solution of MC is little affected by acid and alkali with its aqueous solution stable in wide pH range from 3.0 to 11.0. In fact, MC gel has been widely used in the field of iontophoresis on humans (Calkin *et al.* 2002, Noon *et al.* 1998, Schmelz *et al.* 1997).

Because the process of reverse iontophoresis is pH sensitive (Santi and Guy 1996), solutions used to prepare the MC gel should have the ability to maintain its pH throughout the whole process of reverse iontophoresis and be safe to apply on human. To avoid the pH shift in the MC gel during reverse iontophoresis, buffer species were added to formulations to increase the buffer capacity. Accordingly, phosphate buffer solution can be used to prepare the MC gel as it is safe to apply on humans and is able to main a stable pH (British Pharmacopoeia 2003).

2.10 SAMPLING TECHNIQUES ON THE EXTRACTED METABOLITES

Several sampling techniques can be use for the quantification of the amount of the extracted metabolites, such as High Performance Liquid Chromatography (HPLC) and enzymatic assay.

HPLC is a separation technique, which utilizes differences in distribution of compounds to two phases. The two phases are stationary phase designating a thin

layer created on the surface of fine particles, and mobile phase designating the liquid flowing over the particles. Because each component in a sample, under a certain dynamic condition, has a different distribution equilibrium depending on solubility in the phases and/or molecular size, therefore the components move at different speeds over the stationary phase and are thereby separated from each other.

A HPLC system basically includes a pump, injector, column, detector and recorder or data system, connected as shown in Figure 2.15 & 2.16. The heart of the system is the column, a stainless steel (or resin) tube packed with micrometer size porous particles, where separation occurs. A high pressure pump is used to constantly move the mobile phase into the column inlet at a constant rate. A sample is injected from a sample injector, which is located near the column inlet. The injected sample goes into the column with the mobile phase and the components in the sample migrate through it, passing between the stationary and mobile phases. Compounds move in the column only when is in the mobile phase. Compounds migrate faster through the column when they tend to be distributed in the mobile phase, whereas compounds migrate slower through the column when they tend to be distributed in the stationary phase. In this manner, each component is separated on the column and sequentially elutes from the outlet. A detector can then be used to detect each compound eluting from the column and the detector is connected to the outlet of the column.

A chromatogram is obtained once the separation process is monitored by the recorder starting at the time the sample is injected. The time required for a compound to elute (called retention time) and the relationship between compound concentration and peak area depend on the characteristics of the compound. Therefore, retention time is used as an index for qualitative determination and peak surface area (or height) is used as an index for quantitative determination. Based on data obtained in advance by analyzing a sample with known quantities of the reference standards (highly purified target compounds in general), the concentration for each unit of peak area and the retention time of the target compounds can then be calculated.

HPLC is a very accurate technique on separating different types of molecules and quantifying the amount of the same type of molecule. However, it is relatively expensive to run this technique.

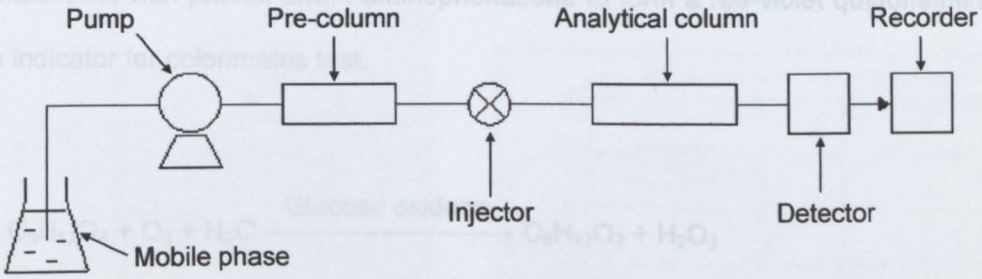

Figure 2.15 – Schematic diagram showing the parts of a high performance liquid chromatography system.

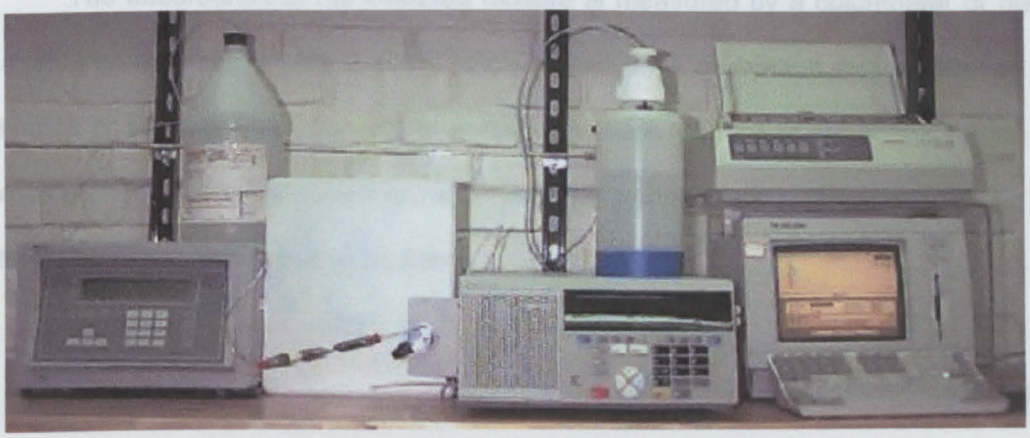

Figure 2.16 – Picture of a high performance liquid chromatography system. (*Source: http://elchem.kaist.ac.kr/vt/chem-ed/sep/lc/hplc.htm*)

Enzymatic assays use enzyme to specifically catalyse specific compounds or molecules. After the enzymatic reaction, a product is generated and the generated product either has a specific colour or is further reacted with other with chemicals to give out a colour. For example, glucose is determined after enzymatic oxidation in the presence of glucose oxidase. The hydrogen peroxide formed reacts, under catalysis of peroxidase, with phenol and 4-aminophenazone to form a red-violet quinoneimine dye as indicator for colorimetric test.

$$C_6H_{12}O_6 + O_2 + H_2O \xrightarrow{\text{Glucose oxidase}} C_6H_{12}O_7 + H_2O_2$$

$$2\ H_2O_2 + C_{11}H_{13}N_3O + C_6H_6O \xrightarrow{\text{Peroxidase}} \text{Quinoneimine} + 4\ H_2O$$

The absorbance of the coloured mixture is measured by a colorimeter or plate reader. Figure 2.17a shows a colorimeter. Based on a calibration curve obtained in advance showing the variation of the absorbance as a function of the concentration of the reference standards (see Figure 2.17b), the concentration of the substance of interest can then be calculated as below:

$$y = mx + b \tag{2.8}$$

where:

y = Absorbance

m = Slope of the calibration cure (see Figure 2.17b)

x = Concentration

b = y-intercept of the calibration cure (see Figure 2.17b)

The enzymatic assay is low-cost and fast. This makes the enzymatic assay ideal for multiple sample experiments. The enzymatic assay is employed in this study.

(a) (b)

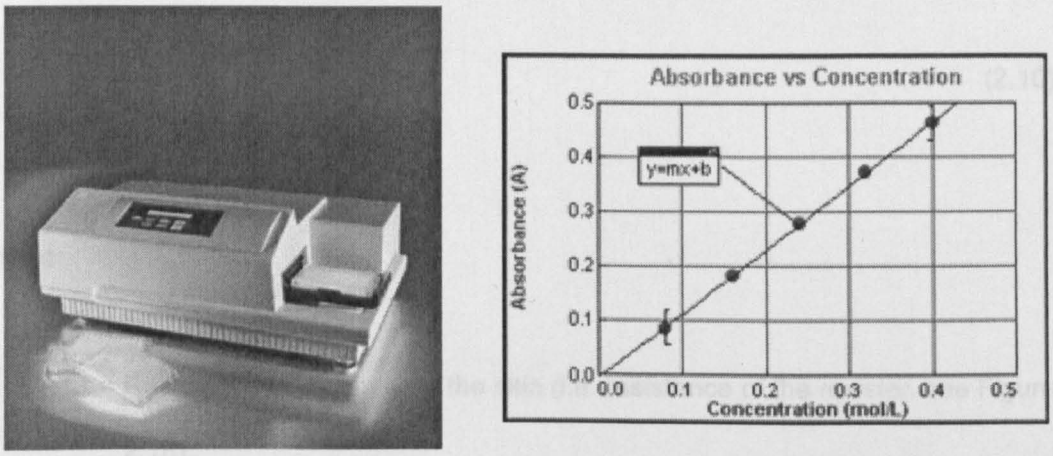

Figure 2.17 – (a) Picture of a colorimeter (*Source: http://www.moleculardevices.com*). (b) A calibration curve showing the variation of the absorbance as a function of the concentration of the reference standards (highly purified target compounds in general).

2.11 SKIN IMPEDANCE MEASUREMENT

Electrical impedance is a measure of the manner and degree that a component resists the flow of alternating current if a given voltage is applied. The impedance of different tissues has different resistive and reactive (capacitive) components. The impedance of tissue may be measured with applied currents at different frequencies (Lozano *et al.* 1990). The frequencies may be selected so that characteristics of different aspects of the tissue can be studied or the separation of the behaviour of different types of tissues is maximized.

The Cole-Cole plot (Cole and Cole 1941) helps in demonstrating the behaviour of tissue impedance as a function of frequency (see Figure 2.19). Skin impedance can be electrically represented by a simple equivalent circuit of a parallel combination of a

resistance and a capacitance (Yamamoto and Yamamoto 1976) (see Figure 2.18). Based on Figure 2.18, the skin impedance can then be mathematically expressed as:

$$\frac{1}{Z} = \frac{1}{R} + \frac{1}{R_C} \tag{2.9}$$

$$\frac{1}{Z} = \frac{1}{R} + \frac{1}{1/j\omega C} \tag{2.10}$$

where:

Z = Skin impedance

R = Resistance component of the skin (i.e. resistance of the resistor, see Figure 2.18)

R_C = Reactance component of the skin (i.e. reactance of the capacitor, see Figure 2.18)

ω = Angular frequency = $2\pi f$

f = Frequency

j = Unit imaginary number

C = Capacitance of the capacitor

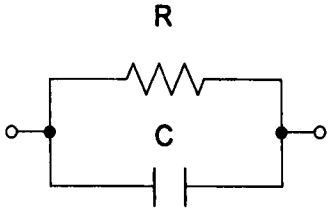

Figure 2.18 – Equivalent circuit of skin impedance, where R and C are the resistance and capacitance components of the skin, respectively.

Equation 2.10 can be simplified to give:

$$Z = \frac{R}{1 + j\omega CR} \tag{2.11}$$

It is possible to determine the real and imaginary components of the skin impedance by expanding Equation 2.11 as:

$$Z = \frac{R(1 - j\omega CR)}{(1 + j\omega CR)(1 - j\omega CR)} \tag{2.12}$$

Equation 2.12 can be rewritten to give:

$$Z = \frac{R - j\omega CR^2}{1 + \omega^2 C^2 R^2} \tag{2.13}$$

$$Z = \frac{R}{1 + \omega^2 C^2 R^2} - \frac{j\omega CR^2}{1 + \omega^2 C^2 R^2} \tag{2.14}$$

Based on Equation 2.14, the real component of skin impedance is illustrated in Equation 2.15, while the imaginary component of skin impedance can be expressed as in Equation 2.16.

$$Z' = \frac{R}{1 + \omega^2 C^2 R^2} \tag{2.15}$$

$$Z'' = -\frac{j\omega CR^2}{1 + \omega^2 C^2 R^2} \tag{2.16}$$

where:

Z' = The real component of skin impedance

Z" = The imaginary component of skin impedance

When Equation 2.14 is plotted as a function of frequency, a complex plane plot (generally semi-circular in shape) can be obtained and it is called Cole-Cole plot (Cole and Cole 1941) (see Figure 2.19). As shown in Figure 2.19, if this figure represents the Cole-Cole plot of the skin impedance, the impedance of skin is equal to (R_0 - R_∞), where R_0 is the impedance of skin as frequency near-zero and R_∞ is the impedance of skin as frequency near-infinity.

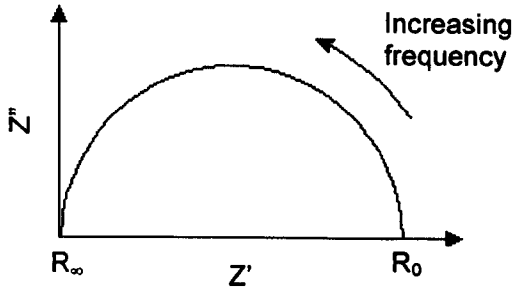

Figure 2.19 – Cole-Cole plot for impedance with a circuit containing a resistor and a capacitor in parallel. Where Z" is the imaginary component of impedance and Z' is the real component of impedance. R_0 is the impedance as frequency near-zero and R_∞ is the impedance as frequency near-infinity.

2.11.1 Effects of Reverse Iontophoresis on the Skin Impedance

Several studies have reported the effect of iontophoresis on the electrical properties of human skin. Oh and Guy (1995) studied the change in resistance of human skin, in response to DC iontophoresis, and they found that application of current (10, 50 and 100 $\mu A/cm^2$) caused skin resistance to drop rapidly, with increasing the

current density resulting in a greater reduction in the value of the skin resistance (reduced to 45, 20 and 10% of pre-treatment value at 10, 50 and 100 $\mu A/cm^2$ respectively) and a slower recovery rate (8, 15 and 30 minutes required for 80% recovery of skin resistance after 10 minutes of current passage at the current density of 10, 50 and 100 $\mu A/cm^2$ respectively). Kalia and Guy (1995) also studied the effect of DC iontophoresis upon the impedance properties of human skin and they had a similar finding. Kalia *et al.* (1996) also demonstrated that DC iontophoresis altered the impedance of the skin, as a function of current density and the time of application. Curdy *et al.* (2002) report that a decrease in skin impedance after DC iontophoresis is not a manifestation of damage to the barrier but a natural response to the relevant electrical potential and ion concentration gradients involved. During DC iontophoresis, the concentration of ions in the skin is increased and this increases the conductivity of the skin, resulting in the reduction of skin resistance. In general, DC iontophoresis can reduce the impedance of the skin.

Up till now, nothing has been reported about the effect of long duration bipolar DC iontophoresis on the electrical properties of skin or membranes. Therefore, this study focused on a study of the long duration bipolar DC at 3 different durations conditions using a pre-clinical model iontophoresis system to investigate its effect on artificial membrane and human skin.

2.12 AIMS AND SCOPE OF THE STUDY

The scope of this study was to develop and test a prototype monitoring system for non-invasive monitoring of glucose and lactate on human *in vivo*. These metabolites are of major importance for large patient groups as diabetes mellitus and critical care patients. There were six principal objectives of this thesis and they are: (1) to find out the optimum switching manner for the reverse iontophoresis on glucose and lactate

extraction, (2) to design and develop a low-cost, low-power, miniature, programmable constant current device used for reverse iontophoresis, (3) to design and develop a low-cost and reliable screen-printed electrode used for reverse iontophoresis, (4) to investigate the effect of long duration bipolar direct current on human transdermal extraction of glucose and lactate, (5) to investigate the effect of long duration bipolar direct current on the electrical properties of human skin and (6) to correlate the real blood glucose/lactate levels with the extracted glucose/lactate levels.

■ *Chapter 3*

Materials and Methodology

Part I: Reverse Iontophoresis Optimisation on Glucose and Lactate Extraction

3.1 Materials And Methods
- 3.1.1 Materials for iontophoresis *in vitro* experiments with artificial skin membrane
- 3.1.2 Experimental procedure
- 3.1.3 Analysis of pre- and post-iontophoresis impedance spectrum
- 3.1.4 Quantification of the extracted glucose and lactate

3.2 Error Estimations
- 3.2.1 Error from the fabrication of the Ag/AgCl electrodes
- 3.2.2 Error in the passage of the iontophoresis current

3.3 Statistical Analysis Of Part I

Part II: Construction and Evaluation of a Constant Current Device for Reverse Iontophoresis

3.4 Materials And Methods
- 3.4.1 Materials
- 3.4.2 Circuit design
- 3.4.3 Experimental procedures for the evaluation of the circuit design
- 3.4.4 Measurements and quantifications of the evaluation

3.5 Error Estimations

3.6 Statistical Analysis Of Part II

Part III: Construction of a Screen-Printed Electrode for Reverse Iontophoresis

3.7 Materials And Methods
- 3.7.1 Materials
- 3.7.2 Construction of screen-printed electrodes for reverse iontophoresis
- 3.7.3 Experimental procedure
- 3.7.4 Analysis of pre- and post-iontophoresis impedance spectrum of human skin
- 3.7.5 Quantification of the extracted glucose and lactate from the MC gel

3.8 Error Estimations
- 3.8.1 Error from the construction of screen-printed electrodes
- 3.8.2 Error in the removal of MC gel from the screen-printed electrodes after experiments

3.9 Statistical Analysis Of Part III

Chapter 3 Materials and Methodology

This chapter consists of three main parts. Part I is the reverse iontophoresis optimisation on glucose and lactate extraction, Part II is the construction and evaluation of a constant current device for reverse Iontophoresis and Part III is the construction of a screen-printed electrode for reverse iontophoresis.

In Part I, *in vitro* experiments are detailed, using a model artificial membrane and diffusion cell. The objectives were to ascertain the optimum current waveform and duration for the reverse iontophoresis of glucose and lactate, to investigate the effect of different current waveforms on glucose and lactate extraction and to investigate the effect of different current waveforms on the electrical properties of the membrane. The results obtained in this part of the study were used in the design of the final iontophoresis system for human experiments which was designed and constructed as described in Part II and Part III of this study.

In Part II, the objectives were to design and develop a programmable constant current device and to evaluate the capability of the use of the newly-developed constant current device on glucose and lactate extraction. The working principles of the constant current device are described in this part of the chapter. The newly-developed constant current device was used in Part III experiments.

In Part III, the objectives were to design and develop a low-cost and reliable screen-printed electrode, to investigate the use of the newly-developed electrode on glucose and lactate extraction, to investigate the effect of long duration bipolar direct current on human transdermal extraction of glucose and lactate and to investigate the effect of long duration bipolar direct current on the electrical properties of human skin.

For all experiments detailed in this part, all currents were supplied by the newly-developed constant current device, which was developed in Part II.

Part I: Reverse Iontophoresis Optimisation on Glucose and Lactate Extraction

Reverse iontophoresis as previously explained refers to the passage of a low level of current through a synthetic or biological membrane to promote the transport of both charged and neutral molecules (Merino *et al.* 1997). In the present study a model artificial membrane and diffusion cell were first adapted for *in vitro* experiments. These were performed using vertical diffusion cells (see Figure 3.1) and results obtained were used in the design of the final iontophoresis system for human experiments which was designed and constructed as part of this study. In the vertical diffusion cell a low level of current (0.3 mA/cm^2) in a range of waveforms was passed for a fixed period of time via Ag/AgCl electrodes inserted into the electrode chambers of the diffusion cells. At the end of the current passage, solutions at the electrode chambers were carefully removed for spectrometric analysis of glucose and lactate. The electrical impedance spectrum of the electrodes and membrane was also recorded before and immediately after the application of current to study changes in the electrical characteristics of the system. The use of an artificial membrane which had skin-like properties (nanoporous, negatively charged) for the first part of the study meant that electrical properties of the electrodes and to some extent the behaviour of glucose and lactate under applied current could be studied without the added complication of individual human skin variations.

There were three objectives in the first part of the study. They were:

(1) to investigate the effect of different current waveforms on glucose and lactate extraction

(2) to ascertain the optimum current waveform and duration for the reverse iontophoresis of glucose and lactate as well as

(3) to investigate the effect of different current waveforms on the electrical properties of the membrane.

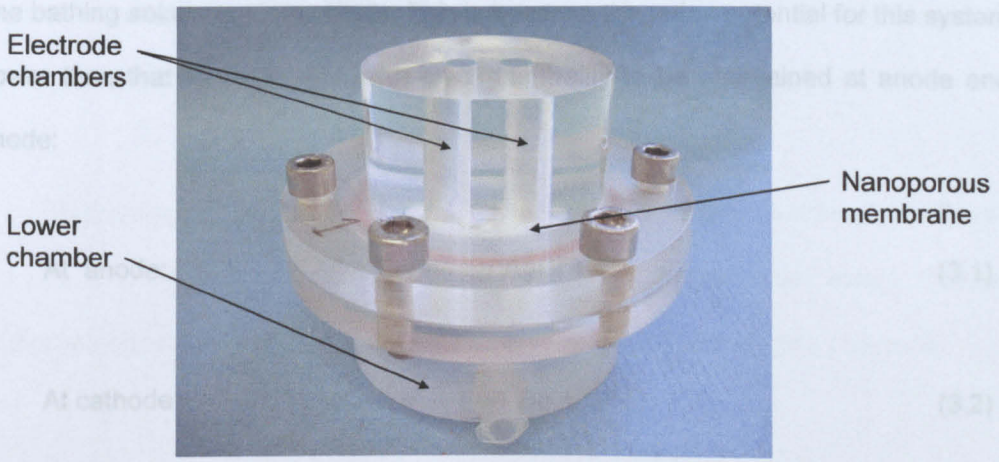

Figure 3.1 – Vertical diffusion cell for *in vitro* reverse iontophoresis experiments.

3.1 MATERIALS AND METHODS

3.1.1 Materials for iontophoresis *in vitro* experiments with artificial skin membrane

Chemicals: N-2-hydroxyethylpiperazine-N'-2-ethanesulphonic acid (HEPES), sodium chloride (NaCl), sodium hydroxide (NaOH), potassium chloride (KCl), hydrochloric acid (HCl), calcium chloride dihydrate ($CaCl_2 \cdot 2H_2O$), ethanol and lactate were purchased from Sigma Chemical Company (St. Louis, MO). Glucose and nitric acid was purchased from BDH Limited (Poole, England). Glucose reagents (GL 26233) and lactate reagents (LC 2389) were purchased from Randox Laboratories Limited (Antrim, UK). De-ionized water (resistivity $\geq 18 \times 10^6$ Ωcm) that had been purified by a Millipore System (Milli-Q UFplus; Bedford, MA) was used to prepare all solutions.

Electrodes: Silver-silver chloride (Ag/AgCl) electrodes were used for the application of both the alternating current, required for the impedance measurements, and the iontophoresis current. Ag/AgCl electrodes were used in this study because they are capable of delivering significantly currents without inducing changes in the pH of the bathing solutions (Jahn 1900). This is because the redox potential for this system is lower than that for water enabling electroneutrality to be maintained at anode and cathode:

At anode: $Ag + Cl^- \longrightarrow AgCl + e^-$ (3.1)

At cathode: $AgCl + e^- \longrightarrow Ag + Cl^-$ (3.2)

Ag/AgCl electrodes, prepared in the usual fashion, were manufactured by electrodeposition of AgCl onto polished silver wires (purchased from Aldrich Chemical Company Inc., Milwaukee, WI). The nominal purity of the commercially acquired silver wire was 99.99% and the wire diameter was 0.1 cm. The silver wire was lightly polished with ultra-fine emery paper first and then rinsed in the sequence of de-ionized water (10 s), 70% ethanol (10 s), de-ionized water (10 s), 1 M nitric acid (10 s) and de-ionized water (10 s). The polished silver wire, 2.5 cm in length, was then anodized in 0.1 M HCl solution stirred continuously at 25°C in conditions of room light for 90 minutes at 314 μA (i.e. 0.4 mA/cm^2). Assuming 100% coulombic efficiency, each electrode was calculated to have 17.57 μM AgCl in the deposited film. The surface area for each electrode was calculated from the length of the cylindrical wire exposed to anodizing solutions. Measurements of length were accurate to 0.05 cm. The surface area of the electrode was 0.785 cm^2 approximately and computed film density was about 22.4×10^{-6} mol/cm^2. The colour of electrodes anodized in this way was dark brownish-grey. Electrodes were rinsed in de-ionized water (10 s) and soaked in

solutions of 1 M KCl in a dark container for 3 days prior to their use in the experiments (see Appendix G). Electrical impedance was measured and total resistance determined for each pair of electrodes where it was assumed that electrodes chlorided at the same time would have near identical impedance values. The standard deviation of the mean resistance among the electrodes used was never more than 13.48 Ω when measured in a solution of 142 mM NaCl with 2.5 mM $CaCl_2 \cdot 2H_2O$ (see Table 3.3).

Membrane: Nanoporous membrane with a net negative charge at pH 7 was used as the artificial skin model (Spectra/Por® CE (cellulose ester) Dialysis Membranes Molecular Weight Cut-Off: 500, Spectrum Laboratories, Inc., Canada).

3.1.2 Experimental procedure

All experiments were carried out on vertical diffusion cells (see Figures 3.1 and 3.2; see Appendix H for the technical drawing of the vertical diffusion cell), in which both electrode chambers were located on the same surface side of the nanoporous membrane (Connolly *et al.* 2002). This is presentative of how iontophoresis electrodes are placed in practice, side by side, on human skin. In the model system they were filled with a buffer solution and the electrodes were placed in this. The lower chamber mimics the interstitial fluid and blood in the skin which carries the molecules of interest. Thus physiological solutions of glucose or lactate would be present in this chamber during the iontophoresis experiments.

Having assembled the diffusion cell with the nanoporous membrane in place, the lower chamber of the diffusion cell were filled with an electrolyte solution comprising 133 mM NaCl, buffered to pH 7.4 with 25 mM HEPES, and either 5 mM glucose or 10 mM lactate. In all experiments, both electrode chambers were each loaded with 350 μl solution, comprising 133 mM NaCl, dissolved in 25 mM HEPES and

pH adjusted to pH 7.4. Each electrode chamber (diameter = 0.5 cm) contained an Ag/AgCl electrode and the surface area of the nanoporous membrane exposed to the electrode, in each electrode chamber, was 0.2 cm^2. A silicon gasket cut to fit the chamber bore holes was placed between the upper and lower chambers to effect a good seal. Thus the exposed are a of membrane for molecular transmission was 0.2 cm^2 in each chamber. The electrode chambers were 1.1 cm apart.

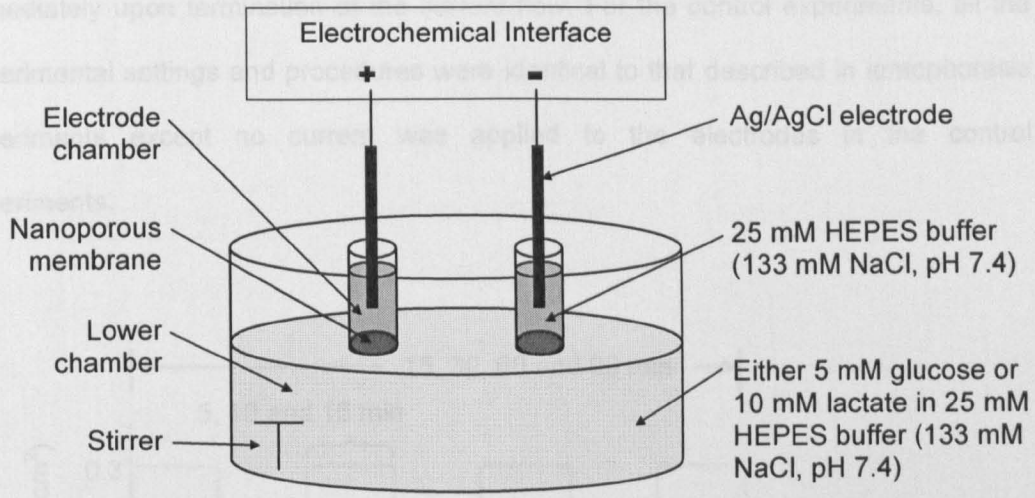

Figure 3.2 – Schematic illustration of the vertical diffusion cell for iontophoresis experiment. For the control experiment, the experimental setting was identical to the iontophoresis experiment except no current flowed through the Ag/AgCl electrodes.

A pre-iontophoresis electrical impedance spectrum was recorded using an impedance analyzer (SI 1260, Schlumberger Technologies, England) to provide a reference point of the system electrical characteristics for later comparison. As given by the manufacturer in the manual, the accuracy of the impedance analyzer on measuring impedance spectrum in the frequency range of 10 μHz up to 32 MHz is ± 0.1 %. Then, an iontophoresis current (delivered using an electrochemical interface SI1286, Schlumberger Technologies, England) of 0.3 mA/cm^2 at 4 different switching modes

(the polarity of electrodes reversing at intervals of 5, 10 and 15 minutes, or without reversing) was passed between the Ag/AgCl electrodes in conditions of ambient light and temperature (22 – 24°C) for a period of either 15, 30, 60 or 90 minutes (see Figure 3.3). As given by the manufacturer in the manual, the electrochemical interface has a resolution of 1 pA in current. The entire content of the electrode chambers were removed at the end of the experiment and stored in microcentrifuge tubes at 4°C for later quantification of glucose or lactate. After refilling electrode chambers with fresh solution, the post-iontophoresis electrical impedance spectrum was recorded immediately upon termination of the current flow. For the control experiments, all the experimental settings and procedures were identical to that described in iontophoresis experiments except no current was applied to the electrodes in the control experiments.

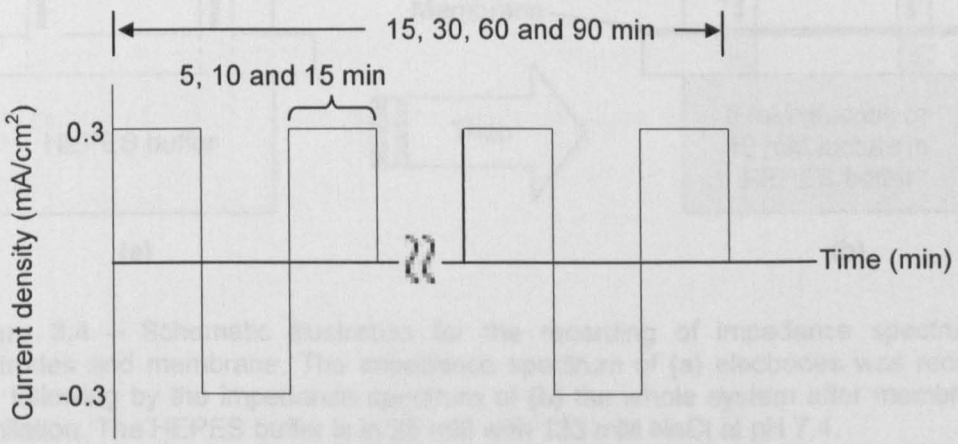

Figure 3.3 – Waveform of the long duration bipolar direct current used in reverse iontophoresis.

3.1.3 Analysis of pre- and post-iontophoresis impedance spectrum

To investigate whether long duration bipolar DC iontophoresis had a significant effect on the membrane impedance, pre- and post-iontophoresis electrical impedance

spectra were recorded. Impedance Analyzer (SI 1260, Schlumberger Technologies, England) and Ag/AgCl electrodes were used. All recordings were conducted at room temperature (22 – 24°C) and all impedance spectra were recorded over the frequency range 1 – $10x10^6$ Hz with 10 frequency points per logarithmic decade. The amplitude of the perturbing wave was limited to 200 mV. The impedance of the Ag/AgCl electrodes were recorded first and the same Ag/AgCl electrodes were then used to record the impedance of the whole system (see Figure 3.4). Two readings per sample were obtained and only the second trial reading was used in order to eliminate the preconditioning effect (see Appendix A for the detail of the preconditioning effect).

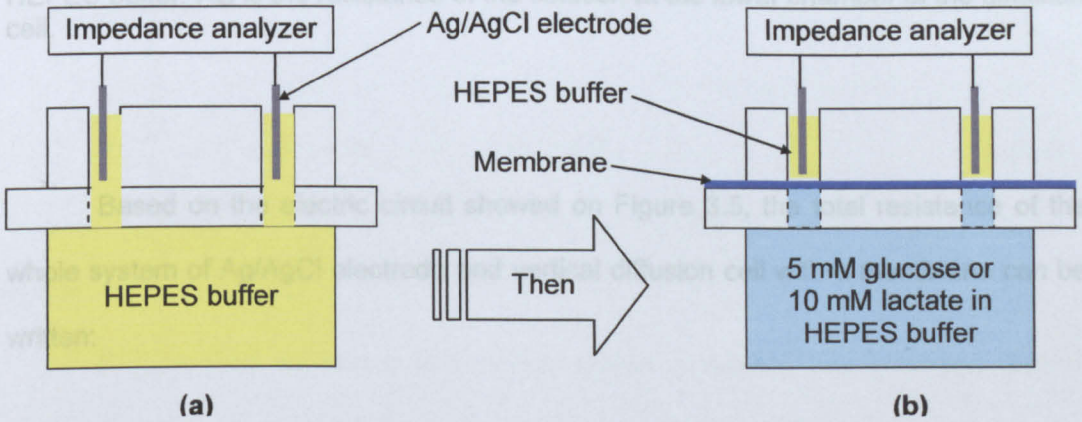

Figure 3.4 – Schematic illustration for the recording of impedance spectrum of electrodes and membrane. The impedance spectrum of **(a)** electrodes was recorded first, following by the impedance spectrum of **(b)** the whole system after membrane's installation. The HEPES buffer is in 25 mM with 133 mM NaCl at pH 7.4.

Assuming that the membrane, just like a skin, can be electrically represented in impedance terms as a parallel combination of resistance and capacitance (Yamamoto and Yamamoto 1976), an equivalent circuit of the impedance of the whole system of Ag/AgCl electrode and vertical diffusion cell with a membrane could be established as shown in Figure 3.5.

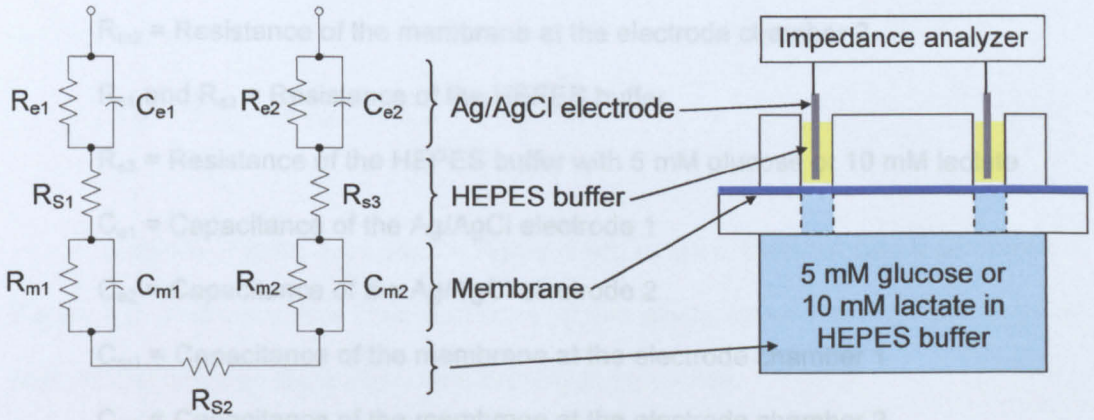

Figure 3.5 – Equivalent circuit of the impedance of the whole system of Ag/AgCl electrode and vertical diffusion cell with a membrane. R_{e1} and R_{e2} as well as C_{e1} and C_{e2} are the resistance and capacitance component of the Ag/AgCl electrodes, respectively. R_{m1} and R_{m2} as well as C_{m1} and C_{m2} are the resistance and capacitance component of the membrane, respectively. R_{s1} and R_{s3} are the resistance of the HEPES buffer. R_{s2} is the resistance of the solution at the lower chamber of the diffusion cell.

Based on the electric circuit showed on Figure 3.5, the total resistance of the whole system of Ag/AgCl electrode and vertical diffusion cell with a membrane can be written:

$$R_{TME} = \frac{R_{e1}}{1+\omega C_{e1} R_{e1}} + R_{s1} + \frac{R_{m1}}{1+\omega C_{m1} R_{m1}} + R_{s2} + \frac{R_{m2}}{1+\omega C_{m2} R_{m2}} + R_{s3} + \frac{R_{e2}}{1+\omega C_{e2} R_{e2}} \quad (3.3)$$

where:

R_{TME} = Total resistance of the whole system of Ag/AgCl electrode and vertical diffusion cell with a membrane

R_{e1} = Resistance of the Ag/AgCl electrode 1

R_{e2} = Resistance of the Ag/AgCl electrode 2

R_{m1} = Resistance of the membrane at the electrode chamber 1

R_{m2} = Resistance of the membrane at the electrode chamber 2

R_{s1} and R_{s2} = Resistance of the HEPES buffer

R_{s3} = Resistance of the HEPES buffer with 5 mM glucose or 10 mM lactate

C_{e1} = Capacitance of the Ag/AgCl electrode 1

C_{e2} = Capacitance of the Ag/AgCl electrode 2

C_{m1} = Capacitance of the membrane at the electrode chamber 1

C_{m2} = Capacitance of the membrane at the electrode chamber 2

ω = Angular frequency = $2\pi f$

When the frequency approaches zero (i.e. ω approaching zero), Equation 3.3 can be rewritten:

$$R_{TME}^{f\to 0} = R_{e1} + R_{s1} + R_{m1} + R_{s2} + R_{m2} + R_{s3} + R_{e2} \qquad (3.4)$$

where:

$R_{TME}^{f\to 0}$ = Total resistance of the whole system of Ag/AgCl electrode and vertical diffusion cell with a membrane as frequency near-zero

When the frequency approaches infinity (i.e. ω approaching infinity), Equation 3.3 can be rewritten:

$$R_{TME}^{f\to \infty} = R_{s1} + R_{s2} + R_{s3} \qquad (3.5)$$

where:

$R_{TME}^{f\to \infty}$ = Total resistance of the whole system of Ag/AgCl electrode and vertical diffusion cell with a membrane as frequency near-infinity

Equation 3.4 subtracted from Equation 3.5 gives:

$$R_{m1} + R_{m2} = \left(R_{TME}^{f \to 0} - R_{TME}^{f \to \infty}\right) - \left(R_{e1} + R_{e2}\right) \quad (3.6)$$

Similarly, Figure 3.4a can be represented by an equivalent circuit as shown in Figure 3.6. Therefore, the total resistance of the whole system of Ag/AgCl electrode and vertical diffusion cell with no membrane can be written:

$$R_{TE} = \frac{R_{e1}}{1 + \omega C_{e1} R_{e1}} + R_{x1} + \frac{R_{e2}}{1 + \omega C_{e2} R_{e2}} \quad (3.7)$$

where:

R_{TE} = Total resistance of the whole system of Ag/AgCl electrode and vertical diffusion cell with no membrane

R_{x1} = Resistance of the solution inside the vertical diffusion cell

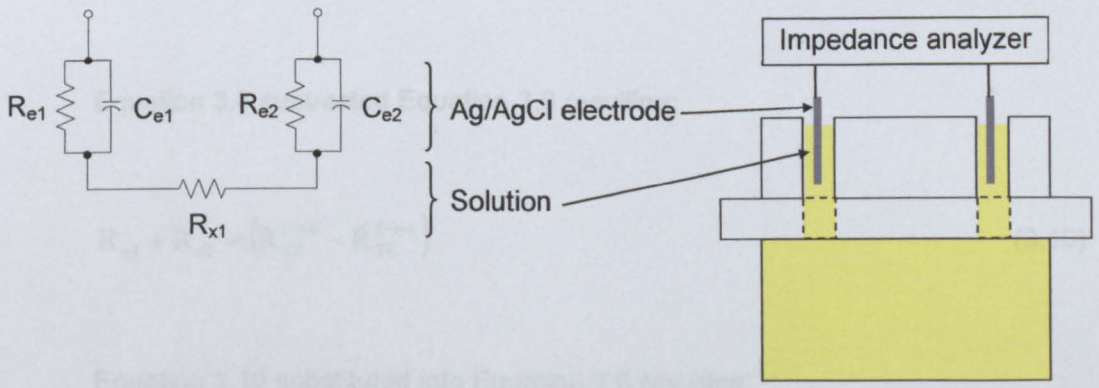

Figure 3.6 – Equivalent circuit of the impedance of the whole system of Ag/AgCl electrode and vertical diffusion cell with no membrane. R_{e1} and R_{e2} as well as C_{e1} and C_{e2} are the resistance and capacitance component of the Ag/AgCl electrodes, respectively. R_{x1} is the resistance of the solution inside the diffusion cell.

When the frequency approaches zero (i.e. ω approaching zero), Equation 3.7 can be rewritten:

$$R_{TE}^{f\to 0} = R_{e1} + R_{x1} + R_{e2} \tag{3.8}$$

where:

$R_{TE}^{f\to 0}$ = Total resistance of the whole system of Ag/AgCl electrode and vertical diffusion cell with no membrane as frequency near-zero

When the frequency approaches infinity (i.e. ω approaching infinity), Equation 3.7 can be rewritten:

$$R_{TE}^{f\to \infty} = R_{x1} \tag{3.9}$$

where:

$R_{TE}^{f\to \infty}$ = Total resistance of the whole system of Ag/AgCl electrode and vertical diffusion cell with no membrane as frequency near-infinity

Equation 3.8 subtracted Equation 3.9 resulting:

$$R_{e1} + R_{e2} = \left(R_{TE}^{f\to 0} - R_{TE}^{f\to \infty}\right) \tag{3.10}$$

Equation 3.10 substituted into Equation 3.6 resulting:

$$R_{m1} + R_{m2} = \left(R_{TME}^{f\to 0} - R_{TME}^{f\to \infty}\right) - \left(R_{TE}^{f\to 0} - R_{TE}^{f\to \infty}\right) \tag{3.11}$$

The impedance analyser used in the experiments allowed the impedance to be measured and recorded over a range of frequency from high to low values. Therefore, the impedance of membrane, $2R_m$, can be calculated by subtracting $\left(R_{TME}^{f\to 0} - R_{TME}^{f\to\infty}\right)$ and $\left(R_{TE}^{f\to 0} - R_{TE}^{f\to\infty}\right)$. The value of $\left(R_{TME}^{f\to 0} - R_{TME}^{f\to\infty}\right)$ is obtained from the impedance spectrum of the whole system of Ag/AgCl electrode and vertical diffusion cell with a membrane as shown in Figure 3.4b, while $\left(R_{TE}^{f\to 0} - R_{TE}^{f\to\infty}\right)$ is obtained from the impedance spectrum of the whole system of Ag/AgCl electrode and vertical diffusion cell with no membrane (see Figure 3.4a).

In general, the impedance data were presented in a conventional electrical manner as Cole- Cole plots (Yamamoto and Yamamoto 1976) showing the variation of the imaginary component of the impedance, Z", as a function of the real component of the impedance, Z' (see Figure 3.7). Using Figure 3.7 as an example, $R_{TE}^{f\to 0}$, $R_{TE}^{f\to\infty}$, $R_{TME}^{f\to 0}$ and $R_{TME}^{f\to\infty}$ were about 480, 60, 3000 and 700 Ω, respectively. Based on Equation 3.11, the resistive part of electrical impedance, $2R_m$, was about 1880 Ω and therefore the electrical resistance R_m of the membrane was about 940 Ω.

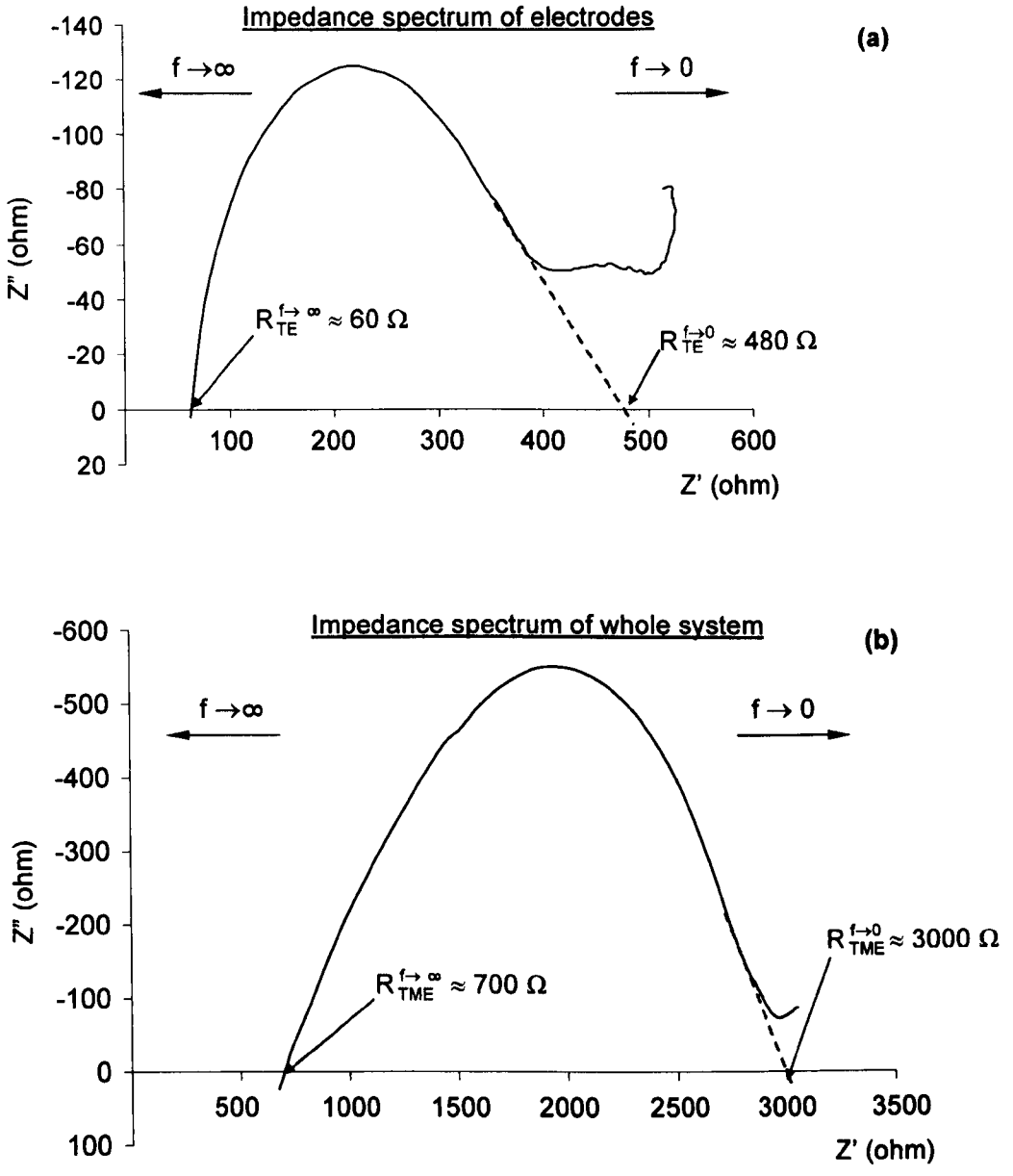

Figure 3.7 – Complex plane impedance spectra of **(a)** electrodes and **(b)** whole system. Based on Equation 3.11, the impedance of the membrane is about 940 Ω, (i.e. {[3000 - 700] - [480 – 60]} / 2 = 940 Ω).

3.1.4 Quantification of the extracted glucose and lactate

Glucose quantification: The amount of glucose extracted through the nanoporous membrane was determined by spectrometric assay using glucose reagents (GL 26233) purchased from Randox Laboratories Limited (Antrim, UK) and

spectrometer (Multiskan Ascent®, Labsystems Oy, Finland) (see Figure 3.8). As given by the manufacturer in the manual, the accuracy of the spectrometer on measuring absorbance is ± 1 %. The contents of glucose reagent are mainly phenol, 4-aminophenazone, glucose oxidase (GOD) and peroxidase (POD). The working principle of the glucose reagent in determining glucose is that glucose is determined after enzymatic oxidation in the presence of glucose oxidase. The hydrogen peroxide formed reacts, under catalysis of peroxidase, with phenol and 4-aminophenazone to form a red-violet quinoneimine dye as indicator.

$$C_6H_{12}O_6 + O_2 + H_2O \xrightarrow{GOD} C_6H_{12}O_7 + H_2O_2 \quad (3.12)$$

$$2\ H_2O_2 + C_{11}H_{13}N_3O + C_6H_6O \xrightarrow{POD} \text{quinoneimine dye} + 4H_2O \quad (3.13)$$

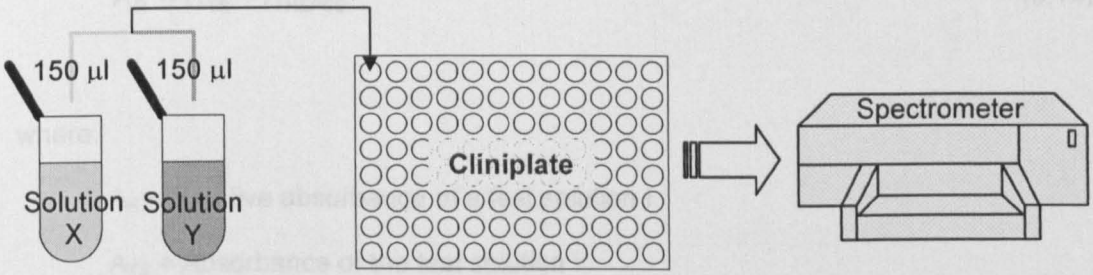

Figure 3.8 – Schematic illustration for the procedures of the spectrometric assay of glucose. 150 µl of solution X was pipetted into a well of the Cliniplate and then 150 µl of solution Y was pipetted into the same well. The Cliniplate was immediately put into the spectrometer for incubation and then the absorbance of the mixture was measured at its optimum wavelength. Solution X represents either extracted glucose sample or standard glucose solution at the concentrations of 0, 0.125, 2.5, 5, 10 and 20 µM. Solution Y represents glucose reagents.

Before performing glucose quantification all microcentrifuge tubes, with the extracted glucose sample, were placed in room temperature (22 – 24°C) for 10

minutes. To test, 150 μl of the extracted glucose sample was pipetted from each microcentrifuge tube to a 96 wells Cliniplate (Multiskan Ascent®, Labsystems Oy, Finland). Standard glucose solutions (150 μl for each concentration) at the concentrations of 0.125, 2.5, 5, 10 and 20 μM, and 25 mM HEPES solution (150 μl), containing 133 mM NaCl buffered at pH 7.4 (represented as 0 μM standard glucose solution), were also pipetted to the Cliniplate. 150 μl of the glucose reagent was then pipetted to each well of the Cliniplate. The Cliniplate was immediately placed on the spectrometer. The programme setting of the spectrometer was (1) incubation temperature 37°C, (2) incubation time 90 minutes and (3) absorbance measured at 500 nm.

Based on the absorbance data of HEPES-only buffered solution (with test reagents) which was used as the blank control, the relative absorbance of a test solution can be expressed as:

$$A_R = A_{TS} - A_{HEPES} \tag{3.14}$$

where:

A_R = Relative absorbance of a test solution i

A_{TS} = Absorbance of the test solution i

A_{HEPES} = Absorbance of the HEPES buffered solution

All the absorbance data of the standard glucose solutions, HEPES buffered solution and extracted glucose samples were converted into relative absorbance data using Equation 3.14. By the use of the relative absorbance data of the standard glucose solutions and the HEPES buffered solution, a calibration curve was plotted showing the variation of the relative absorbance as a function of the concentration of the standard glucose solutions (see Table 3.1) (see Figure 3.9a). An excellent linear

relationship between glucose concentration and relative absorbance was found with the R^2 value being greater than 0.98, allowing the glucose concentration to be calculated simply by linear regression. The concentration of the extracted glucose sample can then be calculated by the linear regression of the calibration curve.

Lactate quantification: The amount of lactate extracted through the nanoporous membrane was determined by using the same method described in glucose quantification: Spectrometric assay. Lactate reagents (LC 2389) purchased from Randox Laboratories Limited (Antrim, UK) and a spectrometer were used. The contents of lactate reagent are mainly N-Ethyl-N-(2 hydroxy-3-sulphopropyl) m-toluidin (TOOS), 4-aminoantipyrine, peroxidase (POD) and lactate oxidase (LOD). The working principle of the lactate reagent in determining lactate is that lactate is determined after enzymatic oxidation in the presence of lactate oxidase. The hydrogen peroxide formed reacts, under catalysis of peroxidase, with TOOS and 4- aminoantipyrine to form a violet quinoneimine dye as indicator.

$$\text{Lactate} + O_2 \xrightarrow{\text{LOD}} \text{pyruvate} + H_2O_2 \qquad (3.15)$$

$$H_2O_2 + \text{4- aminoantipyrine} + \text{TOOS} \xrightarrow{\text{POD}} \text{quinoneimine dye} + 4H_2O \qquad (3.16)$$

All the experimental arrangements and procedures were identical to the glucose quantification except: (1) glucose reagents were replaced by lactate reagents, (2) extracted glucose sample was replaced by extracted lactate sample and (3) standard glucose solutions were replaced by standard lactate solutions of concentration of 3.125, 6.25, 12.5, 25 and 50 μM. The programme setting of the spectrometer was (1) incubation temperature 37°C, (2) incubation time 90 minutes and (3) absorbance measured at 550 nm.

Table 3.1 – Relative absorbance data of the standard glucose solution for the generation of the glucose calibration curve.

	Relative Absorbance					
[Glucose] (μM)	0	0.125	2.5	5	10	20
Trial 1	0.000	0.002	0.006	0.013	0.025	0.052
Trial 2	0.000	0.002	0.006	0.014	0.024	0.048
Trial 3	0.000	0.002	0.005	0.013	0.027	0.051
Trial 4	0.000	0.003	0.006	0.013	0.025	0.048
Mean	0.000	0.002	0.006	0.013	0.025	0.050
SD	0.000	0.000	0.001	0.001	0.001	0.002
Coefficient of variation (%)		22.222	8.696	3.774	4.983	4.144

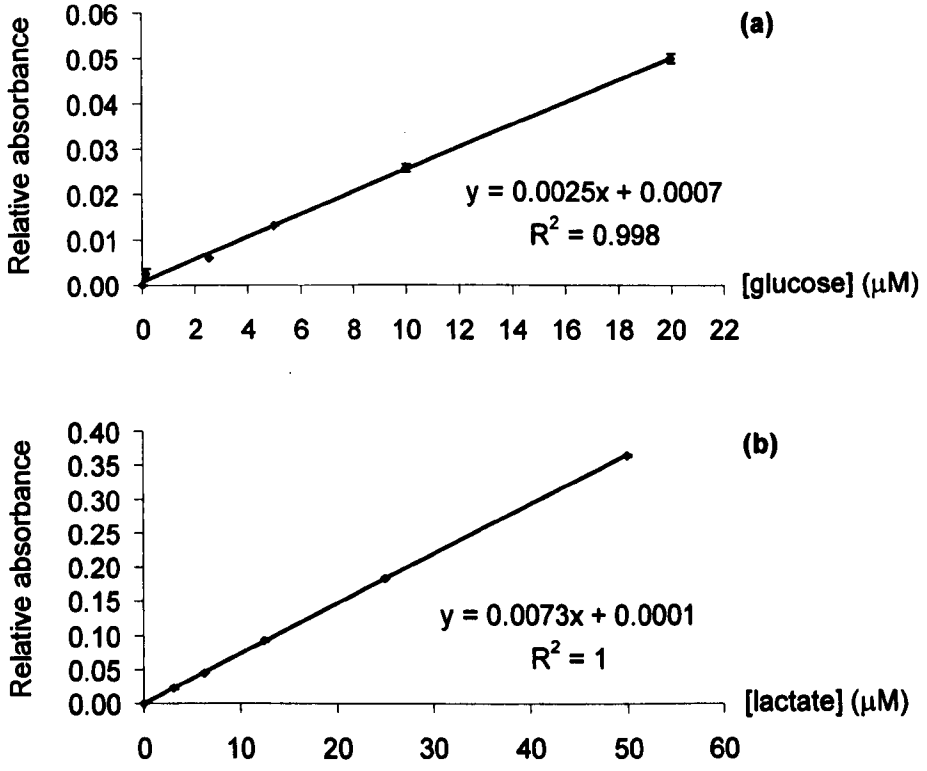

Figure 3.9 – Calibration curves with each point (n = 4) representing the mean ± standard deviation. **(a)** The glucose calibration curve. **(b)** The lactate calibration curve.

All the absorbance data of the standard lactate solutions, HEPES buffered solution and extracted lactate sample were converted into relative absorbance data using Equation 3.14. A calibration curve was plotted, based on the relative absorbance data of the standard lactate solutions and the HEPES buffered solution, to show the variation of the relative absorbance as a function of the concentration of the standard lactate solutions (see Table 3.2) (see Figure 3.9b). An excellent linear relationship ($R^2 \cong 1.00$) was found between lactate concentration and relative absorbance, allowing the lactate concentration to be calculated straightforwardly by linear regression. Using the lactate calibration curve, the concentration of the extracted lactate sample can be calculated by the linear regression.

Table 3.2 – Relative absorbance data of the standard lactate solution for the generation of the lactate calibration curve.

	Relative Absorbance					
[Lactate] (μM)	0	3.125	6.25	12.5	25	50
Trial 1	0.000	0.022	0.045	0.092	0.182	0.362
Trial 2	0.000	0.021	0.046	0.091	0.185	0.367
Trial 3	0.000	0.024	0.045	0.092	0.183	0.365
Trial 4	0.000	0.023	0.045	0.093	0.184	0.364
Mean	0.000	0.023	0.045	0.092	0.184	0.365
SD	0.000	0.001	0.001	0.001	0.001	0.002
Coefficient of variation (%)		5.738	1.105	0.887	0.704	0.571

3.2 ERROR ESTIMATIONS

An effort was made to quantify the errors in the experimental procedures. Sources of error included: a variation in the fabrication of the Ag/AgCl electrodes and passage of the iontophoresis current. Error was quantified as the coefficient of variation of a repeated measure.

3.2.1 Error from the fabrication of the Ag/AgCl electrodes

In order to determine the error from the fabrication of the Ag/AgCl electrodes, 5 pairs of Ag/AgCl electrodes were fabricated based on the method described in section 3.1.1. The impedance spectra of each pair of the Ag/AgCl electrodes were recorded twice in solutions of 142 mM NaCl with 2.5 mM $CaCl_2 \cdot 2H_2O$ using the impedance analyzer (SI 1260, Schlumberger Technologies, England). The first recording of the impedance spectrum was not used to eliminate the preconditioning effects (see Appendix A for the detail of the preconditioning effect) while the second recording was used to compute the resistance of the electrode. The resistance of each pair of the Ag/AgCl electrodes was computed by (using the Equation 3.10 but with different denotation):

$$R_x + R_y = \left(R^{f \to 0} - R^{f \to \infty}\right) \tag{3.17}$$

where:

R_x = Resistance of Ag/AgCl x

R_y = Resistance of Ag/AgCl y

$R^{f \to 0}$ = Resistance of the Ag/AgCl electrodes as frequency near-zero

$R^{f \to \infty}$ = Resistance of the Ag/AgCl electrodes as frequency near-infinity

The mean, standard deviation and coefficient of variation of the resistance of the Ag/AgCl electrodes were computed (see Table 3.3).

Table 3.3 – Evaluation of the error on the fabrication of the Ag/AgCl electrodes.

Pairs of electrodes	Resistance (Ω) of pairs of Ag/AgCl electrodes
1st	442
2nd	428
3rd	438
4th	458
5th	418
Mean	436.80
SD	13.48
Coefficient of variation (%)	3.1

3.2.2 Error in the passage of the iontophoresis current

The accuracy of the electrochemical interface (SI1286, Schlumberger Technologies, England) to deliver an iontophoresis current of 0.3 mA/cm^2 was evaluated. As given by the manufacturer in the manual, the electrochemical interface has a resolution of 1 pA in current.

The experimental arrangement here was identical to that described in section 3.1.2 (see Figure 3.2). The electrochemical interface was connected to a computer with electrochemical measurement software (Corrware v1.3 SOLARTRON, Farnborough, England). The electrochemical interface was controlled and monitored by Corrware. The electrochemical interface was set to deliver a constant current of 58.90 μA. The magnitude of the constant current was measured for 120 seconds by Corrware. The mean and standard deviation of the magnitude of the constant current were 58.89 μA and 5.33 nA, respectively (Coefficient of variation = 0.009%) (see Figure 3.10). The ripple on Figure 3.10 is background or Johnson noise. Therefore, the background noise on the signal was equal to ± 0.009%.

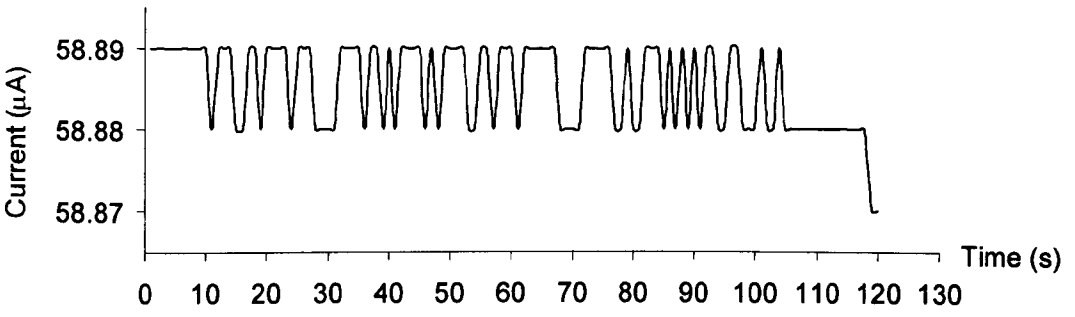

Figure 3.10 – The evaluation of the accuracy of the electrochemical interface (SI1286, Schlumberger Technologies, England) to deliver a constant current of 58.90 μA.

3.3 STATISTICAL ANALYSIS OF PART I

The results were expressed as the mean ± standard deviation. Two-way analysis of variance (ANOVA) was used to determine whether there were significant differences between switching modes and iontophoresis application time (i.e. 30, 60 and 90 min) for the glucose and lactate extraction, and whether there was a significant interaction between switching mode and iontophoresis application time. Identification of a significant interaction led to further analysis of a simple main effect for switching mode with one-way ANOVA and post hoc analysis of significant simple main effects with the LSD (Least Significant Difference) procedure. Also, when a significant interaction was identified, one-way ANOVA was used to determine whether there were significant differences between iontophoresis application time within a switching mode for the glucose and lactate extraction and the post hoc comparisons were made with LSD procedure.

Two-way ANOVA was also conducted to determine whether there were significant differences between switching modes and iontophoresis treatments (i.e. before and after experiment) for the impedance spectrum of the membrane and whether there was a significant interaction between switching mode and iontophoresis

treatment. Identification of a significant interaction led to further analysis of a simple main effect for switching mode with one-way ANOVA and post hoc analysis of significant simple main effects with the LSD procedure. Also, when a significant interaction was identified, paired t-test was used to determine whether there were significant differences between pre- and post-iontophoresis within a switching mode for the impedance spectrum of the membrane.

All tests were carried out using SPSS v.10 software (SPSS Inc., Chicago, Illinois, USA) with the level of statistical significance set at 0.05.

Part II: Construction and Evaluation of a Constant Current Device for Reverse Iontophoresis

Iontophoresis for transdermal drug delivery or for non-invasive monitoring of patients could allow a new generation of medical devices to be developed for low-cost healthcare. The existing iontophoresis systems today are bulky, expensive or non-programmable. In the present study, a miniature, low-cost and programmable device was developed and evaluated. A circuit is described herein which provides a variety of waveforms (DC, pulsed DC, bipolar DC and pulsed bipolar DC) of current for iontophoresis.

There are two objectives of the present study. They are (1) to design and develop a constant current device and (2) to evaluate the capability of the use of the newly-developed constant current device on glucose and lactate extraction.

3.4 MATERIALS AND METHODS

3.4.1 Materials

Electrical and electronic components: Integrated circuits (MAX1044, MAXIM-DALLAS; ICL7136CPL, MAXIM-DALLAS) were purchased from MICROMARK C & CD (Berks, UK). Microprocessor (BS1-IC, PARALLAX) was purchased from Milford Instruments Ltd (Leeds, England). Diodes (1N5817, FAIRCHILD SEMICONDUCTOR), capacitors (MR35V106M4X7, MULTICOMP; CB1V104M2ACB, MULTICOMP; SR151C103KTA, AVX; SR305C474KTA, AVX; SR211C473KTA, AVX; TZ03Z500E169B00, MURATA), fixed-value resistors (MF12100R, MULTICOMP;

MF12220R, MULTICOMP; MF12300R, MULTICOMP; MF121K, MULTICOMP; MF1210K, MULTICOMP; MF1218K, MULTICOMP; MF1239K, MULTICOMP; MF1243K, MULTICOMP; MF1247K, MULTICOMP; MF1256K, MULTICOMP; MF1282K, MULTICOMP; MF12100K, MULTICOMP; MF12180K, MULTICOMP; MF12200K, MULTICOMP; MF12220K, MULTICOMP; MF12560K, MULTICOMP; MF121M, MULTICOMP), variable resistors (MCWIW3296Z-203, MULTICOMP; MCWIW3296Z-503, MULTICOMP; MCWIW3296Z-105, MULTICOMP), double pole double throw switch (MFS201N, KNITTER-SWITCH), LED indicator (TLRY4450, VISHAY), IC-voltage detector (TC54VN4302EZB, TELCOM SEMICONDUCTOR), 3.5 digit length LCD display (VI303-DPRC, VARITRONIX) and plastic enclosure case (75-227911D, VERO) were purchased from Farnell InOne (Leeds, UK). Double pole double throw relay (G6K2PY5DC, OMRON), single pole single throw relay (SIL05-1A72-71D, MEDER), transistor (2N5550, ON SEMICONDUCTOR), cable plug (PAGM02GLAC52A, LEMO), chassis socket (PKGM02GLLA, LEMO), crocodile clip (930126101, ABB), PP3 battery (39170005, ULTRALIFE), pitch pin header (M222011806, HARWIN) and buzzer (RS stock number: 2281627) were purchased from RS Components Ltd (Northants, UK).

Chemicals: All chemicals, identical to that described in section 3.1.1, were used for the evaluation of the constant current device on *in vitro* reverse iontophoresis of glucose and lactate.

Electrodes and membrane: Silver-silver chloride (Ag/AgCl) electrodes and nanoporous membrane, identical to that described in section 3.1.1, were used for the evaluation of the constant current device on *in vitro* reverse iontophoresis of glucose and lactate.

3.4.2 Circuit design

The schematic circuit diagram and the actual subject of the constant current device are respectively shown in Figure 3.11 and 3.12. This circuit is battery-powered (9V) and able to maintain a constant current in the range of 1 μA to 300 μA. The circuit is composed of five parts: Voltage booster, constant current source, current-waveform generator, battery voltage monitor and on-board ammeter.

Voltage booster: This consists of an integrated circuit (**IC**, MAX1044, MAXIM-DALLAS), six diodes (**D1** to **D6**, 1N5817, FAIRCHILD SEMICONDUCTOR) and six 10 μF 35V capacitors (**C1** to **C6**, MR35V106M4X7, MULTICOMP) as shown in Figure 3.13. The IC is a charge pump converter. Pin 1 of the IC is connected to +9V to increase the oscillator frequency (7 – 10 kHz) by a factor of six, preventing the occurrence of ripple on the boosted voltage. The working principle is that the IC switches pin 2 between +9V and 0V at the frequency of about 42 to 60 kHz. When pin 2 is switched to 0V, C1, C3 and C5 charge to +9V through D1, D1 to D3 inclusive and D1 to D5 inclusive. When pin 2 is switched to +9V, negative terminals of C1, C3 and C5 are pulled up to +9V. Because D1 blocks the current flowing back into the battery, charge in C1 flows into C2 through D2. So, C2 is boosted to almost +18V (+9V from the battery plus +9V from C1). Similarly, D3 blocks the current flowing backward, charge in C3 flows through D4 into C4. Therefore, C4 is charged to +27V (+18V from C2 plus +9V from C3). As before, D5 blocks the current flowing back, charge in C5 flows through D6 into C6. So, C6 is boosted to about +36V (+27V from C4 plus +9V from C5). Therefore, +36V can be obtained from C6 when operating the constant current source.

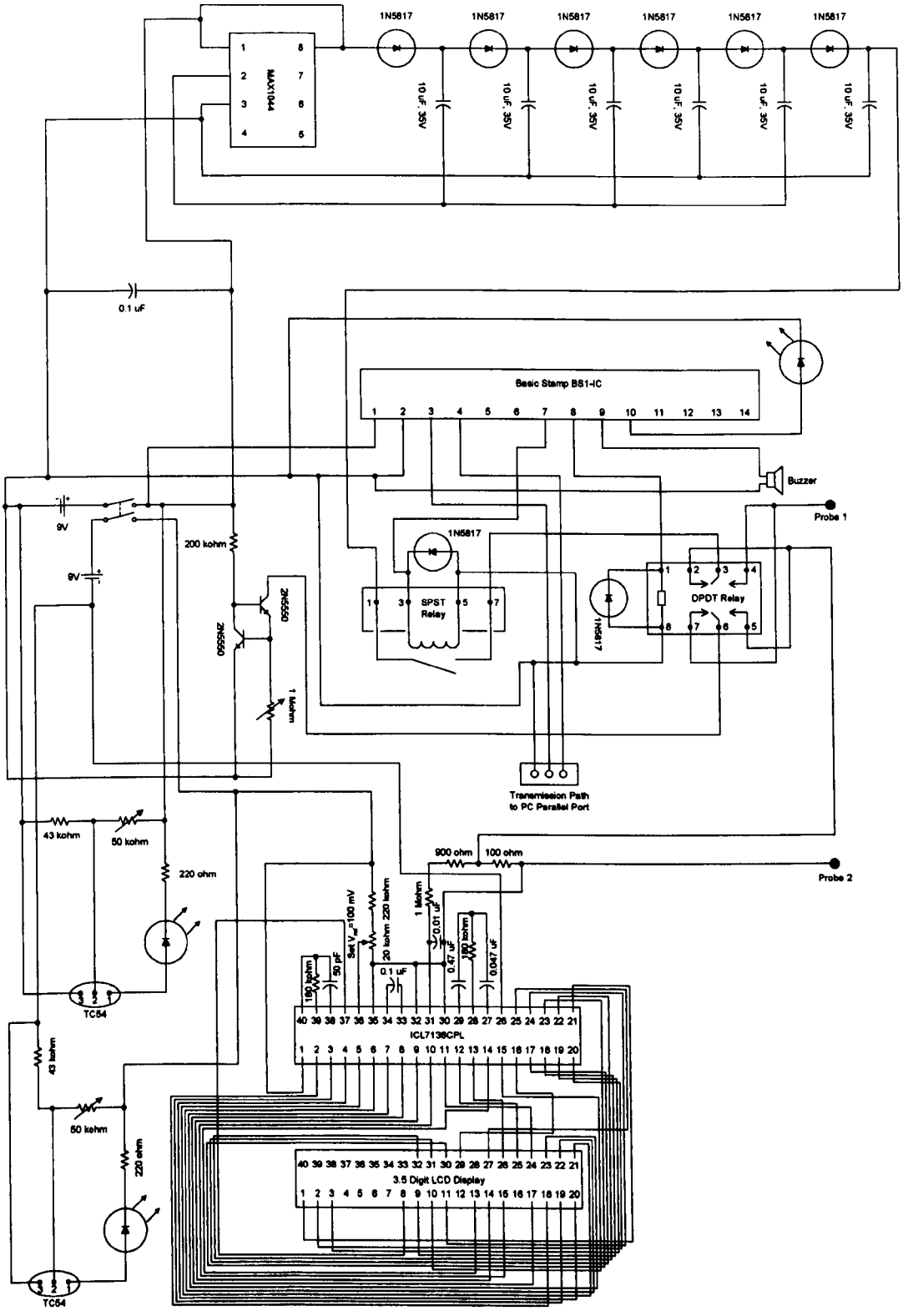

Figure 3.11 – Circuit diagram of the constant current device. It consists of 5 parts: Voltage booster (see Figure 3.13), constant current source (see Figure 3.14), current-waveform generator (see Figure 3.15), battery voltage monitor (see Figure 3.17) and on-board ammeter (see Figure 3.18).

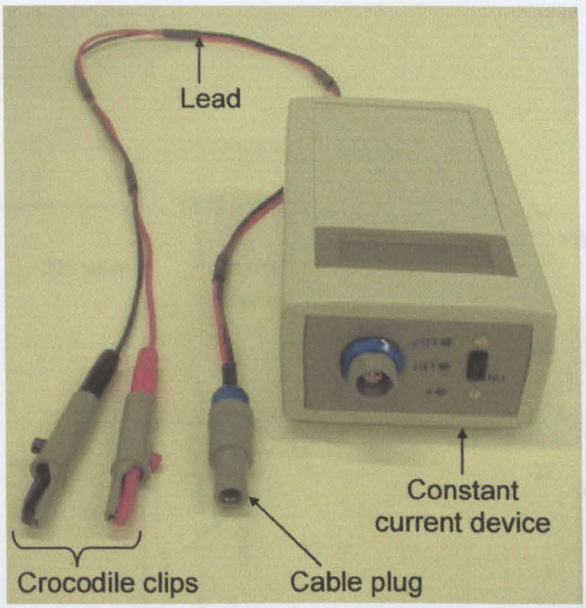

Figure 3.12 – The photo of the constant current device and its accessories. The crocodile clips provide a mean for the connection with electrodes.

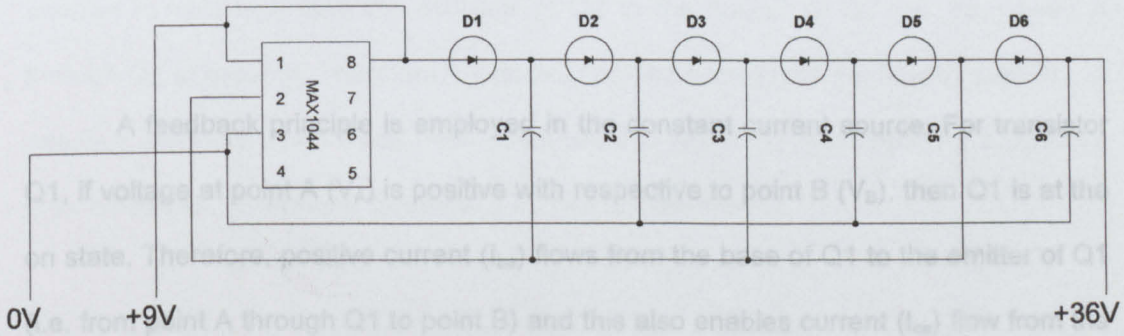

Figure 3.13 – Circuit diagram of the part of voltage booster. The supply of +9V into this voltage booster can generate +36V output.

Constant current source: This consists of two transistors (**Q1** and **Q2**, 2N5550, ON SEMICONDUCTOR), one fixed-value resistor 200 kΩ ± 1% (**R1**, MF12200K, MULTICOMP) and one variable resistor 0 – 1 MΩ ± 10% (**R2**, MCWIW3296Z-105, MULTICOMP) as shown in Figure 3.14a. For the sake of clarity on the explanation of

the working mechanism, the circuit of the constant current source is simplified as Figure 3.14b.

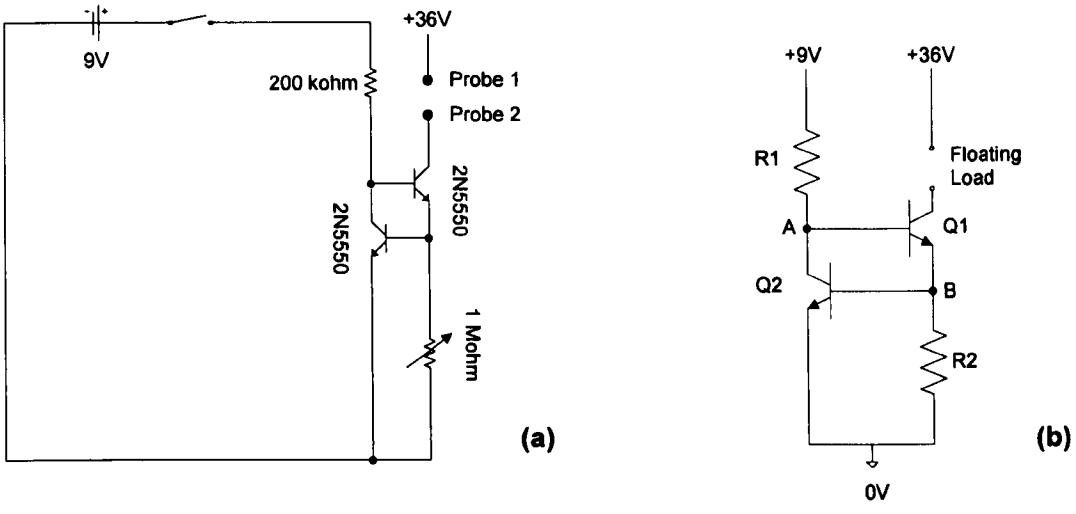

Figure 3.14 – Circuit diagram of the part of constant current source. **(a)** The comprehensive circuit and **(b)** the simplified circuit. Its function is to maintain a constant current to pass through the floating load no matter the resistance of the floating load increase or decrease.

A feedback principle is employed in the constant current source. For transistor Q1, if voltage at point A (V_A) is positive with respective to point B (V_B), then Q1 is at the on state. Therefore, positive current (I_{be}) flows from the base of Q1 to the emitter of Q1 (i.e. from point A through Q1 to point B) and this also enables current (I_{ce}) flow from the collector of Q1 to the emitter of Q1 (i.e. from +36V through Q1 to point B). Therefore, the current passing through R2 is equal to (I_{be} + I_{ce}). Thus, V_B can be expressed as:

$$V_B = R2 \cdot (I_{be} + I_{ce}) \tag{3.18}$$

$$V_B = V_A - 0.6 \tag{3.19}$$

where:

V_B = Voltage at point B

R2 = Resistance of R2

I_{be} = Current flowing from the base of Q1 to the emitter of Q1

I_{ce} = Current flowing from the collector of Q1 to the emitter of Q1

V_A = Voltage at point A

0.6 is the voltage drop between the base and emitter of Q1.

Combining Equations 3.18 and 3.19 forms:

$$\frac{V_A - 0.6}{R2} = I_{be} + I_{ce} \tag{3.20}$$

As long as V_B rises above 0.6V, Q2 is in the on state. Then, current flows from the base of Q2 to the emitter of Q2 (i.e. from point B through Q2 to ground). This also enables current flow from the collector of Q2 to the emitter of Q2 (i.e. from point A through Q2 to ground). Therefore, V_A decreases and a lower current flow through R2. A negative feedback system has been established in which Q2 is maintaining a constant 0.6V across R2. Therefore, Equation 3.20 can be rewritten as:

$$\frac{0.6}{R2} = I_{be} + I_{ce} \tag{3.21}$$

As there is a relationship between I_{be} and I_{ce} ($I_{ce} = \beta \cdot I_{be}$, where β is the gain of the transistor) and β is very large, typically between 50 and 200, I_{be} can be neglected. Equation 3.21 can be rewritten as:

$$I_{ce} \approx \frac{0.6}{R2} \tag{3.22}$$

Therefore, the magnitude of the constant current (I_{ce}) flowing through the floating load, which is represented as the resistance of human skin, can be determined and adjusted by R2. In this circuit design, R1 is 200 kΩ ± 1% and its function is to limit both minimum (1 μA) and maximum (300 μA) currents flowing through human skin. The averaged resistance of skin is about 100 kΩ (Yamamoto and Yamamoto 1976) although this are varied according to the hydration of the skin, thus, passing a current of 300 μA through skin requires +30V according to Ohm's Law. To make sure a constant current can be maintained, the voltage supply to skin is set to +36V.

Current-waveform generator: This consists of a microprocessor Basic Stamp I (BS1-IC, PARALLAX), a single pole single throw relay (**SPST**, SIL051A72BV669, Meder), a double pole double throw relay (**DPDT**, G6K2PY5DC, OMRON), two diodes (1N5817, FAIRCHILD SEMICONDUCTOR), a buzzer (RS stock number: 2281627), three pitch pin headers (M222011806, HARWIN), a LED indicator (TLRY4450, VISHAY) and two probes, i.e. cable plug (PAGM02GLAC52A, LEMO), chassis socket (PKGM02GLLA, LEMO) and crocodile clips (930126101, ABB), as shown in Figure 3.15. Both SPST and DPDT relays are operated at +5V.

The microprocessor is used to control both SPST and DPDT relays in order to change the waveform of the constant current generated by the constant current source. When the SPST relay is switched on, the function of the DPDT relay is to change the polarity of the current output (i.e. to produce a bipolar current waveform). For example, if the DPDT relay is switched on, current flows from probe 2 to probe 1. Conversely, if the DPDT relay is switched off, current then flows from probe 1 to probe 2.

The function of the SPST relay is to produce a pulsed current waveform. For instance, if the SPST relay is switched on, current flows from either probe 1 to probe 2 or probe 2 to probe 1, depending on the state of the DPDT relay. However, if the SPST

relay is switched off, no current flows through the two probes. The buzzer and the LED indicator give a signal once the programmed treatment is completed.

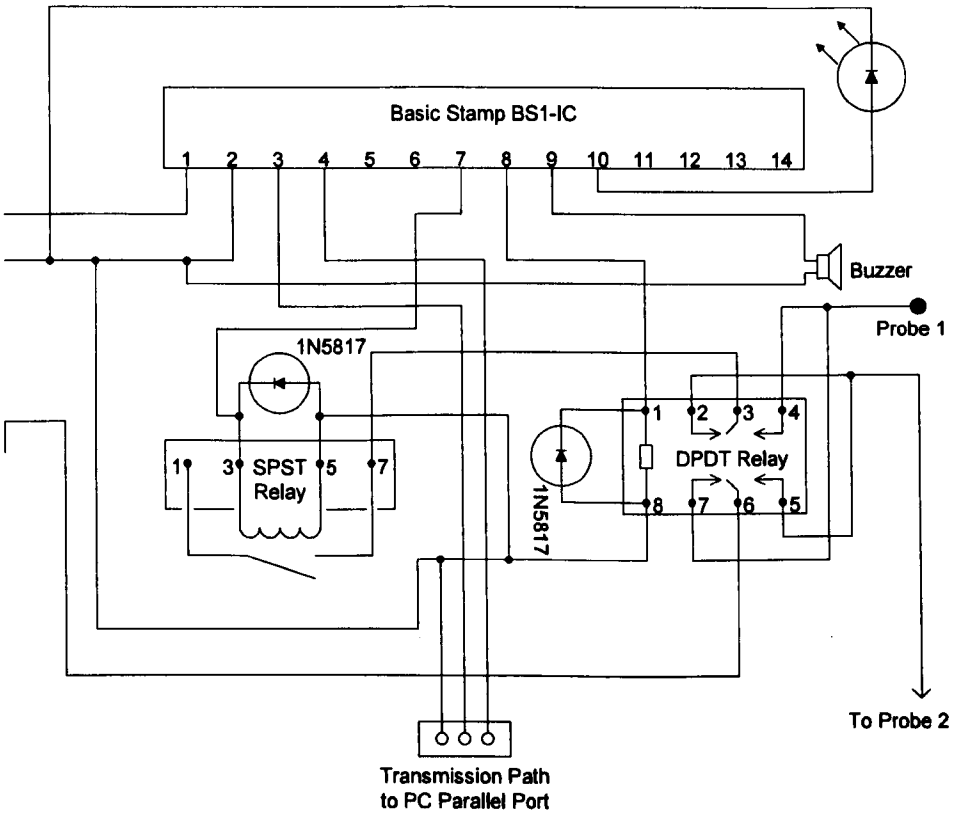

Figure 3.15 – Circuit diagram of the part of current-waveform generator. The Basic Stamp controls the operation of both relays to generate different current waveforms, depending on the program stored inside the Basic Stamp. SPST relay is responsible for pulsed current waveform while DPDT relay is responsible for the polarity of the current output.

Programs for six different waveforms of current (see Appendix B for the details of the programs stored inside the microprocessor) can be stored inside the microprocessor through a parallel port cable, connected between a computer and the transmission path (i.e. the three pitch pin headers). The six different waveforms of current are direct current (DC), pulsed DC (PDC), bipolar DC (BDC), pulsed bipolar DC

(PBDC), bipolar DC including intervals of no applied current (BDC-NO) and pulsed bipolar DC including intervals of no applied current (PBDC-NO) (see Figure 3.16).

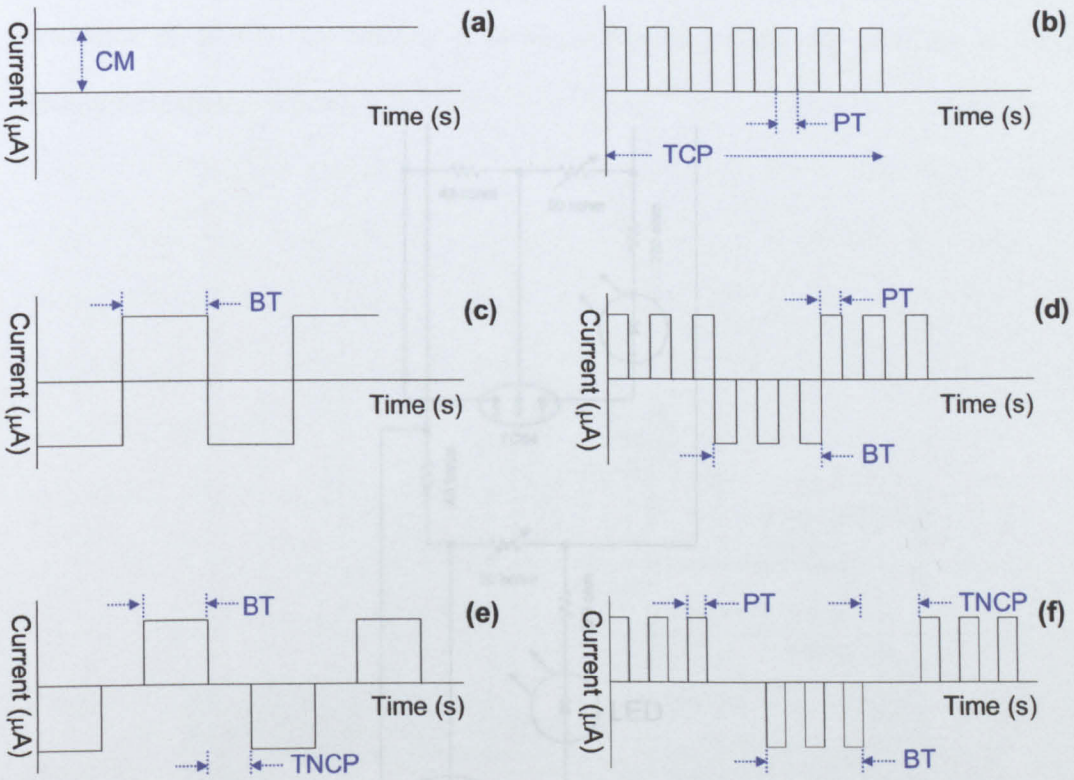

Figure 3.16 – Schematic illustration of the current waveform generated by the constant current device. **(a)** Direct current (DC). **(b)** Pulsed DC. **(c)** Bipolar DC. **(d)** Pulsed bipolar DC. **(e)** Bipolar DC including intervals of no applied current. **(f)** Pulsed bipolar DC including intervals of no applied current. CM is the magnitude of current. PT and BT are the pulse time and bipolar time, respectively. TCP and TNCP are the time of current passage and time of no current passage, respectively.

Battery voltage monitor: This consists of two IC-voltage detectors (TC54VN4302EZB, TELCOM SEMICONDUCTOR), fixed-value resistors 43 kΩ ± 1% (MF1243K, MULTICOMP) and 220 Ω ± 1% (MF12220R, MULTICOMP), two variable resistors 0 – 50 kΩ ± 10% (MCWIW3296Z-503, MULTICOMP) and two LED indicators (TLRY4450, VISHAY) as shown in Figure 3.17. The low voltage alert was set to 7.5V

for the constant current source and 6.0V for the on-board ammeter by the adjustment of the resistance of the variable resistors. Once the detected voltages are below the preset voltages, the LED indicators will be switched on to remind user to replace a new battery.

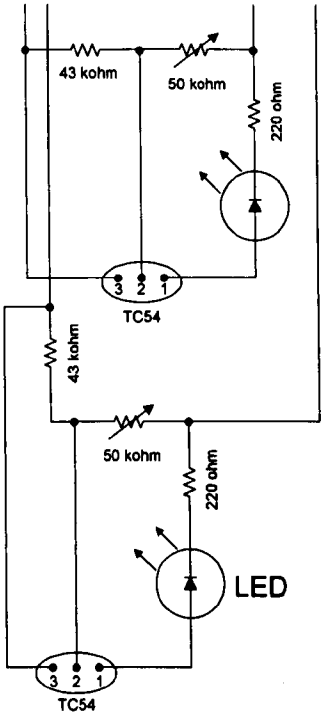

Figure 3.17 – Circuit diagram of the part of battery voltage monitor. Its function is to make sure the constant current device works properly. When the voltage of the battery is below the preset value, the LED will switch on.

On-board ammeter: This consists of an integrated circuit (ICL7136CPL, MAXIM-DALLAS), 3.5 digit length LCD display (VI303-DPRC, VARITRONIX), fixed-value resistors 100 Ω ± 1% (MF12100R, MULTICOMP), 300 Ω ± 1% (MF12300R, MULTICOMP), 180 kΩ ± 1% (MF12180K, MULTICOMP), 220 kΩ ± 1% (MF12220K, MULTICOMP) and 1 MΩ ± 1% (MF121M, MULTICOMP), one variable resistor 0 – 20 kΩ ± 10% (MCWIW3296Z-203, MULTICOMP) and capacitors 50 pF

(TZ03Z500E169B00, MURATA), 0.1 μF (CB1V104M2ACB, MULTICOMP), 0.01 μF (SR151C103KTA, AVX), 0.47 μF (SR305C474KTA, AVX) and 0.047 μF (SR211C473KTA, AVX) as shown in Figure 3.18. This on-board ammeter is able to measure milliampere current in the range of 0 mA to 2 mA (3 reading/second) with resolution of ±0.001. Its function is to show the magnitude and direction of current flowing through the probes.

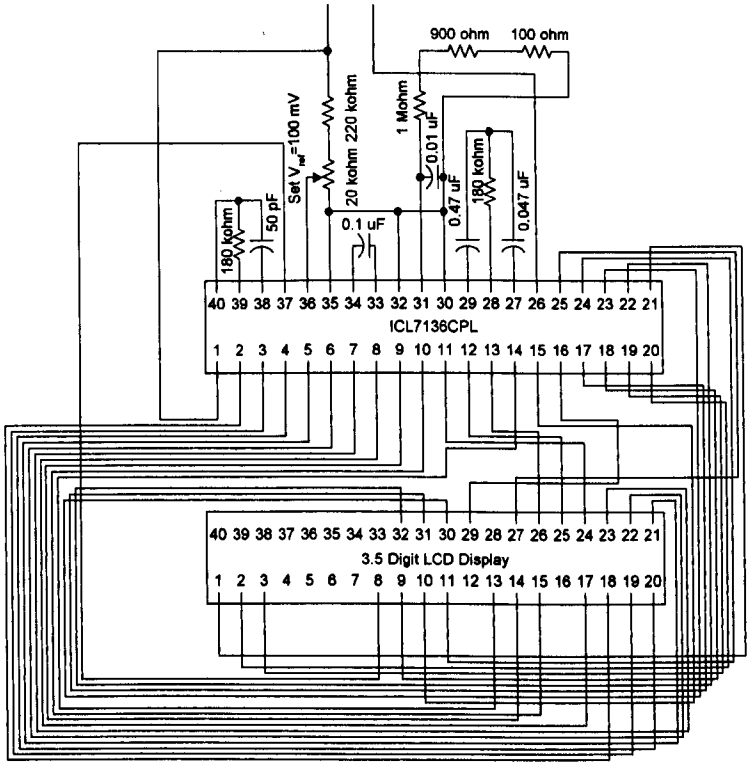

Figure 3.18 – Circuit diagram of the part of on-board ammeter. Its function is to show the connectivity (i.e. to check the contact of electrodes on skin) as well as the magnitude and direction of current output.

3.4.3 Experimental procedures for the evaluation of the circuit design

Electronic evaluation: The accuracy of the constant current device in delivering a constant current (1, 100, 200 and 300 μA) was evaluated. Fixed-value resistors with

resistance of 49 kΩ (*49 kΩ = 39 kΩ ± 1% + 10 kΩ ± 1%*, MF1239K, MULTICOMP; MF1210K, MULTICOMP) and 110 kΩ (*110 kΩ = 100 kΩ ± 1% + 10 kΩ ± 1%*, MF12100K, MULTICOMP; MF1210K, MULTICOMP) were used to simulate the resistance of human skin (Yamamoto and Yamamoto 1976) and they were separately attached to probe 1 and probe 2 of the device. On each setting of constant current delivery, a computer based oscilloscope (ADC-40, Pico Technology Limited, UK) was used to measure the potential difference across the 10 kΩ ± 1% resistor and the magnitude of the current flowing through the resistor can be calculated based on Ohm's Law (Voltage = Current x Resistance). By using the same experimental setting, the accuracy of the device in delivering a constant current (300 μA) at six different waveforms (DC, PDC, BDC, PBDC, BDC-NO, PBDC-NO) was also evaluated. On each setting, data was captured for 3 hours.

The ability of the constant current device in maintaining a constant current (300 μA) at different load resistance values was evaluated. Fixed-value resistors with resistance of 0 Ω (a metal wire), 1 kΩ ± 1% (MF121K, MULTICOMP), 82 kΩ ± 1% (MF1282K, MULTICOMP) and 100 kΩ ± 1% (MF12100K, MULTICOMP) were separately connected in series with the probes of the device and a digital ammeter (Solartron 7045 digital multimeter, The Solartron Electronic Group LTD, England). On each resistance, the reading at the digital ammeter was captured at every 30 seconds up to 300 seconds. For the resistance of 0 and 100 kΩ, an extra experiment with the same setting was conducted with the capture of the reading at 30, 60 and 120 minutes.

The accuracy of the on-board ammeter of the constant current device to show the magnitude of current flowing through the probes was evaluated. A fixed-value resistor 47 kΩ ± 1% (MF1247K, MULTICOMP) was connected in series with the probes of the device and a digital ammeter (Solartron 7045 digital multimeter, The Solartron Electronic Group LTD, England). On each setting of constant current delivery (1, 100, 200 and 300 μA), a digital camera (FINEPIX 2600, FUJI) was used to capture the

reading at the on-board ammeter and the digital ammeter at every 10 seconds up to 60 seconds.

The usable life of the device before battery recharging is required was also evaluated. A fixed-value resistor 100 kΩ ± 1% (MF12100K, MULTICOMP) was attached to probe 1 and probe 2 of the device. A digital voltmeter (Solartron 7045 digital multimeter, The Solartron Electronic Group LTD, England) was used to measure the voltage of the battery. The current setting stored inside the device is 300 μA. A bipolar DC setting (15 minutes bipolar time for the first 5 hours following by 5 minutes bipolar time for another 5 hours) was installed. A digital camera (FINEPIX 2600, FUJI) was used to capture the reading at the on-board ammeter and the digital voltmeter at every 20 minutes up to 10 hours.

In vitro reverse iontophoresis evaluation: The vertical electrode chamber diffusion cells described earlier incorporated with nanoporous membrane (Connolly *et al.* 2002) was used here. This evaluation was to determine whether the constant current device was able to be used as a device for reverse iontophoresis. The whole experimental procedures were identical to that described in section 3.1.2, except that the iontophoresis current was delivered by the constant current device and only one switching mode (the polarity of electrodes reversing at intervals of 15 minutes) was used in this evaluation.

3.4.4 Measurements and quantifications of the evaluation

Electronic evaluation: After the calculation of the magnitude of the current flowing through resistors, these current data were presented as plots showing the variation of the current magnitude as a function of time. From each plot, the magnitude

of current, pulse time, bipolar time, time of current passage and time of no current passage were extracted (see Figure 3.16).

Readings indicated at the on-board ammeter and the digital ammeter/voltmeter was extracted from the digital photos captured by the digital camera.

In vitro reverse iontophoresis evaluation: The recordings of pre- and post-iontophoresis impedance spectrum of a membrane and quantification of the extracted glucose and lactate were conducted. All measurements and quantifications were identical to that described in section 3.1.3 and 3.1.4.

3.5 ERROR ESTIMATIONS

During electronic evaluation, two instruments were used and they were the computer based oscilloscope (ADC-40, Pico Technology Limited, UK) and the digital multimeter (Solartron 7045 digital multimeter, The Solartron Electronic Group LTD, England). Resistors were also used on the electronic evaluation.

As given by the manufacturer in the manual, the accuracy of the computer based oscilloscope on measuring potential difference in the spectrum range of 0 Hz up to 10 kHz is ± 1% and the accuracy of the digital multimeter on measuring current is ± 2%. Resistors have resistance tolerance of ± 1%.

Therefore, if the computer based oscilloscope is used together with a resistor on evaluating the accuracy of the constant current device, there was ± 2% (i.e. ± 1% from the resistor and ± 1% from the computer based oscilloscope) on the measurement.

On the other hand, if the digital multimeter is used together with a resistor on evaluating the accuracy of the constant current device, there was ± 3% (i.e. ± 1% from the resistor and ± 2% from the digital multimeter) on the measurement.

3.6 STATISTICAL ANALYSIS OF PART II

The results were expressed as the mean ± standard deviation. Percentage errors were calculated to evaluate the circuit design.

One-way analysis of variance (ANOVA) was used to determine whether there were significant differences among iontophoresis application time (i.e. 30, 60 and 90 min) for the glucose and lactate extraction. Identification of a significant difference led to further post hoc analysis of significant simple main effects with the LSD procedure. On the other hand, an independent t-test was used to determine whether there were significant differences between the control and reverse iontophoresis (15 minutes electrode polarity reversing) for the glucose and lactate extraction.

The paired t-test was used to determine whether there were significant differences between iontophoresis treatments (i.e. before and after experiment) for the impedance spectrum of the membrane, while an independent t-test was used to determine whether there were significant differences between the control and reverse iontophoresis (15 minutes electrode polarity reversing) for the impedance spectrum of the membrane.

All tests were carried out using SPSS v.10 software (SPSS Inc., Chicago, Illinois, USA) with the level of statistical significance set at 0.05.

Part III: Construction of a Screen-Printed Electrode for Reverse Iontophoresis

Reverse iontophoresis is gaining acceptance in human medicine in the fields of non-invasive diagnosis (Merino *et al.* 1999, Numajiri *et al.* 1993) and patient monitoring (Potts *et al.* 2002, Pitzer *et al.* 2001, Tierney *et al.* 2001). To determine the amount of interested substances extracted by reverse iontophoresis, the extracted substances should pass into a capture media such as gel or liquid and be determined by analytical methods such as biosensor technology and spectrometric assay. For the clinical use, it is much better to have a solid form of capture media for ease of use and handling.

In the present study, a screen-printed electrode was designed and developed. *In vitro* experiments and human experiments were performed using the newly-developed electrode. A low level current was passed for a fixed period of time via the electrodes attached onto the human skin (via a buffered gel) or a specially designed diffusion cell which allowed the gel and electrodes to be tested. At the end of the current passage, the gel at the electrodes could be carefully removed for spectrometric analysis of glucose and lactate. The impedance of the human skin or of the nanoporous membrane of the diffusion cell were also recorded before and immediately after the application of current.

There were four objectives in this section of the study. They were (1) to design and develop a low-cost and reliable screen-printed electrode, (2) to investigate the use of the newly-developed electrode on glucose and lactate extraction, (3) to investigate the effect of long duration bipolar direct current on human transdermal extraction of glucose and lactate and (4) to investigate the effect of long duration bipolar direct current on the electrical properties of human skin.

3.7 MATERIALS AND METHODS

3.7.1 Materials

Chemicals: All chemicals described in section 3.1.1 were used. Litmus paper was purchased from BDH Limited (Poole, England). Methylcellulose (MC) was purchased from The DOW Chemical Company (USA). Sodium phosphate monobasic (USP grade) was purchased from Sigma Chemical Company (St. Louis, MO). 0.1 M phosphate buffer solution (PBS) was prepared by dissolving 1.1998g of sodium phosphate monobasic in 100 ml de-ionized water and adjusting the pH to 7.4 using a 40% w/v solution of sodium hydroxide. MC gel (4%) was prepared by mixing 4 g of methylcellulose with 100 ml of 0.1 M PBS. During gel making, ¼ of the required total amount of the 0.1 M PBS (i.e. 25 ml) was heated up to 80 °C and 4 g methylcellulose was then added into the 0.1 M PBS (80 °C). After the methylcellulose had totally dissolved into the 0.1 M PBS (80 °C) by gentle stirring, the remaining volume (i.e. 75 ml) of the 0.1 M PBS (at room temperature) was then added into the mixture. After further gentle stirring, the mixture was then stored at 4 °C for 3 days before use to ensure air bubbles trapped inside the gel had escaped.

Others: Polyvinyl chloride (PVC) sheet was purchased from Stockline Plastics Limited (Glasgow, UK). Screen printing unit was purchased from Dick Blick Art Materials (Galesburg, IL). Silver paste and Silver-silver chloride (Ag/AgCl) paste were purchased from Advanced Conductive Materials (Atascadero, CA). Insulating paste (Polyurethane) was purchased from Measurement Group UK LTD (Hants, UK). Silicon sheet was purchased from Altec Products Limited (Cornwall, UK). 3M™ Micropore™ Surgical Tape was purchased from 3M Health Care Ltd (Leicestershire, UK). Cellulose membrane was purchased from Sigma Chemical Company (St. Louis, MO).

Nanoporous membrane was used (Spectra/Por® CE (cellulose ester) Dialysis Membranes MWCO: 500, Spectrum Laboratories, Inc., Canada).

3.7.2 Construction of screen-printed electrodes for reverse iontophoresis

The six construction steps of a screen-printed electrode (SPE) are shown schematically in Figure 3.19. The SPEs were constructed using a conventional screen printing technique (Hart and Turner 1996). There are three different layers for each SPE: Insulation shroud, Ag/AgCl pad and conducting track. These three different layers were printed on a clear cellulose membrane sheet one after the other.

Sheets of clear cellulose membrane were cut into pieces approximately 70 mm x 210 mm. Batches of 28 individual SPE were simultaneously printed onto each piece.

Insulation shrouds of insulating paste (polyurethane) were printed to the pieces of cellulose membrane and allowed to dry at room temperature for 3 hours. The screen used to print the insulation shrouds had a mesh size of 390 counts per inch and an emulsion thickness of 25 μm.

Ag/AgCl paste was then printed adjacent to the end of each insulation shroud to form a circular Ag/AgCl pad (diameter = 11.3 mm), the screen for this layer having a mesh size of 390 counts per inch and an emulsion thickness of 25 μm. The Ag/AgCl pad was allowed to dry at room temperature for 3 hours.

After the Ag/AgCl pad was dry, silver paste was printed on top of each Ag/AgCl pad and insulation shroud to form a conducting track and allowed to dry at room temperature for 3 hours. The screen used to print the tracks had a mesh size of 390 counts per inch and an emulsion thickness of 25 μm.

Each batch of the SPE was then reinforced. A PVC sheet (70 mm x 210 mm) with 28 windows was adhered to the printed side of each batch of the SPE by the use of double side adhesive tape. The windows of the PVC sheet should match the end of

the conducting tracks so that connection areas for crocodile clip were still remained (see Figure 3.19f).

After the reinforcement of batches of the SPE, each individual SPE was then separated by the use of scalpel from each batch (see Figure 3.20). A silicon O ring (inner diameter = 11.3 mm, outer diameter = 13 mm, thickness = 1 mm) was adhered to the unprinted side of an individual SPE by the use of double side adhesive tape, with the centre of the silicon O ring located at the centre of the Ag/AgCl pad (see Figure 3.19g).

Finally, the SPEs were stored dry and dark at room temperature.

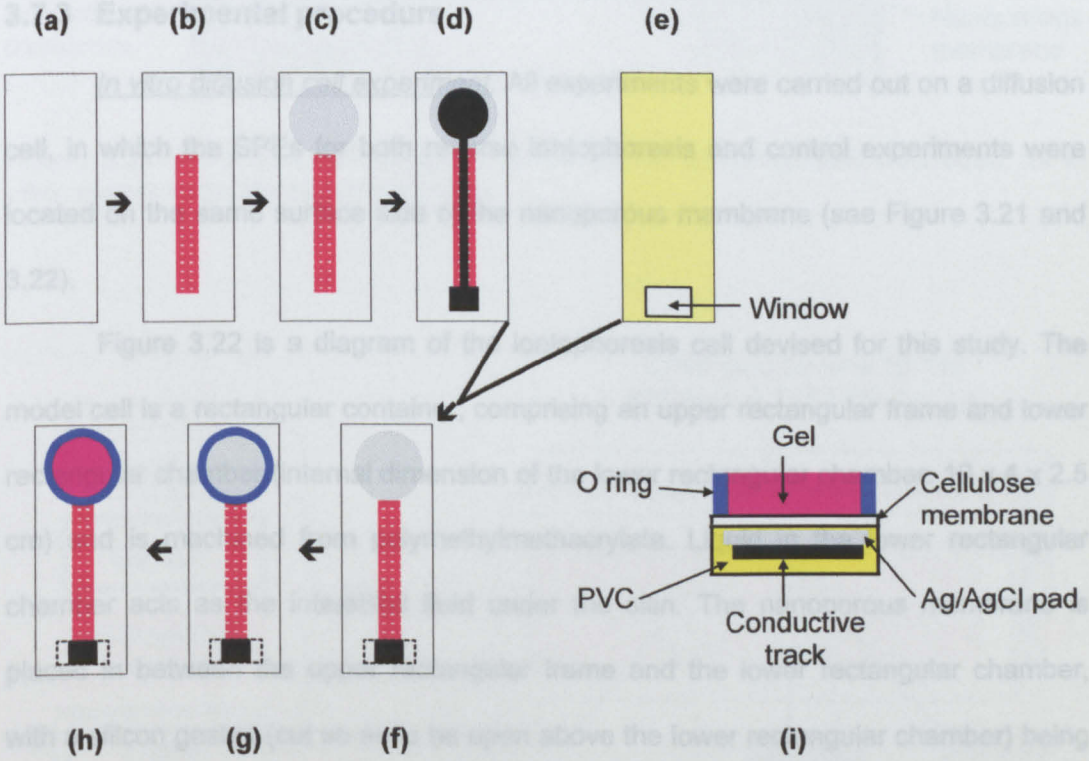

Figure 3.19 – Construction steps for the screen-printed electrode (SPE). **(a)** Support material, cellulose membrane; **(b)** printing of insulation layer; **(c)** printing of Ag/AgCl pad; **(d)** printing of conducting silver track; **(e)** polyvinyl chloride (PVC) sheet with a window; **(f)** reinforcement of the SPE by adhering the PVC sheet to the printed side of the SPE; **(g)** attachment of a silicon O ring on the unprinted side of the SPE; **(h)** filling of 4% MC gel within the O ring boundary (this step will be done just prior to its use in experiments); **(i)** cross-sectional view.

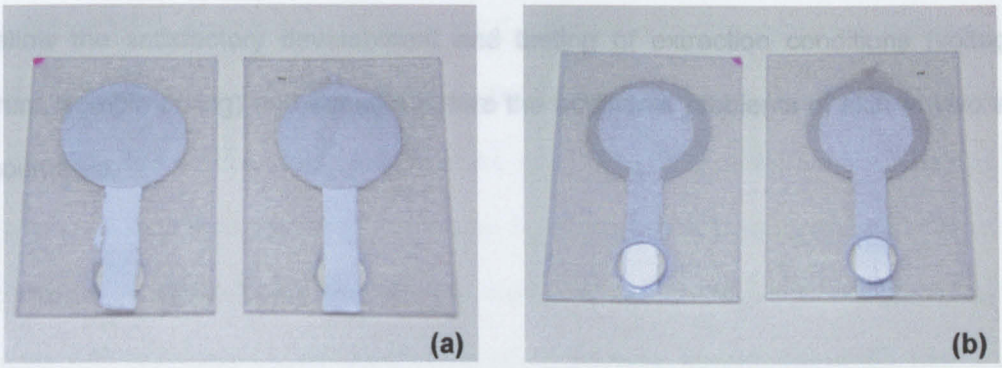

Figure 3.20 – The screen-printed electrodes. **(a)** The front view, with methylcellulose gel (4%) pipetted to this side. **(b)** The back view, with circular window for crocodile clip connection.

3.7.3 Experimental procedure

In vitro diffusion cell experiment: All experiments were carried out on a diffusion cell, in which the SPEs for both reverse iontophoresis and control experiments were located on the same surface side of the nanoporous membrane (see Figure 3.21 and 3.22).

Figure 3.22 is a diagram of the iontophoresis cell devised for this study. The model cell is a rectangular container, comprising an upper rectangular frame and lower rectangular chamber (internal dimension of the lower rectangular chamber: 10 x 4 x 2.5 cm) and is machined from polymethylmethacrylate. Liquid in the lower rectangular chamber acts as the interstitial fluid under the skin. The nanoporous membrane is placed in between the upper rectangular frame and the lower rectangular chamber, with a silicon gasket (cut so as to be open above the lower rectangular chamber) being placed between the nanoporous membrane and the lower rectangular chamber to ensure a good liquid seal. When the model cell has been assembled with the nanoporous membrane in place, filling of the lower rectangular chamber takes place via the inlet port. The nanoporous membrane substitutes for skin in this system. The nanoporous membrane has a negative charge at pH values 7.0 and a molecular cut-off

(for filtration by concentration gradient) of 500 daltons. This model system is designed to allow the satisfactory development and testing of extraction conditions (voltage, current, sample timing) and sensors before the additional problems of skin *in vivo* are encountered.

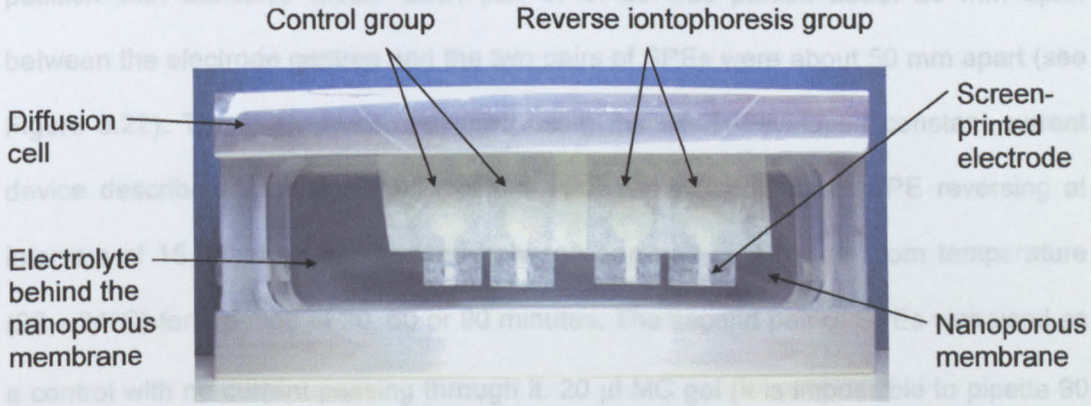

Figure 3.21 – Diffusion cell, designed for the use of screen-printed electrodes, for *in vitro* reverse iontophoresis experiments.

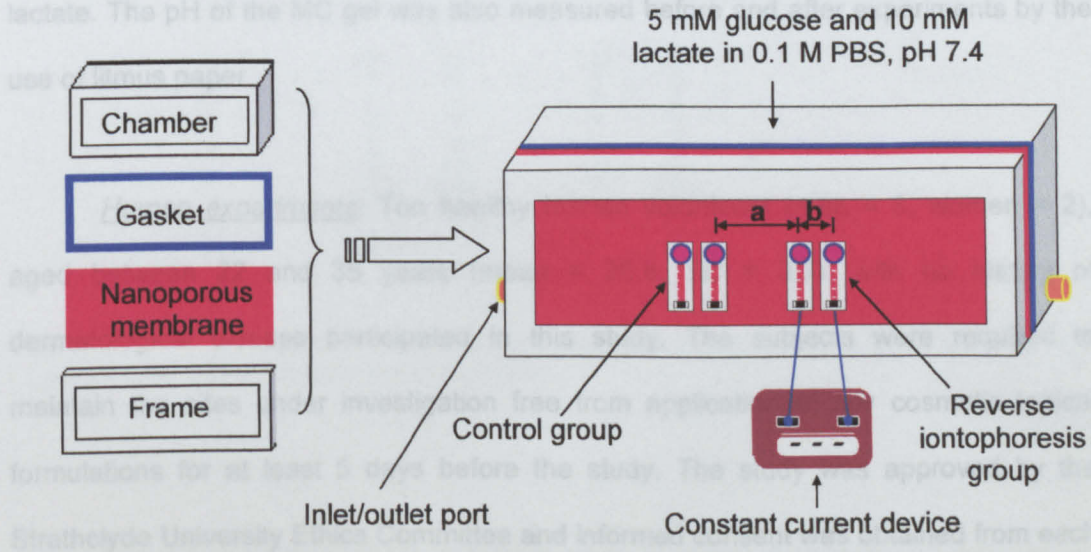

Figure 3.22 – Schematic illustration of the diffusion cell for reverse iontophoresis and control experiments. Where **a** and **b** are 50 mm and 23 mm, respectively.

Having assembled the diffusion cell with the nanoporous membrane in place (see Figure 3.22), the diffusion cell was filled with an electrolyte solution comprising 0.1 M PBS at pH 7.4, 5 mM glucose and 10 mM lactate. Appropriate quantities (90 μl) of a 4% MC gel were pipetted to four SPE at the geometrically defined windows formed by the silicon O ring (see Figure 3.19h). After 5 minutes of MC gel application, the four SPEs were placed onto the nanoporous membrane of the diffusion cell and fixed in position with adhesive tapes. Each pair of SPEs was placed about 23 mm apart between the electrode centres and the two pairs of SPEs were about 50 mm apart (see Figure 3.22). Then, a current (delivered using the newly-developed constant current device described in section 3.4.2) of 0.3 mA/cm^2, with polarity of SPE reversing at intervals of 15 minutes, was passed between one pair of SPEs at room temperature (22 – 24°C) for a period of 30, 60 or 90 minutes. The second pair of SPEs was used as a control with no current passing through it. 20 μl MC gel (It is impossible to pipette 90 μl MC gel back but 20 μl MC gel is guarantee to be pipetted back out of the 90 μl MC gel) was carefully pipetted from each SPE at the end of the experiment and stored separately in microcentrifuge tubes at 4°C for later quantification of glucose and lactate. The pH of the MC gel was also measured before and after experiments by the use of litmus paper.

Human experiments: Ten healthy human volunteers (men = 8, women = 2), aged between 22 and 35 years (mean = 26.8, SD = 3.7), with no history of dermatological disease participated in this study. The subjects were required to maintain the sites under investigation free from application of any cosmetic topical formulations for at least 5 days before the study. The study was approved by the Strathclyde University Ethics Committee and informed consent was obtained from each volunteer. The study instruction and consent form are shown in Appendix C.

MC gel (4%) was pipetted onto four SPEs (90 μl for each SPE). After 5 minutes of MC gel application, the four SPE were placed onto a silver plate and fixed in position with adhesive tapes. Each pair of SPE was about 23 mm apart between the electrode centres and the two pairs of SPE were about 50 mm apart (see Figure 3.23). Each pair of SPEs was then connected to Impedance Analyzer (1294 Impedance Interface in conjunction with SI 1260, Schlumberger Technologies, England) to measure its impedance over the frequency range 1 – $10x10^6$ Hz at increments of 10 frequency points per logarithmic decade with the amplitude of the applied voltage limited to 200 mV. For each pair of SPEs, two measurements were taken. The first measurement was used to eliminate the preconditioning effects (see Appendix D for the detail of the preconditioning effect) while the second measurement was used for determining the impedance of the SPE. After the impedance measurements, MC gel was gently wiped away from each SPE by the use of tissue paper and fresh MC gel was then pipetted to the same SPE (90 μl for each SPE).

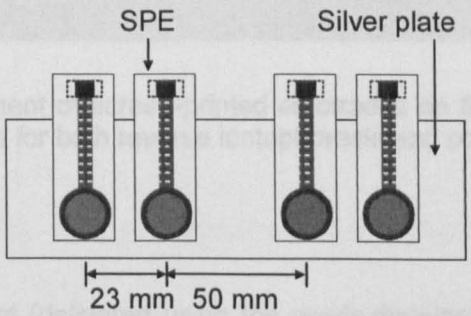

Figure 3.23 – Placement of screen-printed electrodes (SPE) onto a silver plate for the measurement of the impedance of the SPE.

The areas of skin of the subject's inner forearm where the four SPE to be located were prepared by briskly rubbing the areas for 6-8 seconds with alcohol prep pads to remove dry skin, oils and other contaminants. The areas were then allowed to

dry thoroughly. After that, the four SPEs were positioned on the subject's inner forearms and fixed in position with surgical tapes. Each pair of SPE was about 23 mm apart between the electrode centres and the two pairs of SPE were about 50 mm apart (see Figure 3.24). Each pair of SPEs was then connected to Impedance Analyzer (1294 Impedance Interface in conjunction with SI 1260, Schlumberger Technologies, England) to measure the combined impedance of the SPE and the subject's skin twice, with only the second measurement used for impedance analysis.

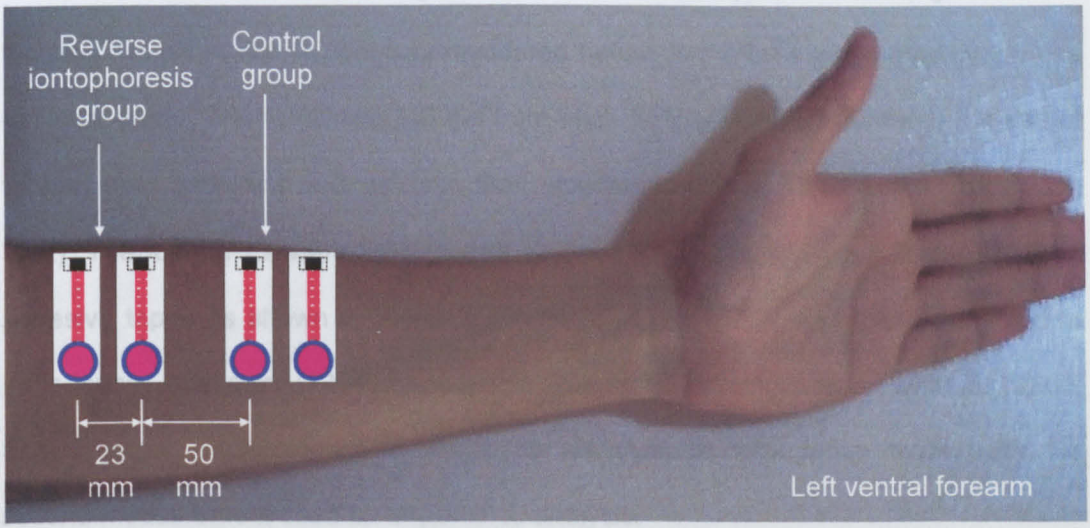

Figure 3.24 – Placement of screen-printed electrodes on the left ventral forearm of a healthy human subject for both reverse iontophoresis and control experiments.

Then, a current (delivered using the newly-developed constant current device described in section 3.4.2) of 0.3 mA, with the polarity of the SPEs reversing at intervals of 15 minutes, was passed between one pair of SPEs at room temperature (22 – 24°C) for a period of 60 minutes. The second pair of SPEs was used as control with no current passing through them. The internal blood glucose and lactate levels were measured before and after experiments by finger stick measurements with a portable glucose meter (FreeStyle Blood Glucose Monitoring System, TheraSense Ltd.,

UK) and portable lactate meter (Accutrend® Lactate, Roche Diagnostics GmbH, Germany), respectively.

At the end of current passage, each pair of SPEs was immediately connected to Impedance Analyzer (1294 Impedance Interface in conjunction with SI 1260, Schlumberger Technologies, England) to measure the combined impedance of the SPE and the subject's skin twice and only the second measurement was used for impedance analysis. After the impedance measurements, all SPEs were removed from the subject's inner forearm. 20 μl MC gel was carefully pipetted from each SPE and stored separately in microcentrifuge tubes at 4°C for later quantification of glucose and lactate. The pH of the MC gel was measured before and after experiments by the use of litmus paper. The remaining MC gel from each SPE was wiped gently by the use of tissue paper and fresh MC gel was then pipetted to the same SPE (90 μl for each SPE). The four SPEs were then placed onto a silver plate and fixed in position with adhesive tapes as shown in Figure 3.23. Each pair of SPEs was then connected to Impedance Analyzer (1294 Impedance Interface in conjunction with SI 1260, Schlumberger Technologies, England) to measure its impedance twice, with the second measurement used for impedance analysis.

3.7.4 Analysis of pre- and post-iontophoresis impedance spectrum of human skin

The skin can be electrically represented in impedance terms as a parallel combination of resistance and capacitance (Yamamoto and Yamamoto 1976), an equivalent circuit of the impedance of the whole system of the screen-printed electrode and human skin can be established as shown in Figure 3.25. Importantly from this, as will be shown, it is possible to determine the dc resistance of human skin which determines the electrical properties of the skin at ultra-low frequencies. This can be an

important guide to skin permeability during and after iontophoresis. The resistances of the skin represents direct charge transport routes (such as ionic current routes) whereas the capacitance is largely due to lipids, particularly in the stratum corneum.

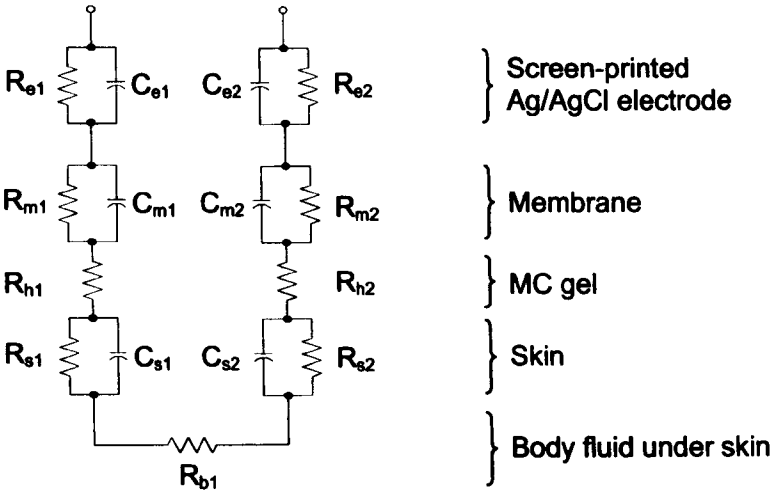

Figure 3.25 – Equivalent circuit of the impedance of the whole system of screen-printed Ag/AgCl electrode and human skin. R_{e1} and R_{e2} as well as C_{e1} and C_{e2} are the resistance and capacitance component of the screen-printed Ag/AgCl electrodes, respectively. R_{m1} and R_{m2} as well as C_{m1} and C_{m2} are the resistance and capacitance component of the membrane of the electrode, respectively. R_{h1} and R_{h2} are the resistance of the MC gel which is mainly resistance even though some polymer molecules exist in the gel. R_{s1} and R_{s2} as well as C_{s1} and C_{s2} are the resistance and capacitance component of the human skin, respectively. R_{b1} is the resistance of the body fluid under skin.

Based on the electric circuit showed on Figure 3.25, the total resistance of the whole system of the screen-printed electrode and human skin could be written:

$$R_{TSE} = \frac{R_{e1}}{1+\omega C_{e1}R_{e1}} + \frac{R_{m1}}{1+\omega C_{m1}R_{m1}} + R_{h1} + \frac{R_{s1}}{1+\omega C_{s1}R_{s1}} + R_{b1} + \frac{R_{e2}}{1+\omega C_{e2}R_{e2}} + \frac{R_{m2}}{1+\omega C_{m2}R_{m2}} + R_{h2} + \frac{R_{s2}}{1+\omega C_{s2}R_{s2}} \quad (3.23)$$

where:

R_{TSE} = Total resistance of the whole system of the screen-printed electrode and human skin

R_{e1} = Resistance of the Ag/AgCl electrode 1

R_{e2} = Resistance of the Ag/AgCl electrode 2

R_{m1} = Resistance of the membrane of the electrode 1

R_{m2} = Resistance of the membrane of the electrode 2

R_{s1} = Resistance of the human skin 1

R_{s2} = Resistance of the human skin 2

R_{h1} and R_{h2} = Resistance of the MC gel

R_{b1} = Resistance of the body fluid under skin

C_{e1} = Capacitance of the Ag/AgCl electrode 1

C_{e2} = Capacitance of the Ag/AgCl electrode 2

C_{m1} = Capacitance of the membrane of the electrode 1

C_{m2} = Capacitance of the membrane of the electrode 2

C_{s1} = Capacitance of the human skin 1

C_{s2} = Capacitance of the human skin 2

ω = Angular frequency = $2\pi f$

When the frequency approaches zero (i.e. ω approaching zero), Equation 3.23 can be rewritten:

$$R_{TSE}^{f\to 0} = R_{e1} + R_{m1} + R_{h1} + R_{s1} + R_{b1} + R_{c2} + R_{m2} + R_{h2} + R_{s2} \qquad (3.24)$$

where:

$R_{TSE}^{f\to 0}$ = Total resistance of the whole system of the screen-printed electrode and human skin as frequency near-zero

When the frequency approaches infinity (i.e. ω approaching infinity), Equation 3.23 can be rewritten:

$$R_{TSE}^{f\to\infty} = R_{h1} + R_{b1} + R_{h2} \tag{3.25}$$

where:

$R_{TSE}^{f\to\infty}$ = Total resistance of the whole system of the screen-printed electrode and human skin as frequency near-infinity

Equation 3.24 subtracted Equation 3.25 resulting:

$$R_{s1} + R_{s2} = \left(R_{TSE}^{f\to 0} - R_{TSE}^{f\to\infty}\right) - \left(R_{e1} + R_{m1} + R_{e2} + R_{m2}\right) \tag{3.26}$$

Similarly, an equivalent circuit of the impedance of the Ag/AgCl electrodes (i.e. screen-printed Ag/AgCl electrode + membrane + MC gel) can be represented as shown in Figure 3.26. Therefore, the total resistance of the whole system of the Ag/AgCl electrode and a silver plate can be written:

$$R_{TXE} = \frac{R_{e1}}{1+\omega C_{e1}R_{e1}} + \frac{R_{m1}}{1+\omega C_{m1}R_{m1}} + R_{h1} + R_{x1} + \frac{R_{e2}}{1+\omega C_{e2}R_{e2}} + \frac{R_{m2}}{1+\omega C_{m2}R_{m2}} + R_{h2} \tag{3.27}$$

where:

R_{TXE} = Total resistance of the whole system of the Ag/AgCl electrode and a silver plate

R_{x1} = Resistance of the silver plate

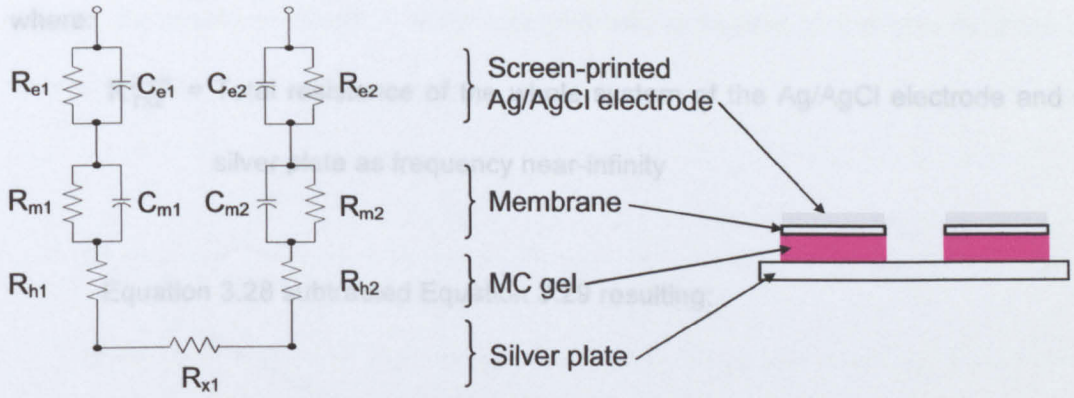

Figure 3.26 – Equivalent circuit of the impedance of the whole system of screen-printed Ag/AgCl electrode and silver plate. R_{e1} and R_{e2} as well as C_{e1} and C_{e2} are the resistance and capacitance component of the screen-printed Ag/AgCl electrodes, respectively. R_{m1} and R_{m2} as well as C_{m1} and C_{m2} are the resistance and capacitance component of the membrane of the electrode, respectively. R_{h1} and R_{h2} are the resistance of the MC gel. R_{x1} is the resistance of the silver plate.

When the frequency approaches zero (i.e. ω approaching zero), Equation 3.27 can be rewritten:

$$R_{TXE}^{f\to 0} = R_{e1} + R_{m1} + R_{h1} + R_{x1} + R_{e2} + R_{m2} + R_{h2} \quad (3.28)$$

where:

$R_{TXE}^{f\to 0}$ = Total resistance of the whole system of the Ag/AgCl electrode and a silver plate as frequency near-zero

When the frequency approaches infinity (i.e. ω approaching infinity), Equation 3.27 can be rewritten:

$$R_{TXE}^{f\to \infty} = R_{h1} + R_{x1} + R_{h2} \quad (3.29)$$

where:

$R_{TXE}^{f\to\infty}$ = Total resistance of the whole system of the Ag/AgCl electrode and a silver plate as frequency near-infinity

Equation 3.28 subtracted Equation 3.29 resulting:

$$R_{e1} + R_{m1} + R_{e2} + R_{m2} = \left(R_{TXE}^{f\to 0} - R_{TXE}^{f\to\infty}\right) \tag{3.30}$$

Equation 3.30 substituted into Equation 3.26 resulting:

$$R_{s1} + R_{s2} = \left(R_{TSE}^{f\to 0} - R_{TSE}^{f\to\infty}\right) - \left(R_{TXE}^{f\to 0} - R_{TXE}^{f\to\infty}\right) \tag{3.31}$$

Therefore, the impedance of human skin, $2R_s$, can be calculated by subtracting $\left(R_{TSE}^{f\to 0} - R_{TSE}^{f\to\infty}\right)$ and $\left(R_{TXE}^{f\to 0} - R_{TXE}^{f\to\infty}\right)$. The value of $\left(R_{TSE}^{f\to 0} - R_{TSE}^{f\to\infty}\right)$ is obtained from the impedance spectrum of the whole system of the screen-printed electrode and human skin as shown in Figure 3.24, while $\left(R_{TXE}^{f\to 0} - R_{TXE}^{f\to\infty}\right)$ is obtained from the impedance spectrum of the whole system of the Ag/AgCl electrode and a silver plate (see Figure 3.23).

The impedance data were presented as plots showing the variation of the impedance magnitude as a function of frequency (see Figure 3.27). Using Figure 3.27 as an example, $R_{TSE}^{f\to 0}$, $R_{TSE}^{f\to\infty}$, $R_{TXE}^{f\to 0}$ and $R_{TXE}^{f\to\infty}$ were about 246.03, 0.04, 25.03 and 0.05 kΩ, respectively. Based on Equation 3.31, the resistive part of electrical impedance, $2R_s$, was about 221.01 kΩ and therefore the electrical resistance R_s of human skin was about 110.51 kΩ in this example. Importantly this is the near dc value of electrical impedance of skin. It is mostly resistance rather than capacitance and this

reflects the electrical situation when iontophoresis is applied to the skin as it too is essentially dc.

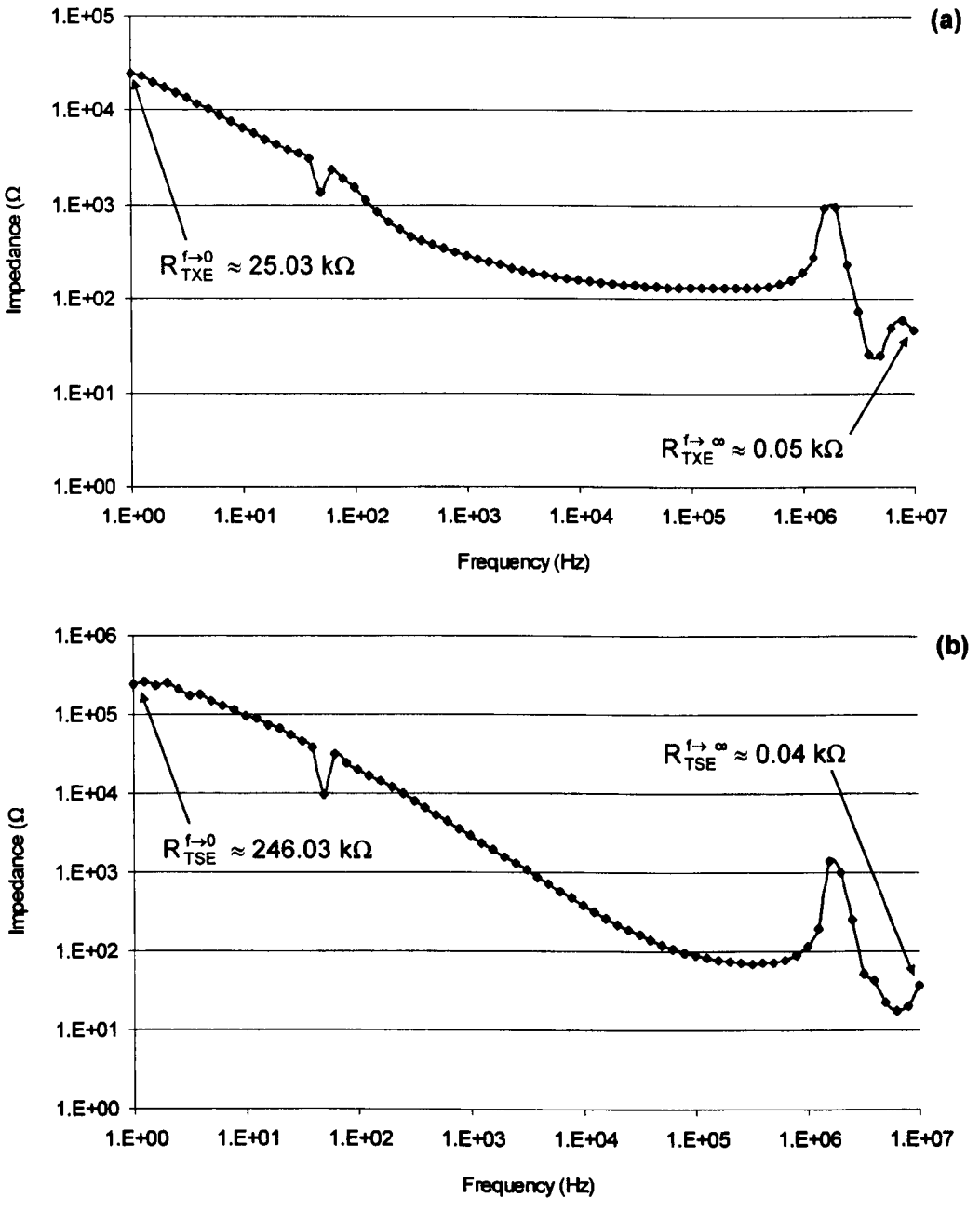

Figure 3.27 – The impedance spectra (data from subject B) of **(a)** a pair of screen-printed electrodes (SPE) measured on a silver plate and **(b)** the human skin plus the pair of SPE. Based on Equation 3.31, the electrical impedance of the human skin is about 110.51 kΩ, (i.e. {[246.03 - 0.04] - [25.03 - 0.05]} / 2 = 110.51 kΩ). The results are shown in Bode Plot form (i.e. total impedance vs. frequency).

3.7.5 Quantification of the extracted glucose and lactate from the MC gel

Glucose and lactate quantification: The amount of glucose and lactate extracted was determined by spectrometric assay using glucose reagents (GL 26233) and lactate reagents (LC 2389) purchased from Randox Laboratories Limited (Antrim, UK) and spectrometer (Multiskan Ascent®, Labsystems Oy, Finland).

All microcentrifuge tubes, with the extracted MC gel after control and reverse iontophoresis experiments, were placed in room temperature (22 – 24°C) for 10 minutes before performing glucose and lactate quantification. Then, 180 μl of 0.1 M PBS was pipetted to each microcentrifuge tube and the mixture of the PBS and extracted MC gel (20 μl) were mixed well with a vortex. 80 μl (for the quantification of glucose) and another 80 μl (for the quantification of lactate) of the mixture were then pipetted from each microcentrifuge tube to a 96 wells Cliniplate (Multiskan Ascent®, Labsystems Oy, Finland) (see Figure 3.28).

Standard solutions for calibration curve were prepared (see Table 3.4). In each standard solution, it contained both glucose and lactate at different concentrations. Standard solution for 0 μM glucose and 0 μM lactate was 0.1 M PBS only while all other standard solutions were prepared by dissolving both glucose and lactate in 0.1 M PBS to achieve the required concentration. Then, standard solutions (480 μl for each concentration) were separately pipetted to 7 new microcentrifuge tubes, with each microcentrifuge tube containing 120 μl of fresh MC gel (4%). The concentrations of the standard solutions for glucose and lactate were therefore changes based on Equation 3.32 (see Table 3.4). The mixture of the standard solution and fresh MC gel were mixed well with a vortex. After that, 80 μl of the mixture was pipetted from each microcentrifuge tube to the same Cliniplate with six replicate wells (see Figure 3.28).

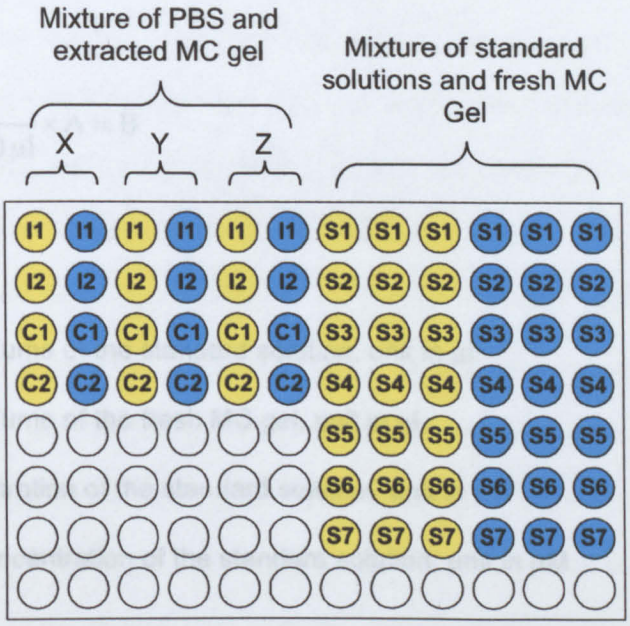

Figure 3.28 – Arrangement of samples and enzymes for the spectrometric analysis of glucose and lactate. Each coloured circle has 80 µl sample and 80 µl enzyme. The yellow and blue circle represented for the glucose and lactate quantification, respectively. Symbols X, Y, and Z represented for 30, 60 and 90 minutes experimental time for control and reverse iontophoresis, respectively. Symbols I1 and I2 represented for the screen-printed electrode 1 and 2 for reverse iontophoresis, respectively. Symbols C1 and C2 represented for the screen-printed electrode 1 and 2 for control, respectively. Symbols S1 to S7 represented for standard solutions of glucose and lactate at different concentrations (see Table 3.4 for the detail of the standard solutions).

Table 3.4 – Standard solutions for the calibration curves of glucose and lactate.

	Standard solutions						
	S1	S2	S3	S4	S5	S6	S7
Glucose concentration (µM)	0	0.125	2.5	5	10	20	50
Lactate concentration (µM)	0	2.5	5	10	20	40	100
Glucose concentration (µM) (after mixing 480 µl standard solution with 120 µl fresh 4% MC gel)	0	0.1	2	4	8	16	40
Lactate concentration (µM) (after mixing 480 µl standard solution with 120 µl fresh 4% MC gel)	0	2	4	8	16	32	80

$$\frac{480\,\mu l}{480\,\mu l + 120\,\mu l} \times A = B \tag{3.32}$$

where:

480 μl = Volume of the standard solution, unit in μl

120 μl = Volume of the fresh MC gel, unit in μl

A = Concentration of the standard solution, unit in μM

B = New concentration of the standard solution, unit in μM

Finally, 80 μl of the glucose reagent was pipetted to the well of the Cliniplate where glucose quantification was performed while 80 μl of the lactate reagent was pipetted to the well of the Cliniplate where lactate quantification was performed (see Figure 3.28). The Cliniplate was immediately placed on the spectrometer and incubated at 37°C for 90 minutes. After incubation, spectrometric analysis of glucose (measured at 500 nm) and lactate (measured at 550 nm) was performed.

All the absorbance data of the standard glucose solutions, standard lactate solutions and extracted glucose and lactate at the MC gel sample were presented in relative absorbance data using Equation 3.33.

$$A_R = A_{TS} - A_{BLANK} \tag{3.33}$$

where:

A_R = Relative absorbance of a test solution i

A_{TS} = Absorbance of the test solution i

A_{BLANK} = Absorbance of the standard solution with 0 μM glucose and 0 μM lactate

By the use of the relative absorbance data of the standard glucose solutions and standard lactate solutions, calibration curves were plotted showing the variation of the relative absorbance as a function of the concentration of the standard glucose/lactate solutions (see Figure 3.29). An excellent linear relationship between glucose concentration and relative absorbance was found with R^2 value being greater than 0.98. An excellent linear relationship ($R^2 \cong 1$) was also found between lactate concentration and relative absorbance. This allows the glucose and lactate concentration to be calculated simply by linear regression. Because the extracted MC gel (20 μl) was mixed with 180 μl of 0.1 M PBS before spectrometric analysis of glucose and lactate, the concentration of the extracted glucose and lactate at the extracted MC gel can be written:

$$\frac{20\,\mu l}{180\,\mu l + 20\,\mu l} \times A = B \tag{3.34}$$

$$A = 10 \text{ x } B \tag{3.35}$$

where:

20 μl = Volume of the extracted MC gel, unit in μl

180 μl = Volume of the 0.1 M PBS, unit in μl

A = Concentration of the extracted glucose/lactate at the extracted MC gel, unit in μM

B = Concentration of the extracted glucose/lactate at the mixture of the 0.1 M PBS (180 μl) and the extracted MC gel (20 μl), unit in μM

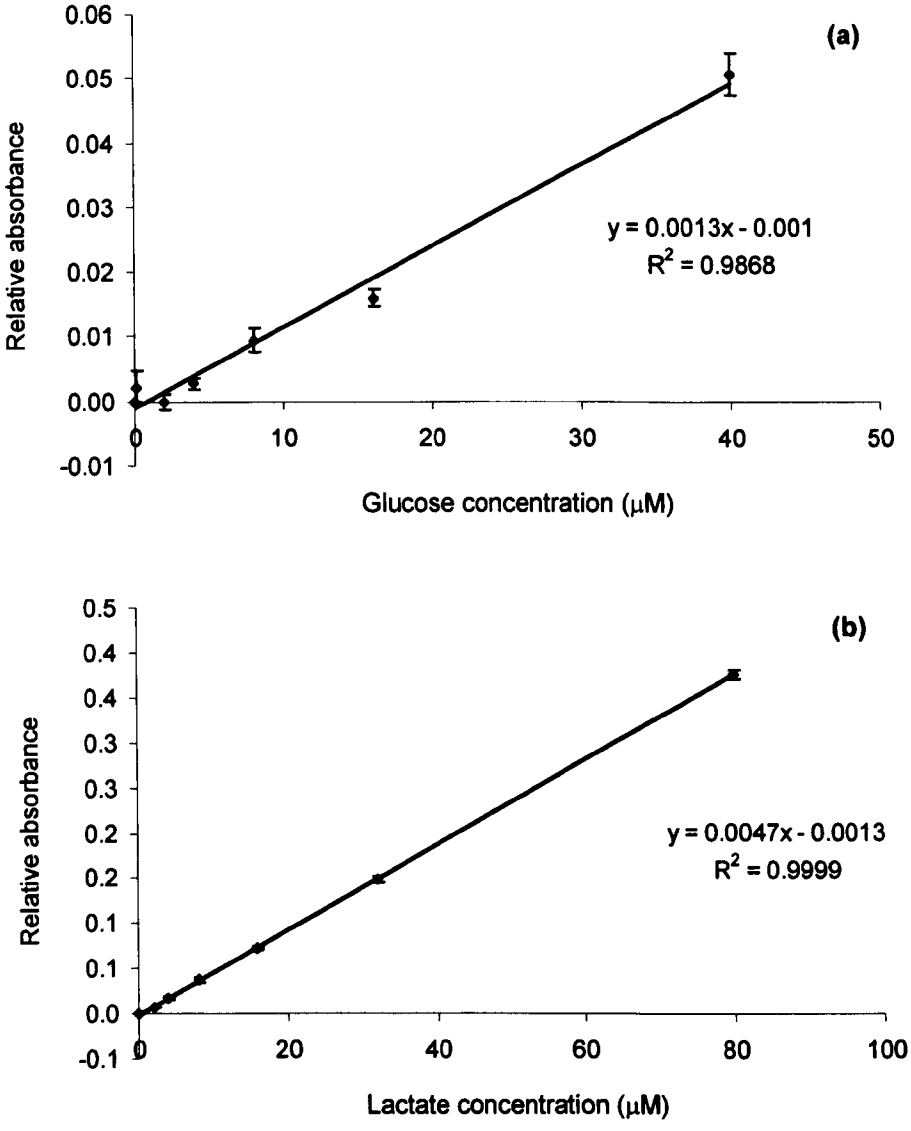

Figure 3.29 – Calibration curves with each point (n = 5) representing the mean ± standard deviation. Standard solutions for the calibration curves are the mixture of 480 μl of 0.1 M PBS, 120 μl of fresh 4% methylcellulose gel and appropriate amount of glucose and lactate. **(a)** The glucose calibration curve. **(b)** The lactate calibration curve.

3.8 ERROR ESTIMATIONS

An effort was made to quantify the total experimental errors in the experimental procedures. Sources of error included the construction of screen-printed electrodes

(SPE) and the removal of MC gel from the SPE after experiments. Error was quantified as the coefficient of variation of a repeated measure.

3.8.1 Error from the construction of screen-printed electrodes

In order to determine the error on the construction of SPE, 5 pairs of SPE were fabricated based on the method described in section 3.7.2. The impedance spectrums of each pair of the SPE were recorded twice in a silver plate, as shown in Figure 3.23, using the impedance analyzer (1294 Impedance Interface in conjunction with SI 1260, Schlumberger Technologies, England). The first trial of the recording of the impedance spectrum was not used to eliminate the preconditioning effects (see Appendix D for the detail of the preconditioning effect) while the second trial of recording was used to compute the resistance of the SPE. Based on Equation 3.30, the resistance of each pair of the SPE was computed. The mean, standard deviation and coefficient of variation of the resistance of the SPE were computed (see Table 3.5).

Table 3.5 – Evaluation of the error on the construction of the screen-printed electrodes.

	Pairs of screen-printed electrode (SPE)				
	1^{st}	2^{nd}	3^{rd}	4^{th}	5^{th}
Resistance ($k\Omega/cm^2$) of the pair of SPE	24.1	27.2	25.0	24.0	27.9
Mean			25.6		
SD			1.8		
Coefficient of variation (%)			7.0		

3.8.2 Error in the removal of MC gel from the screen-printed electrodes after experiments

So as to determine the error in the removal of MC gel from the SPE after experiments, 10 SPE were used. 20 μl MC gel was carefully pipetted from each SPE and stored separately in pre-weighted microcentrifuge tube. Then, the weight of the pre-weighted microcentrifuge tube, having MC gel, was measured again.

The mean, standard deviation and coefficient of variation of the weight of the MC gel, pipetted from the SPE, were computed (see Table 3.6).

Table 3.6 – The result of the evaluation of error on the removal of MC gel from the screen-printed electrode after experiments.

Trial	Weight of the MC gel extracted (g)	Mean (g)	SD (g)	Coefficient of variation (%)
1	0.0164	0.0169	0.0004	2.4
2	0.0168			
3	0.0165			
4	0.0178			
5	0.0174			
6	0.0170			
7	0.0167			
8	0.0169			
9	0.0166			
10	0.0171			

3.9 STATISTICAL ANALYSIS OF PART III

The results of glucose and lactate extraction were expressed as the mean ± standard deviation. For both *in vitro* diffusion cell and human experiment, the independent t-test was used to determine whether there was significant difference

between the electrodes of the control group and the electrodes of reverse iontophoresis groups for the glucose and lactate extraction.

For the *in vitro* diffusion cell experiment, two-way ANOVA was conducted to determine whether there were significant differences between iontophoresis application time (i.e. 30, 60 and 90 min) and group (i.e. control and reverse iontophoresis group) for the glucose and lactate extraction and whether there was a significant interaction between group and iontophoresis application time. Identification of a significant interaction led to further analysis of a simple main effect for groups with an independent t-test. Also, when a significant interaction was identified, one-way ANOVA was used to determine whether there were significant differences between iontophoresis application time within a group for the glucose and lactate extraction and the post hoc comparisons were made with LSD procedure.

For the human experiment, an independent t-test was used to determine whether there was significant difference between control and reverse iontophoresis group for the glucose and lactate extraction.

For the pre-iontophoresis and post-iontophoresis resistance of human skin, two-way ANOVA was conducted to determine whether there were significant differences between groups (i.e. control and reverse iontophoresis groups) and iontophoresis treatments (i.e. before and after experiment) and whether there was a significant interaction between groups and iontophoresis treatments. Identification of a significant interaction led to further analysis of a simple main effect for groups with an independent t-test. Also, when a significant interaction was identified, paired t-test was used to determine whether there were significant differences between iontophoresis treatment within a group for the impedance spectrum of the human skin.

All tests were carried out using SPSS v.10 software (SPSS Inc., Chicago, Illinois, USA) with the level of statistical significance set at 0.05.

■ *Chapter 4*

Results

Part I: Reverse Iontophoresis Optimisation on Glucose and Lactate Extraction

4.1 Error Analysis
4.2 Long Duration Bipolar Direct Current Iontophoresis Effects On Glucose Extraction
4.3 Long Duration Bipolar Direct Current Iontophoresis Effects On Lactate Extraction
4.4 Long Duration Bipolar Direct Current Iontophoresis Effects On Membrane Impedance

Part II: Construction and Evaluation of a Constant Current Device for Reverse Iontophoresis

4.5 Error Analysis
4.6 Electronic Evaluation Of The Circuit Design
4.7 In Vitro Reverse Iontophoresis Evaluation Of The Constant Current Device

Part III: Construction of a Screen-Printed Electrode for Reverse Iontophoresis

4.8 Error Analysis
4.9 In Vitro Reverse Iontophoresis Evaluation Of The Screen-Printed Electrodes
4.10 Long Duration Bipolar Direct Current In Human Transdermal Extraction Of Glucose And Lactate
4.11 Long Duration Bipolar Direct Current Effects On The Electrical Properties Of Human Skin
4.12 Correlation On The Real Blood Glucose/Lactate Levels With The Extracted Glucose/Lactate Levels
4.13 Relationship Between The Skin Impedance, The Real Blood Glucose/Lactate Levels And The Extracted Glucose/Lactate Levels
4.14 Summary

Chapter 4 Results

This chapter consists of three parts. Part I gives the results of the reverse iontophoresis optimisation on glucose and lactate extraction, Part II gives the results of the construction and evaluation of a constant current device for reverse Iontophoresis and Part III details the results of the construction of a screen-printed electrode for reverse iontophoresis.

In Part I, the results cover (1) the error analysis of Part I experiments, (2) the long duration bipolar direct current iontophoresis effects on glucose extraction, (3) the long duration bipolar direct current iontophoresis effects on lactate extraction, and (4) the long duration bipolar direct current iontophoresis effects on membrane impedance.

In Part II, the results cover (1) the error analysis of Part II experiments, (2) the electronic evaluation of the circuit design, and (3) the *in vitro* reverse iontophoresis evaluation of the constant current device.

In Part III, the results of (1) the error analysis of Part III experiments, (2) the *in vitro* reverse iontophoresis evaluation of the screen-printed electrodes, (3) the long duration bipolar direct current in human transdermal extraction of glucose and lactate, (4) the long duration bipolar direct current effects on the electrical properties of human skin, (5) the correlation on the real blood glucose/lactate levels with the extracted glucose/lactate levels, and (6) the relationship between the skin impedance, the real blood glucose/lactate levels and the extracted glucose/lactate levels are illustrated.

Part I: Reverse Iontophoresis Optimisation on Glucose and Lactate Extraction

4.1 ERROR ANALYSIS

This section deals with the effects of experimental error in the experimental arrangements and measurements.

In the fabrication of the Ag/AgCl electrodes, the average variation on the resistance of pair of electrodes due to the chlorination of the silver wire was found to be about ±3.1% (see Table 3.3).

Accuracy of the electrochemical interface (SI1286, Schlumberger Technologies, England) to deliver an iontophoresis current of 0.3 mA/cm^2 was ±0.009%, as revealed by the coefficient of variation of the current measurements (see Figure 3.10).

There is a specific error in readings from the impedance analyser (SI1260, Schlumberger Technologies, England), ± 0.1 % in impedance measurement in the frequency range of 10 μHz up to 32 MHz, which is calculated and given by the manufacturer in the instrument manual.

There is a specific error in readings from the spectrometer (Multiskan Ascent®, Labsystems Oy, Finland), ± 1 % in absorbance measurement, which is calculated and given by the manufacturer in the instrument manual.

In summary, Ag/AgCl electrodes were fabricated to have a small variation in their resistance. The electrochemical interface was found to be precise enough on delivering a constant iontophoresis current. The impedance analyzer and spectrometer were accurate enough in their applications.

4.2 LONG DURATION BIPOLAR DIRECT CURRENT IONTOPHORESIS EFFECTS ON GLUCOSE EXTRACTION

This section deals with the effects of reversing electrode polarity (at 5, 10 and 15 minutes intervals) on glucose extraction over iontophoresis periods of 15, 30, 60 and 90 minutes of total iontophoresis application time. All experiments were carried out on a vertical diffusion cell (see Figure 3.1 and 3.2 for the details of the experimental arrangements).

With no current applied to the model iontophoresis cell (i.e. control experiment), small amounts of glucose were detected in the electrode chambers showing that some diffusion of glucose into the electrode chambers across the nanoporous membrane does occur. With the application of iontophoresis current, more glucose was extracted into both electrode chambers as compared with that of the control experiment and the amount of glucose extracted depended on the switching mode and the duration of the iontophoresis (see Figure 4.1). This confirmed that passage of a current facilitated movement of glucose across the membrane and this is consistent with other researchers (Rao *et al.* 1995).

The experimental results are summarized in Table 4.1 and Figure 4.1. Two-way ANOVA (sample size for each parameter ≥ 12) with iontophoresis application time and switching mode as the fixed factors and glucose extracted as the dependent variable was used to analyse the effect of the periodic electrode polarity reversing and duration of current passage on the glucose extraction. A significant interaction between iontophoresis application time and switching mode was found ($p<0.001$) on the glucose extraction. One-way ANOVA (sample size for each parameter ≥ 12) was then used to investigate the differences among iontophoresis application time and switching mode.

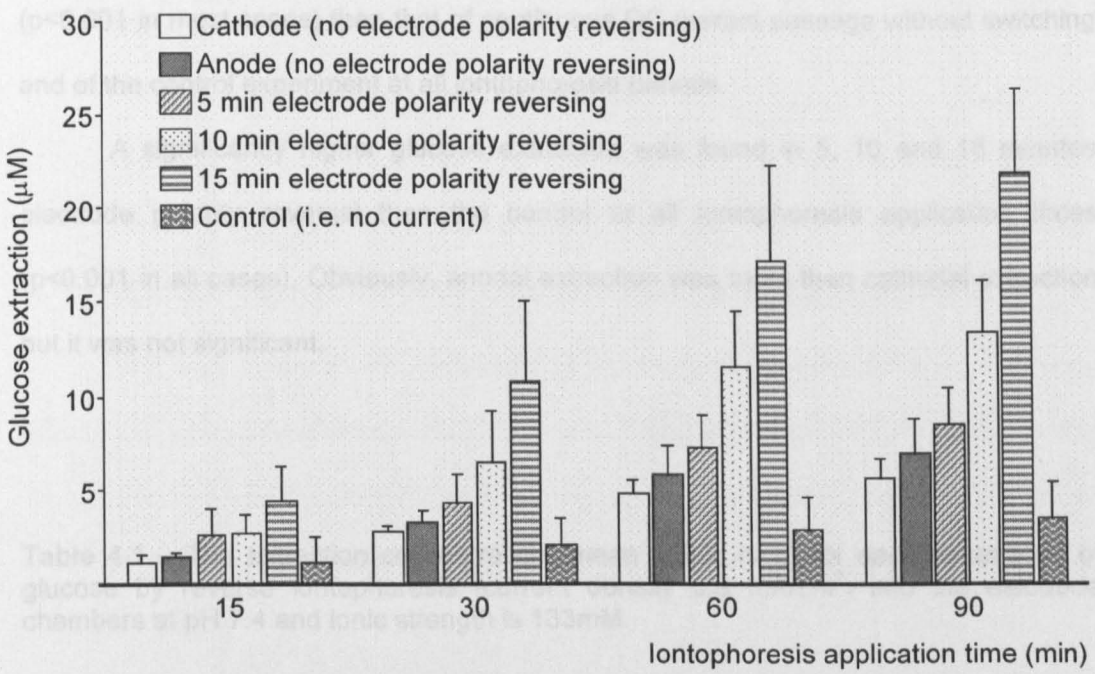

Figure 4.1 – Reverse iontophoresis extraction of glucose (mean ± SD; n≥12 for each bar), as a function of iontophoresis application time. The iontophoresis current was 0.3 mA/cm^2. The electrolyte in the electrode chambers of the diffusion cell was 25 mM, pH 7.4, HEPES buffer containing 133 mM NaCl. The lower chamber of the diffusion cell were filled with an electrolyte solution comprising 133 mM NaCl, buffered to pH 7.4 with 25 mM HEPES, and 5 mM glucose. The results of control and 5, 10 and 15 min electrode polarity reversing are the results from both electrodes.

Comparison of the switching modes against iontophoresis application time using one-way ANOVA (sample size for each parameter ≥ 12) showed that there was a significant difference between the glucose extraction of any of the four switching modes at the four iontophoresis periods (15, 30, 60 and 90 minutes) ($p<0.001$ in all cases). Post-hoc multiple comparisons (a comparison test uses to determine which means differ, once differences exist among the means) using LSD (least significant difference) criteria (sample size for each parameter ≥ 12) showed a significantly high glucose extraction ($p<0.001$ in all cases) with 15 minute electrode polarity reversal against all other switching modes for all iontophoresis periods.

Also, glucose extraction at 10 minute polarity reversal was significantly higher ($p<0.001$ in most cases) than that of continuous DC current passage without switching and of the control experiment at all iontophoresis periods.

A significantly higher glucose extraction was found in 5, 10 and 15 minutes electrode polarity reversal than the control at all iontophoresis application times ($p<0.001$ in all cases). Obviously, anodal extraction was more than cathodal extraction but it was not significant.

Table 4.1 – The extraction concentration (mean ± SD; n≥12 for each parameter) of glucose by reverse iontophoresis (current density 0.3 mA/cm^2) into the electrode chambers at pH 7.4 and ionic strength is 133mM.

Switching mode	Glucose extracted (μM)			
	15 min IT	30 min IT	60 min IT	90 min IT
Cathode	1.17 ± 0.43	2.74 ± 0.31	4.84 ± 0.72	5.69 ± 0.91
Anode	1.41 ± 0.31	3.28 ± 0.61	5.85 ± 1.51	7.01 ± 1.79
5 min EPR	2.56 ± 1.37	4.31± 1.50	7.21 ± 1.75	8.51 ± 1.92
10 min EPR	2.63 ± 1.05	6.40 ± 2.84	11.52 ± 3.00	13.38 ± 2.81
15 min EPR	4.43 ± 1.80	10.75 ± 4.23	17.21 ± 5.15	21.90 ± 4.52
Control	1.14 ± 1.00	2.07 ± 1.17	2.87 ± 1.57	3.47 ± 1.97

Where: • **EPR** is the electrode polarity reversal; **IT** is the iontophoresis application time

Comparison with iontophoresis application times against switching mode using one-way ANOVA (sample size for each parameter ≥ 12) showed that there was a significant difference between the glucose extraction of any of the four iontophoresis periods ($p<0.001$ in all cases). Post-hoc multiple comparisons using LSD criteria (sample size for each parameter ≥ 12) showed consecutive significant increases in glucose extraction were found as the iontophoresis application time increased at each

switching mode ($p<0.05$ in all cases) (see Table 4.1). As expected, the longer the iontophoresis application time, the more glucose is extracted.

4.3 LONG DURATION BIPOLAR DIRECT CURRENT IONTOPHORESIS EFFECTS ON LACTATE EXTRACTION

This section deals with the effects of reversing electrode polarity (at 5, 10 and 15 minutes intervals) on lactate extraction over iontophoresis periods of 15, 30, 60 and 90 minutes of total iontophoresis application time. All experiments were carried out on a vertical diffusion cell (see Figure 3.1 and 3.2 for the details of the experimental arrangements).

Without any applied current (i.e. control experiment) in the model cell, small quantities of lactate were detected in the solution within electrode chambers. This showed that diffusion of lactate into the electrode chambers across the nanoporous membrane took place. With iontophoresis, more lactate was detected in the electrode chambers as compared with the control. Switching mode and the iontophoresis application time were found to be important factors for the determination of the amount of lactate to be extracted across the membrane (see Figure 4.2). Obviously, the results confirmed that passage of a current facilitates movement of lactate across the membrane and this is consistent with work of other researchers (Numajiri *et al.* 1993).

Table 4.2 and Figure 4.2 show the experimental results of long duration bipolar direct current iontophoresis on lactate extraction. Two-way ANOVA (sample size for each parameter ≥ 16) with iontophoresis application time and switching mode as the fixed factors and lactate extracted as the dependent variable was used to analyse the effect of the periodic electrode polarity reversing and duration of current passage on the lactate extraction. It was found that there was a significant interaction between iontophoresis application time and switching mode ($p<0.001$) on the extraction of

lactate. One-way ANOVA was then used to investigate the differences among switching mode and iontophoresis application time.

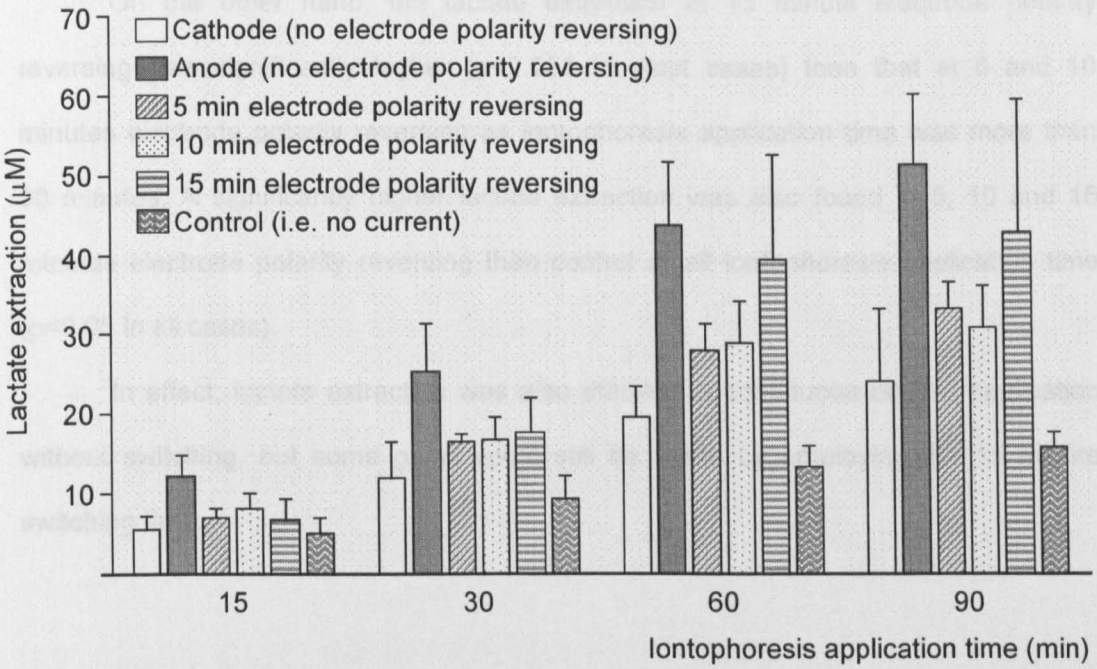

Figure 4.2 – Reverse iontophoresis extraction of lactate (mean ± SD; n≥16 for each bar), as a function of iontophoresis application time. The iontophoresis current was 0.3 mA/cm^2. The electrolyte in the electrode chambers of the diffusion cell was 25 mM, pH 7.4, HEPES buffer containing 133 mM NaCl. The lower chamber of the diffusion cell were filled with an electrolyte solution comprising 133 mM NaCl, buffered to pH 7.4 with 25 mM HEPES, and 10 mM lactate. The results of control and 5, 10 and 15 min electrode polarity reversing are the results from both electrodes.

By the use of one-way ANOVA (sample size for each parameter ≥ 16) to compare different switching modes (reversal of polarity every 5, 10 or 15 minutes) over iontophoresis application times (15, 30, 60 and 90 minutes), a significant difference was found between the four switching modes at the four iontophoresis application times ($p<0.001$ in all cases), with lactate extraction steadily increasing with iontophoresis application time or switching time.

Post-hoc multiple comparisons using LSD criteria (sample size for each parameter ≥ 16) showed a significantly higher lactate extraction ($p<0.001$ in all cases) at the anode during continuous current passage (no polarity reversal) than at the cathode, consistent with the expected behaviour of the negatively charged lactate ion.

On the other hand, the lactate extraction at 15 minute electrode polarity reversing was significantly higher ($p<0.001$ in most cases) than that at 5 and 10 minutes electrode polarity reversing as iontophoresis application time was more than 30 minutes. A significantly higher lactate extraction was also found in 5, 10 and 15 minutes electrode polarity reversing than control at all iontophoresis application time ($p<0.05$ in all cases).

In effect, lactate extraction was also efficient at continuous current application without switching, but some gains could still be made by employing the 15 minute switching time.

Table 4.2 – The extraction concentration (mean ± SD; n≥16 for each parameter) of lactate extracted by reverse iontophoresis (current density 0.3 mA/cm^2) into the electrode chambers at pH 7.4 and ionic strength is 133mM.

Switch manners	**Lactate extracted (μM)**			
	15 min IT	**30 min IT**	**60 min IT**	**90 min IT**
Cathode	5.39 ± 1.81	12.00 ± 4.37	19.56 ± 3.93	24.09 ± 9.23
Anode	12.30 ± 2.53	25.33 ± 5.86	43.76 ± 7.81	51.36 ± 8.96
5 min EPR	6.93 ± 1.23	16.39 ± 1.08	28.00 ± 3.35	33.16 ± 3.28
10 min EPR	8.09 ± 1.99	16.80 ± 2.87	28.92 ± 5.27	30.89 ± 5.11
15 min EPR	6.66 ± 2.70	17.78 ± 4.29	39.45 ± 13.08	42.69 ± 16.90
Control	5.04 ± 1.78	9.35 ± 2.81	13.50 ± 2.44	15.70 ± 1.93

Where: • **EPR** is the electrode polarity reversal; **IT** is the iontophoresis application time

Comparison between iontophoresis application times against switching mode using one-way ANOVA (sample size for each parameter ≥ 16) showed that there was a significant difference between the lactate extraction across the four iontophoresis application times with all switching modes ($p<0.001$ in all cases). Post-hoc multiple comparisons using LSD criteria (sample size for each parameter ≥ 16) showed that consecutive significant increases in lactate extraction were found, as the iontophoresis application time increased, at continuous current passage without switching (i.e. cathode and anode), 5 minute electrode polarity reversing and control ($p<0.05$ in all cases) (see Table 4.2). A successive significant increase in lactate extraction was also found, as the iontophoresis application time increased from 15 minute to 60 minute, at 10 and 15 minutes electrode polarity reversal ($p<0.05$ in all cases). Obviously, the longer the iontophoresis application time, the more lactate is extracted.

4.4 LONG DURATION BIPOLAR DIRECT CURRENT IONTOPHORESIS EFFECTS ON MEMBRANE IMPEDANCE

This section deals with the effects of iontophoresis with reversing electrode polarity (at 5, 10 and 15 minutes intervals) on membrane impedance. The membrane impedance was measured before and after iontophoresis.

The impedance spectra were basically semi-circular in shape. The electrical impedance of the membrane was calculated based on Equation 3.11 (see section 3.1.3 for the detail of the calculation of the electrical impedance of the membrane). In brief, a subtraction of the points crossing the x-axis of the impedance spectra of electrode (see Figure 3.4a for the detail of the experimental setting and Figure 3.7a for the detail of points crossing the x-axis of the impedance spectra of electrode) gave the impedance value of the electrode whereas a subtraction of the points crossing the x-axis of the impedance spectra of membrane (see Figure 3.4b for the detail of the experimental

setting and Figure 3.7b for the detail of points crossing the x-axis of the impedance spectra of membrane) gave the impedance value of the membrane plus the electrode. A subtraction of the impedance value of the membrane plus the electrode and the impedance value of the electrode gave the impedance value of the membrane (see Figure 3.7 for the detail of the calculation of the electrical impedance of membrane).

Initial resistance of the nanoporous membrane was typically 3.3 – 8.3 kΩ/cm^2 at 1 Hz. All pre- and post-iontophoresis impedance spectra exhibited curvature towards the real axis at low frequency, with low frequency data points located at the right hand side of the figure (see Figure 4.3).

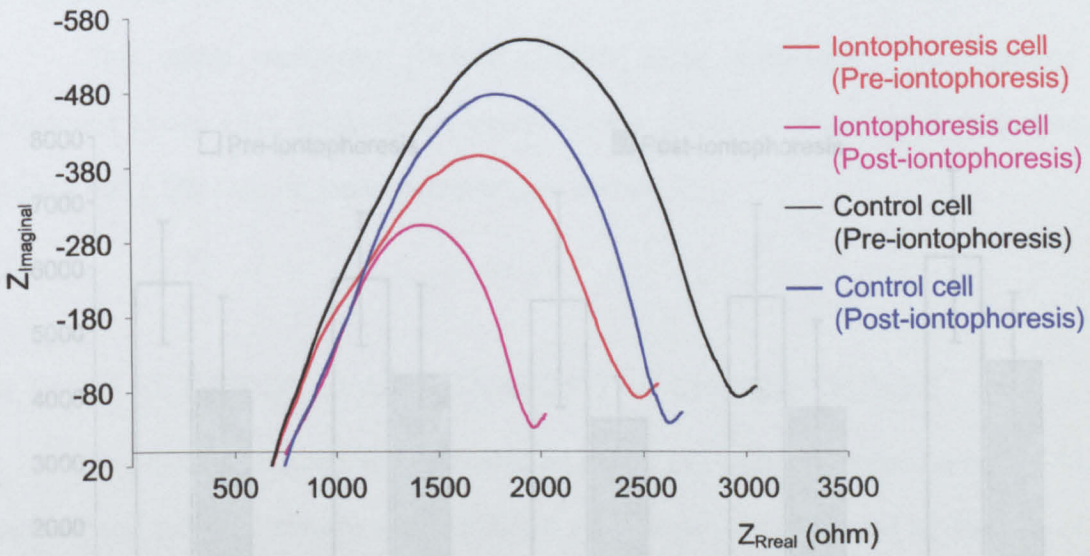

Figure 4.3 – Complex plane impedance spectra of the whole system before and after to the application of an iontophoresis current of 0.3 mA/cm^2.

The experimental results of membrane impedance are summarized in Figure 4.4. Impedance here is calculated at a frequency of 1 Hz to reflect the near dc values of interest for iontophoresis. At this frequency the impedance is effectively only resistive not capacitive. Impedance spectra, measured in glucose and lactate

extraction experiments, were combined together for statistical analysis. Two-way ANOVA (sample size for each parameter ≥ 5) with iontophoresis treatment (i.e. pre- and post-iontophoresis) and switching mode as the fixed factors and membrane impedance as the dependent variable was used to analyse the effect of the iontophoresis treatment and switching mode on the impedance value. The effect of iontophoresis treatment ($p<0.001$), but not switching mode, was found to have a significant effect on the membrane impedance. Post-hoc comparisons using paired t-test criteria (sample size for each parameter ≥ 5) showed that the pre-iontophoresis impedance values was significantly greater ($p<0.001$) than post-iontophoresis impedance values.

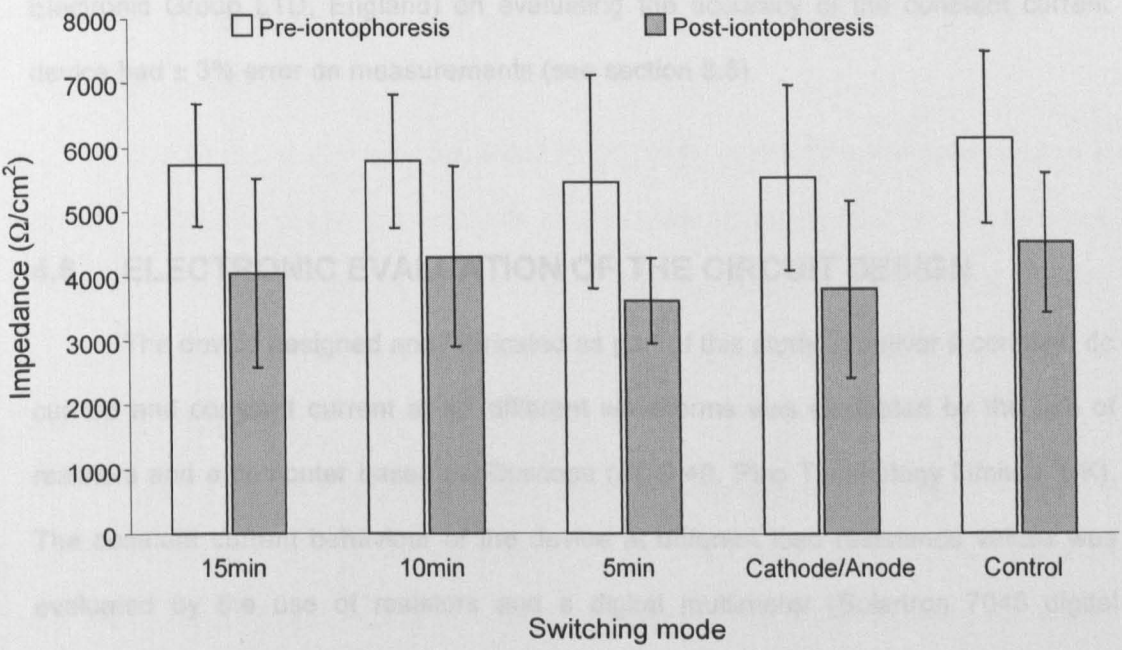

Figure 4.4 – Effect of iontophoresis (0.3 mA/cm^2) on the membrane impedance (mean ± SD; n≥5) at 1 Hz. At this frequency the membrane is almost totally resistive not capacitive.

Part II: Construction and Evaluation of a Constant Current Device for Reverse Iontophoresis

4.5 ERROR ANALYSIS

This section deals with the effects of experimental error in the complete experimental arrangements and measuring system

The computer based oscilloscope (ADC-40, Pico Technology Limited, UK) on evaluating the accuracy of the constant current device had ± 2% error on measurements (see section 3.5).

The digital multimeter (Solartron 7045 digital multimeter, The Solartron Electronic Group LTD, England) on evaluating the accuracy of the constant current device had ± 3% error on measurements (see section 3.5).

4.6 ELECTRONIC EVALUATION OF THE CIRCUIT DESIGN

The device designed and fabricated as part of this study to deliver a constant dc current and constant current at six different waveforms was evaluated by the use of resistors and a computer based oscilloscope (ADC-40, Pico Technology Limited, UK). The constant current behaviour of the device at different load resistance values was evaluated by the use of resistors and a digital multimeter (Solartron 7045 digital multimeter, The Solartron Electronic Group LTD, England). Level of current and battery life were checked.

The results of the evaluation are summarized in Figures 4.5, 4.6 and 4.7 as well as Tables 4.3, 4.4, 4.5 and 4.6. It was found that the accuracy of the device in

delivering constant current, as revealed by the maximum percentage error of current measurements, was about ±0.7% (see Table 4.3).

For different waveforms of applied current (as described in section 3.4.2, see Figure 3.16 for the detail of the different waveforms), the maximum percentage error of the device in terms of current magnitude was found to be about ±1.2% for pulsed DC, ±1% for bipolar DC, ±1.3% for pulsed bipolar DC, ±0% for bipolar DC with a specific rest period where no current was applied and ±1% for pulsed bipolar DC with a specific rest period where no current was applied (see Table 4.4). The accuracy of the device in generating pulsed and bipolar waveforms of currents, as revealed by the maximum percentage error of the measurements of pulsed time and bipolar time, was about ±3% and ±1.5%, respectively (see Table 4.4).

The ability of the device in maintaining a constant current at different load resistance values was found to be about ±1.0% (see Table 4.5), as revealed by the maximum percentage error.

The on-board ammeter appeared to be highly accurate when compared to a digital ammeter in showing the magnitude of current flowing through the probes (see Table 4.6). The best that can be assumed is that the on-board ammeter has ± 0.2% error on measuring current magnitude as the digital ammeter itself has a ± 0.2% error on measuring current.

The device was found to consume very little energy (see Figure 4.7). The current drawn by the whole circuit is about 4 – 27 mA, dependent on the waveform of current required. To generate a DC waveform requires less power (about 36 mW) while more power is required in generating a pulsed bipolar DC waveform (about 243 mW).

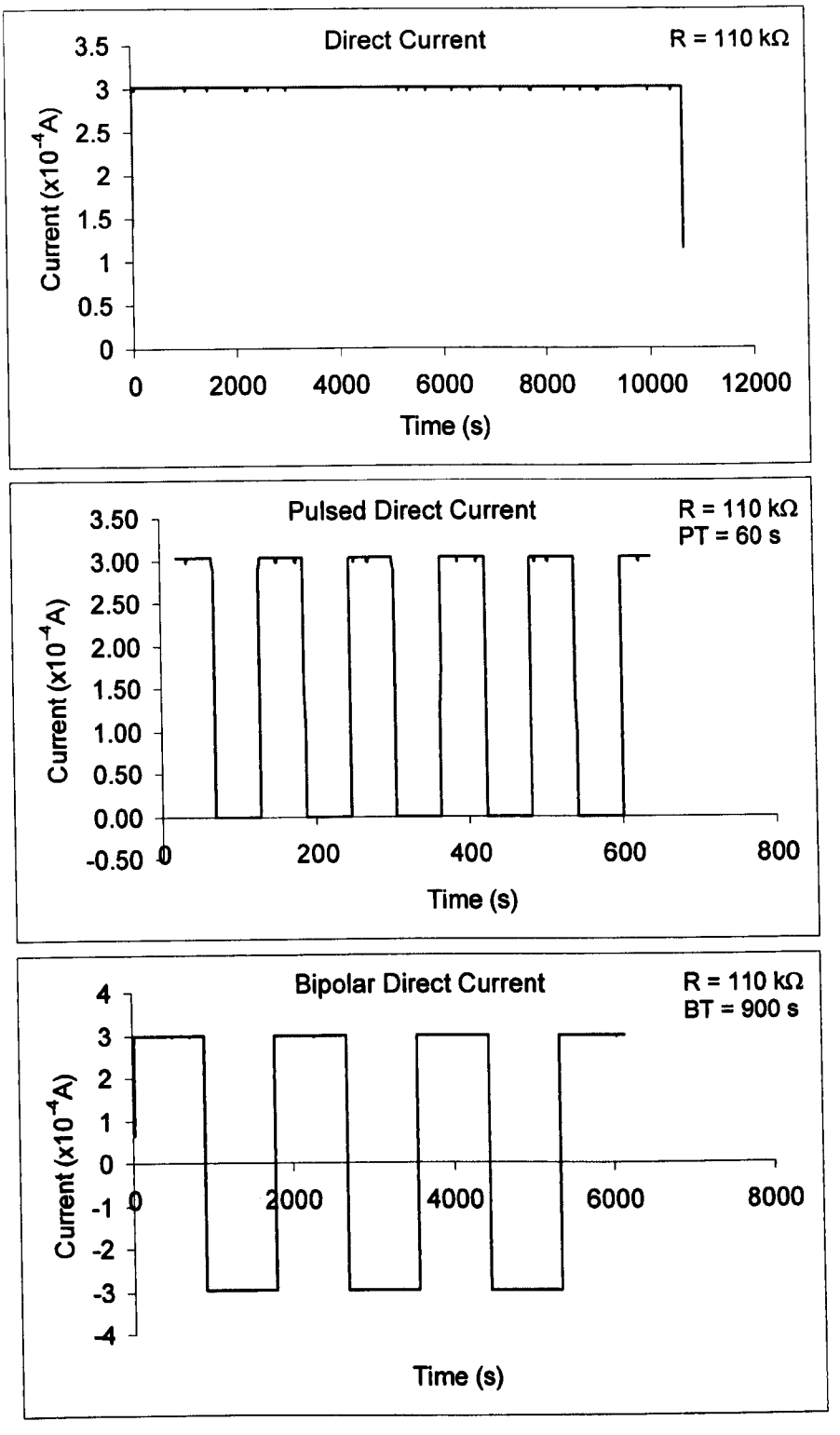

Figure 4.5 – The waveforms of current generated by the constant current device. R is the resistance of the resistor used for evaluation. PT and BT are the programmed pulse time and bipolar time stored inside the microprocessor, respectively. The current setting stored inside the device is 300 μA.

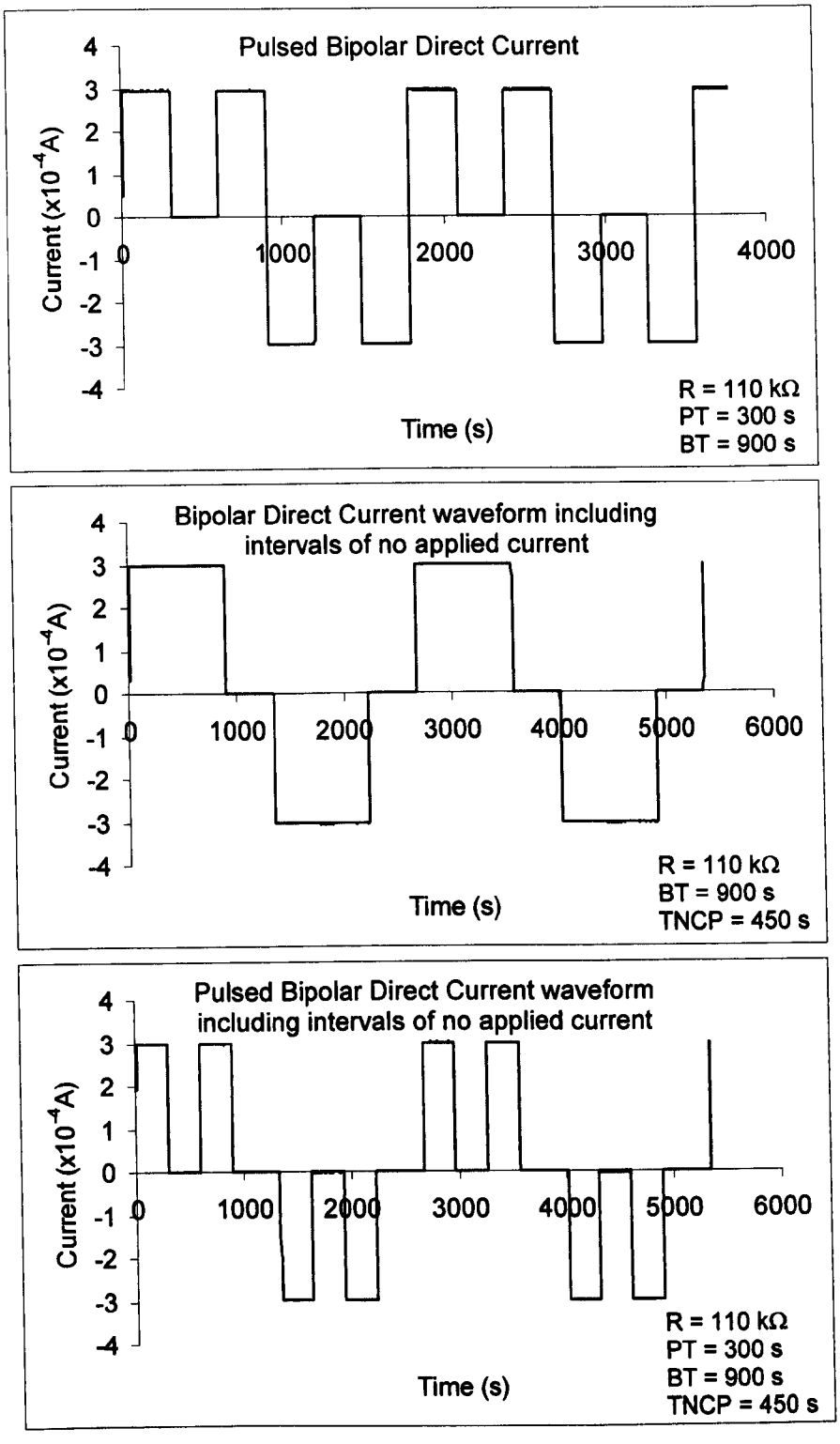

Figure 4.6 – The waveforms of current generated by the constant current device. R is the resistance of the resistor used for evaluation. PT and BT are the programmed pulse time and bipolar time stored inside the microprocessor, respectively. TNCP is the programmed time of no current passage stored inside the microprocessor. The current setting stored inside the device is 300 μA.

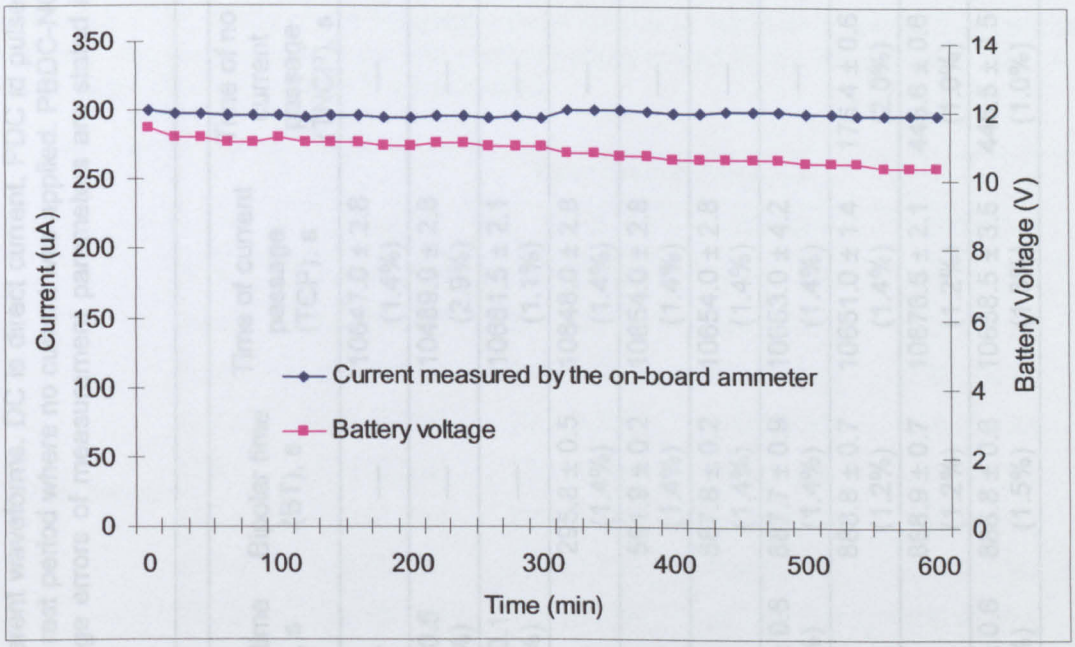

Figure 4.7 – The power consumption of the constant current device. A resistor 100 kΩ ± 1% was connected to the probe of the device. The current setting stored inside the device is 300 μA. A bipolar DC setting (15 minutes bipolar time for the first 5 hours followed by 5 minutes bipolar time for another 5 hours) was programmed into the device.

Table 4.3 – The result (mean ± SD) of the accuracy of the constant current device in delivering constant currents at different magnitude. Percentage errors of current generation, comparison between current setting stored inside the device and the measured current, are stated in parentheses.

Waveform of current	Current setting (I) stored inside the device, μA	Resistance of resistor, kΩ	Measured parameter
			Current , μA
Direct Current	I = 1	49	1.0 ± 0.02 (0.0%)
		110	1.0 ± 0.03 (0.0%)
	I = 100	49	100.0 ± 0.01 (0.0%)
		110	100.0 ± 0.01 (0.0%)
	I = 200	49	200.0 ± 0.01 (0.0%)
		110	200.0 ± 0.01 (0.0%)
	I = 300	49	302.0 ± 0.02 (0.7%)
		110	302.0 ± 0.02 (0.7%)

Table 4.4 – The result (mean ± SD) of the accuracy of the constant current device for different waveforms. DC is direct current. PDC id pulsed DC. BDC is bipolar DC. PBDC is pulsed bipolar DC. BDC-NO is bipolar DC with a specific rest period where no current was applied. PBDC-NO is pulsed bipolar DC with a specific rest period where no current was applied. Percentage errors of measurement parameters are stated in parentheses.

Waveform of current	Program setting stored inside the microprocessor (I = 300μA, TCP = 10800s)	Resistance of resistor, kΩ	Measured parameters				
			Current (I), μA	Pulse time (PT), s	Bipolar time (BT), s	Time of current passage (TCP), s	Time of no current passage (TNCP), s
DC		49	302.0 ± 0.018 (0.7%)	—	—	10647.0 ± 2.8 (1.4%)	—
		110	302.0 ± 0.024 (0.7%)				
PDC	PT = 10 s	49	296.4 ± 0.064 (1.2%)	9.7 ± 0.5 (3.0%)	—	10489.0 ± 2.8 (2.9%)	—
		110	296.5 ± 0.063 (1.2%)				
	PT = 60 s	49	301.4 ± 0.042 (0.5%)	59 ± 0.1 (1.7%)	—	10681.5 ± 2.1 (1.1%)	—
		110	301.4 ± 0.042 (0.5%)				
BDC	BT = 300 s	49	299.9 ± 0.108 (0.0%)	—	295.8 ± 0.5 (1.4%)	10648.0 ± 2.8 (1.4%)	—
		110	299.7 ± 0.094 (0.1%)				
	BT = 600 s	49	299.8 ± 0.081 (0.1%)	—	591.9 ± 0.2 (1.4%)	10654.0 ± 2.8 (1.4%)	—
		110	300.1 ± 0.107 (0.0%)				
	BT = 900 s	49	296.9 ± 0.069 (1.0%)	—	887.8 ± 0.2 (1.4%)	10654.0 ± 2.8 (1.4%)	—
		110	297.6 ± 0.069 (0.8%)				
PBDC	PT =300 s, BT = 900 s	49	296.8 ± 0.133 (1.1%)	295.9 ± 0.6 (1.4%)	887.7 ± 0.9 (1.4%)	10653.0 ± 4.2 (1.4%)	—
		110	296.2 ± 0.120 (1.3%)				
BDC-NO	BT = 900 s, TNCP = 180 s	49	299.9 ± 0.068 (0.0%)	—	888.8 ± 0.7 (1.2%)	10651.0 ± 1.4 (1.4%)	176.4 ± 0.6 (2.0%)
		110	300.0 ± 0.068 (0.0%)				
	BT = 900 s, TNCP = 450 s	49	300.0 ± 0.068 (0.0%)	—	888.9 ± 0.7 (1.2%)	10676.5 ± 2.1 (1.2%)	445.6 ± 0.6 (1.0%)
		110	300.0 ± 0.068 (0.0%)				
PBDC-NO	PT = 300 s, BT = 900 s, TNCP = 450 s	49	297.0 ± 0.133 (1.0%)	295.6 ± 0.6 (1.5%)	886.8 ± 0.6 (1.5%)	10658.5 ± 3.5 (1.3%)	445.5 ± 0.5 (1.0%)
		110	297.2 ± 0.133 (0.9%)				

Table 4.5 – The ability of the constant current device to maintain a constant current at different load resistance values. The current setting stored inside the device is 300 μA. Percentage errors are stated in parentheses.

		Measured current, μA			
		0 kΩ	**1 kΩ**	**82 kΩ**	**100 kΩ**
Short period	30 s	300 (0.0%)	299 (0.3%)	299 (0.3%)	299 (0.3%)
	60 s	300 (0.0%)	299 (0.3%)	299 (0.3%)	299 (0.3%)
	90 s	299 (0.3%)	299 (0.3%)	299 (0.3%)	300 (0.0%)
	120 s	299 (0.3%)	299 (0.3%)	299 (0.3%)	300 (0.0%)
	150 s	299 (0.3%)	299 (0.3%)	299 (0.3%)	300 (0.0%)
	180 s	299 (0.3%)	299 (0.3%)	299 (0.3%)	300 (0.0%)
	210 s	299 (0.3%)	299 (0.3%)	299 (0.3%)	300 (0.0%)
	240 s	299 (0.3%)	299 (0.3%)	299 (0.3%)	300 (0.0%)
	270 s	299 (0.3%)	299 (0.3%)	299 (0.3%)	300 (0.0%)
	300 s	299 (0.3%)	299 (0.3%)	299 (0.3%)	300 (0.0%)
Long period	30 min	299 (0.3%)			298 (0.7%)
	60 min	299 (0.3%)			298 (0.7%)
	120 min	299 (0.3%)			297 (1.0%)

Table 4.6 – The result (mean ± SD) of the test of accuracy of the on-board ammeter in displaying the magnitude of current flowing through the probes. CID is current setting stored inside the device. DA is the digital ammeter reading. OBA is the on-board ammeter reading. Percentage errors, comparison between DA and OBA, are stated in parentheses.

CID, μA	**Device**	**Measured current, μA**						**Mean, μA**	**SD, μA**
		Trial 1	Trial 2	Trial 3	Trial 4	Trial 5	Trial 6		
1	DA	1.0	1.0	1.0	1.0	1.0	1.0	1.0 (0%) 1.0	0.0 0.0
	OBA	1.0	1.0	1.0	1.0	1.0	1.0		
100	DA	100.0	100.0	100.0	100.0	100.0	100.0	100.0 (0%) 100.0	0.0 0.0
	OBA	100.0	100.0	100.0	100.0	100.0	100.0		
200	DA	200.1	200.1	200.1	200.1	200.1	200.1	200.1 (0%) 200.0	0.0 0.0
	OBA	200.0	200.0	200.0	200.0	200.0	200.0		
300	DA	300.0	300.0	299.9	299.9	299.9	299.9	299.9 (0%) 300.7	0.1 0.5
	OBA	300.0	301.0	300.0	301.0	301.0	301.0		

4.7 *IN VITRO* REVERSE IONTOPHORESIS EVALUATION OF THE CONSTANT CURRENT DEVICE

To evaluate the performance of the constant current device for glucose and lactate extraction by reverse iontophoresis and to measure the change of the electrical properties of the membrane after exposure to the device, a series of different experiments were conducted.

Glucose and lactate extraction by the use of the constant current device

This section deals with the evaluation of the constant current device on the glucose and lactate extraction. All experiments were carried out on a vertical diffusion cell (see Figure 3.1 and 3.2 for the detail of the experimental arrangements). Only one switching mode (the polarity of electrodes reversing at intervals of 15 minutes) was used on glucose and lactate extraction over iontophoresis periods of 15, 30, 60 and 90 minutes of total iontophoresis application time.

The experimental results are summarized in Figure 4.8 and 4.9. With application of iontophoresis current, more glucose and lactate was extracted as compared with that of control. Comparison between the control group and reverse iontophoresis group (15 minutes electrode polarity reversing) over iontophoresis application time using the independent t-test (sample size for each parameter ≥ 4) showed that glucose and lactate extraction by the application of current with 15 minutes electrode polarity reversing was significantly higher than that by diffusion alone at all four iontophoresis periods ($p<0.001$ in all cases). Comparison among iontophoresis application times using one-way ANOVA with post-hoc multiple comparisons using LSD criteria (sample size for each parameter ≥ 4) showed that consecutive significant increases in glucose and lactate extraction were found as reverse iontophoresis application time is increased ($p<0.001$ in all cases). Obviously,

the longer the iontophoresis application time, the more glucose and lactate are extracted.

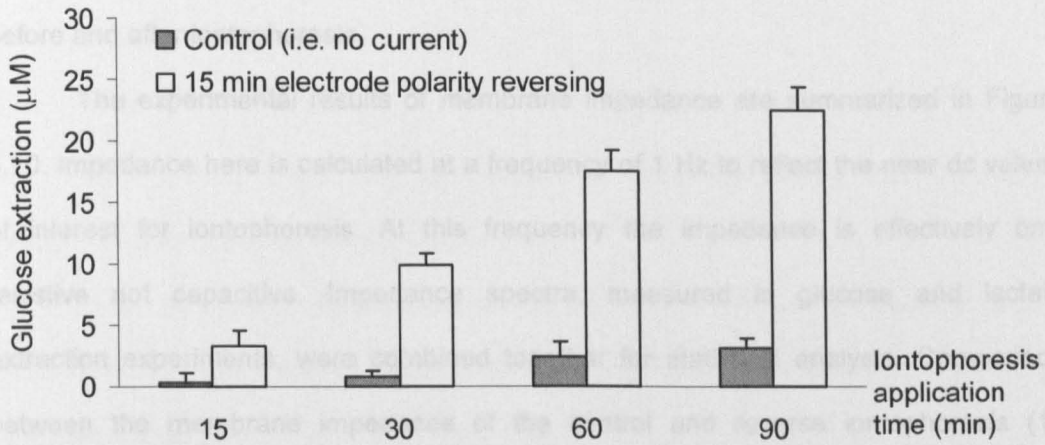

Figure 4.8 – Reverse iontophoresis extraction of glucose (mean ± SD; n≥4 for each bar), as a function of iontophoresis application time. The iontophoresis current (0.3 mA/cm^2) was delivered by the constant current device. The electrolyte in the electrode chambers of the diffusion cell was 25 mM, pH 7.4, HEPES buffer containing 133 mM NaCl. The lower chamber of the diffusion cell were filled with an electrolyte solution comprising 133 mM NaCl, buffered to pH 7.4 with 25 mM HEPES, and 5 mM glucose.

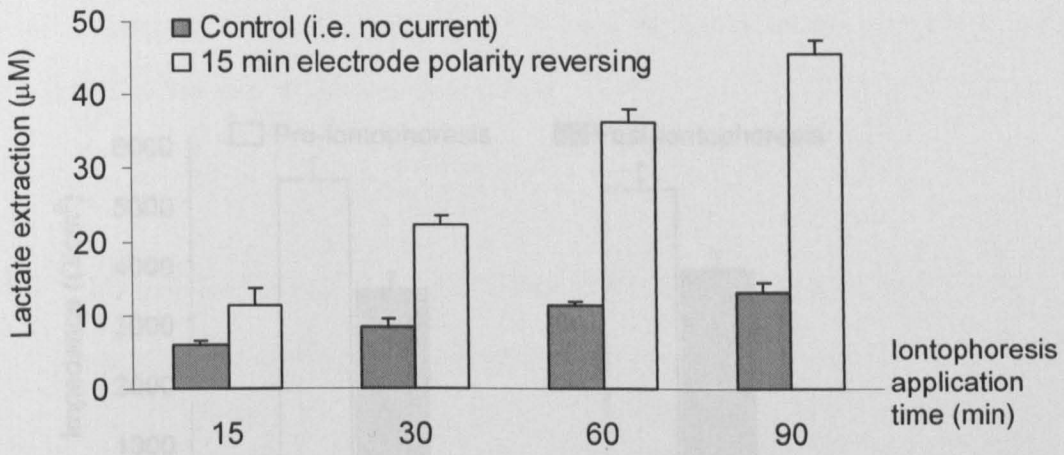

Figure 4.9 – Reverse iontophoresis extraction of lactate (mean ± SD; n≥4 for each bar), as a function of iontophoresis application time. The iontophoresis current (0.3 mA/cm^2) was delivered by the constant current device. The electrolyte in the electrode chambers of the diffusion cell was 25 mM, pH 7.4, HEPES buffer containing 133 mM NaCl. The lower chamber of the diffusion cell were filled with an electrolyte solution comprising 133 mM NaCl, buffered to pH 7.4 with 25 mM HEPES, and 10 mM lactate.

The effects of the use of the constant current device on the membrane impedance

This section deals with the effects of iontophoresis, performed by the constant current device, on membrane impedance. The membrane impedance was measured before and after iontophoresis.

The experimental results of membrane impedance are summarized in Figure 4.10. Impedance here is calculated at a frequency of 1 Hz to reflect the near dc values of interest for iontophoresis. At this frequency the impedance is effectively only resistive not capacitive. Impedance spectra, measured in glucose and lactate extraction experiments, were combined together for statistical analysis. Comparison between the membrane impedance of the control and reverse iontophoresis (15 minutes electrode polarity reversing) using independent t-test (sample size for each parameter = 4) showed no significant difference ($p>0.05$ in all cases). Paired t-test (sample size for each parameter = 4) showed that the pre-iontophoresis membrane impedance was significantly greater ($p<0.05$ in all cases) than post-iontophoresis membrane impedance.

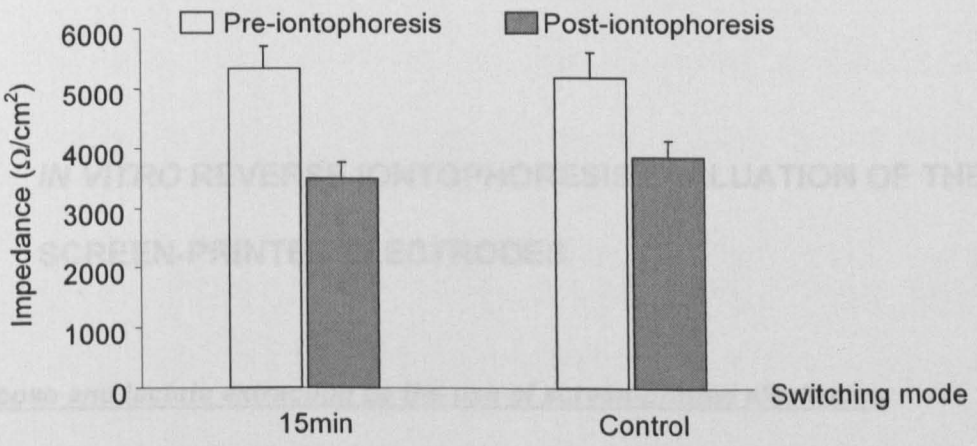

Figure 4.10 – Effect of reverse iontophoresis (0.3 mA/cm^2 delivered by the constant current device) on the membrane impedance (mean ± SD; n=4 for each bar).

Part III: Construction of a Screen-Printed Electrode for Reverse Iontophoresis

4.8 ERROR ANALYSIS

This section deals with the effects of error introducing into the whole experimental arrangements and measurements.

In the fabrication of the screen-printed electrodes, the average variation on the resistance of pair of electrodes due to the fabrication process was found to be about ±7% (see Table 3.5).

The error in the removal of methylcellulose gel from the screen-printed electrode after experiments was about ±2.4%, as revealed by the coefficient of variation of the weight measurement of the removed methylcellulose gel from the screen-printed electrode (see Table 3.6).

In summary, screen-printed electrodes were fabricated to have a small variation in their resistance. The removal method of the methylcellulose gel from the screen-printed electrode was reliable and repeatable.

4.9 *IN VITRO* REVERSE IONTOPHORESIS EVALUATION OF THE SCREEN-PRINTED ELECTRODES

Glucose and lactate extraction by the use of screen-printed electrodes

This section deals with the evaluation of the screen-printed electrodes on the glucose and lactate extraction. All experiments were carried out on a specially-designed diffusion cell (see Figure 3.21 and 3.22 for the detail of the experimental

arrangements). The newly-developed constant current device was used to provide a constant current. Only one switching mode (the polarity of electrodes reversing at intervals of 15 minutes) was used on glucose and lactate extraction over iontophoresis periods of 30, 60 and 90 minutes of total iontophoresis application time.

The experimental results are summarized in Table 4.7 and Figure 4.11. Small amounts of glucose and lactate were detected at the control groups showed that diffusion of glucose and lactate into the methylcellulose gel of the SPE across the nanoporous membrane took place. It was also found that the pH of the methylcellulose gel remained the same (midway between pH 7 and pH 8 as measured by litmus paper) after reverse iontophoresis.

Table 4.7 – *In vitro* evaluation of the screen-printed electrodes showing the extraction (mean ± SD; n=5) of glucose and lactate by reverse iontophoresis (current density 0.3 mA/cm^2) into the 4% methylcellulose gel (preparing in 0.1 M PBS, pH 7.4) of the screen-printed electrodes. Standard deviations are stated in parentheses.

IT (min)	Glucose (μM)				Lactate (μM)			
	Control		Reverse Iontophoresis		Control		Reverse Iontophoresis	
	SPE 1	SPE 2	SPE 3	SPE 4	SPE 1	SPE 2	SPE 3	SPE 4
30	39.98 (11.64)	23.67 (11.95)	164.23 (29.87)	235.13 (62.42)	152.89 (130.31)	187.21 (75.55)	323.86 (116.41)	273.35 (64.45)
60	56.47 (17.90)	41.96 (21.82)	212.51 (86.99)	269.78 (56.60)	228.76 (46.41)	232.41 (88.05)	632.08 (51.97)	535.16 (174.25)
90	79.01 (34.12)	134.86 (39.05)	396.32 (119.06)	312.78 (61.69)	294.62 (89.47)	267.85 (56.88)	709.97 (98.51)	661.82 (96.60)

Where: SPE1, SPE2, SPE3 and SPE4 are the screen-printed electrodes.
IT is the iontophoresis application time.

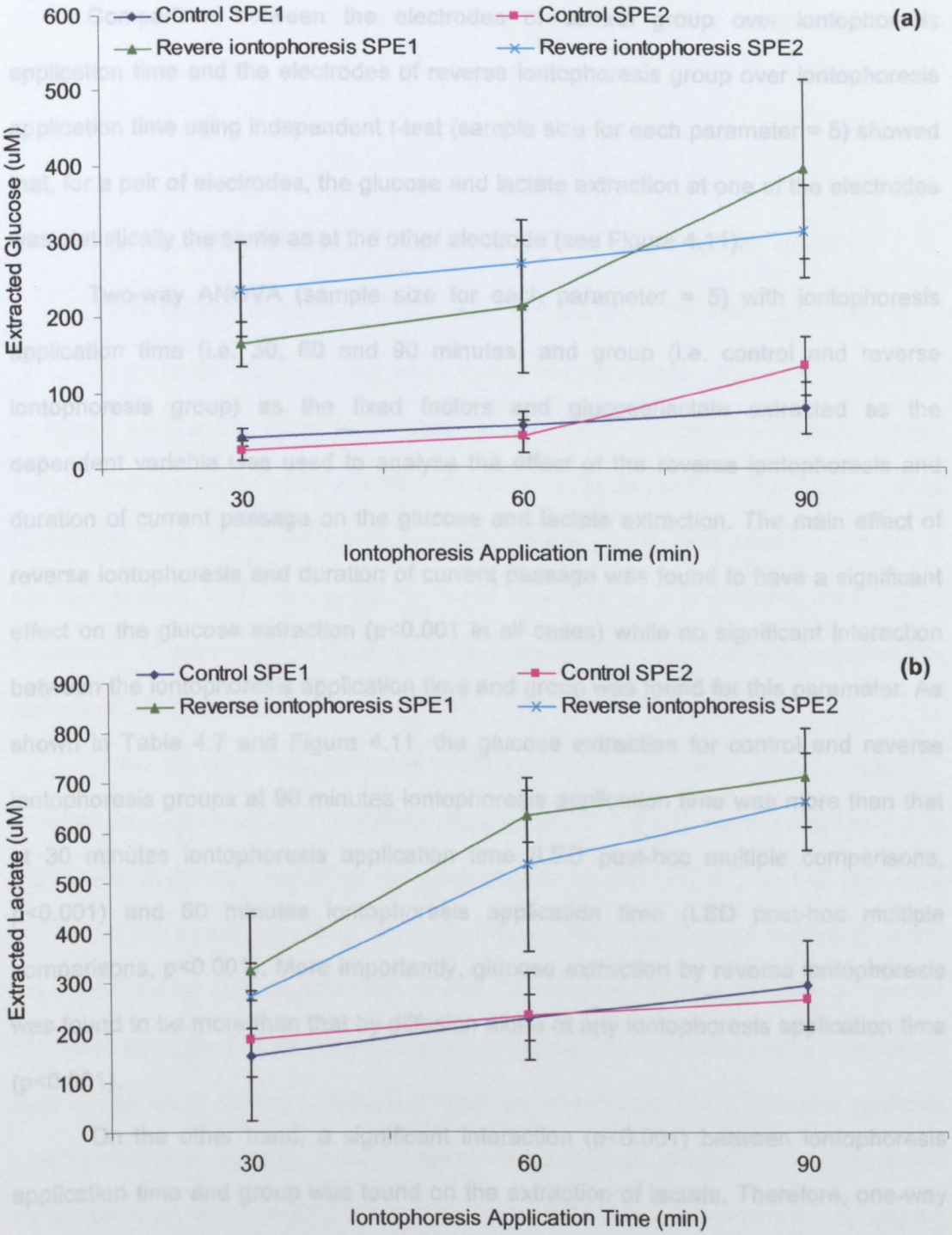

Figure 4.11 – *In vitro* evaluation of the screen-printed electrodes showing the reverse iontophoresis extraction of glucose and lactate by the use of screen-printed electrodes (mean ± SD; n=5 for each point), as a function of iontophoresis application time. The iontophoresis current was 0.3 mA/cm^2. The electrolyte in the diffusion cell was 0.1 M PBS, pH 7.4 containing 5 mM glucose and 10 mM lactate. The gel at the screen-printed electrodes was 4% methylcellulose gel in 0.1 mM PBS, pH 7.4. **(a)** glucose extraction and **(b)** lactate extraction.

Comparison between the electrodes of control group over iontophoresis application time and the electrodes of reverse iontophoresis group over iontophoresis application time using independent t-test (sample size for each parameter = 5) showed that, for a pair of electrodes, the glucose and lactate extraction at one of the electrodes was statistically the same as at the other electrode (see Figure 4.11).

Two-way ANOVA (sample size for each parameter = 5) with iontophoresis application time (i.e. 30, 60 and 90 minutes) and group (i.e. control and reverse iontophoresis group) as the fixed factors and glucose/lactate extracted as the dependent variable was used to analyse the effect of the reverse iontophoresis and duration of current passage on the glucose and lactate extraction. The main effect of reverse iontophoresis and duration of current passage was found to have a significant effect on the glucose extraction ($p<0.001$ in all cases) while no significant interaction between the iontophoresis application time and group was found for this parameter. As shown in Table 4.7 and Figure 4.11, the glucose extraction for control and reverse iontophoresis groups at 90 minutes iontophoresis application time was more than that at 30 minutes iontophoresis application time (LSD post-hoc multiple comparisons, $p<0.001$) and 60 minutes iontophoresis application time (LSD post-hoc multiple comparisons, $p<0.001$). More importantly, glucose extraction by reverse iontophoresis was found to be more than that by diffusion alone at any iontophoresis application time ($p<0.001$).

On the other hand, a significant interaction ($p<0.001$) between iontophoresis application time and group was found on the extraction of lactate. Therefore, one-way ANOVA was used (sample size for each parameter = 5). As shown in Table 4.7 and Figure 4.11, a successive significant increase in lactate extraction was found for the reverse iontophoresis group, as the iontophoresis application time increased from 30 minutes to 90 minutes (LSD post-hoc multiple comparisons, $p<0.001$ in most cases). More importantly, lactate extraction by reverse iontophoresis was found to be more

than that by diffusion alone at any iontophoresis application time (independent t-test, $p<0.001$ in all cases).

4.10 LONG DURATION BIPOLAR DIRECT CURRENT IN HUMAN TRANSDERMAL EXTRACTION OF GLUCOSE AND LACTATE

This section deals with the investigation of long duration bipolar direct current on human transdermal extraction of glucose and lactate. All experiments were carried out on healthy subjects under ethical approval from the University of Strathclyde Ethics Committee. The newly-developed constant current device was used to provide a constant current. Only one switching mode (the polarity of electrodes reversing at intervals of 15 minutes) was used for glucose and lactate extraction with iontophoresis periods of 60 minutes total.

In the present study, only one subject (10% of the sample group), Subject D, reported the experience of a very weak tingling sensation as the current was brought to 0.3 mA/cm^2 at the start and when the electrode polarity reversed. Figure 4.12 illustrated the details (when and how long) of the tingling sensation suffered by Subject D during the whole reverse iontophoresis experiment. As shown in Figure 4.12, at time 0 minute of current passage, Subject D experienced a tingling sensation which lasted no longer than two seconds. At time 15 minutes of current passage (i.e. the occasion of electrode polarity reversed), Subject D again experienced a tingling sensation which also lasted no longer than two seconds. After that, Subject D did not experience any tingling sensations until the end of experiment. On the other hand, 4 subjects (40% of the sample group) had very mild erythema at the reverse iontophoresis site and this lasted for 15-30 minutes after termination of current flow.

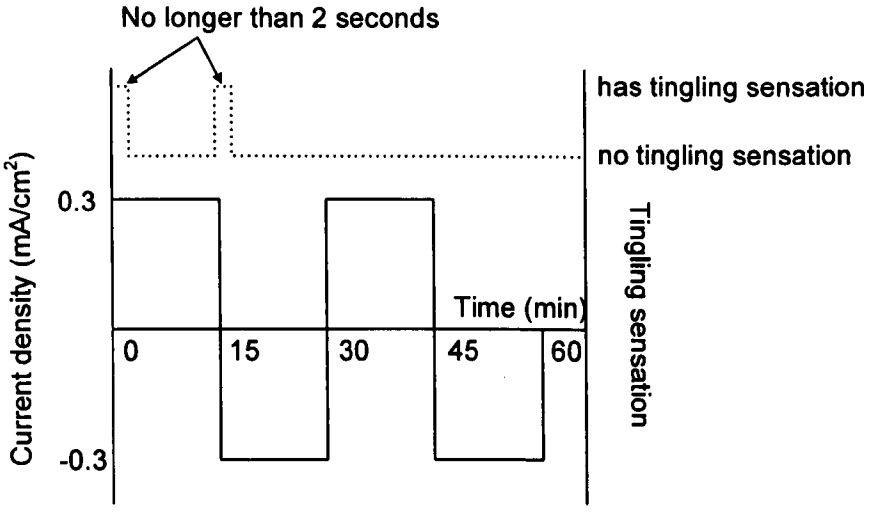

Figure 4.12 – Schematic illustration of the details (when and how long) of the tingling sensation suffered by Subject D during the whole reverse iontophoresis experiment.

The experimental results are summarized in Table 4.8 and Figure 4.13. Diffusion of glucose and lactate across the subject's skin into the methylcellulose gel of the SPE took place and this was proved by the presence of small amounts of glucose and lactate at the control groups. The pH of the methylcellulose gel was found to remain unchanged (midway between pH 7 and pH 8 as measured by litmus paper) after reverse iontophoresis.

The independent t-test (sample size for each parameter = 10) was used for comparison between the electrodes of the control group and the electrodes of the reverse iontophoresis group on the glucose and lactate extraction. For a pair of electrodes, the glucose and lactate extraction at one of the electrodes was found to be statistically the same as at the other electrode (see Figure 4.13).

The independent t-test (sample size for each parameter = 10) was used to compare between the control and reverse iontophoresis measurements for the glucose and lactate extraction. As shown in Figure 4.13, it was found that reverse iontophoresis

significantly promoted more glucose extraction (around 4 times) and lactate extraction (around 2.5 times) than diffusion alone ($p<0.001$ in both cases).

Table 4.8 – Long duration bipolar direct current (current density of 0.3 mA/cm^2, polarity of electrode reversing at intervals of 15 minutes, experimental time of 60 minutes) on human transdermal extraction of glucose and lactate by the use of screen-printed electrodes. The gel at the screen-printed electrodes was 4% methylcellulose gel in 0.1 mM PBS, pH 7.4.

	Extracted Glucose Level (μM)				**Extracted Lactate Level (μM)**			
	Control		Reverse iontophoresis		Control		Reverse iontophoresis	
	SPE 1	SPE 2	SPE 3	SPE 4	SPE 1	SPE 2	SPE 3	SPE 4
Subject A	30.17	30.17	117.1	140.8	109.2	107.1	426.9	350.2
Subject B	70.88	22.37	181.6	96.1	151.7	200.6	374.9	360.0
Subject C	25.00	25.00	202.5	194.4	158.5	149.9	311.5	315.7
Subject D	66.98	27.41	161.9	138.2	182.7	116.6	361.7	238.1
Subject E	41.65	26.10	222.7	222.7	123.5	115.0	377.5	460.6
Subject F	43.77	60.10	148.0	163.7	180.5	140.0	347.9	369.2
Subject G	45.92	14.51	151.7	151.7	128.7	122.3	372.8	285.7
Subject H	25.33	25.33	149.9	174.4	128.2	128.2	415.1	344.7
Subject I	57.61	25.42	115.4	74.3	181.8	132.9	408.0	295.0
Subject J	30.65	53.57	152.9	145.3	108.9	104.6	365.7	312.6
Mean	43.80	31.00	160.4	150.2	145.4	131.7	376.2	333.2
SD	16.75	14.30	34.0	43.4	29.5	28.1	34.0	59.8

Where: SPE1, SPE2, SPE3 and SPE4 are the screen-printed electrodes.

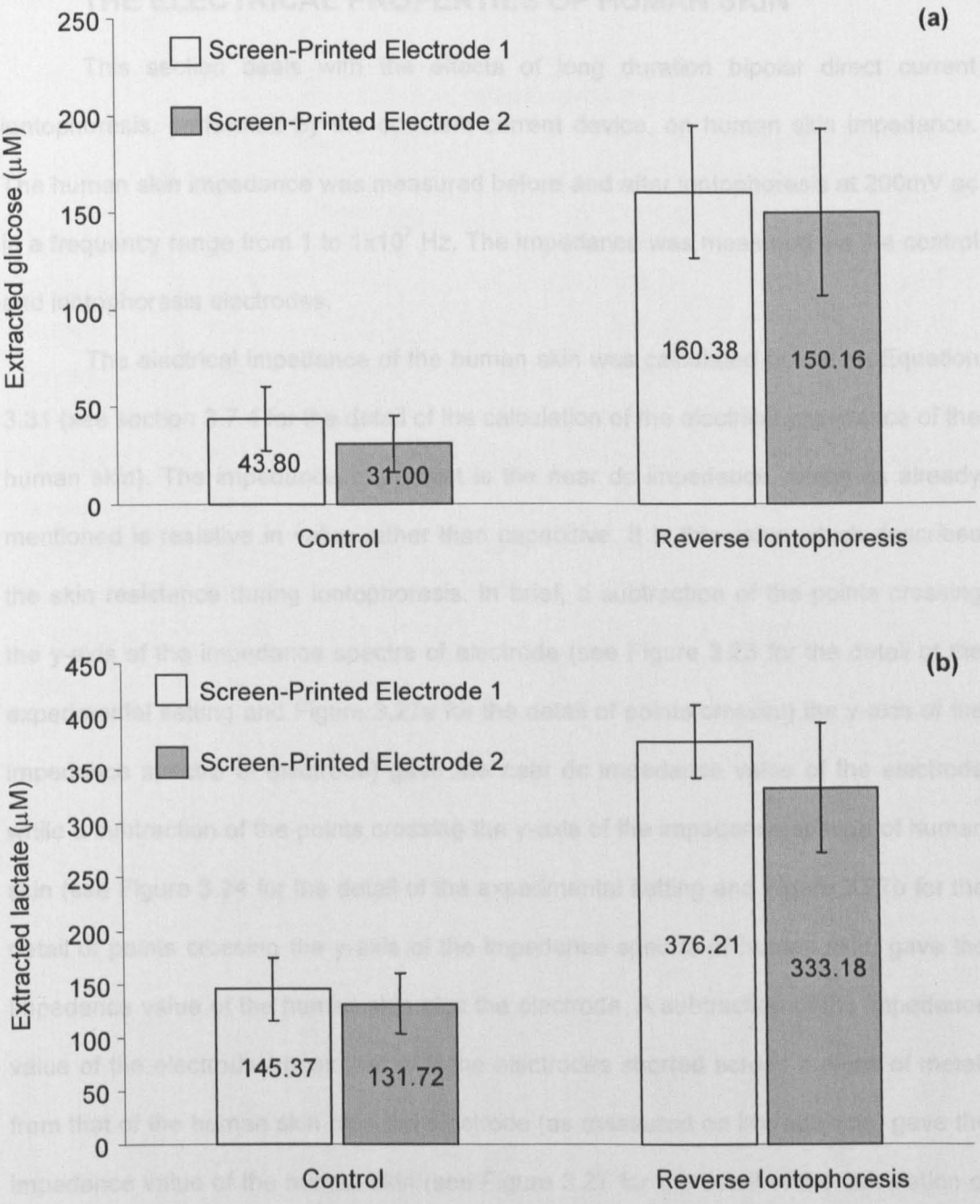

Figure 4.13 – Long duration bipolar direct current (current density of 0.3 mA/cm^2, polarity of electrode reversing at intervals of 15 minutes, experimental time of 60 minutes) on human transdermal extraction of glucose and lactate by the use of screen-printed electrodes (mean ± SD; n=10 for each bar). The gel at the screen-printed electrodes was 4% methylcellulose gel in 0.1 mM PBS, pH 7.4. **(a)** glucose extraction and **(b)** lactate extraction. Extraction of glucose or lactate by reverse iontophoresis was significantly higher ($p<0.001$ in both cases) than that by control (i.e. diffusion alone, where gel and electrodes were applied to subject skin at an adjacent site to iontophoresis electrodes but no current was applied to the control electrodes).

4.11 LONG DURATION BIPOLAR DIRECT CURRENT EFFECTS ON THE ELECTRICAL PROPERTIES OF HUMAN SKIN

This section deals with the effects of long duration bipolar direct current iontophoresis, performed by the constant current device, on human skin impedance. The human skin impedance was measured before and after iontophoresis at 200mV ac in a frequency range from 1 to $1x10^7$ Hz. The impedance was measured via the control and iontophoresis electrodes.

The electrical impedance of the human skin was calculated based on Equation 3.31 (see section 3.7.4 for the detail of the calculation of the electrical impedance of the human skin). The impedance of interest is the near dc impedance, which as already mentioned is resistive in value rather than capacitive. It is this value which describes the skin resistance during iontophoresis. In brief, a subtraction of the points crossing the y-axis of the impedance spectra of electrode (see Figure 3.23 for the detail of the experimental setting and Figure 3.27a for the detail of points crossing the y-axis of the impedance spectra of electrode) gave the near dc impedance value of the electrode while a subtraction of the points crossing the y-axis of the impedance spectra of human skin (see Figure 3.24 for the detail of the experimental setting and Figure 3.27b for the detail of points crossing the y-axis of the impedance spectra of human skin) gave the impedance value of the human skin plus the electrode. A subtraction of the impedance value of the electrode (measured with the electrodes shorted across a piece of metal) from that of the human skin plus the electrode (as measured on live subjects) gave the impedance value of the human skin (see Figure 3.27 for the detail of the calculation of the electrical impedance of human skin). It was found that the initial resistance of the human skin was typically 96.2 – 127.6 $k\Omega/cm^2$ at 1 Hz (see Table 4.9). The experimental results of electrical properties of human skin are summarized in Figure 4.14.

Table 4.9 – The results of the human skin electrical impedance measured before and after experiment at the control and reverse iontophoresis sites of 10 healthy volunteers. Impedance here is calculated at a frequency of 1 Hz to reflect the near dc values of interest for iontophoresis. At this frequency the impedance is effectively only resistive not capacitive.

	Human Skin Impedance (kΩ/cm²)					
	Control Site			Reverse Iontophoresis Site		
	Before Experiment	After Experiment	% Change	Before Experiment	After Experiment	% Change
Subject A	111.2	107.9	-3.0	110.9	67.5	-39.1
Subject B	110.5	103.6	-6.2	108.4	73.2	-32.5
Subject C	119.4	102.8	-13.9	110.0	75.7	-31.2
Subject D	110.2	99.6	-9.6	104.3	70.1	-32.8
Subject E	127.6	108.2	-15.2	112.5	75.9	-32.6
Subject F	117.0	111.8	-4.4	103.9	75.1	-27.7
Subject G	96.2	89.5	-6.9	107.6	80.5	-25.2
Subject H	123.7	111.5	-9.8	115.1	76.8	-33.3
Subject I	107.3	98.0	-8.7	112.2	69.0	-38.5
Subject J	118.0	112.5	-4.7	112.0	78.3	-30.1
Mean	114.1	104.5		109.7	74.2	
SD	9.0	7.4		3.6	4.2	

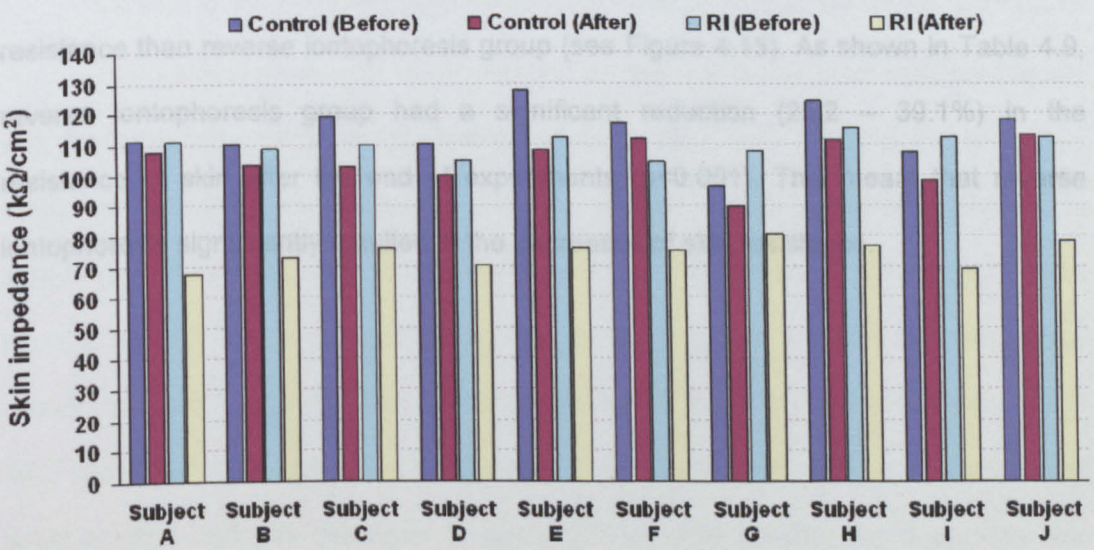

Figure 4.14 – Human skin electrical impedance measured before and after experiment at the control and reverse iontophoresis (RI) sites of 10 healthy volunteers. Impedance here is calculated at a frequency of 1 Hz.

The near dc impedance is the most critical aspect of skin electrical characteristics as far as iontophoresis is concerned as this takes place under largely dc conditions. Two-way ANOVA (sample size for each parameter = 10) with iontophoresis treatments (i.e. control and reverse iontophoresis groups) and group (i.e. control and reverse iontophoresis group) as the fixed factors and skin resistance (at very low frequency, 1 Hz) as the dependent variable was used to analyse the effect of the reverse iontophoresis on the pre-iontophoresis and post-iontophoresis resistance of skin. A significant interaction ($p<0.001$) between iontophoresis treatments and group was found. Paired t-test (sample size for each parameter = 10) was then performed to investigate the effects of iontophoresis treatments, and independent t-test (sample size for each parameter = 10) was used to investigate the differences between groups. As shown in Figure 4.15, before the start of experiments, the resistance of skin at the control group was found to be statistically the same as that at the reverse iontophoresis group. However, after the end of experiments, the resistance of skin at the control group was found to be significantly higher than that at the reverse iontophoresis group ($p<0.001$). Although control group also had a significant decrease ($p<0.001$) on the resistance of skin after the end of experiments, it still had around 1.4 times higher skin resistance than reverse iontophoresis group (see Figure 4.15). As shown in Table 4.9, reverse iontophoresis group had a significant reduction (25.2 – 39.1%) in the resistance of skin after the end of experiments ($p<0.001$). This meant that reverse iontophoresis significantly resulted in the decreases of skin resistance.

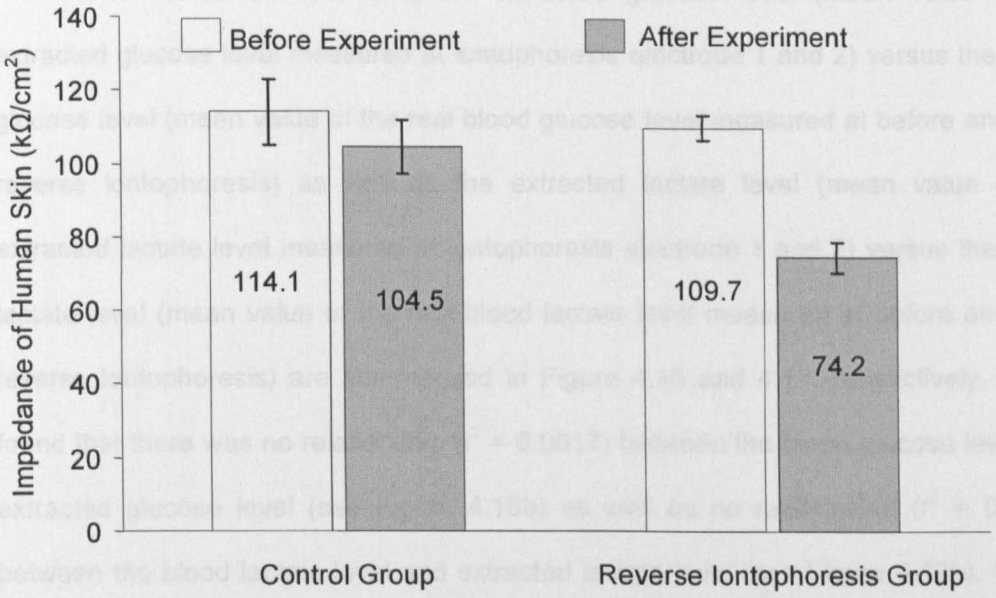

Figure 4.15 – Effect of long duration bipolar direct current (current density of 0.3 mA/cm^2, polarity of electrode reversing at intervals of 15 minutes, experimental time of 60 minutes) on the electrical impedance of human skin (mean ± SD; n=10 for each bar) by the use of screen-printed electrodes with 4% methylcellulose gel (preparing in 0.1 M PBS, pH 7.4). Impedance here is calculated at a frequency of 1 Hz.

4.12 CORRELATION ON THE REAL BLOOD GLUCOSE/LACTATE LEVELS WITH THE EXTRACTED GLUCOSE/LACTATE LEVELS

This section deals with the correlation on the real blood glucose/lactate levels with the extracted glucose/lactate levels. In this study, a current of 0.3 mA (delivered using the constant current device), with the polarity of the electrodes reversed at intervals of 15 minutes, was applied for a period of 60 minutes to the subject's inner forearm through two screen-printed electrodes in conditions of room temperature as shown in Figure 3.24. After the application of current, the amount of extracted glucose and lactate in the gel of the screen-printed electrodes was quantified using spectrometric methods described in section 3.7.5. The internal blood glucose and lactate levels were also measured by finger stick samples, as described in human experiments of section 3.7.3, before and after the application of current

The correlation results of the extracted glucose level (mean value of the extracted glucose level measured at iontophoresis electrode 1 and 2) versus the blood glucose level (mean value of the real blood glucose level measured at before and after reverse iontophoresis) as well as the extracted lactate level (mean value of the extracted lactate level measured at iontophoresis electrode 1 and 2) versus the blood lactate level (mean value of the real blood lactate level measured at before and after reverse iontophoresis) are summarized in Figure 4.16 and 4.17, respectively. It was found that there was no relationship (r^2 = 0.0017) between the blood glucose level and extracted glucose level (see Figure 4.16b) as well as no relationship (r^2 = 0.1711) between the blood lactate level and extracted lactate level (see Figure 4.17b). It must be remembered however that all of these results have been taken in healthy volunteer samples therefore there is no guarantee or suggestion at this stage that a wider population sample would correlate.

However, when outliers were removed from the regression equation (see Figure 4.16a), an improved correlation (r^2 = 0.0288) was found between the blood glucose level and extracted glucose level but again they still had no relationship. Nevertheless, a moderate relationship (r^2 = 0.5213) was found between the blood lactate level and extracted lactate level if outliers were removed from the regression equation (see Figure 4.17a).

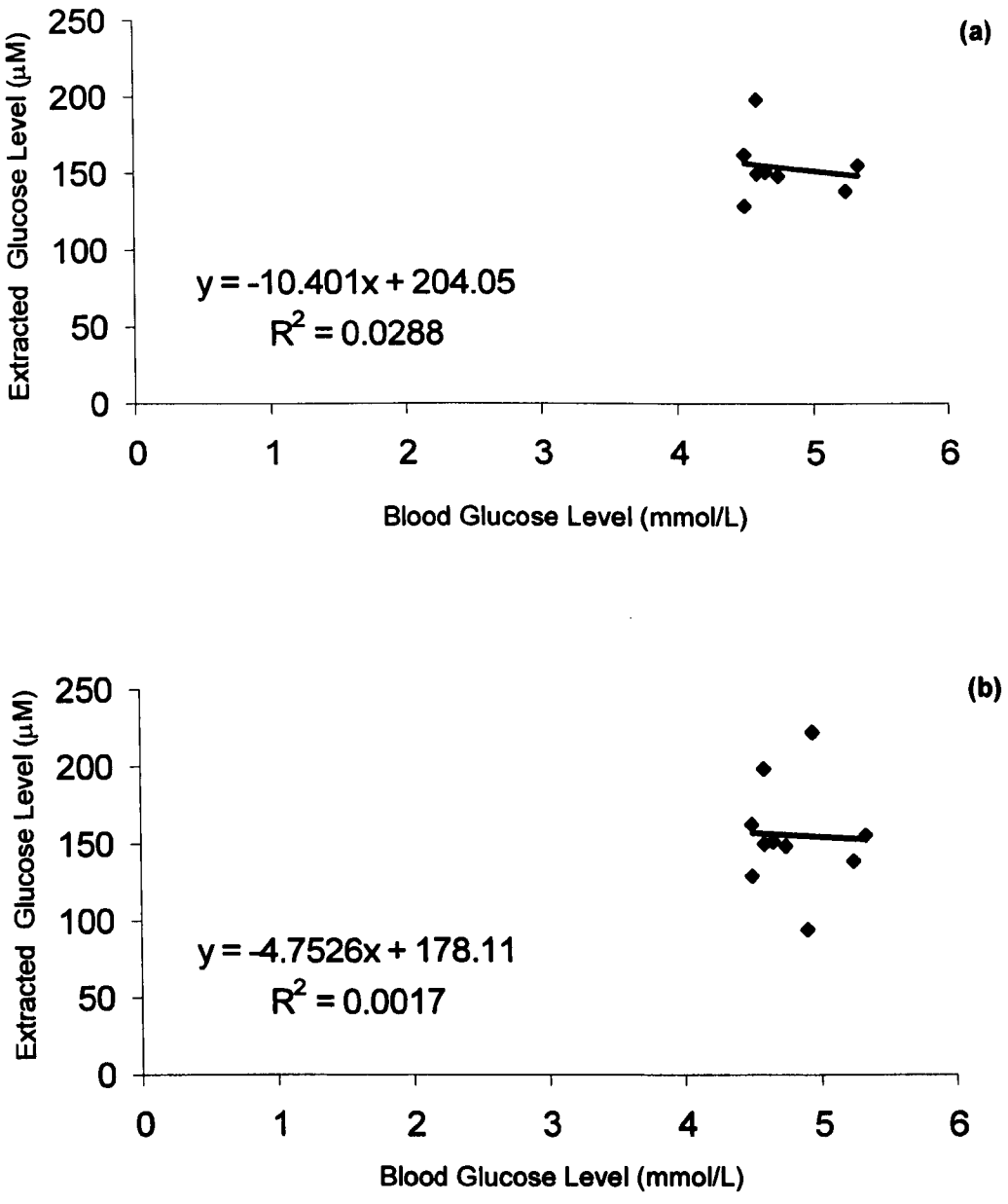

Figure 4.16 – Comparison of real blood glucose levels of healthy subjects and glucose levels in the collection methylcellulose (MC) gel after reverse iontophoresis. **(a)** Correlation analysis excludes outliers (n = 8). **(b)** Correlation analysis includes outliers (n = 10). Outliers markedly affect the correlation and this can be seen in the equations of the correlation lines.

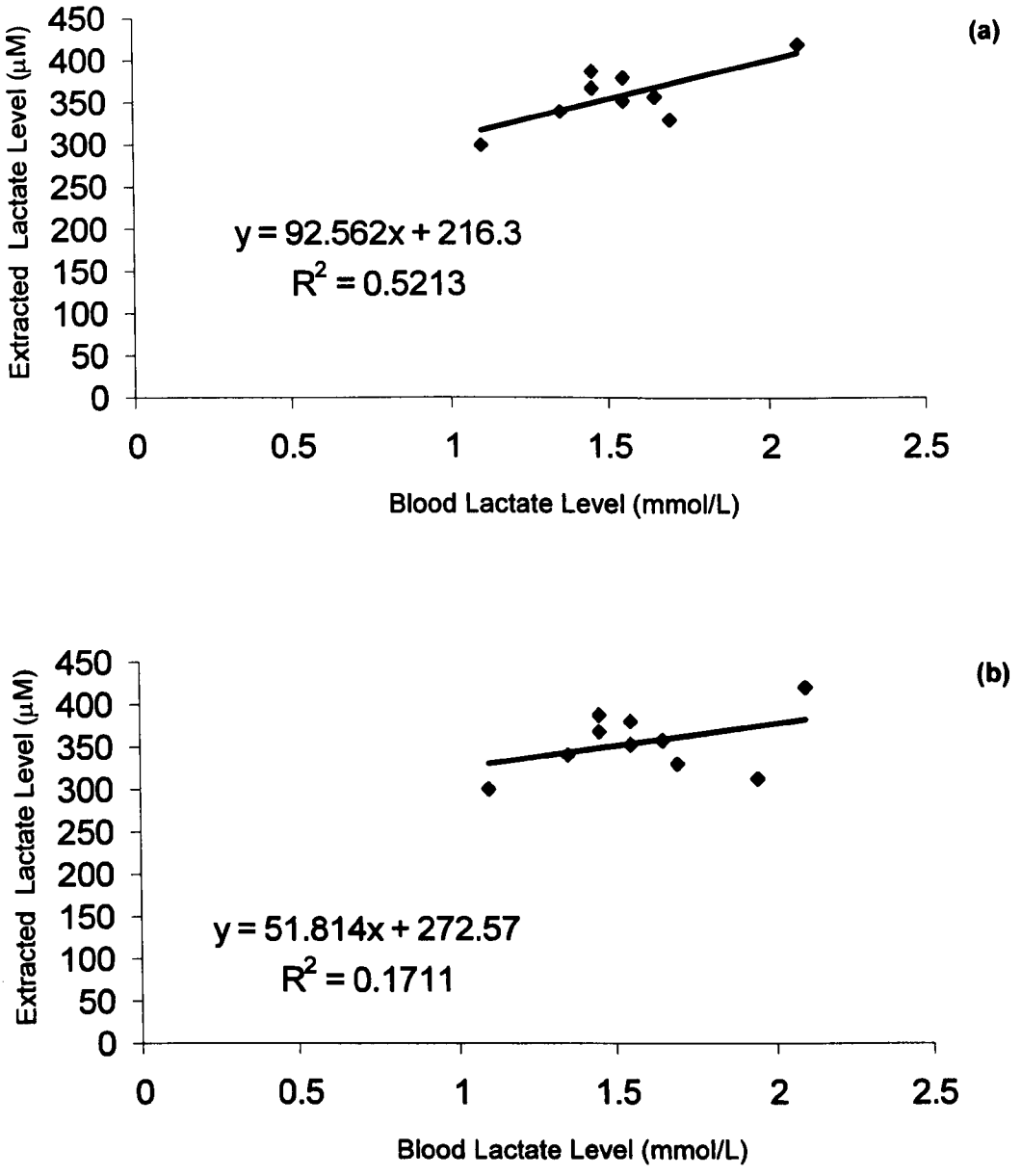

Figure 4.17 – Comparison of real blood lactate levels of healthy subjects and lactate levels in the collection methylcellulose (MC) gel after reverse iontophoresis. **(a)** Correlation analysis excludes outliers (n = 9). **(b)** Correlation analysis includes outliers (n = 10). Outliers markedly affect the correlation and this can be seen in the equations of the correlation lines.

4.13 RELATIONSHIP BETWEEN THE SKIN IMPEDANCE, THE REAL BLOOD GLUCOSE/LACTATE LEVELS AND THE EXTRACTED GLUCOSE/LACTATE LEVELS

This section deals with the correlation between the skin impedance, the real blood glucose/lactate levels and the extracted glucose/lactate levels. Until now, no studies have tried to correlate these parameters simultaneously but they could be an important means of checking or tracking changes in internal blood levels of glucose or lactate against extracted levels by iontophoresis. In this study, a current of 0.3 mA, with the polarity of the electrodes reversed at intervals of 15 minutes, was passed between screen-printed electrode (placed at subject's inner forearm as shown in Figure 3.24) for a period of 60 minutes for simultaneous glucose and lactate extraction as described above. The amount of extracted glucose and lactate were quantified after the application of current, using spectrometric methods. Before and after the application of current, the blood glucose and lactate levels as well as the skin impedance were also measured.

In order to standardize all data in such a way that all results of skin impedance data, real blood glucose/lactate levels data and extracted glucose/lactate levels data could be compared, the concept of normalisation was applied. The skin impedance ratio (i.e. the ratio of the skin impedance before reverse iontophoresis to the skin impedance after reverse iontophoresis for impedance measured at 1 Hz at 200 mV), the glucose ratio (i.e. the ratio of the extracted glucose level to the real blood glucose level) and the lactate ratio (i.e. the ratio of the extracted lactate level to the real blood lactate level) were computed (see Table 4.10 and 4.11).

The correlation results of the glucose ratio versus the skin impedance ratio as well as the lactate ratio versus the skin impedance ratio are summarized in Figure 4.18 and 4.19, respectively. It was found that there was no relationship (r^2 = 0.1326) between the skin impedance ratio and the glucose ratio (see Figure 4.18b) as well as

no relationship (r^2 = 0.1946) between the skin impedance ratio and the lactate ratio (see Figure 4.19b).

However, when outliers were removed from the regression equation (see Figure 4.18a), a good correlation (r^2 = 0.6536) was found between the skin impedance ratio and the glucose ratio. Similarly, a good correlation (r^2 = 0.6624) was found between the skin impedance ratio and the lactate ratio if outliers were removed from the regression equation (see Figure 4.19a). It must be remembered however that all of these results have been taken in healthy volunteer samples therefore there is no guarantee or suggestion at this stage that a wider population sample would correlate.

Table 4.10 – The results of the real blood glucose level (before and after experiment), extracted glucose level and skin electrical impedance (before and after experiment) of the 10 healthy volunteers. Impedance here is at a frequency of 1 Hz. The impedances are given per unit area.

	Real Blood Glucose Level (mmol/L)				Extracted Glucose Level (μM)				Skin Impedance (kΩ)		*GR*	*SIR*
	Before Experiment	After Experiment	Mean	SD	Electrode 1	Electrode 2	Mean	SD	Before Experiment	After Experiment		
Subject A	4.6	4.4	4.5	0.1	117.1	140.8	128.9	16.8	110.9	67.5	28.6	1.6
Subject B	4.8	5.7	5.3	0.6	181.6	96.1	138.8	60.5	108.4	73.2	26.4	1.5
Subject C	4.6	4.6	4.6	0.0	202.5	194.4	198.4	5.7	110.0	75.7	43.1	1.5
Subject D	4.3	4.9	4.6	0.4	161.9	138.2	150.1	16.8	104.3	70.1	32.6	1.5
Subject E	5.3	4.6	5.0	0.5	222.7	222.7	222.7	0.0	112.5	75.9	45.0	1.5
Subject F	5.1	5.6	5.4	0.4	148.0	163.7	155.9	11.1	103.9	75.1	29.1	1.4
Subject G	4.6	4.7	4.7	0.1	151.7	151.7	151.7	0.0	107.6	80.5	32.6	1.3
Subject H	4.6	4.4	4.5	0.1	149.9	174.4	162.2	17.3	115.1	76.8	36.0	1.5
Subject I	4.2	5.6	4.9	1.0	115.4	74.3	94.9	29.1	112.2	69.0	19.4	1.6
Subject J	4.7	4.8	4.8	0.1	152.9	145.3	149.1	5.4	112.0	78.3	31.4	1.4
Mean	4.7	4.9			160.4	150.2			109.7	74.2		
SD	0.3	0.5			34.0	43.4			3.6	4.2		

Remarks: ***GR*** is the glucose ratio (i.e. $\frac{\text{Mean value of the extracted glucose level measured at iontophoresis electrode 1 and 2}}{\text{Mean value of the real blood glucose level measured at before and after reverse iontophoresis}}$)

SIR is the skin impedance ratio (i.e. $\frac{\text{Skin impedance measured before reverse iontophoresis (impedance measured at 1 Hz at 200 mV)}}{\text{Skin impedance measured after reverse iontophoresis (impedance measured at 1 Hz at 200 mV)}}$)

Table 4.11 – The results of the real blood lactate level (before and after experiment), extracted lactate level and skin electrical impedance (before and after experiment) of the 10 healthy volunteers. Impedance here is at a frequency of 1 Hz. The impedances are given per unit area.

	Real Blood Lactate Level (mmol/L)				Extracted Lactate Level (μM)				Skin Impedance (kΩ)		*LR*	*SIR*
	Before Experiment	After Experiment	Mean	SD	Electrode 1	Electrode 2	Mean	SD	Before Experiment	After Experiment		
Subject A	1.8	1.1	1.5	0.5	426.9	350.2	388.6	54.3	110.9	67.5	268.0	1.6
Subject B	1.6	1.3	1.5	0.2	374.9	360.0	367.5	10.5	108.4	73.2	253.4	1.5
Subject C	2.2	1.7	2.0	0.4	311.5	315.7	313.6	3.0	110.0	75.7	160.8	1.5
Subject D	1	1.2	1.1	0.1	361.7	238.1	299.9	87.4	104.3	70.1	272.6	1.5
Subject E	2.4	1.8	2.1	0.4	377.5	460.6	419.0	58.8	112.5	75.9	199.5	1.5
Subject F	1.4	1.9	1.7	0.4	347.9	369.2	358.5	15.1	103.9	75.1	217.3	1.4
Subject G	1.9	1.5	1.7	0.3	372.8	285.7	329.2	61.6	107.6	80.5	193.7	1.3
Subject H	1.5	1.6	1.6	0.1	415.1	344.7	379.9	49.8	115.1	76.8	245.1	1.5
Subject I	1.6	1.5	1.6	0.1	408.0	295.0	351.5	79.9	112.2	69.0	226.8	1.6
Subject J	1.5	1.2	1.4	0.2	365.7	312.6	339.1	37.5	112.0	78.3	251.2	1.4
Mean	1.7	1.5			376.2	333.2			109.7	74.2		
SD	0.4	0.3			34.0	59.8			3.6	4.2		

Remarks: ***LR*** is the lactate ratio (i.e. $\frac{\text{Mean value of the extracted lactate level measured at iontophoresis electrode 1 and 2}}{\text{Mean value of the real blood lactate level measured at before and after reverse iontophoresis}}$)

SIR is the skin impedance ratio (i.e. $\frac{\text{Skin impedance measured before reverse iontophoresis (impedance measured at 1 Hz at 200 mV)}}{\text{Skin impedance measured after reverse iontophoresis (impedance measured at 1 Hz at 200 mV)}}$)

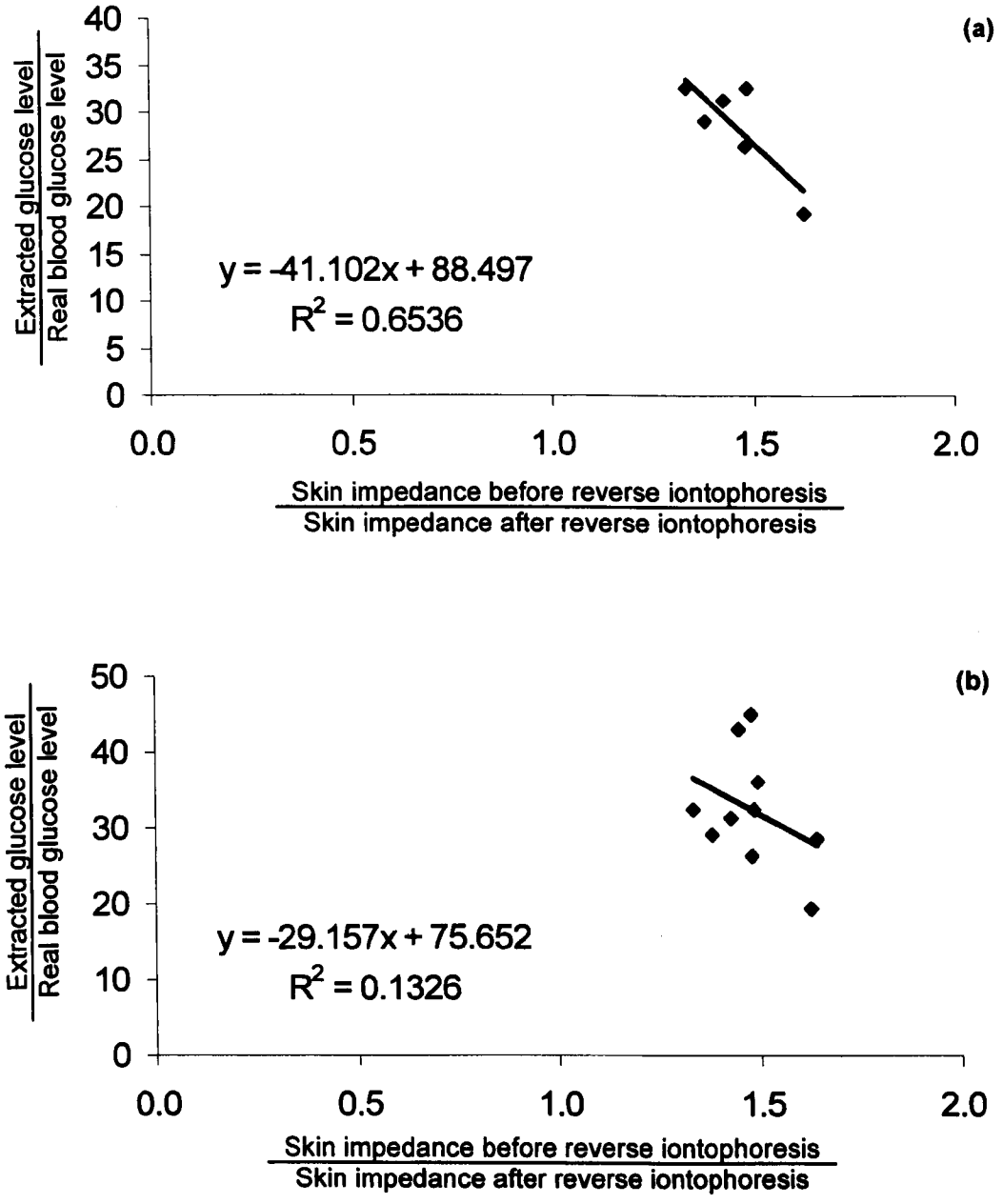

Figure 4.18 – Comparison of the skin impedance ratio (i.e. the ratio of the skin impedance before reverse iontophoresis to the skin impedance after reverse iontophoresis) and the glucose ratio (i.e. the ratio of the extracted glucose level to the real blood glucose level) for 10 different healthy volunteers. **(a)** Correlation analysis excludes outliers (n = 6). **(b)** Correlation analysis includes outliers (n = 10). Outliers markedly affect the correlation and this can be seen in the equations of the correlation lines.

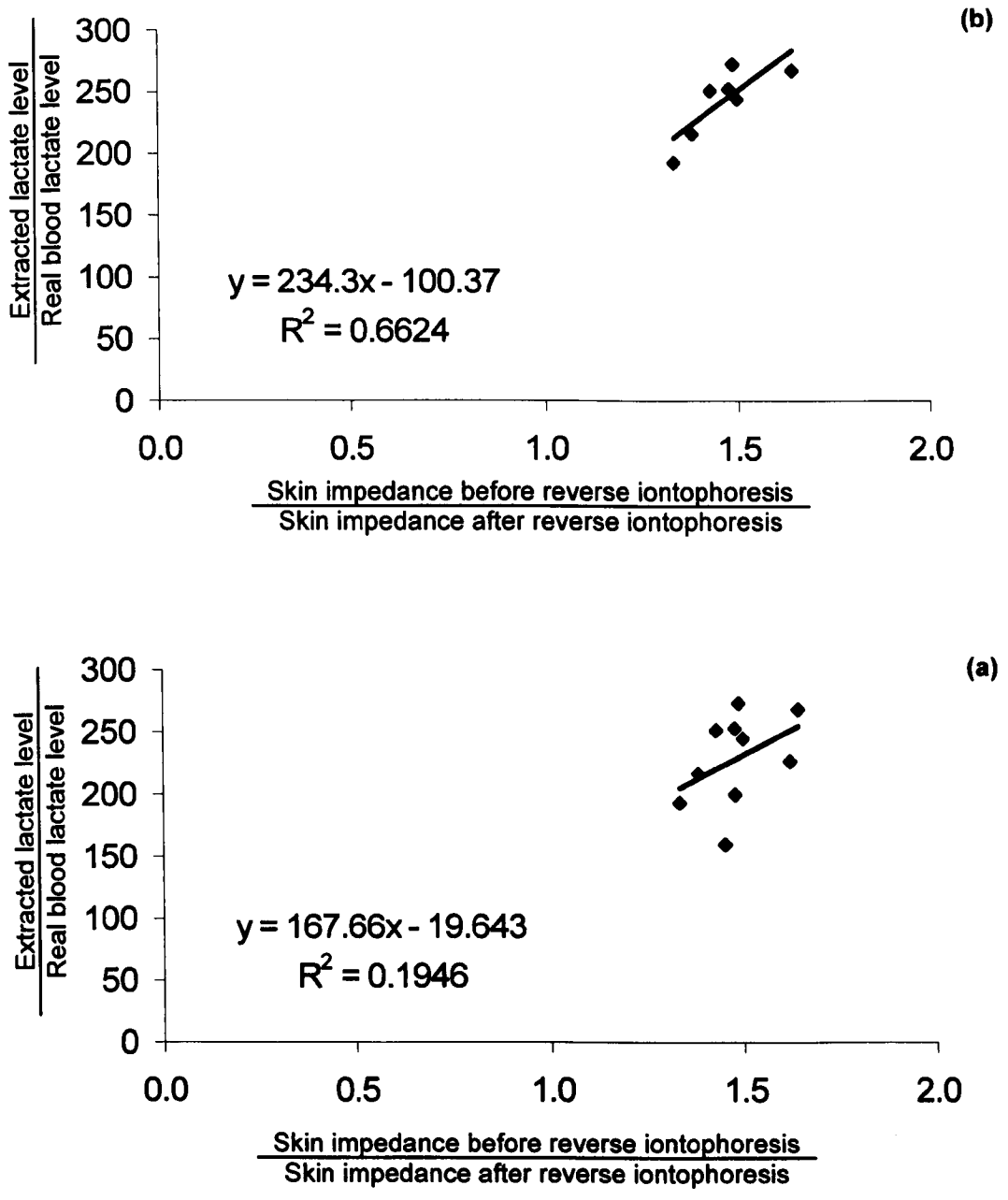

Figure 4.19 – Comparison of the skin impedance ratio (i.e. the ratio of the skin impedance before reverse iontophoresis to the skin impedance after reverse iontophoresis) and the lactate ratio (i.e. the ratio of the extracted lactate level to the real blood lactate level) for 10 different healthy volunteers. **(a)** Correlation analysis excludes outliers (n = 7). **(b)** Correlation analysis includes outliers (n = 10). Outliers markedly affect the correlation and this can be seen in the equations of the correlation lines.

4.14 SUMMARY

In summary, with the new extraction regime and new iontophoresis device, selected to utilise an electrode polarity change every 15 minutes during iontophoresis, optimum glucose extraction and good lactate extraction were obtained both in the model system and in healthy volunteers. Importantly, the near dc resistance of the human subjects' skin also showed some correlation with glucose and lactate extraction. The results will be discussed fully in Chapter 5.

■ *Chapter 5*

Discussion

5.1 Reverse Iontophoresis Optimisation Of Glucose And Lactate Extraction
- 5.1.1 The diffusion cell model
- 5.1.2 The silver-silver chloride electrodes
- 5.1.3 Preconditioning effects in impedance measurement
- 5.1.4 Effects of long duration bipolar direct current iontophoresis on glucose extraction in the model system
- 5.1.5 Effects of long duration bipolar direct current iontophoresis on lactate extraction in the model system
- 5.1.6 Effects of long duration bipolar direct current iontophoresis on membrane impedance
- 5.1.7 Experimental validity and reliability

5.2 Construction And Evaluation Of A Constant Current Device For Reverse Iontophoresis
- 5.2.1 Electronic evaluation of the circuit design
- 5.2.2 In vitro reverse iontophoresis evaluation of the circuit design
- 5.2.3 Limitations of the circuit design
- 5.2.4 Potential clinical applications of the constant current device

5.3 Construction Of A Screen-Printed Electrode For Reverse Iontophoresis
- 5.3.1 The specially-designed diffusion cell
- 5.3.2 Screen-printed electrodes for reverse iontophoresis
- 5.3.3 In vitro reverse iontophoresis evaluation of the screen-printed electrodes
- 5.3.4 Effects of long duration bipolar direct current on human transdermal extraction of glucose and lactate
- 5.3.5 Long duration bipolar direct current on the electrical properties of human skin
- 5.3.6 Experimental validity and reliability

5.4 Correlation On The Real Blood Glucose/Lactate Levels With The Extracted Glucose/Lactate Levels

5.5 Relationship Among The Skin Impedance, The Real Blood Glucose/Lactate Levels And The Extracted Glucose/Lactate Levels

5.6 Limitations Of The Study

5.7 Potential Clinical Applications

5.8 Recommendations For Future Studies

Chapter 5 Discussion

There were six principal objectives of this study and they were: (1) to investigate and establish the optimum switching mode for reverse iontophoresis of glucose and lactate for transdermal extraction, (2) to design and develop a low-cost, low-power, miniature, programmable constant and switchable current device used for reverse iontophoresis, (3) to design, develop and investigate low-cost and reliable screen-printed electrodes for reverse iontophoresis, (4) to investigate the effect of long duration bipolar direct current on human transdermal extraction of glucose and lactate, (5) to investigate the effect of long duration bipolar direct current on the electrical properties of human skin and (6) to correlate the real blood glucose/lactate levels with the extracted glucose/lactate levels.

5.1 REVERSE IONTOPHORESIS OPTIMISATION OF GLUCOSE AND LACTATE EXTRACTION

5.1.1 The diffusion cell model

In this section of the study, cellulose ester nanoporous membranes were used rather than excised animal or human skin samples, in order to avoid large sample-to-sample variations. This allowed the electrical properties of the electrodes and performance of the constant current device for iontophoresis of lactate and glucose to be investigated without the non-uniformities introduced by sample-to-sample variation in animal tissue. In addition, the availability of excised animal or human skin samples

is becoming limited for legal, ethical and safety reasons. Even if excised healthy human skin samples can be obtained, they may be of differing ages, body site or species. In addition, there are many substances in excised animal or human skin samples and this allows interference for the study of the characteristics of an extraction system during reverse iontophoresis. Many of these effects are relatively unpredictable and therefore it is preferable that basic electrical characterisation studies are conducted in as controlled an environment as possible before skin studies commence. Last but not least, systems using animal or human skin *in vitro* are essentially utilising dead tissue which does not fully reproduce *in vivo* skin behaviour.

The best approach to optimize reverse iontophoresis for the transdermal extraction of glucose and lactate is to consider it in its simplest form. Because of the large sample-to-sample differences in the skin of human subjects *in vivo*, a diffusion cell model incorporated with nanoporous membrane was adopted for the first part of the current study. The nanoporous membrane itself has been chosen to mimic some of the key properties of human skin as it has nanoporous and exhibits a negative charge at pH 7. Actually, diffusion cell models incorporated with membranes for molecular permeability studies and for iontophoresis drug delivery measurements have also been widely used in the past (Connolly *et al.* 2002, Foley *et al.* 1992, Morimoto *et al.* 1991, Hatanaka *et al.* 1990). For example, Morimoto *et al.* in 1991 used a 2-chamber diffusion cell equipped with platinum electrodes and a constant current power source to study the effects of ion species and their concentration on the iontophoresis transport of benzoic acid through an artificial membrane. In this study, the nanoporous membrane used for experiments had an average resistance of 5.9 ± 1.3 $k\Omega/cm^2$ before experiments. Because there was no significant difference between the resistances of the nanoporous membrane before experiments, therefore a uniformity model system could be achieved with this small sample-to-sample variation in nanoporous membrane.

5.1.2 The silver-silver chloride electrodes

There are two different types of electrodes, which can be used in reverse iontophoresis experiments, and they are polarizable electrodes (metals such as stainless steel, platinum or aluminium) and non-polarizable electrodes (e.g. silver-silver chloride electrode). Polarizable electrodes, so-called "inert" electrodes, are indeed inert in the sense that they undergo minimum chemical changes during electrochemical reactions; however they are known to cause the electrolysis of water leading to the production of hydroxyl ions at the cathode and hydrogen ions at the anode. This results in a pH change in the system. Such changes result in the reduction of the flux of co-ions and the directional change of electroosmotic flow. For example, Pillai *et al.* (2003) used platinum electrodes for transdermal iontophoretic delivery of insulin peptides using full-thickness rat skin. They observed large pH shifts during iontophoresis and such pH shifts influenced the direction and magnitude of electroosmotic flow. Therefore, polarizable electrodes were not used in this study. Because the redox potential for non-polarizable electrodes system, such as silver-silver electrode, is lower than for water and this enables electroneutrality to be maintained at anode and cathode, non-polarizable electrodes were used in the present study (see section 2.8 for the details of electrodes for reverse iontophoresis).

5.1.3 Preconditioning effects in impedance measurement

It is well known that the electrical impedance of a substance (e.g. electrolyte) normally may not be consistent for the first impedance measurements. This phenomenon is known as a preconditioning effect. In order to achieve consistent results, measurements from the first few impedance tests are usually not taken into account for the determination of the impedance of a substance unless some specific electrochemical phenomenon is being investigated. A pilot study was conducted to

study this preconditioning effect in the current system for measurements of impedance through electrodes and artificial membrane in the model cell. These results were shown in Appendix A. It was found that in the current system the preconditioning effect was not that apparent as the difference between the percentage change in impedance of the second measurement (compared with the first measurement) and the percentage change in impedance of the third measurement (compared with the first measurement) was less than 3% (see Appendix A for the details of the percentage change in impedance after several consecutive impedance measurements). Therefore, the impedance measurements from the second application of voltage onwards were deemed suitable for use in data analysis for all results reported in this study.

5.1.4 Effects of long duration bipolar direct current iontophoresis on glucose extraction in the model system

A current density for iontophoresis of 0.3 mA/cm^2, close to the value recommended as an upper limit by other workers (Ledger 1992), was used. The efficiency of electroosmotic flow is weakly dependent upon current density in the range of 0.14 – 0.55 mA/cm^2 (Delgado-Charro and Guy 1994).

As expected, in the absence of current passage, glucose transport was very low. However, current passage significantly enhanced glucose transport into both electrode chambers, depending on the iontophoresis application time and the switching mode. In this study, glucose extraction was optimised by longer applications of current (90 minutes) with 15 minutes switching time rather than 10 minutes switching time (about 1.6 times less on glucose extraction as compared with that at 15 minutes switching time), 5 minutes switching time (about 2.6 times less on glucose extraction as compared with that at 15 minutes switching time) or 0 minutes switching time, i.e.

continuous DC current, (about 3.1 times less for the anode and 3.8 times less for the cathode on glucose extraction as compared with that at 15 minutes switching time).

As shown in Figure 4.1, glucose extraction by 15 minutes switching time was still more than that by 0 minutes switching time (i.e. continuous DC current) at 15 minutes iontophoresis application time. This might be due to the reason that after a series of experiments starting from 90 minutes iontophoresis application time down to 15 minutes iontophoresis application time, the membrane received 15 minutes switching was still in good condition (no or less polarisation happen on the membrane) but not the membrane received 0 minutes switching (membrane being polarised). Because polarisation of membrane can result in the reduction of the electroosmotic flux, glucose extraction by 15 minutes switching time was more than that by 0 minutes switching time at 15 minutes iontophoresis application time even they both could be assumed as continuous DC current at that moment.

In 1995, Rao *et al.* conducted a reverse iontophoresis experiment to non-invasively extract glucose out of human subjects. They found that direct current iontophoresis at 0.25 mA/cm^2 for a period of 1 hour can significantly extract glucose out of human skin (about 10 times more for cathodal extraction and 3 times more for anodal extraction), as compared with diffusion alone. Although our findings on glucose extraction in model system had the same phenomena that direct current iontophoresis at 0.3 mA/cm^2 for a period of 1 hour can significantly extract glucose out of a nanoporous membrane (about twice as much for both cathodal and anodal extractions as compared with that for diffusion alone), our cathodal extraction (1.68 pmol; i.e. 4.8 μM x 350 μl) was lower than the cathodal extraction (5.83 pmol; i.e. 10.6 μM x 0.55 ml) reported by Rao *et al.* (1995) but our anodal extraction (2.07 pmol; i.e. 5.9 μM x 350 μl) was almost the same as the anodal extraction (1.87 pmol; i.e. 3.4 μM x 0.55 ml) reported by Rao *et al.* (1995). Rao *et al.* (1995) of course were using live subjects but

this does show that our model system behaves in a similar manner to reported iontophoresis systems.

Our findings showed that it was possible to significantly increase ($p<0.05$) the amount of glucose extracted across the nanoporous membrane by either (a) increasing the iontophoresis application time from 15 minutes to 90 minutes (see Table 4.1) or (b) by increasing the time interval between reversal of electrode polarity to 15 minutes rather than 10 minutes or 5 minutes (see Figure 4.1).

Glucose, an uncharged molecule, is mainly extracted by electroosmosis during reverse iontophoresis. Electroosmotic flow is always in the same direction as the flow of counter ions. Since human skin is negatively charged under physiological conditions (Burnette and Ongpipattanakul 1987), the counter ions are cations and the electroosmotic flow is thus from anode to cathode (Pikal 2001, Guy *et al.* 2000). The nanoporous membrane used in this model system is negatively charged. Therefore, electroosmotic flow in the model system should be from anode to cathode during direct current reverse iontophoresis and thus more glucose should be found at cathode rather than anode. However, in the model system, extraction of glucose at anode was greater than that at cathode during direct current reverse iontophoresis but this was not significant. This result was not in agreement with other researchers (Rao *et al.* 1995 and 1993). The reason underlying the anodal extraction is more than cathodal extraction may be due to neutral or positively charged pores existing in the membrane (Pikal and Shah 1990). It is also possible that some masking of negative charge in the nanoporous membrane or some membrane polarisation occurred which reduced the effect of cathodal electroosmosis.

As can be seen in Figure 4.1, the amount of glucose extracted in the model system at either 10 or 15 minutes switching times was significantly more than that at continuous current passage without switching (i.e. cathode and anode held constant) at any iontophoresis application time but this was inconsistent with the results reported by Santi and Guy in 1996. They found that total mannitol extractions were statistically

equivalent for the continuous current passage with or without switching, albeit that a different sugar molecule was studied. The glucose result in this current study for switching of polarities may be due to the electrode polarity reversal allowing depolarisation of the membrane (Banga and Chein 1988). During continuous current passage without switching, sodium and chloride ion pass across the membrane to the cathode and anode, respectively. Continuous transport of these ions possibly leads to the accumulation of the ions at the membrane and the inherent fixed negative charge of the membrane is therefore shielded. This reduction of the electric field in the current conducting pathways diminishes counter-ion migration and therefore reduces the level of electroosmotic flow – the key mechanism of transport for uncharged molecules. Accumulation of ions could also cause membrane polarisation, reducing the level of electroosmosis as well (Lawler *et al.* 1960). For current passage with periodic electrode polarity switching, the level of masking of negative charge in the nanoporous membrane or membrane polarisation can be reduced once the polarity of the electrodes is reversed (Banga and Chein 1988).

Based on the findings, it is postulated that 15 minutes electrode polarity reversing is the best switching mode as it extracts significantly more glucose than the control (at least >3.9 times) and continuous current passage without switching (at least >3.1 times) within the studied iontophoresis application time. According to the results, consecutive significant increases in glucose extraction were found as the iontophoresis application time increased at each switching mode ($p<0.05$ in all cases). Therefore, the longest iontophoresis application time (90 minutes) in this study seems to be the best.

Long application times of current do enhance extraction of molecules from the membrane but in a practical system for use by patients this would need to be balanced with the need for relatively frequent analysis of the extracted molecule, in this case glucose.

5.1.5 Effects of long duration bipolar direct current iontophoresis on lactate extraction in the model system

With the passage of current, more lactate could be extracted across the membrane when compared with the control group. This means that iontophoresis can facilitate lactate extraction and the amount of lactate to be extracted depended on the iontophoresis application time and the switching mode. Based on the result, more lactate could be extracted across the membrane by increasing the iontophoresis application time from 15 minutes to 90 minutes (see Table 4.2 and Figure 4.2).

Lactate is a negatively charged molecule. During continuous current passage without switching, lactate passed across the membrane to the anode because of the electrostatic attraction. Hence more lactate could be detected at the anode than at the cathode.

Obviously, in this study, the time of the application of positive polarity to any chamber during periodic electrode polarity reversal is half of that of the continuous current passage conditions. Hence the lactate extraction in continuous current passage is more than that obtained when electrode polarity reversal is employed.

However, as shown in the results, the differences between continuous current application and polarity reversal did not lead to halving of the lactate extraction when polarity reversal was compared to continuous current conditions. This might be due to membrane depolarisation effects once the polarity of the electrodes was reversed (Banga and Chein 1988) and this may have helped to maintain the transport properties of the membrane. Conversely, for continuous current passage, the membrane will become more negative in the anode chamber with the accumulation of chloride and lactate ions.

Although continuous current passage without switching promoted more lactate extraction compared with other switching modes, in practical devices for patient use it could cause erythrema and stinging (Howard *et al.* 1995). Periodic electrode polarity

reversal could help to depolarise skin at regular intervals (Banga and Chein 1988). In addition skin damage and irritation is minimised with polarity reversal (Tomohira *et al.* 1997). Therefore, 15 minutes electrode polarity reversal during current application was selected for healthy volunteer trials as this still gave good lactate extraction in the model system.

According to the result, consecutive increases in lactate extraction were found as the iontophoresis application time increased at each switching mode. Therefore, the longest iontophoresis application time (90 minutes) in this study seemed to be the best. However, practicalities of sampling for patients or for the healthy volunteer measurements in this study dictate that such long sessions are not desirable. Therefore, short iontophoresis application times (60 minutes) were recommended to be used in the study for the human subjects.

5.1.6 Effects of long duration bipolar direct current iontophoresis on membrane impedance

In the results, no significant difference was found between the pre-iontophoresis impedance for any of the four switching modes. This implied that the sample-to-sample variation was small.

The impedance of membrane post-iontophoresis was significantly smaller than that of the pre-iontophoresis and this was consistent with the results reported by Kalia and Guy in 1995 for human skin. It is possible that iontophoresis punctures the membrane and creates microscopic pores. Since the impedance of the membrane is determined by the ability of ions to flow through it, the barrier function of the membrane is impaired and ion transport therefore becomes easier, thus if the membrane is damaged: the impedance decreases. The decrease in post-iontophoresis impedance of membrane may also be due to increased local ion concentrations following

iontophoresis and the elevated ion levels may have been facilitated by transport through current-induced structural changes in the transport routes (Kalia and Guy 1995, Kasting 1992). This would shield the negative charge on the membrane. Finally, the membrane simply may have become more hydrated during current passage, lowering impedance. The greater the degree of membrane hydration, the more facile ion transport becomes and the lower the impedance (Kalia and Guy 1995). Similarly, Pikal and Shah in 1991 reported that the skin resistance was altered by hydration when iontophoresis was applied. In addition, Burnette and Ongpipattanakul in 1988 reported that skin resistance was decreased by hydration. In view of the above points, the enhancement of membrane hydration could be discussed in terms of membrane resistance. It was possible that the enhancement of membrane hydration was most responsible for the improvement of permeability (Menon *et al.* 1994).

5.1.7 Experimental validity and reliability

The error analysis reported in section 4.1 showed that the experimental technique was sufficiently reliable for the present analysis. The reproducibility of the Ag/AgCl electrodes through chlorination was shown to be very high. Therefore, Ag/AgCl electrodes, fabricated in this way, were good to be used on measuring the impedance of the membrane because of the low electrode-to-electrode variation of the resistance.

Analysis of the accuracy of the electrochemical interface (SI1286, Schlumberger Technologies, England) to deliver a constant current revealed that there was a negligible error (about 0.009%) on maintaining a constant iontophoresis current of 58.90 μA in this experiment. Providing and maintaining of a constant current is very important for reverse iontophoresis experiment as reverse iontophoresis is current dependent. Therefore, the electrochemical interface is highly suitable for this experiment.

For the impedance analyzer (SI1260, Schlumberger Technologies, England), there is a specific error in readings, ± 0.1 % in impedance measurement in the frequency range of 10 μHz up to 32 MHz, which is calculated and given by the manufacturer in the manual. Therefore, there was a negligible error (± 0.1 %) on the computation of the impedance of the membrane. More importantly, precaution was taken to minimise the introduction of error on the impedance spectrum measurement. To eliminate the preconditioning effect the results from the second test of impedance measurement are used for computation of the membrane impedance rather than the first (see Appendix A for the detail of the preconditioning effect).

For the spectrometer (Multiskan Ascent®, Labsystems Oy, Finland), there is a specific error in readings, ± 1 % in absorbance measurement, which is calculated and given by the manufacturer in the manual. Therefore, there was a negligible error (± 1 %) on the computation of the concentration of glucose and lactate. In this study, one of the objectives is to find the optimum switching mode for reverse iontophoresis of glucose and lactate. If the computational method is not accurate, error will be introduced into the results.

5.2 CONSTRUCTION AND EVALUATION OF A CONSTANT CURRENT DEVICE FOR REVERSE IONTOPHORESIS

5.2.1 Electronic evaluation of the circuit design

As shown in Table 4.3, the accuracy of the device in delivering constant currents was about ±0.7%. This ±0.7% error may be partly due to the error of data acquisition because the computer based oscilloscope (ADC-40, Pico Technology Limited, UK) has an accuracy of ±1%. Resistance tolerance (±1%) of the resistor used for evaluation may also contribute this ±0.7% error.

Because the microprocessor has an accuracy limit of ±1% on timing (Manufacturer data from PARALLAX), this contributes some errors in the frequency of the generated waveforms. As shown in Table 4.4, the measured time was always smaller than the preset time stored inside the microprocessor. Therefore, this timing error can be reduced by simply changing the program stored inside the microprocessor (see Appendix E). It was found that the timing error of the microprocessor can be reduced to be least than 0.4% if the preset time stored inside the microprocessor increased by 1%. For example, if we need the constant current device to provide a direct current for 15 minutes, the preset time stored inside the microprocessor should be 15.15 minutes (i.e. 15 minutes X 1.01).

Since the device is able to maintain a constant current at different load resistance with a negligible error of ±1.0%, this reflected that the device is able to maintain a constant current over a wide range of skin impedance. During iontophoresis or reverse iontophoresis, skin impedance decreases. Because the device is capable of maintaining constant current, it can be used for both iontophoresis and reverse iontophoresis as they need constant current for their controllable processes.

As a result, the device is expected to operate effectively for iontophoresis applications *in vivo*. The simplicity of the device is evident since polarity and duration of the applied current can be adjusted by software and stored inside the microprocessor. Since the current waveform is controlled by a program, less electronic components are required to generate different waveforms of current and this reduces the overall device size.

5.2.2 *In vitro* reverse iontophoresis evaluation of the circuit design

Obviously, the reverse iontophoresis experiments on glucose and lactate extraction conducted using the newly-developed constant current device had similar

results as those obtained by the use of the electrochemical interface. The device can effectively and significantly extract glucose and lactate across the nanoporous membrane as compared to diffusion alone. Therefore, it was supposed that the device could be used for reverse iontophoresis on glucose and lactate extraction on humans.

Clearly, the device significantly reduced the impedance of the nanoporous membrane after reverse iontophoresis and this was found to be identical to the results obtained by the use of the conventional electrochemical interface. This phenomenon was explained in section 5.1.6.

5.2.3 Limitations of the circuit design

There are two limitations to this device. First, the pulsed time and bipolar time cannot be very short because they are limited by the operation time of the relays and microprocessor. The typical operation time of the double pole double throw (DPDT) and single pole single throw (SPST) relays is 3 ms and 0.5 ms, respectively. Also, the microprocessor takes 0.5 ms to read in instruction. Therefore, the pulsed time and bipolar time should be greater than 1 ms (i.e. 0.5 ms delay from the SPST relay plus 0.5 ms delay from the microprocessor) and 3.5 ms (i.e. 3 ms delay from the DPDT relay plus 0.5 ms delay from the microprocessor), respectively. This is not a great limitation as the application times for current in iontophoresis are minutes rather than seconds. The software and microprocessor easily allow passage of DC for periods of time up to 20 minutes or greater at any one polarity.

Another limitation is that the delays produced by the PAUSE instruction to the microprocessor, which is used for timing, are ±1%. Therefore, the more extensive the use of the PAUSE instruction and the PAUSE period, the higher the error.

To minimise the problem generated by the use of the DPDT and SPST relays, an analogue switch (e.g. ADG441, ANALOG DEVICES) can be used to replace them providing faster switching times (generally, both $Time_{ON}$ and $Time_{OFF}$ are in

nanoseconds) and lower power consumption (less than 5 mW in general). With this modification a much shorter pulsed time or bipolar time can be achieved and a 9V battery can be use to operate the whole circuit for a much longer time. However, use of the analogue switch in the present circuit design generates another problem, current leakage. Usually, an analogue switch has nanoampere current leakage, which may cause noise in the applied current. Therefore, DPDT and SPST relays were used in the present circuit design rather analogue switches.

Problem, generated by the microprocessor Basic Stamp I (BS1-IC, PARALLAX), can be minimised by the use of a latest version of Basic Stamp, such as BASIC Stamp 2p (BS2P-24, PARALLAX) which has a relatively higher speed of Basic interpreter (12000 Basic instructions per second) compared to the BS1-IC used in the present circuit design (2000 Basic instructions per second). However, the cost of the BS2P-24 (£59) is much more expensive than that of the BS1-IC (£25). Also, the power consumption by the BS2P-24 (60 mA) is much higher than that of the BS1-IC (2 mA). BS1-IC is therefore preferred.

5.2.4 Potential clinical applications of the constant current device

The major application for this device is in iontophoresis drug delivery or reverse iontophoresis extraction of molecules and ions from human skin for non-invasive monitoring of human patients.

Another potential application of this device is cranial electrotherapy stimulation (CES) therapy. CES is the application of low-level, pulsed electrical currents (usually not exceeding one milliampere), applied to the head for medical and/or psychological purposes. The current is applied by easy-to-use clip electrodes that attach on the ear lobes, or by stethoscope-type electrodes placed behind the ears. CES is primarily used for the treatment of anxiety, insomnia, depression and chemical dependency. Numerous experimental and clinical studies have been performed to investigate the

efficacy of CES therapy for these disorders (Klawansky *et al.* 1995, Shealy *et al.* 1989, Schmitt *et al.* 1986 & 1984, Jarzembski 1985, Smith 1982, Moore *et al.* 1975, Rosenthal 1971). These studies have used a variety of CES devices with current levels generally ranging from 50 μA to 5 mA and treatment sessions of approximately 30 min over 5–15 days.

An additional application of the device is transcutaneous electrical nerve stimulation (TENS). TENS is the application of an electrical current (range from microampere to milliampere) through electrodes attached to the skin. The commonest clinical application of TENS is pain control. Many experimental and clinical studies have proven that TENS is effective for localized treatment of pain (De Angelis *et al.* 2003, Chiu *et al.* 1999, Benedetti *et al.* 1997, Wildersmith 1989).

5.3 CONSTRUCTION OF A SCREEN-PRINTED ELECTRODE FOR REVERSE IONTOPHORESIS

5.3.1 The specially-designed diffusion cell

Model systems for reverse iontophoresis studies *in vitro* do exist but there are a number of problems associated with their use which make them less than ideal for device and sensor development. The Franz cell is the most commonly used diffusion cell for pharmaceutical studies of transdermal molecular transmission or extraction (Sage and Riviere 1992) but it does not readily lend itself to sensor development applications. The structural design of the Franz cell for iontophoresis studies is such that electrodes which drive iontophoretic current are placed on either side of a skin sample suspended in bathing solution. However, in the real clinical situation, electrodes are mounted close to each other on the surface of the patient's skin. Therefore, the electric current pathways and applied electric field directions are very different in both

situations. In 1988, Glickfeld *et al.* developed a new diffusion cell for iontophoresis-assisted transdermal drug delivery, closely replicating the real clinical situation, where two iontophoresis chambers were mounted on the outer side of a animal skin sample with a third chamber placed between to aid electrical isolation of the two iontophoresis chambers.

As mentioned in section 5.1.1, there are some problems for a model system using excised animal or human skin samples. Also, the diffusion cell developed by Glickfeld *et al.* (1998) cannot be used for sensor (e.g. hydrogel electrode) development. Therefore, a model system for the study of transdermal molecular transmission or extraction, inspired by the design of Glickfeld *et al.* (1998) and suitable for sensor development and testing has been designed and developed in the bioengineering unit (Connolly *et al.* 2002). The model system was further developed in the course of this project to allow gel electrodes to be directly tested on artificial membrane for iontophoresis. The model system (see Figure 3.21 and 3.22 for the details of the model system) is used with a nanoporous membrane fixed in front of a chamber to mimic the real clinical situation so that both sensors, gel electrodes this time, are mounted close to each other on the surface of the membrane. Once the electrodes were evaluated by this model system, the electrodes were then used on humans.

5.3.2 Screen-printed electrodes for reverse iontophoresis

Reverse iontophoresis is gaining acceptance in human medicine in the field of non-invasive diagnosis (Merino *et al.* 1999, Numajiri *et al.* 1993) and patient monitoring (Potts *et al.* 2002, Pitzer *et al.* 2001, Tierney *et al.* 2001, Tamada *et al.* 1999, Rao *et al.* 1995, Numajiri *et al.* 1993). To determine the concentration of a substance of interest extracted by reverse iontophoresis, the extracted substance should be captured in the electrode contact media, either in liquid (e.g. buffer solution) or in solid form (e.g. solid

gel), so that it can be determined by analytical methods such as biosensor technology or spectrometric assays. For clinical use, it is much better to use the media in solid form rather than in liquid form because of the convenience and ease of use and handing.

Up till now, not so many studies investigated reverse iontophoresis on human skin in live subjects. Some studies (Degim *et al.* 2003, Rao *et al.* 1995) used the electrode contact media in liquid form while other studies (Potts *et al.* 2002, Tierney *et al.* 2001 and 2000) use a solid form. Two groups of favoured materials that have emerged over the last decade for media (in solid form) are electroactive polymers and gels. Normally, gel is preferred as it possesses some very attractive features including high water content, non-toxicity and high chemical and hydrolytic stability. Hence a gel was selected for this study.

To fabricate a low-cost, disposable and reliable electrode for this study, screen-printing techniques were employed. These techniques are used not only because of their precision and reproducibility, but also because of the speed, relative cheapness, flexibility of design, choice of materials and low barrier for technology transfer capability with which electrodes can be produced (Galanvidal *et al.* 1995, Hart and Wring 1994 and 1997, Alvarez-Icaza and Bilitewski 1993, Gilmartin and Hart 1992). Actually, the screen-printing technique is widely used in the production of enzyme-based sensors (Alvarez-Icaza and Bilitewski 1993, Wring and Hart 1992, Kulys and Dcosta 1991).

Circular shape screen-printed electrodes were used in all experiments using the rectangular diffusion cell. This is because a circular electrode with the same area as a rectangular electrode yields 32% lower non-uniformity of the current distribution at the electrode-skin interface (Krasteva and Papazov 2002).

5.3.3 *In vitro* reverse iontophoresis evaluation of the screen-printed electrodes

Obviously, the newly-developed screen-printed electrode can be used to effectively and significantly extract glucose and lactate across the nanoporous membrane as compared to diffusion alone. More importantly, the pH of the methylcellulose (MC) gel remained the same (midway between pH 7 and pH 8 as measured by litmus paper) after revere iontophoresis and this showed that the Ag/AgCl part of the screen-printed electrode in addition to the buffer used was effective in maintaining the pH of the MC gel. This is very important for the reverse iontophoresis of glucose. At physiological pH (about pH 7.4), the skin is negatively charged and cation permselective (Burnette *et al.* 1987). Thus, current passage causes a net convective solvent flow in the anode-to-cathode direction, facilitating cation transport, inhabiting that of anions, and enabling the enhanced transdermal transport of neutral, polar solutes (Kim *et al.* 1993, Burnette *et al.* 1987).

On the other hand, no significant difference was found on the amount of glucose and lactate extracted by the use of screen-printed electrode or traditional rod-type Ag/AgCl electrode (see Figure 5.1). This means that the screen-printed electrode can work as efficiently as the traditional rod-type Ag/AgCl electrode.

5.3.4 Effects of long duration bipolar direct current on human transdermal extraction of glucose and lactate

Maintaining a constant pH of the methylcellulose (MC) gel during reverse iontophoresis is very important not only for maintaining of the direction of the electroosmotic flow, but also for preventing skin irritation (Tapper 1983). In this study of human transdermal extraction of glucose and lactate, the pH of the MC gel was found to remain unchanged after reverse iontophoresis. Therefore, 40% of the subjects

having very mild erythema might be due to the effects of current application during reverse iontophoresis.

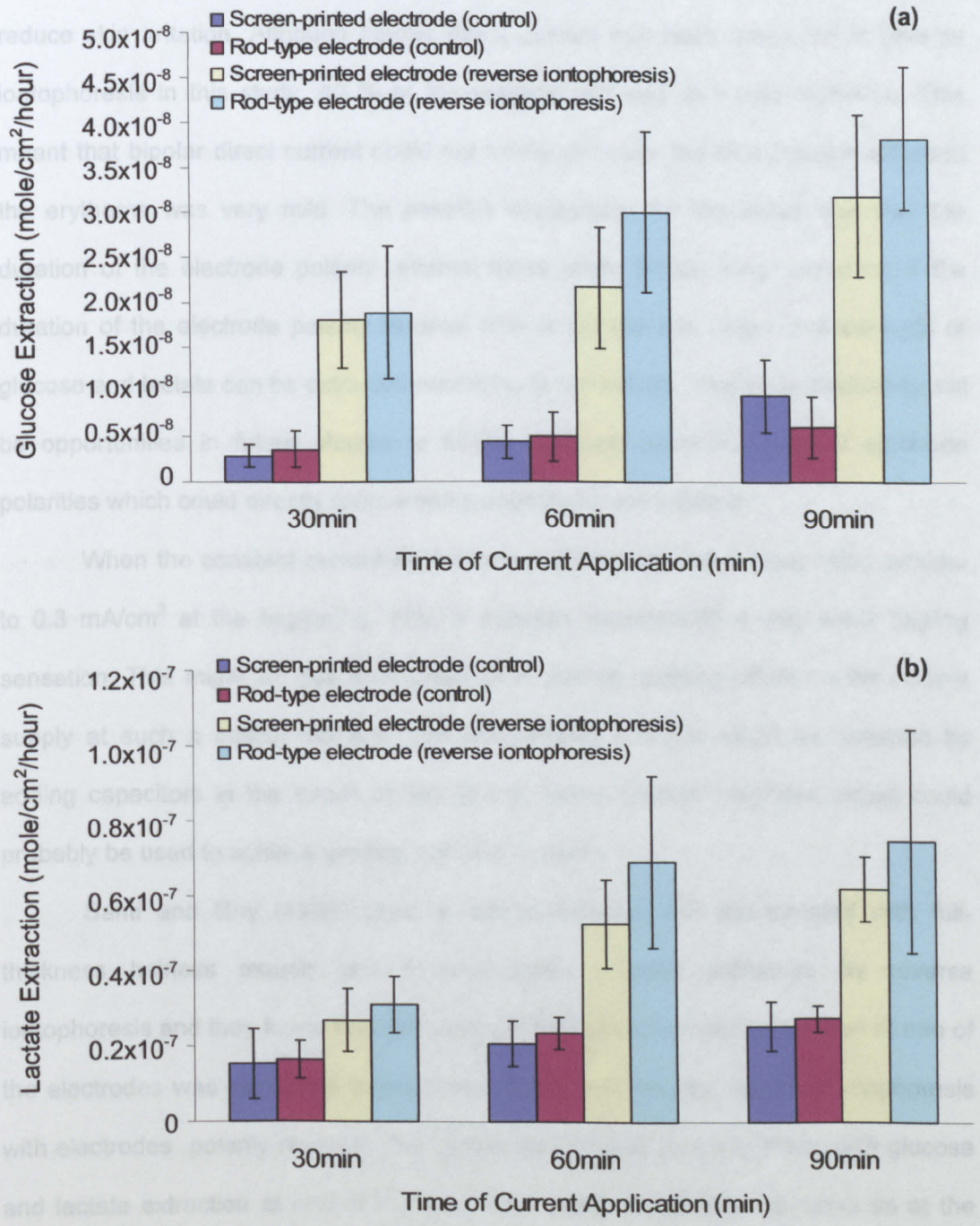

Figure 5.1 – Comparison on the amount of **(a)** glucose and **(b)** lactate extracted by the use of screen-printed electrode or traditional rod-type Ag/AgCl electrode. Results are expressed as mean ± SD (n≥10 for each bar).

It is well known that direct current can cause skin polarisation (Howard *et al.* 1995) and skin polarisation results in skin irritation. Polarised skin as a consequence of direct current passage is believed to be repolarised once the direction of the direct current flow is reversed. In this study, it was postulated that bipolar direct current could reduce skin irritation. Although bipolar direct current has been employed in reverse iontophoresis in this study, 40 % of the subjects still had very mild erythema. This meant that bipolar direct current could not totally eliminate the skin irritation although the erythema was very mild. The possible explanation for this result was that the duration of the electrode polarity reversal times might be too long. However, if the duration of the electrode polarity reversal time is set too low, only small amounts of glucose and lactate can be extracted according to our results. Therefore, there may still be opportunities in future studies to further optimise switching times of electrode polarities which could directly reduce some aspects of skin irritation.

When the constant current device was switched on with current being brought to 0.3 mA/cm^2 at the beginning, 10% of subjects experienced a very weak tingling sensation. This might be due to the lack of a gradual ramping effect on the current supply at such a critical moment. Gradual ramping currents might be obtained by adding capacitors in the circuit of the device. Some special integrated circuit could probably be used to achieve gradual ramping currents.

Santi and Guy (1996) used a vertical diffusion cell incorporated with full-thickness hairless mouse skin to investigate mannitol extraction by reverse iontophoresis and they found that, for a pair of electrodes, mannitol extraction at one of the electrodes was significant different from the other one after reverse iontophoresis with electrodes polarity reversal. Our finding was inconsistent with them, with glucose and lactate extraction at one of the electrodes being statistically the same as at the other electrode. Our finding suggested that the initial polarity of the electrode was not important for reverse iontophoresis with polarity reversal which would be the logical

expectation if both chambers of a device get to be both anode and cathode for equal duration during extraction.

Not many researchers have investigated glucose extraction by reverse iontophoresis in human subjects (Rao *et al.* 1995, Sieg *et al.* 2004a, Sieg *et al.* 2004b, Sieg *et al.* 2003) and no researchers have studied the effects of reverse iontophoresis on lactate extraction both in human subjects and *in vitro*. In the past twenty years, several papers (Rao *et al.* 1995, Sieg *et al.* 2004a, Sieg *et al.* 2004b, Sieg *et al.* 2003) were found for the reverse iontophoresis of glucose in humans, but only one relevant paper (Rao *et al.* 1995) was found with which could be used for comparison with our findings. On the other hand, no relevant paper was found for the reverse iontophoresis of lactate in human subjects. Rao *et al.* (1995) passed a direct current (0.25 mA/cm^2) across the human skin (ventral forearm) of subjects for a period of 60 minutes to extract glucose out of the skin and they found that around 5.83 pmol of glucose could be extracted at the cathode using that criteria. However, our finding was not in agreement with them. In this study (i.e. current density = 0.3 mA/cm^2, time of current application = 60 minutes, electrode polarity reversal = every 15 minutes), it was found that around 13.95 pmol (i.e. 155 μM x 90 μl) of glucose could be extracted by long duration bipolar direct current. The possible explanation might be that we used a higher current density (0.3 mA/cm^2) compared to Rao *et al.* (1995). More importantly, we used a bipolar direct current rather than a direct current. Bipolar direct current can prevent skin polarisation (Banga and Chein 1988) and skin polarisation can reduce the level of electroosmosis (Lawler *et al.* 1960). Because glucose is mainly extracted out of the skin by electroosmosis and bipolar direct current can prevent the reduction in the level of electroosmosis, bipolar direct current can promote more glucose extraction than direct current.

Obviously, long duration bipolar direct current could significantly promote more glucose and lactate extraction than diffusion alone.

5.3.5 Long duration bipolar direct current on the electrical properties of human skin

In this study, human skin electrical resistance was found to be about 96.2 – 127.7 kΩ/cm^2 at 1 Hz (see Table 4.9 and Figure 4.14) and this is very close to that reported by Yamamoto and Yamamoto (1976). They reported that the human skin electrical resistance was about 95 kΩ/cm^2 at dc. In this study, ten subjects were recruited for participation and there was no large difference between their skin electrical impedances before the experiment. Therefore, any changes on the skin electrical resistance after the experiment could reflect the effect of long duration bipolar direct current on skin electrical properties.

As reported in our findings (see Table 4.9), long duration bipolar direct current significantly reduced the skin electrical resistance from 109.7 kΩ/cm^2 to 74.2 kΩ/cm^2 (i.e. 32.4 % reduction in the skin electrical resistance after iontophoresis; impedance here is at frequency of 1 Hz) and this was consistent with the findings reported by Kalia and Guy in 1995 except that they noted a much larger percentage reduction in the impedance measured. They studied the effect of iontophoresis current density on the electrical resistance properties of human skin *in vivo* and they found that passage of a current (0.1 mA/cm^2) for 15 minutes caused a significant reduction in the magnitude of the skin electrical resistance from 176.3 kΩ/cm^2 to 4.7 kΩ/cm^2 (i.e. 97.3 % reduction in the skin resistance after iontophoresis; impedance here is at frequency of 1 Hz). The reason underlying the huge difference in the percentage reduction in the skin electrical resistance after iontophoresis between our findings and the Kalia and Guy (1995) findings may be due to different electrode systems being used to apply the iontophoresis current. Our electrode system uses screen-printed Ag/AgCl electrodes filled with gel whereas the electrode system used by Kalia and Guy (1995) is based upon electrode chambers filled with solution and they used rod-type Ag/AgCl electrodes to pass iontophoresis current to the solution at the electrode chambers.

Therefore, our electrode system might have a better uniformity of iontophoresis current density while their electrode system may have non-uniformity in the distribution of iontophoresis current as the current in their electrode system is spreading from electrode to the solution. Therefore, their electrode system might have a greater chance to form a localised high current density spots and this might increase the chances to puncture (electroporate) the skin, creating more microscopic pores.

In general, the possible explanation for the reduction in skin electrical resistance after passage of a current is that current may puncture the skin and create microscopic pores. Increased local ion concentrations following passage of a current may also contribute to the reduction in skin electrical resistance (Kalia and Guy 1995, Kasting 1992).

Kalia and Guy (1995) reported that low skin electrical resistance reflected the high degree of skin hydration. Also, it was reported that skin electrical resistance was decreased by hydration (Pikal and Shah 1991, Burnette and Ongpipattanakul 1988). In this study, the average skin electrical resistance at the control site (i.e. no current passage) reduced from 114.1 $k\Omega/cm^2$ to 104.5 $k\Omega/cm^2$ (i.e. 8.4 % reduction in the skin resistance after experiment; impedance here is at a frequency of 1 Hz). According to the finding reported by Kalia and Guy (1995), Pikal and Shah (1991) as well as Burnette and Ongpipattanakul (1988), the reduction in skin electrical resistance at the control site after the experiment is due to the skin being hydrated. Based on the findings of the control experiments in the present study, skin being hydrated at the reverse iontophoresis site after the passage of long duration bipolar direct current is one of the reasons for the reduction in skin electrical resistance at the reverse iontophoresis site. However, the further reduction in skin electrical resistance at the reverse iontophoresis site after the passage of long duration bipolar direct current as compared with the control experiments may be due to the creation of microscopic pores at skin after current passage, skin being further hydrated by liquid flow due to current, increased local ion concentrations following passage of a current, or a

combination of all. Which one is the dominant factor underlying the further reduction in skin electrical resistance at the reverse iontophoresis site after the passage of long duration bipolar direct current as compared with the control experiment is not known at this time. However, one thing is clear, the resistance change on passage of current is significantly different from the hydration-only effects observed at the control electrode.

5.3.6 Experimental validity and reliability

The error analysis reported in section 4.8 showed that the experimental technique was sufficiently reliable for the present analysis. The reproducibility of the screen-printed electrodes was shown to be acceptable with ±7% variation on fabrication process. This ±7% variation on the fabrication process of screen-printed electrodes might be dramatically reduced by using computerised screen-printing technique rather than manual screen-printing technique.

Error in the removal of methylcellulose (MC) gel from the screen-printed electrode after experiments was negligible (about ±2.4%). The removal method of MC gel was very important for the computation of the amount of glucose and lactate to be extracted by reverse iontophoresis as both extracted glucose and lactate are in the region of μM. In this study, one of the objectives is to find the long duration bipolar direct current in human transdermal extraction of glucose and lactate. If the removal method of MC gel from the screen-printed electrode after experiments is not accurate, error will be introduced into the results.

Precautions were taken to minimise the introduction of error on the impedance spectrum measurement. The first impedance measurement of any set is used to eliminate the precondition effect while the second trial of impedance measurement is used for computation of the skin impedance (see Appendix D for the detail of the preconditioning effect).

5.4 CORRELATION ON THE REAL BLOOD GLUCOSE/LACTATE LEVELS WITH THE EXTRACTED GLUCOSE/LACTATE LEVELS

As shown in Figures 4.16b and 4.17b, no relationship was found between the glucose in the healthy subjects' blood and the extracted glucose levels of the collection electrode methylcellulose (MC) gel after reverse iontophoresis as well as no relationship was found between the subject's blood lactate and the extracted lactate levels of the collection MC gel after reverse iontophoresis. However, when outliers were removed from the regression equations during correlation analysis, improved correlations were obtained. The possible explanation for that might be due to the small sample size (10 healthy volunteers in this study) leading to high variations.

It could be seen that the outliers removed from the correlation on the real blood glucose level with the extracted glucose level were far away from the linear regression line (see Figure 4.16). Similarly, outliers removed from the correlation on the real blood lactate level with the extracted lactate level were far away from the linear regression line (see Figure 4.17). In correlation analysis, the correlation coefficients (r^2), an index to reflect a quantitative measure of the relationship between two variables, are affected by sample size, the types of variable being studied, and so on. Therefore, better correlations without the elimination of outliers from the linear regression lines can be obtained if the sample size is big enough so that the variations of data are low as well as data are more random. Moreover, only not healthy subjects data but also patient subjects (e.g. diabetic patients) data should be included in the correlations analysis because this will provide a wider range of data making the correlations analysis more reliable. However, it may be that no such correlation will exist in a wider sample.

Apart from using data (i.e. blood glucose level, extracted glucose level, blood lactate level and extracted lactate level) to perform correlation analyses between the blood glucose level and extracted glucose level as well as correlation analyses between the blood lactate level and extracted lactate level, all these data could benefit

in the other types of correlation. The details of the other types of correlation were described in the flowing section 5.5.

5.5 RELATIONSHIP AMONG THE SKIN IMPEDANCE, THE REAL BLOOD GLUCOSE/LACTATE LEVELS AND THE EXTRACTED GLUCOSE/LACTATE LEVELS

A good relationship was found between the skin impedance ratio (impedance was measured at a frequency of 1 Hz) and the glucose ratio. Besides, the skin impedance ratio was found to have a good relationship with the lactate ratio. This suggests that subject's blood glucose or lactate levels could be estimated by linear regression equations with more physical parameters (e.g. skin impedance). For a healthy population, it is possible to obtain an estimate of the glucose level in a subject's blood by the use of the linear regression equation ($y = -41.10x + 88.50$; where y is the glucose ratio and x is the skin impedance ratio) as showed in Figure 4.18a, as well as the lactate level in the subject's blood by the use of the linear regression equation ($y = 234.30x - 100.37$; where y is the lactate ratio and x is the skin impedance ratio) as showed in Figure 4.19a. This is a significant result for iontophoresis practical systems and one which we shall pursue in future studies. However, it must be remembered that all of these results have been taken in healthy volunteer samples therefore there is no guarantee or suggestion at this stage that a wider population sample would correlate.

Again, some outliers have been removed to improve the correlation in the correlation analysis because of the small sample size leading to high variations. As mentioned in the above section 5.4, better correlations without the elimination of outliers from the linear regression lines can be obtained if the sample size is big enough and patient subjects (e.g. diabetic patients) data is included.

By the use of the two linear regression equations as mentioned above, one's blood glucose and lactate level could be estimated non-invasively for a healthy subject. If this method could be extended to a wider population it would bring benefit to some patients, such as diabetic patients. Most type 1 diabetic patients measure their own blood glucose at several times a day by obtaining finger-prick capillary samples and applying the blood to a reagent strip for analysis in a portable meter (Pickup 2003). However, this method is painful, cumbersome, aesthetically unpleasant and inconvenient. More importantly, this method is not a continuous monitoring method and therefore blood glucose monitoring cannot be performed during sleeping and whilst the subject is occupied, such as during driving a motor vehicle.

It can be foreseen that this method (i.e. reverse iontophoresis extraction of glucose and lactate as well as skin electrical impedance measurement) can possibly be able to work with glucose (see Appendix F for the details of the construction and performances of the glucose biosensor) and lactate biosensors to provide an automatically, continuously and non-invasively determination of both glucose and lactate level at the same time in the patient's blood.

5.6 LIMITATIONS OF THE STUDY

Like many other research studies, limitations are inevitable. In the part of the reverse iontophoresis optimisation on glucose and lactate extraction, owing to time constraints, only four time intervals (5, 10, 15 minutes or dc) electrodes polarity reversal were investigated in the current study. Other time intervals from 1 minute up to 15 minutes designed at intervals of 1 minute, are suggested in future study so as to obtain a more comprehensive picture of the effects of the switching modes on the reverse iontophoresis of glucose and lactate extraction.

Although a monitoring system for non-invasive monitoring of metabolites in human subjects has been developed, this system was only semi-automatic for the whole process of monitoring. After the automatic reverse iontophoresis extraction of glucose and lactate across the human skin into the methylcellulose (MC) gel of the screen-printed electrode, it is necessary to extract the MC gel from the screen-printed electrode manually and quantify the amount of the extracted glucose and lactate manually by spectrometric assay. To make this system operate automatically, the MC gel screen-printed electrode should be incorporate glucose and lactate biosensors together with a modified iontophoresis device to automatically quantify the amount of the extracted glucose and lactate.

Due to the time constraints only ten normal subjects were recruited. The sample size is small and variations are therefore high. That's why some outliers have been removed from the regression equation in order to get a good correlation between the blood glucose level and extracted glucose level as well as the blood lactate level and extracted lactate level. More normal subjects for the correlation analysis are suggested in future studies so as to increase the reliability of the correlation analysis.

By reason of the time constraints, clinical patient subjects have not been recruited for the current study. Participation of clinical patient subjects is critical for future studies so as to analysis the feasibility of the application of the monitoring system on patients.

5.7 POTENTIAL CLINICAL APPLICATIONS

Results of the current study have shown that the monitoring system could effectively and non-invasively extract metabolites, glucose and lactate, across the human skin in live subjects and the amount of the extracted glucose and lactate could be quantified by spectrometric analysis of the gel of the electrode. Apart from glucose

and lactate monitoring, this monitoring system can be used to monitor the other metabolites which can be extracted by reverse iontophoresis. For example, this monitoring system could be possibly employed in monitoring of prostaglandin E_2, a small negatively charged molecule at physiological pH, during the initiation and development of irritant or allergic response (Mize *et al.* 1997). Urea is another example. Urea is a small, uncharged and hydrophilic molecule. Just like glucose, urea can be extracted by electroosmotic flow during reverse iontophoresis (Degim *et al.* 2003). Therefore, this monitoring system could be possibly employed in monitoring of the urea level of patients with insufficient kidney function (e.g. renal failure) for understanding the need for dialysis (Degim *et al.* 2003).

On the other hand, the constant current device has its own potential clinical applications. Apart from the clinical applications on cranial electrotherapy stimulation therapy and transcutaneous electrical nerve stimulation as mentioned in section 5.2.4, the device possibly can be employed in reducing edema (Mohr *et al.* 1987), due to the results of surgery or injuries. The idea is that the device could electrically induce muscle contraction, which helps stimulate circulation by pumping fluid and blood through veins and lymphatic channels back into the heart.

5.8 RECOMMENDATIONS FOR FUTURE STUDIES

The present study has thoroughly examined the monitoring system for non-invasive monitoring of glucose and lactate. However, much further research work still needs to be done so that the monitoring system can operate automatically.

It should be noted that 40 % of the subjects have very mild erythema. This is possibly due to the long time intervals (15 minutes) between reversals of the electrode polarities. Future investigations for short time intervals between polarity reversals (1 to

15 minutes at intervals of 1 minute) are suggested so as to obtain an optimum time interval with perhaps less skin irritation but efficient glucose and lactate extraction.

Another requirement for future studies is the automatic measurement, within the iontophoresis system of glucose and lactate in the gel. This will require the incorporation of biosensors into the device. Many types of biosensors exist today for glucose (Gala´n-Vidal *et al.* 1998, Nagata *et al.* 1995) and lactate (Hart *et al.* 1996, Collier *at al.* 1996) therefore expediting the development of this part of the system.

One long-term outcome of this work and similar studies might be the use of these findings and devices to build an artificial pancreas, i.e. mimicking the physiological situation to supply insulin according to glucose levels(Jaremko and Rorstad 1998, Shichiri *et al.* 1984 and 1982), This would require the use of the monitoring system (requiring further investigation for automatic operation as described in the previous paragraph) developed in this study and an iontophoresis technique or implanted pump for transdermal or internal insulin delivery. With such a system, the glucose biosensor readings would be immediately transferred to a microprocessor that could calculate the necessary insulin infusion rates by means of an appropriate feedback algorithm.

■ *Chapter 6*

Conclusion

Chapter 6 Conclusion

In the first part of the study, it was demonstrated that reverse iontophoresis using long duration bipolar direct current facilitated glucose and lactate extraction. It was shown that the efficiency of the glucose and lactate extraction could be maximised by alternating the duration interval (time between polarity switching) of the long duration bipolar direct current. Results also suggested that current passage with periodic electrode polarity reversal significantly promoted more glucose extraction than continuous current passage without switching. In this study, 15 minutes between electrode polarity reversals provides an optimum condition for glucose extraction as compared with other switching modes. On the other hand, continuous current passage (without switching) led to more lactate extraction than all other switching modes. However, in this study, passage of current combined with electrode polarity reversal every 15 minutes since this was the best glucose extraction condition and lactate extraction under these conditions was still good. More importantly, current passage with electrode polarity reversing could reduce skin irritation. Finally, long duration bipolar direct current was found to result in a reduction in the electrical resistance of an artificial skin membrane (cellulose ester).

In the second part of the study, it was demonstrated that a low-cost, low-power, miniature, programmable constant current device designed for this study could operate effectively. Based on the results obtained, it is concluded that the constant current device is accurate enough, with about ±0.7% error, for delivery of continuous constant current in the range of 1 μA and 300 μA. However, it is necessary to bear in mind that there is a certain amount of error (0% up to ±1.3%, depending on the waveform of current selected), in the magnitude of the delivered current. It was demonstrated that

the constant current device could be used for reverse iontophoresis of glucose and lactate across a membrane.

In the third part of the study, it was shown that a low-cost and reliable screen-printed electrode has been developed. The reproducibility of the screen-printed electrodes was demonstrated to be acceptable with ±7% error on the fabrication process as measured by electrical impedance differences. It was demonstrated that long duration bipolar direct current with 15 minutes electrode polarity reversal facilitated glucose and lactate extraction across the human skin *in vivo* and resulted in a reduction in the electrical resistance of the human skin *in vivo*. A good relationship was found between the skin impedance ratio as defined by pre- and post- iontophoresis measurements and the extracted to internal blood glucose ratio. In addition, the skin impedance ratio was similarly found to have a good relationship with the lactate ratio.

In a nutshell, a prototype monitoring system for non-invasive monitoring of metabolites, glucose and lactate, has been developed.

References

References

Abramson D, Scalea TM, Hitchcock R, Trooskin SZ, Henry SM and Greenspan J (1993). Lactate clearance and survival following injury. Journal of Trauma-Injury and Critical Care; 35: 584-589.

Al-Asadi L, Dellinger R, Deutch J and Nathan S (1996). Clinical impact of closed versus open provider care in a medical intensive care unit. American Journal of Respiratory and Critical Care Medicine; 153: A360.

Almeida NF and Mulchandani AK (1993). A mediated amperometric enzyme electrode using tetrathiafulvalene and L-glutamic acid. Analytica Chimica Acta; 282: 353-361.

Alvarez-Figueroa MJ and Blanco-Mendez J (2001). Transdermal delivery of methotrexate: iontophoretic delivery from hydrogels and passive delivery from microemulsions. International Journal of Pharmaceutics; 215: 57-65.

Alvarez-Icaza M and Bilitewski U (1993). Mass-Production of Biosensors. Analytical Chemistry; 65: A525-A533.

American Diabetes Association (1998). Economic consequences of diabetes mellitus in the U.S. in 1997. Diabetes Care; 21: 296-309.

American Diabetes Association (2003). Economic costs of diabetes in the U.S. in 2002. Diabetes Care; 26: 917-932.

Amos AF, McCarty DJ and Zimmet P (1997). The rising global burden of diabetes and its complications: estimates and projections to the year 2010. Diabetic Medicine; 14 (Suppl. 5): S1-S85.

Angus DC, Kelley MA, Schmitz RJ, White A, Popovich J Jr and Committee on Manpower for Pulmonary and Critical Care Societies (COMPACCS) (2000). Caring for the critically ill patient. Current and projected workforce requirements for care of the critically ill and patients with pulmonary disease: can we meet the requirements of an aging population? Journal of the American Medical Association; 284: 2762-2770.

Artru F, Jourdan C, Perret-Liaudet A, Charlot M and Mottolese C (1998). Low brain tissue oxygen pressure: incidence and corrective therapies. Neurological Research; 20 (Suppl 1): S48-S51.

Back DM, Michalska DF and Polavarapuu PL (1984). Fourier transform infrared spectroscopy as a powerful tool for the study of carbohydrates in aqueous solution. Applied Spectroscopy; 38: 173-180.

Bakker J, Coffernils M, Leon M, Gris P and Vincent JL (1991). Blood lactate levels are superior to oxygen-derived variables in predicting outcome in human septic shock. Chest; 99: 956-962.

Banga AK and Chein YW (1988). Iontophoretic delivery of drugs: Fundamentals, developments and biomedical applications. Journal of Controlled Release; 7: 1-24.

Banga AK and Chien YW (1993). Hydrogel-based iontophoretic delivery devices for transdermal delivery of peptide/protein drugs. Pharmaceutical Research; 10: 697-702.

Bantle JP and Thomas W (1997). Glucose Measurement in Patients with Diabetes Mellitus with Dermal Interstitial Fluid. Journal of Laboratory and Clinical Medicine; 130: 436-441.

Beh SK, Moody GJ and Thomas JDR (1991). Studies on enzyme electrodes with ferrocene and carbon paste bound with cellulose triacetate. Analyst; 116: 459-462.

Behnam AB, Nguyen D, Moran SL and Serletti JM (2003). TRAM flap breast reconstruction for patients with advanced breast disease. Annals of Plastic Surgery; 50: 567-571.

Bell DSH (1994). Stroke in the diabetic patient. Diabetes Care; 17: 213-219.

Benedetti F, Amanzio M, Casadio C, Cavallo A, Cianci R, Giobbe R, Mancuso M, Ruffini E and Maggi G (1997). Control of postoperative pain by transcutaneous electrical nerve stimulation after thoracic operations. Annals of Thoracic Surgery; 63: 773-776.

Bild DE, Selby JV, Sinnock P, Browner WS, Braveman P and Showstack JA (1989). Lower-extremity amputation in people with diabetes. Epidemiology and prevention. Diabetes Care; 12: 24-31.

Boyle DIR, Morris AD and MacDonald TM (1998). A record linkage capture-recapture technique to create a diabetes disease register for epidemiological research. http://www.dundee.ac.uk/memo/dougie.htm

Brancati FL, Whelton PK, Randall BL, Neaton JD, Stamler J and Klag MJ (1997). Risk of end-stage renal disease in diabetes mellitus: a prospective cohort study of men screened for MRFIT. Multiple Risk Factor Intervention Trial. Journal of the American Medical Association; 278: 2069-2074.

Brand RM and Iversen PL (1996). Iontophoretic delivery of a telomeric oligonucleotide. Pharmaceutical Research; 13: 851-854.

British Pharmacopoeia (2003). Appendix. London: Stationery Office, 2003. pp. A130.

Burnette RR (1989). Iontophoresis Transdermal Drug Delivery ed J Hadgraft and R H Guy (New York: Marcel Dekker) pp 247-291.

Burnette RR and Marrero D (1986). Comparison between the iontophoretic and passive transport of thyrotropin releasing hormone across excised nude mouse skin. Journal of Pharmaceutical Sciences: 738-743.

Burnette RR and Ongipipattanakul B (1988). Characterization of the pore transport properties and tissue alteration of excised human skin during iontophoresis. Journal of Pharmaceutical Sciences; 77: 132-137.

Burnette RR and Ongpipattanakul B (1987). Characterization of the perm selective properties of excised human skin during iontophoresis. Journal of Pharmaceutical Sciences; 76: 765-773.

Caduff A, Hirt E, Feldman Y, Ali Z and Heinemann L (2003). First human experiments with a novel non-invasive, non-optical continuous glucose monitoring system. Biosensors & Bioelectronics; 19: 209-217.

Cairns CB, Moore FA, Haenel JB, Gallea BL, Ortner JP, Rose SJ and Moore EE (1997). Evidence for early supply independent mitochondrial dysfunction in patients developing multiple organ failure after trauma. Journal of Trauma-Injury Infection and Critical Care; 42: 532-536.

Calkin AC, Sudhir K, Honisett S, Williams MRI, Dawood T and Komesaroff PA (2002). Rapid potentiation of endothelium-dependent vasodilation by estradiol in postmenopausal women is mediated via cyclooxygenase 2. Journal of Clinical Endocrinology and Metabolism; 87: 5072-5075.

Cameron BD, Gorde HW and Coté GL (1999). Development of an Optical Polarimeter for in vivo Glucose Monitoring. Proceedings of the Society of Photo-Optical Instrumentation Engineers (SPIE) 3599; 43-49.

Cameron JS and Challah S (1986). Treatment of end-stage renal failure due to diabetes in the United Kingdom, 1975-84. Lancet; 2: 962-966.

Carrier M, Trudelle S, Thai P and Pelletier L (1998). Ischemic threshold during cold blood cardioplegic arrest: monitoring with tissue pH and pO2. Journal of Cardiovascular Surgery (Torino); 39: 593-597.

Cass AEG (1990). "Biosensors: A practical approach", Oxford University Press, Oxford.

Cass AEG, Davis G, Francis GD, Hill HAO, Aston WJ, Higgins IJ, Plotkin EV, Scott LDL and Turner APF (1984). Ferrocene-mediated enzyme electrode for amperometric determination of glucose. Analytical Chemistry; 56: 667-671.

Cattrall RW (1997). "chemical sensors", Oxford University Press, Oxford.

Chien YW, Lelawongs P, Siddiqui O, Sun Y and Shi WM (1990). Facilitated transdermal delivery of therapeutic peptides and proteins by iontophoretic delivery devices. Journal of Controlled Release; 13: 263-278.

Chien YW, Siddiqui O, Sun Y, Shi WM and Liu JC (1987). Transdermal iontophoretic delivery of therapeutic peptides/proteins. I: Insulin. Annals of the New York Academy of Sciences; 507: 32-51.

Chiu JH, Chen WS, Chen CH, Jiang JK, Tang GJ, Lui WY and Lin JK (1999). Effect of transcutaneous electrical nerve stimulation for pain relief on patients undergoing hemorrhoidectomy - Prospective, randomized, controlled trial. Diseases of the Colon & Rectum; 42: 180-185.

Chung H, Arnold MA, Rhiel M and Murhammer DW (1996). Simultaneous measurements of glucose, glutamine, ammonia, lactate, and glutamate in aqueous solutions by near-infrared spectroscopy. Applied Spectroscopy; 50: 270-276.

Cole KS and Cole RH (1941). Dispersion and absorption in dielectrics. Journal of Chemical Physics; 9: 341-351.

Collier WA, Janssen D and Hart AL (1996). Measurement of soluble L-lactate in dairy products using screen-printed sensors in batch mode. Biosensors & Bioelectronics; 11: 1041-1049.

Connolly P, Cotton C and Morin F (2002). Opportunities at the Skin Interface for Continuous Patient Monitoring: A Reverse Iontophoresis Model tested on Lactate and Glucose. IEEE Transactions in Nanobioscience; 1: 37-41.

Cosnier S (1999). Biomolecule immobilization on electrode surfaces by entrapment or attachment to electrochemically polymerized films. A reviews. Biosensors & Bioelectronics; 14: 1443-1456.

Cote GL, Fox MD and Northrop RB (1992). Noninvasive optical polarimetric glucose sensing using a true phase measurement technique. IEEE Transactions on Biomedical Engineering; 39: 752-756.

Cullander C (1992). What are the pathways of iontophoretic current flow through mammalian skin?. Advanced Drug Delivery Reviews; 9: 119-135.

Curdy C, Kalia YN and Guy RH (2002). Post-iontophoresis recovery of human skin impedance in vivo. European Journal of Pharmaceutics and Biopharmaceutics; 53: 15-21.

Currie CJ, Kraus D, Morgan CL, Gill L, Stott NC and Peters JR (1997). NHS acute sector expenditure for diabetes: the present, future, and excess in-patient cost of care. Diabetic Medicine; 14: 686-692.

Davis BL, Kuznicki J, Praveen SS and Sferra JJ (2004). Lower-extremity amputations in patients with diabetes: pre- and post-surgical decisions related to successful rehabilitation. Diabetes-Metabolism Research and Reviews; 20 (Suppl 1): S45-S50.

Dawson KG, Gomes D, Gerstein H, Blanchard JF and Kahler KH (2002). The economic cost of diabetes in Canada, 1998. Diabetes Care; 25: 1303-1307.

De Angelis C, Perrone G, Santoro G, Nofroni I and Zichella L (2003). Suppression of pelvic pain during hysteroscopy with a transcutaneous electrical nerve stimulation device. Fertility and Sterility; 79: 1422-1427.

de Boer J, Potthoff H, Mulder PO, Dofferhoff AS, van Thiel RJ, Plijter-Groendijk H and Korf J (1994). Lactate monitoring with subcutaneous microdialysis in patients with shock: a pilot study. Circulatory Shock; 43: 57-63.

De la Guardia M (1995). Biochemical sensors: the state of art. Microchimica Acta; 120: 243-255.

Degim IT, Ilbasmis S, Dundaroz R and Oguz Y (2003). Reverse iontophoresis: a non-invasive technique for measuring blood urea level. Pediatric Nephrology; 18: 1032-1037.

Degoute CS, Ray MJ, Manchon M, Claustrat B and Banssillon V (1989). Intraoperative glucose infusion and blood lactate: endocrine and metabolic relationships during abdominal aortic surgery. Anesthesiology; 71: 355-361.

Del Terzo S, Bhel CR and Nash RA (1989). Iontophoretic transport of a homologous series of ionized and nonionized model compounds: Influence of Hydrophobicity and mechanistic interpretation. Pharmaceutical Research; 6: 85-90.

Delgado-Charro MB and Guy RH (1994). Characterization of convective solvent flow during iontophoresis. Pharmaceutical Research; 11: 929-935.

Diabetes test nixed (1996). USA Today, 27 February 1996: Sect. D, p. 1

Diabetes UK (2004). Diabetes in the UK 2004. http://www.diabetes.org.uk/infocentre/reports/in_the_UK_2004.doc.

Eddowes MJ (1990). Theoretical methods for analysing performance, Biosensors – A practical approach, edited by Cass AEG, pp211-263.

Edsander-Nord A, Rojdmark J and Wickman M (2002). Metabolism in pedicled and free TRAM flaps: a comparison using the microdialysis technique. Plastic and Reconstructive Surgery; 109: 664-673.

Elia S, Liu P, Hilgenberg A, Skourtis C and Lappas D (1991). Coronary haemodynamics and myocardial metabolism during weaning from mechanical ventilation in cardiac surgical patients. Canadian Journal of Anaesthesia-Journal Canadien D Anesthesie; 38: 564-571.

Elias PM (1983). Epidermal lipids, barrier function, and desquamation. Journal of Investigative Dermatology; 80: 44-49.

Evans J (1995). Causes of blindness and partial sight in England and Wales 1990-1991. HMSO.

Fischbacher C, Jagemann KU, Danzer K, Müller UA, Papenkordt L and Schüler J (1997). Enhancing calibration models for non-invasive near-infrared spectroscopical blood glucose determination. Fresenius Journal of Analytical Chemistry; 359: 78-82.

Foley D, Corish J and Corrigan OI (1992). Iontophoretic delivery of drugs through membranes including human stratum corneum. Solid State Ionics; 53-56: 184-196.

Forrest RD, Jackson CA and Yudkin JS (1986). Glucose intolerance and hypertension in north London: the Islington Diabetes Survey. Diabetic Medicine; 3: 338-342.

Gaboriau HP and Murakami CS (2001). Skin anatomy and flap physiology. Otolaryngologic Clinics of North America; 34: 555-569.

Gala´n-Vidal CA, Mun˜oz J, Domı´nguez C and Alegret S (1998). Glucose biosensor strip in a three electrode configuration based on composite and biocomposite materials applied by planar thick film technology. Sensors and Actuators B; 52: 257-263.

Galanvidal CA, Munoz J, Dominguez C and Alegret S (1995) Chemical sensors, biosensors and thick-film technology. Trac-Trends in Analytical Chemistry; 14: 225-231.

Gatling W, Budd S, Walters D, Mullee MA, Goddard JR and Hill RD (1998). Evidence of an increasing prevalence of diagnosed diabetes mellitus in the Poole area from 1983 to 1996. Diabetic Medicine; 15: 1015-1021.

Gatling W, Houston AC and Hill RD (1985). The prevalence of diabetes mellitus in a typical English community. Journal of the Royal College of Physicians of London; 19: 248-250.

Gersh BJ and Anderson JL (1993). Thrombolysis and myocardial salvage. Results of clinical trials and the animal paradigm--paradoxic or predictable? Circulation; 88: 296-306.

Gilmartin MAT and Hart JP (1992). Voltammetric and amperometric behaviour of uric-acid at bare and surface-modified screen-printed electrodes – studies towards a disposable uric-acid sensor. Analyst; 117: 1299-1303.

Glikfeld P, Cullander C, Hinz RS and Guy RH (1988). A new system for in vitro studies of iontophoresis. Pharmacological Research; 5: 443-446.

Goldstein RJ and Chiang HD (1985). Measurement of temperature and heat transfer. In Handbook of Heat Transfer Applications. Rohenow WM, Hartnett JP, Ganic EN, Eds. New York, McGraw-Hill, p. 12-1-12-94.

Goodman JC, Valadka AB, Gopinath SP, Uzura M and Robertson CS (1999). Extracellular lactate and glucose alterations in the brain after head injury measured by microdialysis. Critical Care Medicine; 27: 1965-1973.

Gorton L (1995). Carbon paste electrodes modified with enzymes, tissues, and cells. Electroanal; 1: 23-45.

Green P, Shroot B, Bernerd F, Pilgrim WR and Guy RH (1992). In vitro and in vivo iontophoresis of a tripeptide across nude rat skin. Journal of Controlled Release; 20: 209-218.

Groeger JS, Guntupalli KK, Strosberg M, Halpern N, Raphaely RC, Cerra F and Kaye W (1993). Descriptive analysis of critical care units in the United States: patient characteristics and intensive care unit utilization. Critical Care Medicine; 21: 279-291.

Guilbault G (1988). Non-invasive in vivo glucose measurements. Artificial Organs; 13: 172.

Gunasingham H and Tan CH (1990). Carbon paste tetrathiafulvalene amperometric enzyme electrode for the determination of glucose in flowing systems. Analyst; 115: 35-39.

Gunther A and Bilitewski U (1995). Characterization of inhibitors of acetylcholinesterase by an automated amperometric flow-injection system. Analytica Chimica Acta; 300: 117-125.

Guy RH (1998). Iontophoresis - recent developments. Journal of Pharmacy and Pharmacology; 50: 371-374.

Guy RH, Delgado-Charro MB and Kalia YN (2001). Iontophoretic transport across the skin. Skin Pharmacology and Applied Skin Physiology; 14: 35-40.

Guy RH, Kalia YN, Delgado-Charro MB, Merino V, Lopez A and Marro D (2000). Iontophoresis: electrorepulsion and electroosmosis. Journal of Controlled Release; 64: 129-132.

Haaland DM, Robinson MR, Koepp GW, Thomas EV and Eaton RP (1992). Reagentless near-infrared determination of glucose in whole blood using multivariate calibration. Applied Spectroscopy; 46: 1575-1578.

Habicht JM, Wolff T, Langemann H and Stulz P (1998). Intraoperative and postoperative microdialysis measurement of the human heart--feasibility and initial results. Swiss Surgery; (Suppl 2): 26-30.

Hale PD, Boguslavsky LI, Karan HI, Lan HL, Lee HS, Okamoto Y and Skothem TA (1991). Investigation of violgen dericatives as electron-transfer mediators in amperometric glucose sensors. Analytica Chimica Acta; 248: 155-161.

Halhal M, Renard G, Courtois Y, BenEzra D and Behar-Cohen F (2004). Iontophoresis: from the lab to the bed side. Experimental Eye Research; 78: 751-757.

Hall JW and Pollard A (1992). Near-infrared spectrophotometry: a new dimension in clinical chemistry. Clinical Chemistry; 38: 1623-1631.

Harris MI, Hadden WC, Knowler WC and Bennett PH (1987). Prevalence of diabetes and impaired glucose tolerance and plasma glucose levels in U.S. population aged 20-74 yr. Diabetes; 36: 523-534.

Hart AL, Turner APF and Hopcroft D (1996). On the use of screen- and ink-jet printing to produce amperometric enzyme electrodes for lactate. Biosensors & Bioelectronics; 11: 263-270.

Hart JP and Wring SA (1994). Screen-printed voltammetric and amperometric electrochemical sensor for decentralised testing. Electroanalysis; 6: 617-624.

Hart JP and Wring SA (1997). Recent developments in the design and application of screen-printed electrochemical sensors for biomedical, environmental and industrial analyses. Trac-Trends in Analytical Chemistry; 16: 89-103.

Hatanaka T, Inuma M, Sugibayashi K and Morimoto Y (1990). Prediction of skin permeability of drugs I. Comparison with artificial membrane. Chemical & Pharmaceutical Bulletin; 38: 3452-3459.

Hidalgo DA, Disa JJ, Cordeiro PG and Hu QY (1998). A review of 716 consecutive free flaps for oncologic surgical defects: refinement in donor site selection and technique. Plastic and Reconstructive Surgery; 102: 722-732.

Hildingsson U, Sellden H, Ungerstedt U and Marcus C (1996). Microdialysis for metabolic monitoring in neonates after surgery. Acta Paediatrica; 85: 589-594.

Hirvonen J, Hueber F and Guy RH (1995). Current profile regulates iontophoretic delivery of amino acids across the skin. Journal of Controlled Release; 37: 239-249.

Holbrook KA and Wolff K (1993). The structure and development of skin. In: Dermatology in general medicine, vol 1, 4th ed., Eds. TB Fitzpatrick, AZ Eisen, K Wolff, IM Feedberg and KF Austen. McGraw Hill, Inc., New York, pp. 97-145.

Howard JP, Drake TR and Kellogg DL (1995). Effects of alternating current iontophoresis on drug delivery. Archives of Physical Medicine and Rehabilitation; 76: 463-466.

International Diabetes Federation (2003). Diabetes Atlas 2003. 2nd edition, Brussels, International Diabetes Federation.

Jadoul A, Bouwstra JA and Preat V (1999). Effects of iontophoresis and electroporation on the stratum corneum: review on the biophysical studies. Advanced Drug Delivery Reviews; 35: 89-105.

Jager A and Bilitewski U (1994). Screen printed enzyme electrode for the determination of lactose. Analyst; 119: 1251-1255.

Jahn H (1900). Uber den dissociationsgrad und das dissociationsgleichgewicht stark dissociierter elektrolyte. Zeitschrift Fur Physikalische Chemie. International Journal of Research in Physical Chemistry & Chemical Physics; 33: 545-576.

Jaremko J and Rorstad O (1998). Advances toward the implantable artificial pancreas for treatment of diabetes. Diabetes Care; 21: 444-450.

Jarzembski WB (1985). Electrical stimulation and substance abuse treatment. Neurobehavioral Toxicology and Teratology; 7: 119–123.

Kaiser N (1979). Laser absorption spectroscopy with an ATR prism--noninvasive in vivo determination of glucose. Hormone and Metabolic Research; Suppl 8: 30-33.

Kajiwara K, Uemura T, Kishihawa H, Nishida K, Hashiguchi Y, Uehara M, Sakakida M, Ichinose K and Shichiri M (1993). Noninvasive measurement of blood glucose concentrations by analyzing Fourier transform infra-red absorbance spectra through oral mucosa. Medical & Biological Engineering & Computing; 31: S17-S22.

Kalia Y, Nonato LB and Guy RH (1996). The effect of iontophoresis on skin barrier integrity: Non-invasive evaluation by impedance spectroscopy and tranepidermal water loss. Pharmaceutical Research; 13: 957-960.

Kalia YN and Guy RH (1995). The electrical characteristics of human skin in vivo. Pharmaceutical Research; 12: 1605-1613.

Kalia YN, Naik A., Garrison J and Guy RH (2004). Iontophoretic drug delivery. Advanced Drug Delivery Reviews; 56: 619-658.

Kasting GB (1992). Theoretical models for iontophoretic delivery. Advanced Drug Delivery Reviews; 9: 177-199.

Khan GF and Wernet W (1997). Design of enzyme electrodes for extended use and storage life. Analytical Chemistry; 69: 2682-2687.

Khouri RK (1992). Free flap surgery: the second decade. Clinics in Plastic Surgery; 19: 757-761.

Kim A, Green PG, Rao G and Guy RH (1993). Convective solvent flow across the skin during iontophoresis. Pharmaceutical Research; 10: 1315-1320.

Kind GM, Buntic RF, Buncke GM, Cooper TM, Siko PP and Buncke HJ Jr (1998). The effect of an implantable Doppler probe on the salvage of microvascular tissue transplants. Plastic and Reconstructive Surgery; 101: 1268-1273.

King H and Rewers M. (1993). Global estimates for prevalence of diabetes mellitus and impaired glucose tolerance in adults. WHO Ad Hoc Diabetes Reporting Group. Diabetes Care; 16: 157-177.

Klawansky S, Yeung A, Berkey C, Shah N, Phan H and Chalmers TC (1995). Meta-analysis of randomized controlled trials of cranial electrostimulation: efficacy in treating selected psychological and physiological conditions. Journal of Nervous and Mental Diseases; 183: 478-484.

Klonoff D (1997). Noninvasive blood glucose monitoring. Diabetes Care; 20: 433-437.

Knoblauch P and Moll F (1993). In-vitro pulsatile and continuous trandermal delivery of buserelin by iontophoresis. Journal of Controlled Release; 26: 203-212.

Koschinsky T and Heinemann L (2001). Sensors for glucose monitoring: technical and clinical aspects. Diabetes-Metabolism Research and Reviews; 17: 113-123.

Krasteva VT and Papazov SP (2002). Estimation of current density distribution under electrodes for external defibrillation. Biomedical Engineering Online; 1: 7.

Kroll SS, Schusterman MA, Reece GP, Miller MJ, Evans GR, Robb GL and Baldwin BJ (1996). Choice of flap and incidence of free flap success. Plastic and Reconstructive Surgery; 98: 459-463.

Kulys J and Dcosta EJ (1991). Printed amperometric sensor based on TCNQ and cholinesterase. Biosensors & Bioelectronics; 6: 109-115.

Kurnik RT, Berner B, Tamada J and Potts RO (1998). Design and stimulation of a reverse iontophoretic glucose monitoring device. Journal of Electrochemical Society; 145: 4119-4215.

Kurnik RT, Oliver JJ, Waterhouse SR, Dunn T, Jayalakshmi Y, Lesho M, Tamada J, Lopatin M, Wei C and Potts RO (1999). Application of the mixtures of experts algorithm for signal processing in a noninvasive glucose monitoring system. Sensors and Actuators B; 60: 1-8.

Laing SP, Swerdlow AJ, Slater SD, Botha JL, Burden AC, Waugh NR, Smith AW, Hill RD, Bingley PJ, Patterson CC, Qiao Z and Keen H (1999a). The British Diabetic Association Cohort Study, I: all-cause mortality in patients with insulin-treated diabetes mellitus. Diabetic Medicine; 16: 459-465.

Laing SP, Swerdlow AJ, Slater SD, Botha JL, Burden AC, Waugh NR, Smith AW, Hill RD, Bingley PJ, Patterson CC, Qiao Z and Keen H (1999b). The British Diabetic Association Cohort Study, II: cause-specific mortality in patients with insulin-treated diabetes mellitus. Diabetic Medicine; 16: 466-471.

Lambrechts M and Sansen W (1992). Biosensors: microchemical devices. IOP publishing, Bristol.

Lawler JC, Davis MJ and Griffith E (1960). Electrical characteristics of the skin: The impedance of the surface sheath and deep tissues. Journal of Investigative Dermatology; 34: 301-308.

Ledger PW (1992). Skin biological issues in electrically enhanced transdermal delivery. Advanced Drug Delivery Reviews; 9: 289-307.

Levraut J, Ciebiera JP, Chave S, Rabary O, Jambou P, Carles M and Grimaud D (1998). Mild hyperlactatemia in stable septic patients is due to impaired lactate clearance rather than overproduction. American Journal of Respiratory and Critical Care Medicine; 157: 1021-1026.

Lidman D and Daniel RK (1981). Evaluation of clinical microvascular anastomoses — reasons for failure. Annals of Plastic Surgery; 6: 215-223.

Lin LW and Pisano AP (1999). Silicon-processed microneedles. JOURNAL OF MICROELECTROMECHANICAL SYSTEMS; 8: 78-84.

Lineaweaver W and Buncke HJ (1986). Complications of free flap transfers. Hand Clinics; 2: 347-351.

Lorenzo E, Pariente F, Hernandez L, Tobalina F, Darder M, Wu Q, Maskus M and Abruna HD (1998). Analytical strategies for amperometric biosensors based on chemically modified electrodes. Biosensors & Bioelectronics; 13: 319-332.

Lozano A, Rosell J and Pallás-Areny R (1990). Two-frequency impedance plethysmograph: real and imaginary parts. Medical & Biological Engineering & Computing; 28: 38-42.

Lutz BS, Bagenholm T and Adell R (2004). Angle-to-angle mandibular reconstruction with two free fibular flaps in a patient with two consecutive gingival cancers. Scandinavian Journal of Plastic and Reconstructive Surgery and Hand Surgery; 38: 46-49.

Malchoff CD, Shoukri K, Landau JI and Buchert JM (2002). A novel noninvasive blood glucose monitor. Diabetes Care; 25: 2268-2275.

Manikis P, Jankowski S, Zhang H, Kahn RJ and Vincent JL (1995). Correlation of serial blood lactate levels to organ failure and mortality after trauma. American Journal of Emergency Medicine; 13: 619-622.

Marbach R, Koschinsky T, Gries FA and Heise HM (1993). Noninvasive blood glucose assay by near-infrared diffuse reflectance spectroscopy of the human inner lip. Applied Spectroscopy; 47: 875-881.

March WF, Rabinovitch B and Adams RL (1982). Noninvasive glucose monitoring of the aqueous humor of the eye. II. Animal studies and the scleral lens. Diabetes Care; 5: 259-265.

Marecaux G, Pinsky MR, Dupont E, Kahn RJ and Vincent JL (1996). Blood lactate levels are better prognostic indictors than TNF and IL-6 levels in patients with septic shock. Intensive Care Medicine; 22: 404-408.

Mendelowitsch A, Mergner GW, Shuaib A and Sekhar LN (1998). Cortical brain microdialysis and temperature monitoring during hypothermic circulatory arrest in humans. Journal of Neurology Neurosurgery and Psychiatry; 64: 611-618.

Menon GK, Bommannan DB and Elias PM (1994). High-frequency sonophoresis: permeation pathways and structural basis for enhanced permeation. Skin Pharmacology; 7: 130-139.

Menzel M, Doppenberg EM, Zauner A, Soukup J, Reinert MM and Bullock R (1999). Increased inspired oxygen concentration as a factor in improved brain tissue oxygenation and tissue lactate levels after severe human head injury. Journal of Neurosurgery; 91: 1-10.

Merino V, Kalia YN and Guy RH (1997). Transdermal therapy and diagnosis by iontophoresis. Trends in Biotechnology; 15: 288-290.

Merino V, Lopez A, Hochstrasser D and Guy RH (1999). Noninvasive sampling of phenylalanine by reverse iontophoresis. Journal of Controlled Release; 61: 65-69.

Mize NK, Buttery M, Daddona P, Morales C and Cormier M (1997). Reverse iontophoresis: monitoring prostaglandin E2 associated with cutaneous inflammation in vivo. Experimental Dermatology; 6: 298-302.

Mohr TM, Akers TK and Landry RG (1987). Effect of high voltage stimulation on edema reduction in the rat hind limb. Physical Therapy; 67: 1703-1707.

Montagna W and Parakkal PF (1974). The structure and function of skin. Academic Press, New York.

Moomey CB, Melton SM, Croce MA, Fabian TC and Proctor KG (1998). Prognostic value of blood lactate, base deficit, and oxygenderived variables in an LD50 model of penetrating trauma. Critical Care Medicine; 26: 154-161.

Moore JA, Mellor CS, Standage KF, and Strong H (1975). A double-blind study of electrosleep for anxiety and insomnia. Biological Psychiatry; 10: 59-63.

Morimoto Y, Numajiri S and Sugibayashi K (1991). Effect of ion species and their concentration on the iontophoretic transport of benzoic-acid through poly(vinyl acetate) membrane. Chemical & Pharmaceutical Bulletin; 39: 2412-2416.

Müller UA, Mertes B, Danzer K, Fischbacher C, Jagemann KU, Papenkordt L and Schüler J (1997). Non-invasive blood glucose measurement by means of infrared spectroscopy: calibration models and results. J Artif Org; 20: 285.

Murray MJ, Gonze MD, Nowak LR and Cobb CF (1994). Serum D(-)-lactate levels as an aid to diagnosing acute intestinal ischemia. American Journal of Surgery; 167: 575-578.

Nagata R, Yokoyama K, Clark SA and Karube I (1995). A glucose sensor fabricated by the screen printing technique. Biosensors & Bioelectronics; 10: 261-267.

Neil HA, Gatling W, Mather HM, Thompson AV, Thorogood M, Fowler GH, Hill RD and Mann JI (1987). The Oxford Community Diabetes Study: evidence for an increase in the prevalence of known diabetes in Great Britain. Diabetic Medicine; 4: 539-543.

Nicholson RS and Shain I (1964). Theory of stationary electrode polarography: single scan and cyclic methods applied to reversible, irreversible, and kinetic systems. Analytical Chemistry; 36: 706-723.

Noon JP, Walker BR, Hand MF and Webb DJ (1998). Studies with iontophoretic administration of drugs to human dermal vessels in vivo: cholinergic vasodilatation is mediated by dilator prostanoids rather than nitric oxide. British Journal of Clinical Pharmacology; 45: 545-550.

Numajiri S, Sakurai H, Sugibayashi K, Morimoto Y, Omiya H, Takenaka H and Akiyama N (1993). Comparison of depolarizing and direct current systems on iontophoretic enhancement of transport of sodium benzoate through human and hairless rat skin. Journal of Pharmacy and Pharmacology; 45: 610-613.

Numajiri S, Sugibayashi K and Morimoto Y (1993). Non-invasive sampling of lactic acid ions by iontophoresis using chloride ion in the body as an internal standard. Journal of Pharmaceutical and Biomedical Analysis; 11: 903-909.

Oh SY and Guy RH (1995). Effects of iontophoresis on the electrical properties of human skin in vivo. International Journal of Pharmaceutics; 124: 137-142.

Padmanabhan RV, Phipps JB, Lattin GA and Sawchuk RJ (1990). In vitro and in vivo evaluation of transdermal iontophoretic delivery of hydromorphone. Journal of Controlled Release; 11: 123-135.

Panchagula R, Pillai O, Nair VB and Ramarao P (2000). Transdermal iontophoresis revisited. Current Opinion in Chemical Biology; 4: 468-473.

Panzram G (1987). Mortality and survival in type 2 (non-insulin-dependent) diabetes mellitus. Diabetologia; 30: 123-131.

Pfutzner A, Caduff A, Larbig M, Schrepfer T and Forst T (2004). Impact of posture and fixation technique on impedance spectroscopy used for continuous and noninvasive glucose monitoring. Diabetes Technology & Therapeutics; 6: 435-441.

Phipps JB and Gyory JR (1992). Transdermal ion migration. Advanced Drug Delivery Reviews; 9: 137-176.

Phipps JB, Padmanabhan RV and Lattin GA (1989). Iontophoretic delivery of model inorganic and drug ions. Journal of Pharmaceutical Sciences; 78: 365-369.

Pickup J (2003). Diabetic control and its measurements. In: Pickup, J.C., Williams, G. (Eds.), Textbook of Diabetes, third ed. Blackwell, Oxford, pp. 34.1–34.17.

Pikal MJ (1990). Transport mechanisms in iontophoresis. I. A theoretical model for the effect of electroosmotic flow on flux enhancement in transdermal iontophoresis. Pharmaceutical Research; 7: 118-126.

Pikal MJ (1992). The role of electroosmotic flow in transdermal iontophoresis. Advanced Drug Delivery Reviews; 9: 201-237.

Pikal MJ (2001). The role of electroosmotic flow in transdermal iontophoresis. Advanced Drug Delivery Reviews; 46: 281-305.

Pikal MJ and Shah S (1990). Transport mechanisms in iontophoresis. III. An experimental study of the contributions of electroosmotic flow and permeability change in transport of low and high molecular weight solutes. Pharmaceutical Research; 7: 222-229.

Pikal MJ and Shah S (1991). Study of the mechanisms of flux enhancement through hairless mouse skin by pulsed DC iontophoresis. Pharmaceutical Research; 8: 365-369.

Pillai O and Panchagnula R (2003). Transdermal delivery of insulin from poloxamer gel: ex vivo and in vivo skin permeation studies in rat using iontophoresis and chemical enhancers. Journal of Controlled Release; 89: 127-140.

Pillai O, Kumar N, Dey CS, Borkute S, Nagalingam S and Panchagnula R (2003). Transdermal iontophoresis of insulin. Part 1: A study on the issues associated with the use of platinum electrodes on rat skin. Journal of Pharmacy and Pharmacology; 55: 1505-1513.

Pitzer KR, Desai S, Dunn T, Edelman S, Jayalakshmi Y, Kennedy J, Tamada JA and Potts RO (2001). Detection of hypoglycaemia with the GlucoWatch biographer. Diabetes Care; 24: 881-885.

Portney LG and Watkins MP (1993). Foundations of clinical research applications:

applications to practice. Appleton & Lange: pp 509-514.

Potts RO, Tamada JA and Tierney MJ (2002). Glucose monitoring by reverse iontophoresis. Diabetes Metabolism Research and Reviews; 18: S49-53.

Rao G, Glikfeld P and Guy RH (1993). Reverse iontophoresis: Development of a noninvasive approach for glucose monitoring. Pharmaceutical Research; 10: 1751-1755.

Rao G, Guy RH, Glikfeld P, LaCourse WR, Leung L, Tamada J, Potts RO and Azimi N (1995). Reverse iontophoresis: Noninvasive glucose monitoring in vivo in human. Pharmaceutical Research; 12: 1869-1873.

Rasmussen I, Hillered L, Ungerstedt U and Haglund U (1994). Detection of liver ischemia using microdialysis during experimental peritonitis in pigs. Shock; 1: 60-66.

Riviere JE and Heit MC (1997). Electrically-assisted transdermal drug delivery. Pharmaceutical Research; 14: 687-697.

Robinson MR, Eaton RP, Haaland DM, Koepp GW, Thomas EV, Stallard BR and Robinson PL (1992). Noninvasive glucose monitoring in diabetic patients: a preliminary evaluation. Clinical Chemistry; 38: 1618-1622.

Rojdmark J, Blomqvist L, Malm M, Adams-Ray B and Ungerstedt U (1998). Metabolism in myocutaneous flaps studied by in situ microdialysis. Scandinavian Journal of Plastic and Reconstructive Surgery and Hand Surgery; 32: 27-34.

Rojdmark J, Heden P and Ungerstedt U (2000). Prediction of border necrosis in skin flaps of pigs with microdialysis. Journal of Reconstructive Microsurgery; 16: 129-134.

Rosengren A, Welin L, Tsipogianni A and Wilhelmsen L (1989). Impact of cardiovascular risk factors on coronary heart disease and mortality among middle aged diabetic men: a general population study. British Medical Journal; 299: 1127-1131.

Rosenthal SH (1971). Electrosleep as a psychiatric treatment. Comm Contemp Psych; 1: 25–33.

Sage BH and Riviere JE (1992). Model systems in iontophoresis — Transport efficacy. Advanced Drug Delivery Reviews; 9: 265-287.

Santi P and Guy RH (1996). Reverse iontophoresis — parameters determining electroosmotic flow. I. PH and ionic strength. Journal of Controlled Release; 38: 159-165.

Schmelz M, Schmidt R, Bickel A, Handwerker HO and Torebjork HE (1997). Specific C-receptors for itch in human skin. Journal of Neuroscience; 17: 8003-8008.

Schmidt JB, Binder M, Macheiner W and Bieglmayer C (1995). New treatment of atrophic acne scars by iontophoresis with estriol and tretinoin. International Journal of Dermatology; 34: 53-57.

Schmitt R, Capo T and Boyd E (1986). Cranial electrotherapy stimulation treatment for anxiety in chemically dependent persons. Alcoholism-Clinical and Experimental Research; 10: 158-160.

Schmitt R, Capo T, Frazier H and Boren D (1984). Cranial electrotherapy stimulation treatment of cognitive brain dysfunction in chemical dependence. Journal of Clinical Psychiatry; 45: 60-63.

Schnetz E and Fartasch M (1991). Microdialysis for the evaluation of penetration through the human skin barrier - a promising tool for future research. European Journal of Pharmaceutical Sciences; 12: 165-174.

Schusterman MA, Miller MJ, Reece GP, Kroll SS, Marchi M and Goepfert H (1994). A single center's experience with 308 free flaps for repair of head and neck cancer defects. Plastic and Reconstructive Surgery; 93: 472-478.

Scottish Intensive Care Society Audit Group (2003). ANNUAL REPORT 2003 - An Audit of Intensive Care Units in Scotland. http://www.scottishintensivecare.org.uk

Shealy C, Cady R, Wilkie R, Cox R, Liss S and Clossen W (1989). Depression – a diagnostic, neurochemical profile and therapy with cranial electrical stimulation (CES). Journal of Neurological and Orthopaedic Medicine and Surgery; 10: 301-303.

Shichiri M, Kawamori R, Hakui N, Asakawa N, Yamasaki Y and Abe H (1984). The development of wearable-type artificial endocrine pancreas and its usefulness in glycaemic control of human diabetes mellitus. Biomedica Biochimica Acta; 43: 561-568.

Shichiri M, Kawamori R, Yamasaki Y, Hakui N and Abe H (1982). Wearable artificial endocrine pancreas with needle-type glucose sensor. Lancet; 2: 1129-1131.

Sieg A, Guy RH and Delgado-Charro MB (2003). Reverse iontophoresis for noninvasive glucose monitoring: The internal standard concept. Journal of Pharmaceutical Sciences; 92: 2295-2302.

Sieg A, Guy RH and Delgado-Charro MB (2004a). Simultaneous extraction of urea and glucose by reverse iontophoresis in vivo. Pharmaceutical Research; 21: 1805-1810.

Sieg A, Guy RH and Delgado-Charro MB (2004b). Noninvasive glucose monitoring by reverse iontophoresis in vivo: Application of the internal standard concept. Clinical Chemistry; 50: 1383-1390.

Simmons D, Williams DR and Powell MJ (1991). The Coventry Diabetes Study: prevalence of diabetes and impaired glucose tolerance in Europids and Asians. Quarterly Journal of Medicine; 81: 1021-1030.

Singh J and Bhatia KS (1996). Topical iontophoretic drug delivery: Pathways, principles, factors and skin irritation. Medicinal Research Reviews; 16: 285-296.

Slomovitz BM, Lavery RF, Tortella BJ, Siegel JH, Bachl BL and Ciccone A (1998). Validation of a hand-held lactate device in determination of blood lactate in critically injured patients. Critical Care Medicine; 26: 1523-1528.

Smith A, Yang D, Delcher H, Eppstein J, Williams D and Wilkes S (1999). Fluorescein Kinetics in Interstitial Fluid Harvested from Diabetic Skin during Fluorescein Angiography: Implications for Glucose Monitoring. Diabetes Technology & Therapeutics; 1: 21-27.

Smith RB (1982). Confirming evidence of an effective treatment for brain dysfunction on alcoholic patients. Journal of Nervous and Mental Disease; 170: 275-278.

Stephenson JM, Kenny S, Stevens LK, Fuller JH and Lee E (1995). Proteinuria and mortality in diabetes: the WHO Multinational Study of Vascular Disease in Diabetes. Diabetic Medicine; 12: 149-155.

Takahashi Y, Iwata M and Machida Y (2001). Enhancing effect of switching iontophoresis on transdermal absorption of glibenclamide. Yakugaku Zasshi-Journal of the Pharmaceutical Society of Japan; 121: 161-166.

Talbot NH and Pisano AP (1998). Polymolding: two wafer polysilicon micromolding of closed-flow passages for microneedles and microfluidic devices. IEEE Solid-State Sensor and Actuator Workshop; 4: 265-268.

Tamada JA, Bohannon NJV and Potts RO (1995). Measurement of glucose in diabetic subjects using non invasive transdermal extraction. Nature Medicine; 1: 1198-1201.

Tamada JA, Garg S, Jovanovic L, Pitzer KR, Fermi S and Potts RO (1999). Noninvasive glucose monitoring: Comprehensive clinical results. Jama-Journal of the American Medical Association; 28: 1839-1844.

Tapper R (1983). Design of an electronic antiperspirant device. Journal of Clinical Engineering; 8: 253-259.

Tapper R (1993). Iontophoretic treatment system. US patent no. 5,224,927.

The Diabetes Control and Complication Trial (DCCT) Research Group (1993). The effect of intensive treatment of diabetes on the development and progression of long-term complications of insulin-dependent diabetes mellitus. New England Journal of Medicine; 329: 997-1036.

The UK Prospective Diabetes Study (UKPDS) Group (1998a). Intensive blood-glucose control with sulphonylureas or insulin compared with conventional treatment and risk of complications in patients with type 2 diabetes (UKPDS 33). Lancet; 352: 837-853.

The UK Prospective Diabetes Study (UKPDS) Group (1998b). Effect of intensive blood-glucose control with metformin on complications in overweight patients with type 2 diabetes (UKPDS 34). Lancet; 352: 854-865.

The UK Prospective Diabetes Study Group (1998c). Efficacy of atenolol and captopril in reducing risk of macrovascular and microvascular complications in type 2 diabetes: UKPDS 39. British Medical Journal; 317: 713-720.

The UK Prospective Diabetes Study Group (1998d). Tight blood pressure control and risk of macrovascular and microvascular complications in type 2 diabetes: UKPDS 38. British Medical Journal; 317: 703-713.

Tierney MJ, Garg S, Ackerman NR, Fermi SJ, Kennedy J, Lopatin M, Potts RO snd Tamada JA (2000b). Effect of acetaminophen on the accuracy of glucose measurements obtained with the GlucoWatch biographer. Diabetes Technology & Therapeutics; 2: 199-207.

Tierney MJ, Tamada JA, Potts RO, Eastman RC, Pitzer K, Ackerman NR and Fermi SJ (2000). The GlucoWatch® biographer: a frequent, automatic and non-invasive glucose monitor. Annals of Medicine; 32: 632-641.

Tierney MJ, Tamada JA, Potts RO, Jovanovic L, Garg S and Cygnus Research Team (2001). Clinical evaluation of the GlucoWatch® biographer: a continual, non-invasive glucose monitor for patients with diabetes. Biosensors & Bioelectronics; 16: 621-629.

Tomohira Y, Machida Y, Onishi H and Nagai T (1997). Iontophoretic transdermal absorption of insulin and calcitonin in rats with newly-devised switching technique and addition of urea. International Journal of Pharmaceutics; 155: 231-239.

Udesen A, Lontoft E and Kristensen SK (2000). Monitoring of free TRAM flaps with microdialysis. Journal of reconstructive Microsurgery; 16: 101-106.

Vahjen W, Bradley J, Bilitewski U and Schmid RD (1991). Mediated enzyme electrode for the determination of L-glutamate. Analytical Letters; 24: 1445-1452.

Valadka AB, Goodman JC, Gopinath SP, Uzura M and Robertson CS (1998). Comparison of brain tissue oxygen tension to microdialysis-based measures of cerebral ischemia in fatally head-injured humans. Journal of Neurotrauma; 15: 509-519.

Van Heuvelen A (1987). Blood glucose monitor. US-Pat No.4704029.

Vincent JL (1996). End-points of resuscitation: arterial blood pressure, oxygen delivery, blood lactate, or...? Intensive Care Med; 22: 3-5.

Vincent JL (1998). Blood lactate levels: index of tissue oxygenation. Int J Intensive Care; 49-53.

Volpe G, Moscone D, Compagnone D and Palleschi G (1995). In vivo continuous monitoring of L-lactate coupling subcutaneous microdialysis and an electrochemical biocell. Sensors and Actuators B: Chemical; 24: 138-141.

Wang SL, Head J, Stevens L and Fuller JH (1996). Excess mortality and its relation to hypertension and proteinuria in diabetic patients. The World Health Organization Multinational Study of Vascular Disease in Diabetes. Diabetes Care; 19: 305-312.

Ward KJ, Haaland DM, Robinson MR and Eaton RP (1992). Post-prandial blood glucose determination by quantitative mid-infrared spectroscopy. Applied Spectroscopy; 46: 959-965.

Wearley L and Chien YW (1990). Enhancement of the in vitro skin permeability of azidothymidine (AZT) via iontophoresis and chemical enhancer. Pharmaceutical Research; 7: 34-40.

Website 1. http://www.glucowatch.com/uk/consumer/frame_set.htm

Website 10. http://www.wescor.com/biomedical/html/products.html

Website 2. http://www.empi.com/products/ionto.cfm

Website 3. http://www.drionic.com/

Website 4. http://www.hidrex.de/oldsite/english/seiten/frameset.htm

Website 5. http://www.iomed.com/products/phoresor.htm

Website 6. http://www.life-tech.com/pain/index.html

Website 7. http://www.optisgroup.com/Technology_Eyegate.htm

Website 8. http://www.rafischer.com/prod05.htm

Website 9. http://www.vyteris.com/lda.html

Westgren M, Kruger K, Ek S, Grunevald C, Kublickas M, Naka K, Wolff K and Persson B (1998). Lactate compared with pH analysis at fetal scalp blood sampling: a prospective randomised study. British Journal of Obstetrics and Gynaecology; 105: 29-33.

Westgren M, Kublickas M and Kruger K (1999). Role of lactate measurements during labor. Obstetrical & Gynecological Survey; 54: 43-48.

White SF, Tothill IE, Newman JD and Turner APF (1996). Development of a mass-producible glucose biosensor and flow-injection analysis system suitable for on line monitoring during fermentations. Analytica Chimica Acta; 321: 165-172.

Wild S, Roglic G, Green A, Sicree R and King H (2004). Global Prevalence of Diabetes. Estimates for the year 2000 and projections for 2030. Diabetes Care; 27: 1047-1053.

Wildersmith P (1989). Pain control by TENES in oro-facial pain and dental treatment. Journal of Dental Research; 68: 643-643.

Wilkins E and Atanasov P (1996). Glucose monitoring: State of the art and future possibilities. Medical Engineering & Physics; 18: 273-288.

Wilkins E et al (1996). Principles and fundamentals of glucose monitoring. In Leroith D, Taylor SI, Olefsky JM, Eds. Diabetes Mellitus: A Fundamental and Clinical Text. Philadelphia, PA. Lippincott-Raven Publishers, p. 443-451.

Wilson GS, Zhang Y, Reach G, Moatti-Sirat D, Poitout V, Thevenot DR, Lemonnier F and Klein JC (1992). Progress toward the development of an implantable sensor for glucose. Clinical Chemistry; 38: 1613-1617.

Wood EJ and Bladon PT (1985). The human skin. Edward Arnold, London, pp. 1-31.

Wring SA and Hart JP (1992). Chemically modified, screen-printed carbon electrodes. Analyst; 117: 1281-1286.

Yamamoto T and YamamotoY (1976). Electrical properties of the epidermal stratum corneum. Medical and Biological Engineering; 14: 151-158.

Yoshida NH and Roberts MS (1993). Solute molecular size and transdermal iontophoresis across excised human skin. Journal of Controlled Release; 25: 177-195.

Young M and Birkmeyer J (2000). Potential reduction in mortality rates using an intensivist model to manage intensive care units. Effective Clinical Practice; 3: 284-289.

Zauner A, Doppenberg E, Soukup J, Menzel M, Young HF and Bullock R (1998). Extended neuromonitoring: new therapeutic opportunities?. Neurological Research; 20 (Suppl 1): S85-S90.

Zhang I, Schung KK and Edwards DA (1996). Hydrogels with enhanced mass transfer for transdermal drug delivery. Journal of Pharmaceutical Sciences; 85: 1312-1316.

Appendices

Appendix A The Preconditioning Effects on the Recording of Impedance Spectrum of Ag/AgCl Electrodes

As shown in Table A.1 and Figure A.1, it was found that there was a big difference among the 1st trial and the others on the impedance of electrodes (> 10%), whereas a small difference was found on the impedance of electrodes among the last four trials (< 6%). Therefore, the preconditioning effects on the recording of impedance spectrum of Ag/AgCl electrodes seemed to become steady after the 1st trial. In the present study, data captured in the 2nd trial was hence used to compute the impedance of the Ag/AgCl electrodes.

Table A.1 – The results of the preconditioning effects on the recording of impedance spectrum of Ag/AgCl electrodes.

Impedance (Ω)	**Number of trials**					
	1	2	3	4	5	6
Electrodes 1 & 2	513	442	438	428	438	418
Electrodes 3 & 4	463	428	418	408	408	398
Electrodes 5 & 6	498	438	438	428	413	413
Electrodes 7 & 8	498	458	445	438	438	428
Electrodes 9 & 10	468	418	408	393	388	378
Mean	488.0	436.8	429.4	419.0	417.0	407.0
SD	21.5	15.1	15.6	18.2	21.3	19.5
% Change in impedance (compared with the 1st trial)		-10.49	-12.01	-14.14	-14.55	-16.60
% Change in impedance (compared with the previous trial)		-10.49	-1.69	-2.42	-0.48	-2.40

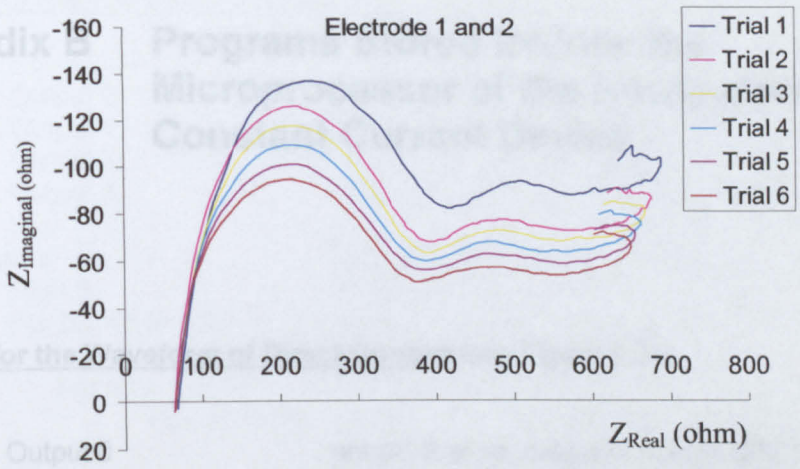

Figure A.1 – The results of the preconditioning effects on the recording of impedance spectrum of Ag/AgCl electrodes. Data from electrodes 1 and 2.

Appendix B Programs Stored Insides the Microprocessor of the Newly-developed Constant Current Device

Program for the Waveform of Direct Current (see Figure A.2a)

```
Main:
        Output 0                'set pin 0 as an output to control SPST relay
        Output 1                'set pin 1 as an output to control DPDT relay
        Output 2                'set pin 2 as an output to control buzzer
        Output 3                'set pin 3 as an output to control LED indicator

Start program:                  'start to run the below program
        High 0                  'switch on SPST relay
        For b2 = 1 to 120       'repeat the loop for 120 times
            Pause 60000         'pause for 60 second
        Next
        Low 0                   'switch off SPST relay
        High 2                  'switch on buzzer
        Pause 100               'pause for 0.1 second
        Low 2                   'switch off buzzer
        High 3                  'switch on LED indicator
```

Program for the Waveform of Pulsed Direct Current (see Figure A.2b)

```
Main:
        Output 0                'set pin 0 as an output to control SPST relay
        Output 1                'set pin 1 as an output to control DPDT relay
        Output 2                'set pin 2 as an output to control buzzer
        Output 3                'set pin 3 as an output to control LED indicator

Start program:                  'start to run the below program
        For b2 = 1 to 120       'repeat the loop for 120 times
            High 0              'switch on SPST relay
            Pause 100           'pause for 0.1 second
            Low 0               'switch off SPST relay
            Pause 100           'pause for 0.1 second
        Next
        High 2                  'switch on buzzer
        Pause 100               'pause for 0.1 second
        Low 2                   'switch off buzzer
        High 3                  'switch on LED indicator
```

Program for the Waveform of Bipolar Direct Current (see Figure A.2c)

```
Main:
        Output 0                    'set pin 0 as an output to control SPST relay
        Output 1                    'set pin 1 as an output to control DPDT relay
        Output 2                    'set pin 2 as an output to control buzzer
        Output 3                    'set pin 3 as an output to control LED indicator

Start program:                      'start to run the below program
        High 0                      'switch on SPST relay
        For b2 = 1 to 120           'repeat the loop for 120 times
            High 1                  'switch on DPDT relay
            For b3 = 1 to 15        'repeat the loop for 15 times
                Pause 60000         'pause for 60 second
            Next
            Low 1                   'switch off DPDT relay
            For b4 = 1 to 15        'repeat the loop for 15 times
                Pause 60000         'pause for 60 second
            Next
        Next
        Low 0                       'switch off SPST relay
        High 2                      'switch on buzzer
        Pause 100                   'pause for 0.1 second
        Low 2                       'switch off buzzer
        High 3                      'switch on LED indicator
```

Program for the Waveform of Pulsed Bipolar Direct Current (see Figure A.2d)

```
Main:
        Output 0                    'set pin 0 as an output to control SPST relay
        Output 1                    'set pin 1 as an output to control DPDT relay
        Output 2                    'set pin 2 as an output to control buzzer
        Output 3                    'set pin 3 as an output to control LED indicator

Start program:                      'start to run the below program
        For b2 = 1 to 120           'repeat the loop for 120 times
            High 1                  'switch on DPDT relay
            For b3 = 1 to 120       'repeat the loop for 120 times
                High 0              'switch on SPST relay
                Pause 100           'pause for 0.1 second
                Low 0               'switch off SPST relay
                Pause 100           'pause for 0.1 second
            Next
            Low 1                   'switch off DPDT relay
            For b4 = 1 to 120       'repeat the loop for 120 times
                High 0              'switch on SPST relay
                Pause 100           'pause for 0.1 second
                Low 0               'switch off SPST relay
                Pause 100           'pause for 0.1 second
            Next
        Next
```

```
Low 0                   'switch off SPST relay
High 2                  'switch on buzzer
Pause 100               'pause for 0.1 second
Low 2                   'switch off buzzer
High 3                  'switch on LED indicator
```

Program for the Waveform of Bipolar Direct Current including Intervals of No Applied Current (see Figure A.2e)

```
Main:
        Output 0                'set pin 0 as an output to control SPST relay
        Output 1                'set pin 1 as an output to control DPDT relay
        Output 2                'set pin 2 as an output to control buzzer
        Output 3                'set pin 3 as an output to control LED indicator

Start program:                  'start to run the below program
        For b2 = 1 to 4         'repeat the loop for 4 times
            High 1              'switch on relay DPDT relay
            High 0              'switch on SPST relay
            For b3 = 1 to 15    'repeat the loop for 15 times
                Pause 60000     'pause for 60 second
            Next
            Low 0               'switch off SPST relay
            For b4 = 1 to 5     'repeat the loop for 5 times
                Pause 60000     'pause for 60 second
            Next
            Low 1               'switch off DPDT relay
            High 0              'switch on SPST relay
            For b5 = 1 to 15    'repeat the loop for 15 times
                Pause 60000     'pause for 60 second
            Next
            Low 0               'switch off SPST relay
            For b6 = 1 to 5     'repeat the loop for 5 times
                Pause 60000     'pause for 60 second
            Next
        Next
        Low 0                   'switch off SPST relay
        High 2                  'switch on buzzer
        Pause 100               'pause for 0.1 second
        Low 2                   'switch off buzzer
        High 3                  'switch on LED indicator
```

Program for the Waveform of Pulsed Bipolar Direct Current including Intervals of No Applied Current (see Figure A.2f)

```
Main:
        Output 0                    'set pin 0 as an output to control SPST relay
        Output 1                    'set pin 1 as an output to control DPDT relay
        Output 2                    'set pin 2 as an output to control buzzer
        Output 3                    'set pin 3 as an output to control LED indicator

Start program:                      'start to run the below program
        For b2 = 1 to 4             'repeat the loop for 4 times
            High 1                  'switch on DPDT relay
            For b3 = 1 to 120       'repeat the loop for 120 times
                High 0              'switch on SPST relay
                Pause 100           'pause for 0.1 second
                Low 0               'switch off SPST relay
                Pause 100           'pause for 0.1 second
            Next
            Low 0                   'switch off SPST relay
            For b4 = 1 to 5         'repeat the loop for 5 times
                Pause 60000         'pause for 60 second
            Next
            Low 1                   'switch off DPDT relay
            For b5 = 1 to 120       'repeat the loop for 120 times
                High 0              'switch on SPST relay
                Pause 100           'pause for 0.1 second
                Low 0               'switch off SPST relay
                Pause 100           'pause for 0.1 second
            Next
            Low 0                   'switch off SPST relay
            For b6 = 1 to 5         'repeat the loop for 5 times
                Pause 60000         'pause for 60 second
            Next
        Next
        Low 0                       'switch off SPST relay
        High 2                      'switch on buzzer
        Pause 100                   'pause for 0.1 second
        Low 2                       'switch off buzzer
        High 3                      'switch on LED indicator
```

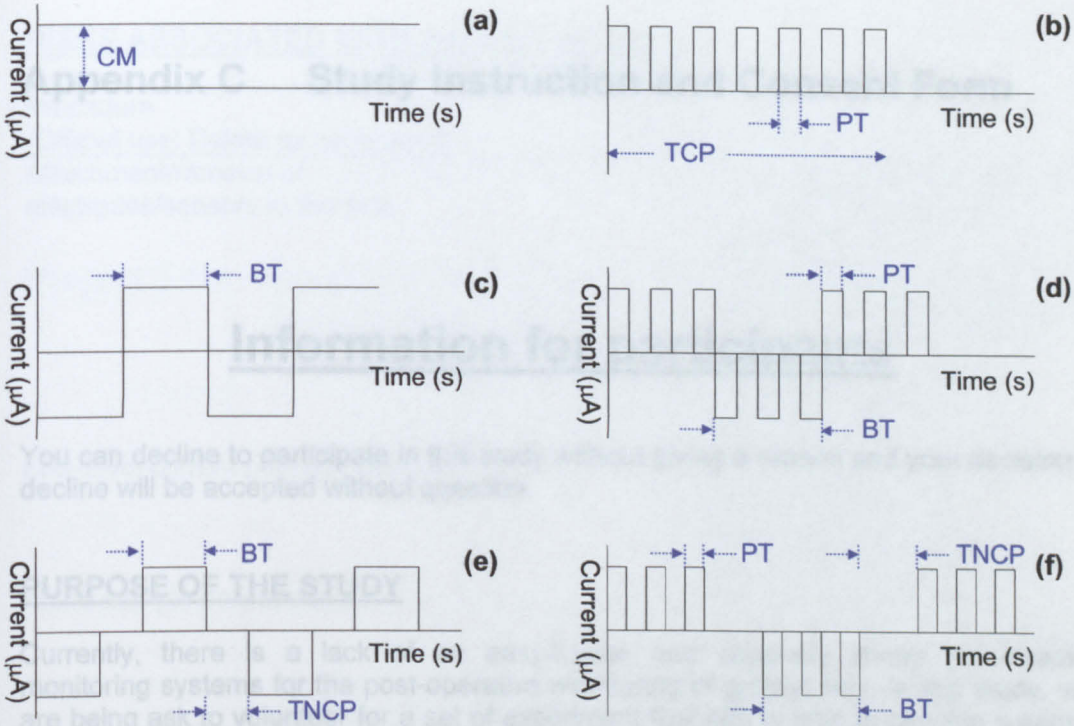

Figure A.2 – Schematic illustration of the current waveform generated by the newly-developed constant current device. (a) Direct current (DC). (b) Pulsed DC. (c) Bipolar DC. (d) Pulsed bipolar DC. (e) Bipolar DC including intervals of no applied current. (f) Pulsed bipolar DC including intervals of no applied current. CM is the magnitude of current. PT and BT are the pulse time and bipolar time, respectively. TCP and TNCP are the time of current passage and time of no current passage, respectively.

Appendix C Study Instruction and Consent Form

Information for participants

You can decline to participate in this study without giving a reason and your decision to decline will be accepted without question.

PURPOSE OF THE STUDY

Currently, there is a lack of an easy-to-use and relatively cheap non-invasive monitoring systems for the post-operative monitoring of grafted skin. In this study, you are being ask to volunteer for a set of experiment that aim to help to develop a sensor system for the post-operative monitoring of grafted skin.

There is no financial reward associated with your participation in these experiments.

Who should volunteer? These studies require the participation of normal health subjects with no current dermatological diseases.

You should not volunteer if you are:

- Ill for any reason
- Using electrically sensitive support systems (e.g. pacemakers)
- Pregnant
- Suffering from diabetes
- Known to have a diagnosed skin condition
- Known to have any infectious disease (e.g. HIV)
- Known to have any allergy

THE EXPERIMENT

The experiment required that you sit down on a comfortable chair. Electrodes will be attached on your inner forearms. A low-level current ($\leq$ 0.5 mA/cm^2) will be applied to the skin via the electrodes for a period of 60 minutes. The skin electrical resistance of your inner forearms will be measured before and after the passage of the current. At the end of current passage, samples of the electrode gel will be collected and your blood glucose and lactate level will be measured at the same time.

RISKS ASSOCIATED WITH PARTICIPATION

Procedure (Official use: Delete as necessary)	Risk
Attachment/removal of electrodes/sensors to the skin	1. Slight irritation of the skin due to cleaning before item attached to skin. 2. Potential allergic reaction to the materials used to make attach electrodes/sensors. 3. Transitory discomfort as electrodes/sensors are removed.
Low-level current passage on skin	1. Slight undue burning or painful sensation below an electrode/sensor site during/after current passage.
Blood sample collection	1. Slight discomfort/painful sensation during blood sample collection. 2. Risk of infection after blood sample collection.

The risk levels associated with participation in this study are considered to be low.

The details of these procedures will be explained to you before the start of an experiment.

As a volunteer you are free to demand that an experiment is stopped and that you can withdraw from the study at any time.

IF YOU AGREE TO PARTICIPATE IN THE STUDY
YOU SHOULD COMPLETE THE ATTACHED CONSENT FORM.

Consent Form

Declaration of Consent

Project Title: Development of Non-Invasive, Iontophoresis Sensor Systems

To be completed by the subject.

	YES	NO
Have you read the information sheet about the study?	☐	☐
Do you confirm that you have no condition, as listed on the information sheet, that makes you unsuitable to take part in the study?	☐	☐
Have you had an opportunity to discuss the study?	☐	☐
Have you received satisfactory answers to your questions?	☐	☐

Who has discussed the study with you?

.....

Are you aware you are free to withdraw at any time from the study?	☐	☐
Do you agree to participate in this study?	☐	☐

In agreeing to participate in this trial, you should be aware that you may be entitled to compensation for accidental Bodily Injury including death or disease arising out the trial, without the need to prove fault. However, such compensation is subject to acceptance of Conditions of Compensation, a copy of which is available upon request.

Name (please print):..... Date of Birth:.....

Signature:..... Date:.....

Witness name (please print):.....

Witness signature:.....

Appendix D The Preconditioning Effects on the Recording of Impedance Spectrum of Screen-Printed Electrodes

As shown in Table A.2 and Figure A.3, it was found that there was a big difference among the 1st trial and the others on the impedance of electrodes (> 12%), whereas a small difference was found on the impedance of electrodes among the last three trials (< 5%). Therefore, the preconditioning effects on the recording of impedance spectrum of screen-printed electrodes seemed to become steady after the 1st trial. In the present study, data captured in the 2nd trial was hence used to compute the impedance of the screen-printed electrodes.

Table A.2 – The results of the preconditioning effects on the recording of impedance spectrum of screen-printed electrodes.

Impedance (kΩ/cm²)	**Number of trials**				
	1	2	3	4	5
Electrodes 1 & 2	26.8	23.5	22.6	21.8	21.1
Electrodes 3 & 4	31.5	27.0	25.9	25.0	24.0
Electrodes 5 & 6	27.0	23.2	22.3	21.5	20.6
Electrodes 7 & 8	26.3	23.0	22.1	21.4	20.7
Electrodes 9 & 10	30.7	26.6	25.4	24.5	23.7
Mean	28.5	24.7	23.7	22.8	22.0
SD	2.4	2.0	1.8	1.8	1.7
% Change in impedance (compared with the 1st trial)		-13.33	-16.84	-20.00	-22.81
% Change in impedance (compared with the previous trial)		-13.33	-4.05	-3.80	-3.51

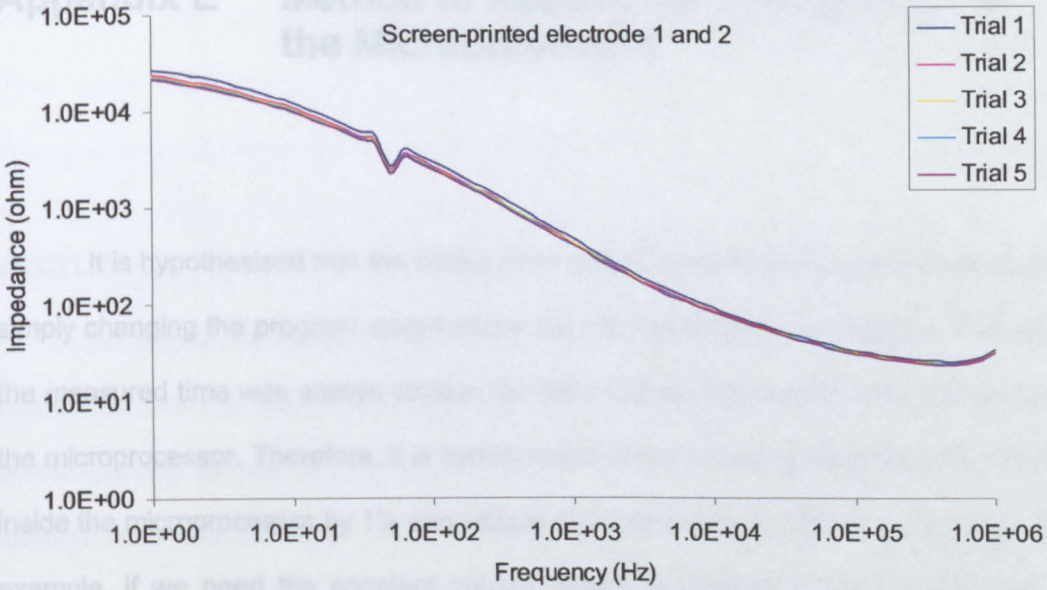

Figure A.3 – The results of the preconditioning effects on the recording of impedance spectrum of screen-printed electrodes. Data from electrodes 1 and 2. The results are shown in Bode Plot form (i.e. total impedance vs. frequency).

Appendix E Method to Reduce the Timing Error of the Microprocessor

It is hypothesised that the timing error of the microprocessor can be reduced by simply changing the program stored inside the microprocessor. As shown in Table 4.4, the measured time was always smaller (at least 1%) than the preset time stored inside the microprocessor. Therefore, it is hypothesised that increasing the preset time stored inside the microprocessor by 1% can reduce the timing error of the microprocessor. For example, if we need the constant current device to provide a direct current for 15 minutes, the preset time stored inside the microprocessor should be 15.15 minutes (i.e. 15 minutes X 1.01).

A set of experiments was performed to prove our hypothesis. The constant current device was set to provide a direct current for 15, 30 or 60 minutes. It was found that the timing error of the microprocessor can be reduced to be least than 0.4% (see Table A.3).

Table A.3 – The results of the method to reduce the timing error of the microprocessor.

Ideal time (minute)	Preset time inside the microprocessor (minute)		Measured time (minute)		Percentage Error (%)	
	As ideal time	101% of ideal time	As ideal time	101% of ideal time	As ideal time	101% of ideal time
15	15	15.15	14.82	14.95	1.21	0.33
30	30	30.30	29.60	29.88	1.35	0.40
60	60	60.60	59.28	59.78	1.20	0.37

Appendix F Screen-Printed Amperometric Ferrocene-Mediated Glucose Biosensor

ABSTRACT

An amperometric ferrocene-mediated glucose biosensor strip based on a three electrodes (working, counter and reference) planar configuration was constructed using screen-printing technique. Different combinations of glucose oxidase and ferrocene loading were dropped coat onto the surface of the amperometric transducer. The amperometric transducer was characterised electrochemically using cyclic voltammetry and its electrochemical characteristics are found to be close to an ideal amperometric transducer. The biosensor on detection of glucose at 200 mV (Ag/AgCl) shows a linear response range for glucose up to 4 mM in 0.01 M phosphate buffered saline solution pH 7.4. The response time of the biosensor was about 10s.

INTRODUCTION

The development of amperometric biosensors is one of the major areas of interest concerning research in the detection of substances. Biosensors may be built by hand, and over thousands of papers reported the properties of hand-made biosensors. One of the major techniques used in the fabrication of enzyme-based biosensors is screen-printing (Alvarez-Icaza and Bilitewski 1993, Wring and Hart 1992, Kulys and D'Costa 1991). In screen-printing, a liquid medium/paste is forced through a mesh screen onto a surface to form an image. Parts of the screen are blocked off, thus preventing the liquid medium/paste from passing through. The "mask" is a negative of part or whole of the desired image, and complex images may be built up through the

use of successive screens. It is attractive not because of its precision, but also because of the speed and relative low cost with which biosensors can be produced.

The most common electrochemical transducers employed to the amperometric biosensors are either inert metal such as platinum or gold (Khan and Wernet 1997, De la Guardia 1995) or carbonaceous materials (Gorton 1995). The widespread use of carbon paste as the supporting matrix for the construction of biosensors is attributed to the simple construction procedures required, the low background current it exhibits, its ability for surface regeneration, and its very low cost.

Amperometric biosensor based on oxidase enzymes that generate H_2O_2 are the most widely used biosensors, the transduction path being the electrochemical oxidation of the peroxide formed in an enzyme reaction (Cattrall 1997). Glucose determination is of important in many fields, such as pharmaceutical and food industries. The development of glucose amperometric biosensors is related to a primary commercial purpose and many efforts have been devoted to the fabrication of compact portable units for personal use by diabetics (Wilkins and Atanasov 1996). Apart from that, glucose simultaneous measurement is of great importance for patient monitoring during intensive care and surgical operation process. In food industries, glucose is an important substrate since it is used as an additive sweeter of foods, and as an essential growth factor of several bacteria that are usually employed in fermentation broths. Therefore, glucose simultaneous measurement is of great importance for quality control in food production.

One serious problem that must be overcome for the use of a glucose biosensor in physiological samples is the presence of metabolites, such as ascorbic and uric acids, that present positive interference due to the fact that they are oxidised at the same potential as H_2O_2 (exceeding 0.7 V). Moreover, the peroxide that is generated is harmful for glucose oxidase, limiting the biosensor's performance. One viable solution for these problems is to replace the natural electron acceptor of glucose oxidase (O_2) by electroactive compounds that will act as redox mediators. An enzyme electrode

based on an electron transfer mediator was reported by Cass *et al.* (1984) 20 years ago. To date the most popular and possibly the most reliable types of biosensors reported on in the literature and utilized commercially are those employing redox enzymes coupled with amperometric detection (Cosnier 1999, Lorenzo *et al.* 1998). Biosensors based on ferrocene derivates (Beh *et al.* 1991, Vahjen *et al.* 1991, Cass *et al.* 1984), tetrathiafulvalene (Almeida and Mulchandani 1993, Gunasingham and Tan 1990) and viologen derivatives (Hale *et al.* 1991) have been reported.

In this paper, the electrochemical characteristics of a screen-printed amperometric transducer (3 electrodes) were evaluated. Different combinations of glucose oxidase and ferrocene loading were dropped coat onto the surface of the amperometric transducer and the sensitivity of these ferrocene-mediated glucose biosensors was evaluated.

METHODOLOGY

Reagents And Solutions

All reagents were commercially available and were employed without further purification. Ferrocene, toluene, 1-cyclo-hexyl-3-(2-morpholinoethyl) carbodiimide-p-methyltoluenesulphate, glucose oxidase (GOD), D(+) glucose, phosphate buffered saline (PBS) tablet, ferrocenemonocarboxylic acid (FMCA), sodium perchlorate, acetate buffer (acetic acid + sodium acetate) were purchased from Sigma Chemical Co. (St. Louis, MO). De-ionized water that had been purified by a Millipore System (Milli-Q UFplus; Bedford, MA) was used to prepare all solutions.

Graphite paste, silver paste, and silver-silver chloride (Ag/AgCl) paste were purchased from Advanced Conductive Materials (Atascadero, CA). Insulating paste (Polyurethane) was purchased from Measurement Group UK LTD (Hants, UK).

Polyvinyl chloride (PVC) sheet was purchased from Stockline Plastics Limited (Glasgow, UK).

Construction Of The Amperometric Transducer And Ferrocene-Mediated Glucose Biosensor

The construction steps of a three-electrode amperometric transducer are shown schematically in Figure A.4. The transducers were constructed using the conventional screen-printing technique (screen mesh size = 390 counts per inch; screen emulsion thickness = 25 μm). There are four different layers for each transducer: Conducting track, insulation shroud, Ag/AgCl pad and graphite pads. These four different layers were printed on a clear PVC sheet one after the other and each layer were allowed to dry at room temperature for 2 hours. Prior to the screen-printing process, the PVC sheets were kept at 80 °C for 1 hour annealing. Silver paste was firstly used to print the conducting tracks. Parts of the conducting tracks were then surrounded by an insulation shroud of insulating paste. Ag/AgCl paste was subsequently applied to the end of conducting tracks to form a Ag/AgCl pad (reference electrode and electrode for reverse iontophoresis) (see Figure A.4). Graphite paste was finally applied to the end of the remaining conducting tracks to form graphite pads (working and counter electrodes).

The same transducer fabrication process explained above was used to ferrocene-mediated glucose biosensor construction. A modified method from Cass (1990) was used to construct the glucose biosensor. 0-0.2 M Ferrocene (in toluene), 0.15 M 1-cyclo-hexyl-3-(2-morpholinoethyl) carbodiimide-p-methyltoluenesulphate (in 0.1 M acetate buffer pH 4.5) and 8.5-16.5 mg/ml glucose oxidase (in 0.1 M acetate buffer pH 4.5) were dropped coat on the surface of one graphite pad (working electrode) of the transducer successively (see Table A.4) and dried for 90 minutes at room temperature. The volume of each solution dropped was 10 μl. A silicon O-ring (10

mm thickness) was then fixed on the surface of the glucose biosensor. The glucose biosensors were kept under 4°C when not in use.

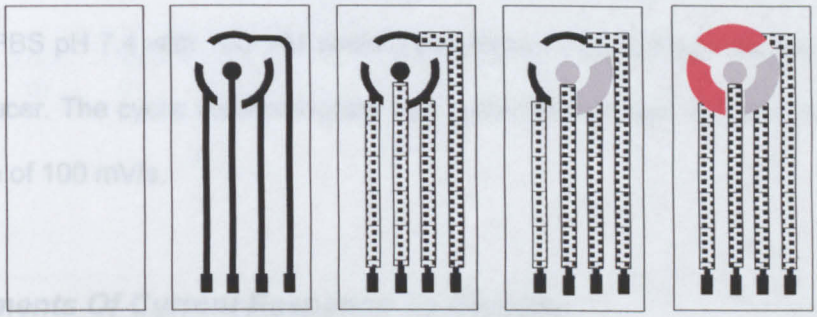

Figure A.4 – Construction steps for the screen-printed amperometric transducer. (a) Support material, polyvinyl chloride; (b) printing of conducting silver basal track; (c) printing of insulation layer; (d) printing of Ag/AgCl pad; (e) printing of graphite pads. The central circular Ag/AgCl pad is for reverse iontophoresis on future study.

Table A.4 – Combinations of glucose oxidase and ferrocene loading for the ferrocene-mediated glucose biosensor construction.

Ferrocene-mediated glucose biosensors	Glucose loading (mg/ml)	Ferrocene loading (M)
1	8.5	0.00
2	8.5	0.05
3	8.5	0.10
4	8.5	0.20
5	12.5	0.00
6	12.5	0.05
7	12.5	0.10
8	12.5	0.20
9	16.5	0.00
10	16.5	0.05
11	16.5	0.10
12	16.5	0.20

Cyclovoltammetric Measurements Of The Amperometric Transducer

The amperometric transducer was connected to a potentiostat (electrochemical interface SI1286, Schlumberger Technologies, England) coupled to a Corrware software (Schlumberger Technologies, England). A solution (500 µl) of 0.5 mM FMCA in 0.01 M PBS pH 7.4 with 100 mM sodium perchlorate was added onto the surface of the transducer. The cyclic voltammogram was recorded between -0.1 and +0.5V using a scan rate of 100 mV/s.

Measurements Of Current Response To Glucose

The ferrocene-mediated glucose biosensor was connected to a potentiostat (electrochemical interface SI1286, Schlumberger Technologies, England) coupled to a Corrware software (Schlumberger Technologies, England) and a potential of 200 mV versus Ag/AgCl pad was applied to the working electrode. A solution (50 µl) of 0.01 M PBS pH 7.4 was added onto the surface (inside the silicon O-ring) of the glucose biosensor. After the current was constant, 200 µl of different concentration of glucose solution was injected into the PBS buffer solution.

Statistics Analysis

One-way analysis of variance (ANOVA) was used to analyse the simple main effect for glucose oxidase loading and ferrocene loading. All statistical analyses were carried out using SPSS v.10 software (SPSS Inc., Chicago, Illinois, USA) with the level of statistical significance set at 0.05.

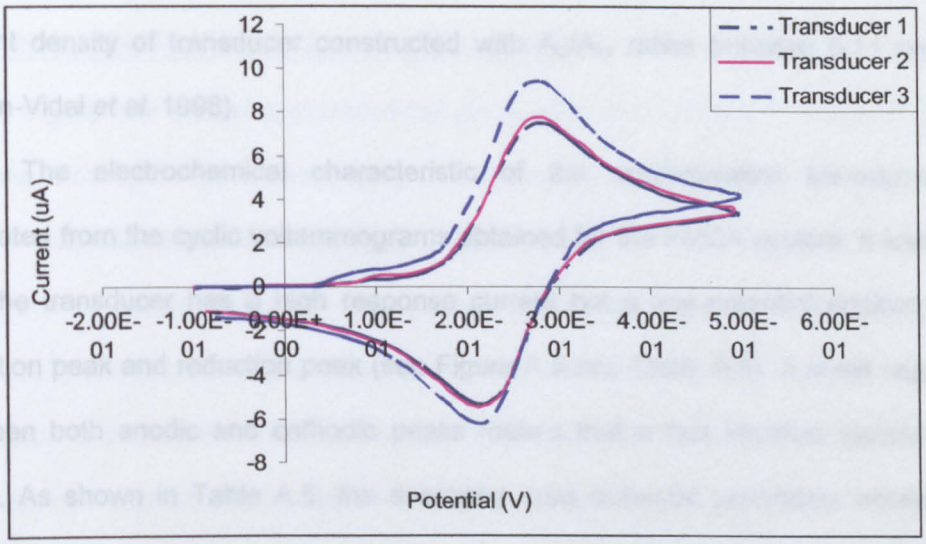

Figure A.5 – Cyclic voltammogram of amperometric transducers. The supporting electrolyte is a 0.5 mM FMCA in 0.01 M PBS pH 7.4 with 100 mM sodium perchlorate. Scan rate is 100 mV/s.

RESULTS AND DISCUSSION

The Amperometric Transducer

One of the major features of the counter electrode material is to have a good inert behavior. Thus, lots of counter electrode materials, such as gold, platinum (Khan and Wernet 1997, De la Guardia 1995), graphite (Gorton 1995), etc have been developed. Galan-Vidal *et al.* (1998) reported that there are no dependence between the current density and the materials used and therefore graphite was used as counter electrode material in this study because it is low cost.

The ratio of the counter electrode area to working electrode area (A_C/A_W) has an influence on supplying a determined current to the working electrode. Several works have been reported and the reporting A_C/A_W ratios are between 1 and 12 (White *et al.* 1996, Nagata *et al.* 1995, Gunther and Bilitewski 1995, Jager and Bilitewski 1994, Lambrechts and Sansen 1992). In this study, the A_C/A_W ratio of 1 was employed on constructing the amperometric transducer because there is no great difference on the

current density of transducer constructed with A_C/A_W ratios between 0.11 and 9.20 (Galan-Vidal *et al.* 1998).

The electrochemical characteristic of the amperometric transducer was evaluated from the cyclic voltammograms obtained for the FMCA system. It was found that the transducer has a high response current but a low potential position of the oxidation peak and reduction peak (see Figure A.5 and Table A.5). A small separation between both anodic and cathodic peaks means that a fast electron transfer takes place. As shown in Table A.5, the averaged peak potential separation between the anodic and cathodic peak (ΔE_p) and the ratio of the anodic peak current to cathodic peak current (I_{pa}/I_{pc}) were found to be close to that of an ideal amperometric transducer reported by Nicholson and Shain (1964), i.e. ideal ΔE_p and I_{pa}/I_{pc} should be 59 mV and 1 respectively.

The reproducibility in the construction of the amperometric transducer was evaluated from standard deviation of ΔE_p and I_{pa}/I_{pc} ratio. As shown in Table A.5, the relative standard deviation of ΔE_p and I_{pa}/I_{pc} ratio indicated a batch reproducibility of transducer construction of about 6% (n = 3).

Table A.5 – The electrochemical characteristics of the amperometric transducers.

	E_{pa} (V)	E_{pc} (V)	I_{pa} (μA)	I_{pc} (μA)	ΔE_p (V)	I_{pa}/I_{pc}
Transducer 1	0.281	0.211	6.50	6.97	0.07	0.93
Transducer 2	0.277	0.213	6.42	7.09	0.06	0.91
Transducer 3	0.275	0.212	6.82	8.16	0.06	0.84
Mean					0.07	0.89
SD					0.00	0.05
Relative SD					5.77	5.60

E_{pa} and E_{pc} are the anodic and cathodic peak potentials.
I_{pa} and I_{pc} are the anodic and cathodic peak currents.
ΔE_p are the peak separation ($\Delta E_p = E_{pa} - E_{pc}$)

The Ferrocene-Mediated Glucose Biosensor

Figure A.6 shows a current-time curve after the addition of glucose solution onto the biosensor. Immediately after the addition of glucose solution, the reductive current was increased and reached a plateau within 10 second in general. The magnitude of current response was plotted against the glucose concentration (see Figure A.7) and the sensitivity of the biosensor was determined by the slope of linear regression of this current response versus glucose concentration plot. It was found that the response current was increased with increasing concentration of glucose and the reductive current response was proportional to the glucose concentration up to 4 mM in general.

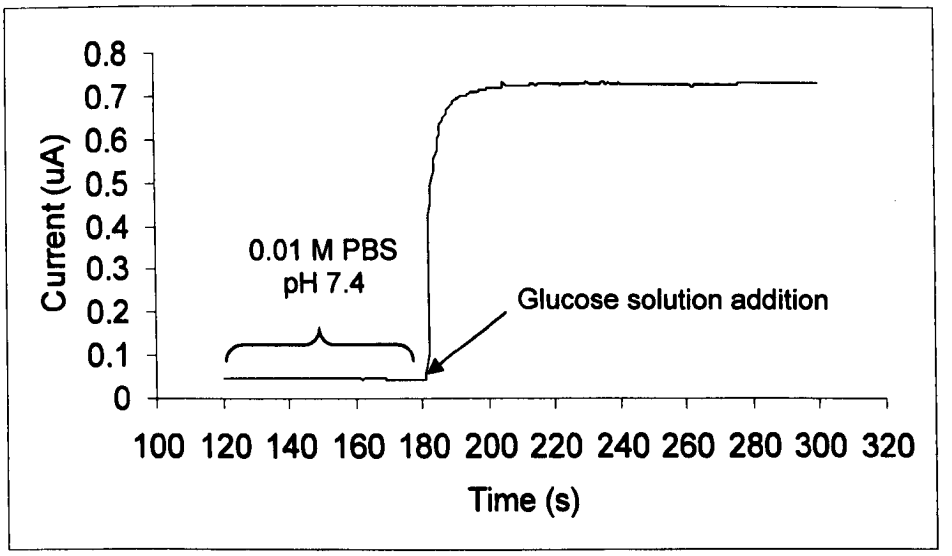

Figure A.6 – Current-time curve obtained by the addition of 4 mM glucose solution on the ferrocene-mediated glucose biosensor. Data is obtained from biosensor with the combination of 12.5 mg/ml glucose oxidase and 0.1 M ferrocene.

The mean values of the sensitivity for each combination of glucose oxidase loading and ferrocene loading are given in Table A.6. The changes in the sensitivity

with different concentration of glucose oxidase and ferrocene are also illustrated (see Figure A.8). As shown in Figure A.8, it was found that the sensitivity was increased with increasing concentration of ferrocene. More importantly, the sensitivity of the ferrocene-mediated glucose biosensor was found to be significantly higher than unmediated glucose biosensor ($p<0.05$). Unmediated glucose biosensor has a lower sensitivity because it needs dioxygen for its reaction to be taken place:

$$\text{Glucose} + \text{GODoxidized} \rightarrow \text{GODreduced} + \text{Gluconolactone} \qquad \text{(A.1)}$$

$$\text{GODreduced} + \text{Oxygen} \rightarrow \text{GODoxidized} + \text{Hydrogen peroxide} \qquad \text{(A.2)}$$

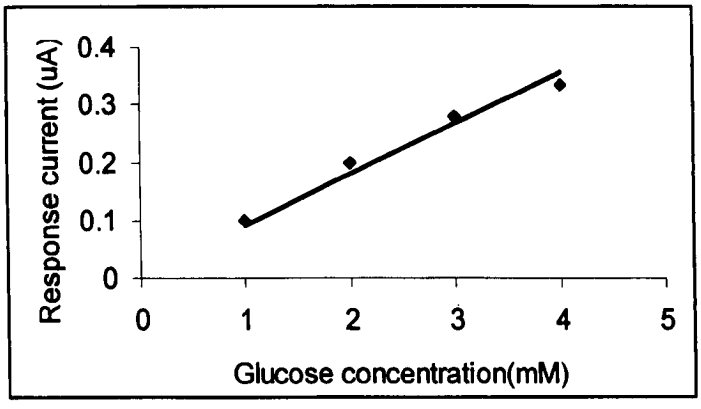

Figure A.7 – Calibration curve of glucose obtained on the ferrocene-mediated glucose biosensor. The line is that of best fit found by linear regression; the intercept has been forced through zero. The sensitivity of the biosensor is the slope of the linear regression line. Data is obtained from biosensor with the combination of 8.5 mg/ml glucose oxidase and 0.05 M ferrocene.

However, ferrocene-mediated glucose biosensor doesn't need dioxygen for its reaction because ferrocene replaces dioxygen as a cofactor for glucose oxidase and thus acts as an electron acceptor; the reduced form of the glucose oxidase is then re-oxidised as shown below:

$$GOD_{reduced} + 2\ Ferrocene^{+} \rightarrow GOD_{oxidized} + 2\ Ferrocene + 2\ H^{+} \quad (A.3)$$

$$2\ Ferrocene \leftrightarrow 2\ Ferrocene^{+} + 2\ e^{-} \quad (A.4)$$

Table A.6 – The sensitivity (nA/mM) of the ferrocene-mediated glucose biosensor at different combinations of glucose oxidase loading and ferrocene loading (n = 3).

Glucose oxidase (mg/ml)	Ferrocene (M)			
	0	0.05	0.1	0.2
8.5	21.5 ± 0.5 (2.3%)	87.7 ± 4.3 (4.9%)	125.1 ± 3.6 (2.9%)	199.0 ± 5.7 (2.9%)
12.5	25.8 ± 1.7 (6.6%)	96.3 ± 1.0 (1.0%)	189.7 ± 1.3 (0.7%)	210.5 ± 4.9 (2.3%)
16.5	23.8 ± 0.1 (0.4%)	103.6 ± 0.1 (0.1%)	150.3 ± 10.4 (6.9%)	186.3 ± 6.0 (3.2%)

Relative standard deviations are stated in parentheses.

As shown in Figure A.8, there is no great influence on the sensitivity with increasing glucose oxidase loading except the biosensor with 0.1 M ferrocene. For biosensor with 0.1 M ferrocene, the sensitivity of 12.5 mg/ml glucose oxidase loading was found to be significantly higher than that of both 8.5 mg/ml and 16.5 mg/ml glucose oxidase loading ($p<0.05$). Interestingly, for biosensor with 0.2 M ferrocene, the sensitivity of 12.5 mg/ml glucose oxidase loading was found to be higher than that of 16.5 mg/ml glucose oxidase loading. This seems to be that higher glucose oxidase loading doesn't take any advantage with higher concentration of ferrocene. Therefore, the optimal ferrocene-mediated glucose biosensor in this study can be either the combination of 12.5 mg/ml glucose oxidase with 0.1 M ferrocene or 12.5 mg/ml glucose oxidase with 0.2 M ferrocene. This finding is similar to that reported by Cass (1990).

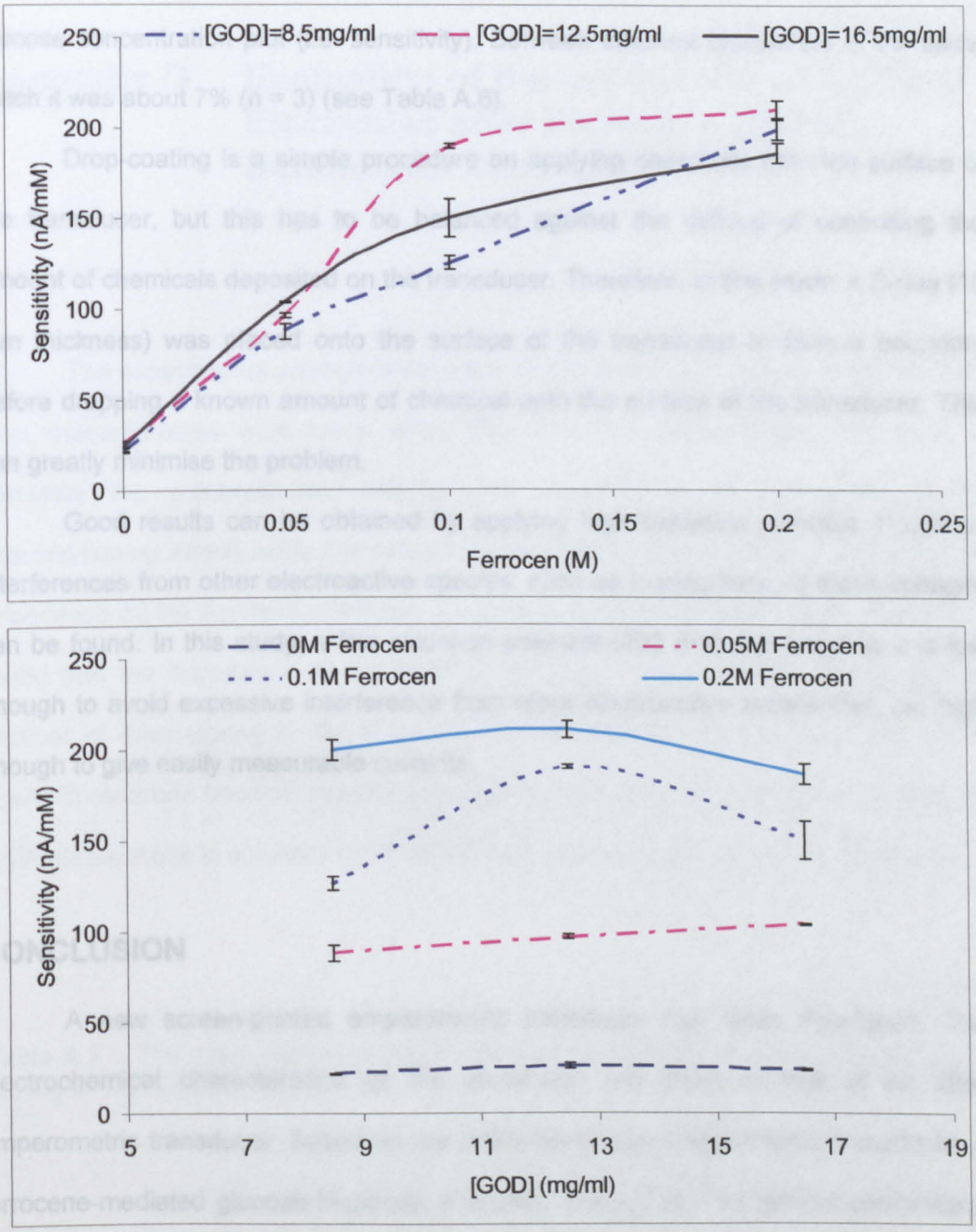

Figure A.8 – The changes in the sensitivity of the ferrocene-mediated glucose biosensor at different combinations of glucose oxidase loading and ferrocene loading (n = 3).

The construction reproducibility of the ferrocene-mediated glucose biosensor was evaluated from relative standard deviation of the slope of current response versus

glucose concentration plot (i.e. sensitivity). Between different biosensors of the same batch it was about 7% (n = 3) (see Table A.6).

Drop-coating is a simple procedure on applying chemicals onto the surface of the transducer, but this has to be balanced against the difficult of controlling the amount of chemicals deposited on the transducer. Therefore, in this study, a C-ring (10 mm thickness) was placed onto the surface of the transducer to form a boundary before dropping a known amount of chemical onto the surface of the transducer. This can greatly minimise the problem.

Good results can be obtained by applying high oxidation potential. However, interferences from other electroactive species, such as L-ascorbate, at these voltages can be found. In this study, a low oxidation potential (200 mV) was used as it is low enough to avoid excessive interference from other electroactive substances, but high enough to give easily measurable currents.

CONCLUSION

A new screen-printed amperometric transducer has been developed. The electrochemical characteristics of the transducer are close to that of an ideal amperometric transducer. Based on the newly-developed amperometric transducer, a ferrocene-mediated glucose biosensor has been developed. The optimal combination of glucose oxidase and ferrocene can either be 12.5 mg/ml glucose oxidase with 0.1 M ferrocene or 12.5 mg/ml glucose oxidase with 0.2 M ferrocene.

Appendix G Evaluation of the Impedance of Ag/AgCl Electrodes after Storing in 1M KCl Solution for Several Days

The experimental arrangements were identical to that described in Figure 3.4a. Two measurements were taken every day. The first measurement was used to eliminate the preconditioning effects (see Appendix A for the detail of the preconditioning effect) while the second measurement was used for determining the impedance of the Ag/AgCl electrode. As shown in Table A.7 and Figure A.9, it was found that the impedance of the Ag/AgCl electrode decreases with increasing the number of days storing in 1M KCl solution. The decrease in the impedance of the Ag/AgCl electrode became steadily after Day 3. Therefore, it is suggested to soak the Ag/AgCl electrode in solutions of 1M KCl for 3 days prior to its use in the experiments.

Table A.7 – The results of the evaluation of the impedance of Ag/AgCl electrode after storing in 1M KCl solution for several days.

	Day					
	1	2	3	4	5	6
Impedance (Ω)	537	530	500	495	490	490
% Change in impedance (compared with Day 1)		-1.3	-6.9	-7.8	-8.8	-8.8
% Change in impedance (compared with the previous day)		-1.3	-5.7	-1.0	-1.0	0.0

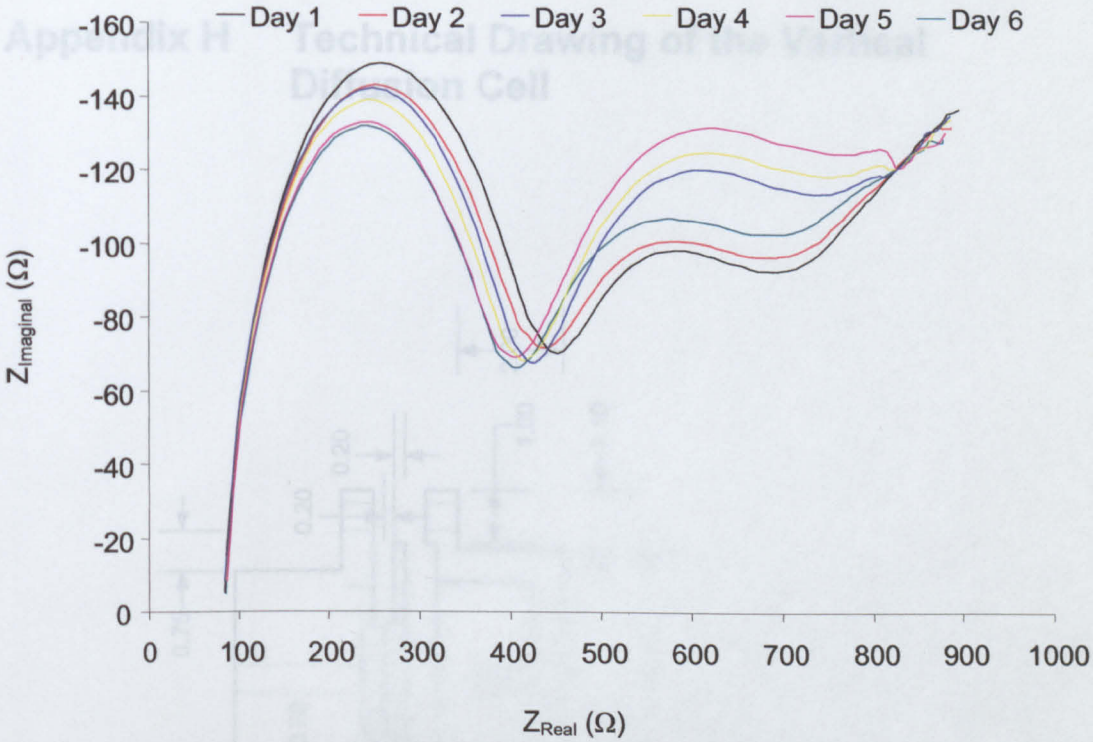

Figure A.9 – The results of the evaluation of the impedance of Ag/AgCl electrode after storing in 1M KCl solution for several days.

Appendix H Technical Drawing of the Vertical Diffusion Cell

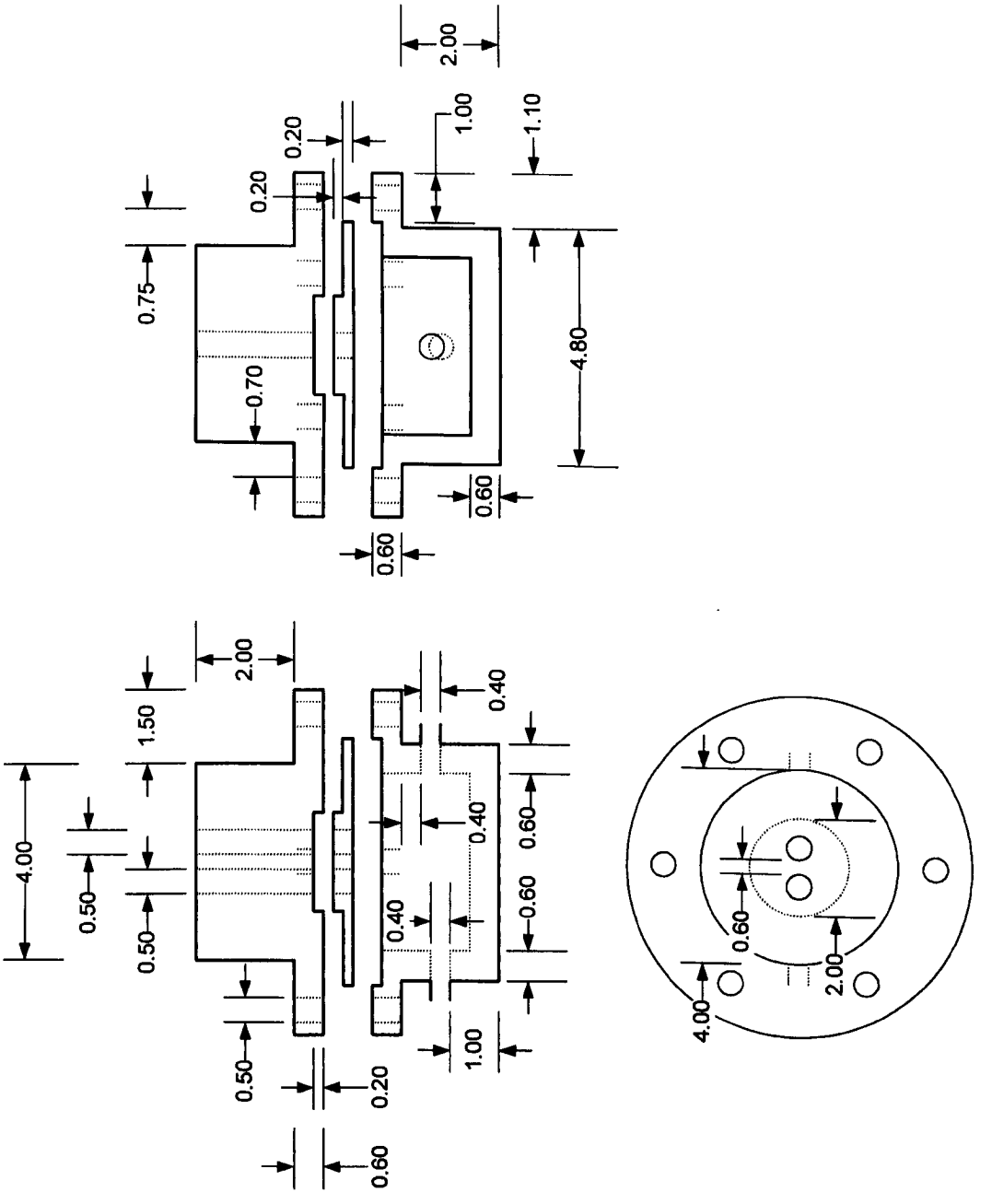

Figure A.10 – Technical drawing of the vertical diffusion cell. Unit is in cm.